Université du Québec

INRS Institut national de la recherche scientifique

INRS Armand-Frappier Santé Biotechnologie

Characterization of TagB and TagC, new chromosomally encoded autotransporters and their roles in the pathogenesis of Extraintestinal pathogenic *Escherichia coli* (ExPEC)

By

Pravil Pokharel

A thesis submitted for the degree of

Doctor of Philosophy (Ph.D.) in Biology

Evaluation committee members

President of Jury and Internal Examiner	Dr. Charles Calmettes Armand-Frappier Santé Biotechnologie, INRS
External Examiner	Dr. Samantha Gruenheid Department of Microbiology and Immunology McGill University
External Examiner	Dr. Josée Harel Department of Microbiology, Infectiology and Immunology Université de Montréal (UdeM)
Supervisor	Dr. Charles M. Dozois Armand-Frappier Santé Biotechnologie

ACKNOWLEDGMENTS

I am indebted to my supervisor, Professor Charles M. Dozois who in all possible ways, helped me go through this journey of Ph.D. I am very fortunate to have had such a great supervisor. His encouragement, supervision, profound enthusiasm, and creative discussion are deeply appreciated. His patient mentoring style has helped me grow as a person and a scientist. I express my appreciation to the thesis evaluation members for their many hours of hard work in reviewing this thesis during this stressful COVID-19 pandemic season – Dr. Josée Harel, Dr. Samantha Gruenheid, and Dr. Charles Calmettes.

I am particularly grateful to a wonderful person, Hicham Bessaiah, a valued labmate and my brother. He has been all around and selflessly given his time to make my manuscripts, experimental designs, critical data analysis as perfect as possible.

My special thanks go to Prof. Alma Lilian Guerrero Barrera and Juan Manuel Diaz from Autonomous University of Aguascalientes, Mexico for the great collaboration and help throughout my work. Your comments helped me immeasurably.

I would like to extend my sincere thanks to Prof. Kessen Patten for collaboration with Zebrafish model and Prof. Nicolas Doucet, Prof. Eric Déziel, Prof. Charles Calmettes, Prof. Richard Villemur and Prof. Frédéric Veyrier for valuable insights. I'd like to recognize the help of Jessy Tremblay for confocal microscopy and Arnaldo Nakamura for electron microscopy. I gratefully acknowledge the assistance of Michel Courcelles whose help cannot be overestimated.

I would also like to thank NSERC Canada Discovery and CRIPA-FRQNT grants for their gracious funding over the years.

I also appreciate and acknowledge the effort of Sebastien and all those friends, Katerina, Hossein, Imene, Jihen, Mariem, Malek, Remi, Daniel, Hajer, Vivian, Isabelle, Sabin, Mahendra, Alex, Sammy, Hamza, Hassan, Pranav, Priyanka, Alina; made throughout the years in the CMD lab; the laughs we shared during my time spent there made the experience so much more memorable.

Finally, I am thankful to my mother and future mother-in-law for their infinite love, encouragement, mental support and prayers.

DEDICATION

To my fiancé Ashna, who sees all that is best in me.

ABSTRACT

Serine protease autotransporters of *Enterobacteriaceae* (SPATE) are associated with various extraintestinal pathogenic *Escherichia coli* (ExPEC) including avian pathogenic *E. coli* (APEC). We have identified three new genes encoding SPATE proteins in APEC strain QT598, two located adjacent to each other on a genomic island and another on the plasmid (QT598 has 5 SPATE genes in total), and we refer to them as "tandem autotransporter genes, *tagB*, and *tagC* and serine-protease hemagglutinin autotransporter, *sha*". The remaining SPATEs, Vat and Tsh are previously characterized. Interestingly, these new autotransporter genes are present in some APEC and in some human uropathogenic *E. coli* (UPEC). The possible function and roles of these new SPATES especially TagB and TagC in the pathogenesis of ExPEC were investigated in my thesis.

Clones expressing TagB and TagC proteins were tested for various phenotypes including adherence to human renal, bladder cell lines and chicken fibroblast, biofilm formation, autoaggregation, cytotoxicity and hemagglutination, which represent possible mechanisms of colonization of the host. Results showed that these SPATEs are autoaggregating, hemagglutinating and can promote adherence to the HEK 293 renal and 5637 bladder human cell lines, chicken fibroblast, but did not contribute significantly to biofilm production. TagB and TagC exhibited cytopathic effects on the bladder epithelial cell line. Further, TagB and TagC induced cytoskeletal damage to bladder epithelial cells characterized by disruption of actin stress fibers. The serine protease motif was essential for oligopeptide cleavage and cytopathic effects, as cytotoxicity was abolished when the active serine was replaced by alanine. However, this residue was not required for secretion of the SPATEs into the external milieu or for autoaggregation. TagB and TagC proteins were internalized by bladder epithelial cells but the serine mutant variant of these proteins were left outside the cell. Following transurethral infection of CBA/J mice with a *tagBC* mutant, no significant difference in colonization was observed. However, the competitive fitness of a mutant lacking all 5 SPATE genes was significantly lower in the kidney as well as when infected in the yolk sac of Zebrafish. This underlines the potential cumulative role of SPATEs for survival and competitive fitness during extra-intestinal infection.

Keywords *Escherichia coli*, SPATEs, Toxins, Adhesins, Poultry, Urinary tract infection, Cytotoxicity, Actin, Mucinase, Pathogenesis

RÉSUMÉ

Les autotransporteurs protéases de sérines des *Enterobacteriaceae* (SPATEs, *Serine Protease Autotransporters of Enterobacteriaceae*) sont associés à différentes souches pathogènes d'*Escherichia coli* extra-intestinaux (ExPEC), y compris les *E. coli* pathogènes aviaires (APEC). Nous avons identifié trois nouveaux gènes codant pour des protéines SPATE dans une souche APEC QT598, deux sont adjacents, situés sur un îlot génomique dans une souche APEC et un autre situé sur un plasmide (QT598 possède 5 gènes SPATE au total), et nous les appelons "tandem autotransporter genes, *tagB*, and *tagC* and serine protease hemagglutinin autotransporter, *sha*". Vat et Tsh sont préalablement caractérisés. En effet, ces nouveaux gènes autotransporteurs sont présents chez certaines souches APEC et également dans certaines souches d'*E. coli* uropathogènes (UPEC). La fonction et les rôles possibles de ces nouveaux SPATES en particulier TagB et TagC dans la pathogenèse d'une souche ExPEC ont été étudiés dans ma thèse.

Les clones exprimant ces protéines TagB et TagC ont été testés pour différents phénotypes, y compris l'adhésion au rein humain, aux lignées cellulaires de la vessie et aux fibroblastes de poulet, la formation de biofilm, l'autoagrégation, la cytotoxicité et l'hémagglutination, qui représentent des mécanismes possibles de colonisation de l'hôte. Les résultats ont montré que ces SPATEs sont autoagrégants, hémagglutinants et peuvent favoriser l'adhérence aux lignées cellulaires humaines rénales HEK 293 et de la vessie 5637, les fibroblastes de poulet, mais n'ont pas contribué de manière significative à la production de biofilm. TagB et TagC ont présenté des effets cytopathiques sur la lignée cellulaire épithéliale de la vessie.

De plus, TagB et TagC ont induit des dommages aux cytosquelettes des cellules épithéliales de la vessie caractérisés par une perturbation des fibres de stress d'actine. Le motif de la sérine protéase était essentiel pour le clivage des oligopeptides et les effets cytopathogènes, car la cytotoxicité a été abolie lorsque la sérine active a été substituée par l'alanine. Cependant, ce résidu n'était pas requis pour la sécrétion des SPATEs dans le milieu extracellulaire ou pour l'autoagrégation. Les protéines TagB et TagC ont été internalisées aux cellules épithéliales de la vessie, mais le mutant sérine de ces protéines n'a pas pu s'internaliser aux cellules. Suite à une infection transurétrale des souris CBA/J avec un mutant *tagBC*, aucune différence significative de colonisation de la vessie et des reins n'a été observée. Cependant, l'aptitude compétitive d'un mutant des 5 SPATE gènes était significativement moins capable de coloniser les reins de souris et le sac vitellin du poisson-zèbre. Cela souligne le rôle cumulatif potentiel des SPATEs pour la survie et la compétitivité pendant les infections extra-intestinales.

Mots-clés *Escherichia coli*, SPATEs, Toxines, Adhésines, Volaille, Infection des voies urinaires, Cytotoxicité, Actine, Mucinase, Pathogenèse

TABLE OF CONTENTS

LIST OF FIGURES

LIST OF TABLES

LIST OF ABBREVIATIONS

ANOVA Analysis of variance

APEC Avian pathogenic *E. coli*

CNF1 Cytotoxic necrotizing factor 1

DAEC Diffuse Adhering *E. coli*

DAPI 4′,6-Diamidino-2-phenylindole

EAEC Enteroaggregative *E. coli*

EHEC Enterohemorrhagic *E. coli*

EPEC Enteropathogenic *E. coli*

ETEC Enterotoxigenic *E. coli*

ExPEC Extraintestinal pathogenic *E. coli*

LDH Lactate dehydrogenase

LEE Locus of enterocyte effacement

LPS Lipopolysaccharides

NMEC Neonatal meningitis *E. coli*

PAS Periodic acid–Schiff

PMSF Phenylmethylsulfonyl fluoride

SPATEs Serine protease autotransporters of *Enterobacteriaceae*

TEM Transmission electron microscopy

UPEC Uropathogenic *E. coli*

1 INTRODUCTION

In addition to intestinal infections like diarrhea or dysentery, *Escherichia coli* is capable of causing extraintestinal infections such as urinary tract infections and meningitis in humans and respiratory and systemic infections in birds (Kaper et al., 2004). Avian pathogenic *E. coli* (APEC) is responsible for global multimillion-dollar losses for the poultry industry while Uropathogenic *E. coli* (UPEC) is the most common bacterial infectious disease encountered in human clinical practice and have a profound medical and socioeconomic impact. Antibiotics are the easiest solution to avoid them, but many *E. coli* strains are becoming more and more resistant, making antibiotics less attractive as a remedy. So, in this antibiotic resistance era, we need to develop antimicrobial agents that can kill or disarm bacteria by targeting factors that are crucial for virulence. We found novel virulent toxic proteins, autotransporters, belonging to serine protease family which is produced by both APEC and UPEC strains. In this thesis, we focused on the better characterization of these proteins to find their role in the pathogenesis of extraintestinal infections. Our hypothesis is the possible contribution of these proteins in the colonization and dissemination of the bacteria in the host.

In the literature review, I introduce and explain the pathogenesis of different *E. coli* pathotypes focusing on the toxins and their possible roles. Afterwards, I present the roles of TagB and TagC in pathogenesis, as well as a review chapter on "serine protease autotransporters" which overviews the broader biological context of this family of toxins. The first article deals with the first objective of this thesis - to find the possible roles of TagB and TagC *in vitro* as well as *in vivo* using cell culture and murine models. Following the findings from the first article as a steppingstone, we worked on the second objective of the thesis which was to elucidate the possible mechanisms of the protease activity of these toxins. Thus, the second article concludes with the coverage of a plausible mechanism of the cytotoxicity of these proteins on the epithelial cells.

2 LITERATURE REVIEW

2.1 *Escherichia coli*

Escherichia coli (*E. coli*) is generally known to cause bacterial diarrheal diseases and is a nearly ubiquitous facultative anaerobic Gram-negative bacteria present in the colon of mammals and birds (Hill & Drasar, 1975). Many strains of *E. coli* are not harmful and can contribute to human health – through synthesis of co-factors such as clotting factor vitamin K (Bentley & Meganathan, 1982), vitamin B2 (Bacher *et al.*, 2000), and may provide colonization resistance against other enteropathogens (Hudault *et al.*, 2001). *E. coli* is a highly diversified bacterial species that is an intestinal commensal, but it is also a versatile bacterial pathogen associated with 3 general types of infections: enteric disease, urinary tract infections (UTIs) and sepsis/meningitis (Kaper *et al.*, 2004). *E. coli* strains are grouped into 7 major phylogenetic groups (A, B1, B2, C, D, E and F) (Clermont *et al.*, 2013). Although these phylogenetic groups do not completely represent the complex diversity of *E. coli,* it has been demonstrated that extra-intestinal pathogenic *E. coli* (ExPEC) are predominantly within groups B2 and D (Boyd & Hartl, 1998; Johnson *et al.*, 2001; Picard *et al.*, 1999). The pathogenic versatility ExPEC is due to the acquisition of genes encoding various virulence factors that are present on different pathogenicity islands or on virulence plasmids. This array of specific virulence factors that enable ExPEC to cause infections outside the GI tract are non-randomly distributed and strains of *E. coli* phylogenetic group B2 show the greatest frequency and diversity of virulence traits (Picard *et al.*, 1999).

Based upon the site of infection and disease caused by *E. coli* in humans, pathogenic *E. coli* strains have been divided into two major groups: intestinal pathogenic *E. coli* and extraintestinal pathogenic *E. coli* (ExPEC) (Figure 2.1). Among intestinal strains causing diarrheagenic infections, there are six well-defined pathotypes: Enteropathogenic *E. coli* (EPEC), Enterohemorrhagic *E. coli* (EHEC), Enterotoxigenic *E. coli* (ETEC), Enteroaggregative *E. coli* (EAEC), Enteroinvasive *E. coli* (EIEC) and Diffusely adherent *E. coli* (DAEC). The ExPEC group includes strains causing disease outside the intestinal tract, including Uropathogenic *E. coli* (UPEC) and Neonatal meningitis *E. coli* (NMEC), and Avian pathogenic *E. coli* (APEC). These pathotypes are briefly described below with the focus on the serine proteases or toxins and will serve as the underpinning for the bacterial pathogenesis presented in subsequent chapters. Various toxins are associated with the above-mentioned pathotypes with diversity in the properties and mode of action influenced by niche and fitness differences.

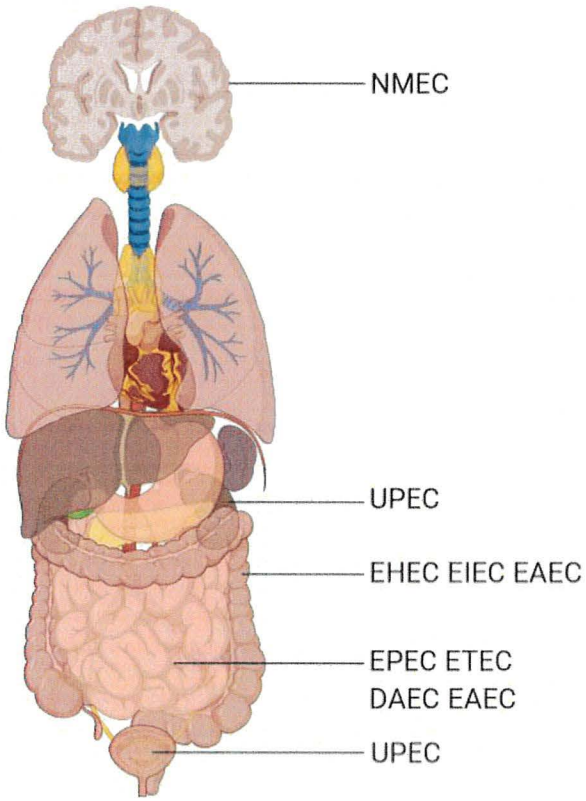

Figure 2.1 Different colonization sites of *E. coli* in humans

At least six pathotypes of diarrheagenic *E. coli* have been described. ETEC strains adhere to the small intestinal mucosa (Girón *et al.*, 1994), EAEC strains bind to small as well as large intestinal cells and tend to clump in small aggregates (Nataro *et al.*, 1987), EPEC strains attach to small intestinal mucosal cells forming attaching and effacing (AE) lesions (Moon *et al.*, 1983), EHEC strains adhere to large intestine to produce AE lesions (Kaper *et al.*, 2004), EIEC strains invade colonic epithelial cells (Nataro & Kaper, 1998), and DAEC bind to the small intestine enterocytes (Benz & Schmidt, 1992). UPEC strains colonize the periurethral area and migrate up the urethra to infect the bladder. Further, bacteria can ascend to the kidney and enter the bloodstream (Kaper *et al.*, 2004). NMEC, the leading cause of gram-negative infant meningitis can invade meninges that form the blood-brain barrier (Dietzman *et al.*, 1974).

2.1.1 Intestinal pathogenic *E. coli*

Enteropathogenic *E. coli* (EPEC)

EPEC are pathogens associated with infant diarrhea in developing countries (Ochoa *et al.*, 2008). The characteristic histopathological hallmark related to this group of *E. coli* is production of lesions known as "Attaching and effacing (A/E)" lesions that are produced when bacteria intimately attach to intestinal epithelial cells and alter the cytoskeleton through accumulation of polymerized actin beneath the adherent bacteria (Moon *et al.*, 1983). A protein called intimin mediates the intimate attachment of the epithelial cells. Intimin is encoded by the *eae* gene located within a 35- kb pathogenicity island called the locus of enterocyte effacement (LEE) (McDaniel *et al.*, 1995). The LEE encodes a type III secretion system (TTSS), translocators (EspA, EspB, and EspD), effectors

(Tir, EspG, EspF, Map, and EspH), chaperones (CesAB, CesD, CesD2, CesF, and CesT), and regulators (Ler, GrlA, and GrlR) (Kenny, 2001). The model for EPEC pathogenesis suggests that EPEC initially adhere to epithelial cells by interaction of intimin with the translocated intimin receptor (Tir) inserted in the membrane. Subsequent effacement of microvilli leads to loss of absorptive surface area, increased intestinal inflammation, and fluid accumulation in the intestinal lumen. In addition, some of the EPEC strains produce an enterotoxin, EspC which belongs to serine protease autotransporter family (Figure 2.2) (Mellies *et al.*, 2001). EspC has no role in the generation of EPEC A/E lesions (Stein *et al.*, 1996) but controls pore formation and cytotoxicity by cleaving EspA/EspD which are the translocator components of the Type III secretion system (T3SS) (Guignot *et al.*, 2015). It is interesting to note that EspC could contribute to EPEC infection by degrading different biological substrates like pepsin, glycoprotein, coagulation factor V, and spectrin (Dutta *et al.*, 2002) and by inducing apoptosis and necrosis in epithelial cells (Serapio-Palacios & Navarro-Garcia, 2016).

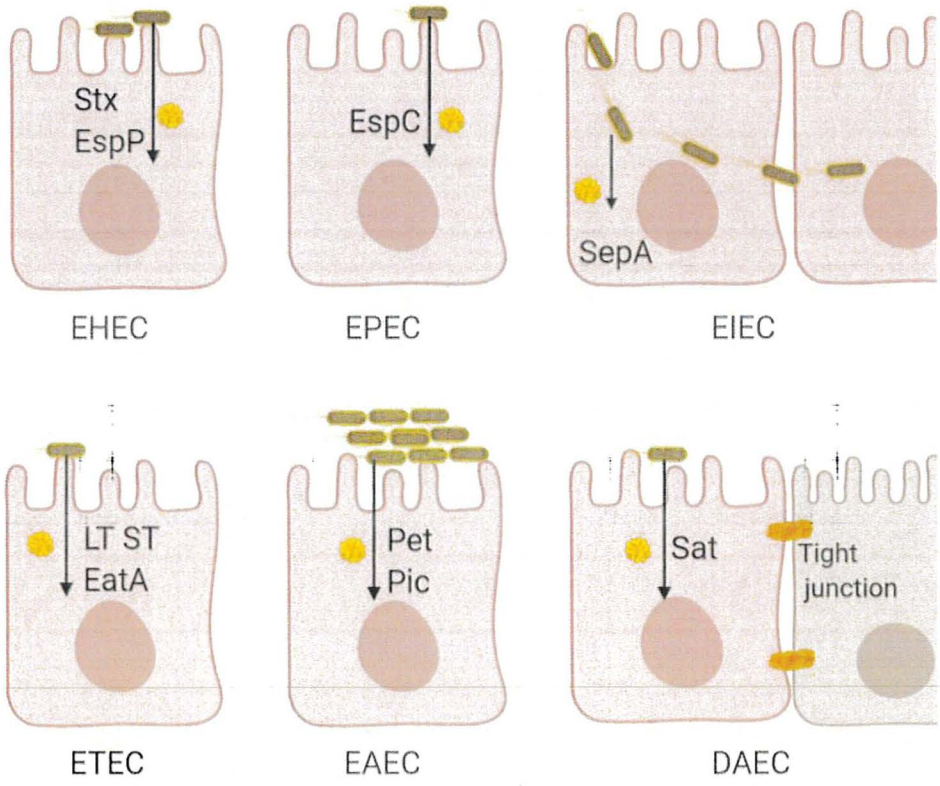

Figure 2.2 Presence of toxins in different intestinal *E. coli*

Diarrheal complication of EHEC is due to Shiga toxin (Stx) (Fraser *et al.*, 2004). EHEC produces EspP an extracellular serine protease cytotoxin which reduces coagulation factor activities and has a role in adherence and biofilm formation (Brunder *et al.*, 1997; Xicohtencatl-Cortes *et al.*, 2010). EPEC produces an enterotoxin EspC, which cleaves spectrin and can induce apoptosis and necrosis (Serapio-Palacios & Navarro-Garcia, 2016). EIEC breach the colonic epithelium, is internalized and then released from vacuoles and can spread laterally to adjacent cells. SepA can facilitate invasion of intestinal cells by disrupting apical poles of the epithelial barrier (Maldonado-Contreras *et al.*, 2017). ETEC produces watery diarrhea by the secretion of heat-labile (LT) and/or heat-stable (ST) enterotoxins (Spangler, 1992). EatA can degrade the intestinal mucosal layer and provide access to ETEC toxins to epithelial cell surfaces (Kumar *et al.*, 2014). EAEC after attaching to the bowel epithelium secretes enterotoxin and cytotoxins. Pet is a cytotoxin that can mediate cellular alteration by degrading fodrin/spectrin (Villaseca *et al.*, 2000). Pic is a mucinase and can significantly reduce complement activation by cleaving complement cascade factors - C3, C4, and C2 (Abreu *et al.*, 2015). DAEC is diffusely associated with the host cells. Sat is a cytotoxin that has been described in relation to the disruption of tight junctions and enterotoxicity activity (Guignot *et al.*, 2007). Adapted from (Kaper *et al.*, 2004).

Enterohemorrhagic *E. coli* (EHEC)

EHEC causes bloody diarrhea (hemorrhagic colitis) and life-threatening hemolytic uremic syndrome (HUS) (Riley *et al.*, 1983). EHEC strains of the O157: H7 serotype have been associated with both outbreaks and sporadic cases of food-associated severe diarrhea. This pathotype contains specific virulence factors and also has the ability to survive in environmental stress conditions including low pH and has a low infectious dose (50 - 100 organisms) (Tuttle *et al.*, 1999). Stx toxins, also known as verotoxins (VT), are a key virulence factor for EHEC. The Shiga toxin family is composed of Stx1 which is nearly identical to the toxin of *Shigella dysenteriae* and differs only at a single amino acid whereas Stx2 shares less than 60% amino acid homology to Stx1 (Fraser *et al.*, 2004). Stx consists of five identical B subunits which bind the holotoxin to the glycolipid globotriaosylceramide (Gb3) on the target cell surface while a single A subunit cleaves ribosomal RNA and halts protein synthesis (Endo *et al.*, 1988). Stx can also induce apoptosis in intestinal epithelial cells (Jones *et al.*, 2000), cause local damage in the colon resulting in hemorrhagic colitis, necrosis and perforation of the intestine (Kaper *et al.*, 2004). EspP is a serine protease autotransporter (Figure 2.2), which contributes to biofilm formation by forming macroscopic rope-like polymers that are refractory to antibiotics and mediates adherence to host cells and cytopathic effects (Xicohtencatl-Cortes *et al.*, 2010; Brunder *et al.*, 1997). EspP can also cleave host coagulation factor V (Brunder *et al.*, 1997) and serpins from human plasma (Weiss *et al.*, 2014) which can result in prolonged hemorrhage and contribute to EHEC pathology.

Enterotoxigenic *E. coli* (ETEC)

This group of bacteria is one of the principal causes of acute "travelers' diarrhea", affecting tourists visiting low-income countries, and is predominant in areas with poor sanitation and inadequate clean water. ETEC strains adhere to the small intestinal mucosa with the help of one or more proteinaceous pili/fimbriae also called colonization factors (CFs) (Girón *et al.*, 1994). Following initial adhesion and colonization, they cause diarrhea not by invading the mucosa but by producing plasmid-encoded heat-labile (LT) and/ or heat-stable (ST) enterotoxin. LTs are closely related in structure and function to cholera enterotoxin produced by *Vibrio cholera* (Spangler, 1992). LTs increase host intracellular cAMP through activation of a cAMP-dependent kinase and activate the main chloride channel of epithelial cells resulting in increased chloride secretion from crypt cells. This ion imbalance causes loss of water from tissue and subsequent diarrhea (Nataro & Kaper, 1998). ETEC is also important veterinary pathogens associated with post-weaning diarrhea in both pigs and cattle, and STb toxin is involved in diarrhea (Khac *et al.*, 2006; Nataro & Kaper, 1998). ETEC also secrete EatA, a serine protease autotransporter of *Enterobacteriaceae* (SPATE) which can cleave substrates identified for cathepsin G (Patel *et al.*, 2004). EatA can also degrade the small intestinal mucus layer and then facilitate entry of ETEC enterotoxins into host enterocytes (Kumar *et al.*, 2014).

Enteroaggregative *E. coli* (EAEC)

EAEC is the cause of several diarrheal outbreaks worldwide. EAEC infection involves colonization of bacterial cells in dense clusters to the intestinal mucosa mediated by aggregative adherence fimbriae (AAF) (Czeczulin *et al.*, 1997; Nataro *et al.*, 1987). This is followed by secretion of EAEC heat-stable enterotoxin (EAST1) and ShET1 (*Shigella* enterotoxin 1) which cause loss of fluid into the intestinal lumen (Fasano *et al.*, 1997; Savarino *et al.*, 1996). EAEC also produces a plasmid-encoded SPATE autotransporter enterotoxin called Pet (Eslava *et al.*, 1998). Pet has enterotoxic activity and induces cytoskeleton changes and epithelial cell rounding due to the breakdown of fodrin/spectrin in host cells (Villaseca *et al.*, 2000). In addition, EAEC produces another SPATE with mucinase activity called Pic (Harrington *et al.*, 2009), which contribute to intestinal colonization by EAEC. Pic was also shown to reduce complement activation by cleaving complement cascade factors - C3, C4 and C2 (Abreu *et al.*, 2015), to also induce polymorphonuclear leucocyte/neutrophil (PMN) activation and programmed T-cell death (Ruiz-Perez *et al.*, 2011). In this context, Pic activity can contribute to immune evasion and promote EAEC virulence.

Enteroinvasive *E. coli* (EIEC)

EIEC is closely related to *Shigella* species. The colonic mucosa is the site of infection and the bacteria invade M cells. Pathogenesis includes a series of steps consisting of - enterocyte invasion, followed by the lysis of the endocytic vacuole, intracellular multiplication and movement to the cytoplasm of adjacent epithelial cells via actin (Nataro & Kaper, 1998). Pathogenesis is the cumulative result of several proteins like IpaA, IpaB, IpaC and IpgD, secreted by a plasmid-encoded type III secretion system (Menard *et al.*, 1993). Further, SepA is one of the major secreted enterotoxin proteins of EIEC strains (Nataro *et al.*, 1995). SepA is a SPATE protein that was shown to be important for the disruption of epithelial barrier integrity during infection to facilitate bacterial transit to adjacent epithelial cells (Maldonado-Contreras *et al.*, 2017).

Diffusely adherent *E. coli* (DAEC)

The DAEC pathotype causes persistent watery diarrhea and demonstrates a characteristic diffuse pattern of adherence (DA) to HEp-2 cells (Benz & Schmidt, 1992; Cookson & Nataro, 1996). DAEC infections are more prevalent among young children in both developing and developed countries (Baqui *et al.*, 1992). The DA adherence pattern is due to the production of adhesins encoded by a family of afa/dra/daa related operons (Bilge *et al.*, 1989; Labigne-Roussel *et al.*, 1984; Pham *et al.*, 1997). In addition, another member of the SPATE proteins, Sat, has been associated with Afa/Dr DAEC strains and was shown to promote lesions in the tight junctions of polarized epithelial Caco-2/TC7 cells (Guignot *et al.*, 2007). Also, Sat triggered pronounced fluid accumulation and villous necrosis in rabbit ileal tissue and morphological changes in Y1 adrenal cells (Taddei *et al.*, 2005).

2.1.2 Extraintestinal pathogenic *E. coli* (ExPEC)

Uropathogenic *E. coli* (UPEC)

Urinary tract infection is a very common bacterial infection, particularly in women, and UPEC strains account for up to 90% of urinary tract infections (UTIs) (Foxman, 2010). UPEC isolates exhibit a high degree of genetic diversity due to the presence of mobile DNA segments which are scattered around the chromosome known as pathogenicity islands (Dobrindt *et al.*, 2001; Rasko *et al.*, 2001). The key virulence factors harbored by UPEC strains are the production of type 1 fimbriae, P fimbriae, mannose-resistant adhesins, hemolysin, serum resistance, siderophore aerobactin and K1 capsule (Kaper *et al.*, 2004). Normally, UTI infection is initiated when uropathogenic *E. coli* originating from the bowel, is transferred to the urogenital region and

ascends towards the periurethral area. Colonization is facilitated by adhesins like Pap (P), type 1 and other fimbriae like S, M, and F1C which can mediate adherence to uroepithelial cells which is an important step in the development of UTI (Connell *et al.*, 1996; Kaper *et al.*, 2004; Wullt *et al.*, 2000). It has been shown that by virtue of type 1 fimbriae, *E. coli* can attach to mannose moieties that coat transitional epithelial cells (Choudhury *et al.*, 1999). Further, several toxins including hemolysin (Dhakal & Mulvey, 2012), a protease autotransporter called Sat (Guyer *et al.*, 2000), Pic (Navarro-Garcia *et al.*, 2010) and cytotoxic necrotizing factor (CNF-1) (Rippere-Lampe *et al.*, 2001) can contribute to the capacity to colonize the urinary tract. But, these virulence factors are not always present among different subgroups of UPEC (Johnson & Stell, 2000), suggesting that there can be multiple mechanisms of UPEC pathogenesis.

Urinary tract infection (UTI)

The urinary tract can be affected by a variety of diseases including microbial colonization of the urine and infection of the urinary tract tissues - kidney, renal pelvis, ureters, bladder and urethra. Clinically, urinary tract infection (UTI) has been categorized as uncomplicated or complicated. Uncomplicated UTIs occur in the normal urinary tract of immunocompetent individuals who are otherwise healthy (Smelov *et al.*, 2016). On the other hand, complicated UTIs are associated with individuals of all sexes and ages that are immunocompromised or have genitourinary structural or functional abnormalities, including urinary obstruction, urinary retention, renal failure, renal transplantation, pregnancy or catheterization (Foxman, 2014). For the typical microbes involved in uncomplicated UTIs, UPEC is followed by *Klebsiella pneumoniae, Staphylococcus saprophyticus, Enterococcus faecalis,* Group B *Streptococcus* (GBS), *Proteus mirabilis, Pseudomonas aeruginosa, Staphylococcus aureus* and *Candida* species. For complicated UTIs, there have been cases of polymicrobial infections. In addition to UPEC, *Enterococcus* spp., *Klebsiella pneumonia*, *Candida* spp., *Staphylococcus aureus*, *Proteus mirabilis, Pseudomonas aeruginosa* and GBS are common agents associated with complicated UTIs (Foxman, 2014).

UTI is characterized by the presence of bacteria and neutrophils in the urine which is known as bacteriuria (presence of uropathogens in urine with more than 10^5 CFU/ml) (Schmiemann *et al.*, 2010). Bacteriuria can be asymptomatic in the host and have adverse outcomes for pregnant women and people undergoing traumatic genitourinary procedures (Nicolle, 2003). UTI can manifest itself into cystitis (inflammation of the bladder) and acute pyelonephritis (kidney infection) (Figure 2.3). Cystitis is typically characterized by symptoms including frequency, burning sensation, urgency, pyuria (leukocytes in urine), dysuria, suprapubic pain and/or lower abdominal discomfort with cloudy urine. If left untreated, these infections can result in pyelonephritis which

is distinguished clinically from cystitis by the presence of flank pain, fever, and nausea (Grabe *et al.*, 2015). Antibiotics are given for the treatment of symptomatic UTI but up to 25% will suffer a recurrence of infection within 6 months following treatment of initial UTI (Foxman, 2014). Mounting evidence is showing that two-thirds of these recurrences are attributable to the identical initial strain recovered from a given patient suffering from uncomplicated UTIs (Brauner *et al.*, 1992; Ejrnæs, 2011; Ejrnaes *et al.*, 2006).

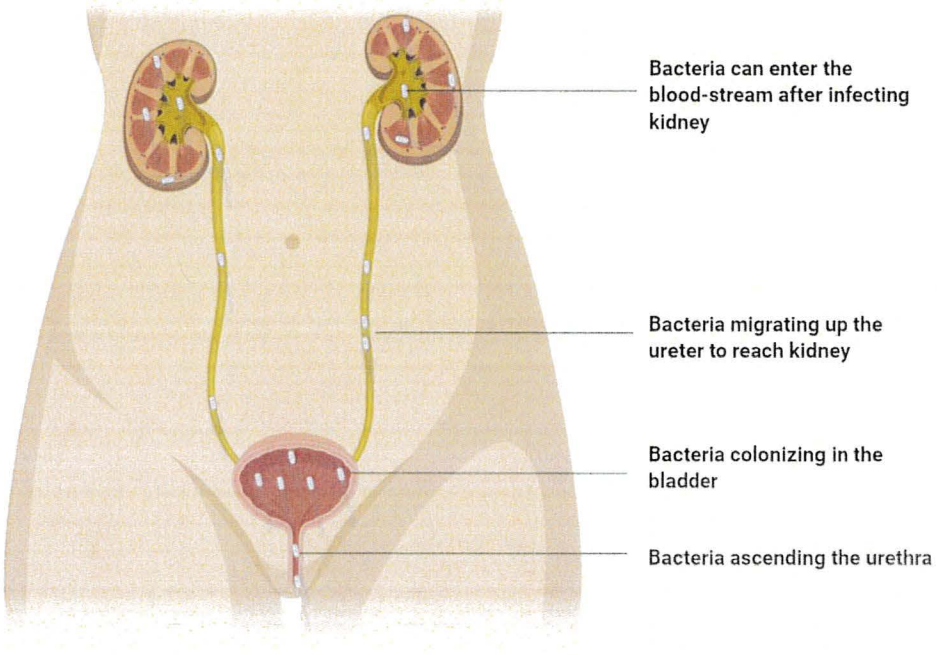

Figure 2.3 Different stages and types of urinary tract infection caused by UPEC

In ascending infection, bacteria colonize the urethra and ascend to the bladder leading to cystitis and sometimes subsequently to the kidneys resulting in pyelonephritis. Different virulence factors including adhesins (Type 1, P, S fimbriae, Dr adhesins), iron acquisition receptors (IreA, IroN), cytotoxic necrotizing factors, autotransporters (Sat, Pic), and hemolysin are involved in the infection.

Recurrent Urinary Tract Infection (rUTI)

A common problem in UTI is a recurrence. A recurrent urinary tract infection (UTI) is defined as a symptomatic UTI that relapses following an earlier episode, usually after appropriate medical treatment. This relapse could be due to the same organism found in the initial infection or by a second bacterial isolate (Hooton, 2001). rUTIs are observed in a quarter of women within 6 months of a UTI episode and in half of the women within one year of a UTI episode even after antimicrobial treatment and these women are healthy and generally have anatomically normal

urinary tracts (Foxman, 1990). The frequency of sexual intercourse is regarded as one of the strongest risk factors for recurrent UTIs in young women (Scholes *et al.*, 2000).

Epidemiology and economic burden

UTIs are among the most common bacterial infectious disease encountered in clinical practice and have a profound medical and socioeconomic impact. Uncomplicated UTIs in the USA result in more than 10 million medical visits and annual societal costs (health care costs and time missed from work) of these infections cost approximately 3 billion dollars in the USA alone (2005 estimates) (Brown *et al.*, 2005). It has been estimated that 1 in 3 women will have 1 UTI by the age of 24 years and 40% to 50% of women will experience at least 1 UTI during their lifetime (Foxman, 2014). A wide range of predisposing factors have been identified for UTI which includes genetic factors (ABO blood group antigens) (Hopkins *et al.*, 1998), biological factors (congenital abnormalities, urinary obstruction, prior history of UTI, diabetes) (Miyazaki & Ichikawa, 2003; Schneeberger *et al.*, 2014), behavioral factors (sexual activity, use of spermicide, condom, diaphragm) (Foxman *et al.*, 1997), bladder catheterization (Hooton *et al.*, 2010) and HIV infection (Schönwald *et al.*, 1999).

Uropathogenesis

The pathogenesis of UTI is complex and influenced by multiple host and microbial factors. Years of research and use of different animal and cellular models have elucidated some of the pathogenic mechanisms. The mechanisms of UPEC infection include adherence to host cells, motility, acquisition of essential metals and other micronutrients, toxin production and evasion of the host immune response.

Adherence of the pathogens to host cells plays a key initial step in colonization and subsequent disease progression. Uropathogens must adhere to or penetrate the mucosal barrier in order to persist. A UTI typically initiates by contamination of the periurethra by a uropathogen from intestinal sources, followed by bacterial colonization of the urethra and bladder through filamentous adhesins known as fimbriae (pili) (Connell *et al.*, 1996). For example, UPEC strain CFT073, a well-characterized reference strain, encodes 12 distinct fimbrial gene clusters which code for type 1, P, F1C, Dr, Auf fimbriae as well as their chaperone and usher proteins (Welch *et al.*, 2002). Type 1 fimbriae have been found essential for colonization, invasion, and persistence of UPEC in the mouse bladder. The FimH adhesin of type 1 fimbriae binds to mannosylated receptors and bladder cell surface known molecules such as uroplakins, $\alpha_3\beta_1$ integrins and the pattern recognition receptor TLR4 (Mossman *et al.*, 2008; Wu *et al.*, 1996; Zhou *et al.*, 2001).

However, a high molecular weight soluble protein named as Tamm-Horsfall protein (THP) is present in human urine to protect the bladder by competing for *E. coli* fimbriae and prevent from adhering to the urothelium (Bates Jr *et al.*, 2004; Pak *et al.*, 2001). The expression of type 1 fimbriae is phase variable and controlled by the orientation of an invertible element in the promoter region (Abraham *et al.*, 1985; Bjarke Olsen & Klemm, 1994).

E. coli expresses another fimbriae known as P fimbriae which have been associated with acute pyelonephritis in humans and showed a subtle role for pathogenesis in the murine model (Lane & Mobley, 2007; Wullt *et al.*, 2000). P fimbriae, specifically mediated by the PapG adhesin protein, bind specifically to glycosphingolipids containing digalactoside moieties found in renal epithelium and also the P blood group antigen which is on the surface of some host erythrocytes (Lund *et al.*, 1987). So, the human population lacking the receptor for P fimbriae may be less susceptible to P-fimbriae-mediated adherence during UTIs caused by UPEC.

Type 1 fimbriae binding to epithelial cells trigger a signal transduction cascade that activates the Rho family of GTP binding proteins, resulting in cytoskeleton rearrangements in host cells and internalization of UPEC by a zippering mechanism in which the plasma membrane engulfs the bacterium (Martinez *et al.*, 2000). This invasion actually benefits bacteria since the intracellular location shelters UPEC from host defenses, may reduce access to antibiotics, and prevent clearance from micturation. Although intracellular UPEC can evade host defenses, expulsion of UPEC in urothelial cells does occur by innate immune defense through lipopolysaccharide (LPS) mediated activation of TLR4 and expulsion of bacteria from epithelial cells (Song *et al.*, 2009). However, a minority of internalized UPEC can escape into the epithelial cell cytoplasm and subvert expulsion and rapidly replicate exponentially in coccoid form, forming an amorphous biofilm-like intracellular bacterial community (IBC) which can cause superficial cells to protrude (Anderson *et al.*, 2003). Later, maturation of IBCs can lead to bacterial dispersion and the cycle of invasion of other urothelial cells (Justice *et al.*, 2004). Alternatively, UPEC can establish quiescent intracellular reservoir (QIRs) in the underlying bladder cells which can later serve as seeds for UPEC revival, releasing bacteria back into the bladder lumen (Mulvey *et al.*, 2001; Mysorekar & Hultgren, 2006). Due to this phenomenon, the source of recurrent infections can be due to recurrent intestinal source contamination, vaginal colonization, or reinfection by latent bacteria within the urinary tract.

Other virulence determinants of some UPEC include three different types of toxins: 1. Hemolysin, 2. Cytotoxic necrotizing factor 1 (CNF1), and 3. Autotransporter proteins. α Hemolysin (HlyA), encoded by the *hlyCABD* operon, oligomerizes and inserts into the cholesterol-rich microdomain

in the host cell membrane in a Ca^{+2} dependent manner (Koschinski *et al.*, 2006). Hemolysin is implicated in pore formation in bladder cells and promotes their lysis and facilitates iron and nutrient acquisition (Dhakal & Mulvey, 2012). Further, it can trigger cell exfoliation, apoptosis, and cytokine production and induce an inflammatory response (Dhakal & Mulvey, 2012; Russo *et al.*, 2005; Smith *et al.*, 2008). CNF1 secreted by some UPEC strains affects actin remodeling and membrane ruffling, which leads to the internalization of UPEC in the host cell through the activation of the members of the Rho family of GTP binding proteins: Rac1, RhoA and CDC42 (Visvikis *et al.*, 2011) and may also play a role in bladder cell exfoliation (Mills *et al.*, 2000). In addition, activation of Rac1 and GTP induces the anti-apoptotic pathway, preventing apoptosis of the colonized uroepithelium and prolonging UPEC survival (Miraglia *et al.*, 2007). Further, another family of toxins – members of the serine protease autotransporters of *Enterobacteriaceae* (SPATEs) including Sat, Pic and Vat have been characterized in UPEC. Sat (secreted autotransporter protein) can cause different effects on biological functions such as cytotoxicity on bladder and kidney cell lines *in vitro* (Guyer *et al.*, 2000); elongation of kidney cells with apparent impairment of cellular junction (Guyer *et al.*, 2002); degradation of fodrin and human coagulation factor V (Dutta *et al.*, 2002); and induction of autophagic cell detachment (Liévin-Le Moal *et al.*, 2011). Another SPATE known as Pic having mucinase function and also the cytotoxin Vat (mistakenly annotated as Tsh) have been expressed during UT infection in mice (Heimer *et al.*, 2004; Parham *et al.*, 2004; Restieri *et al.*, 2007).

To survive and compete in many diverse environmental niches, UPEC has also evolved multiple means of obtaining essential metals, such as iron. The most diverse and broadly distributed iron uptake mechanism used by microorganisms are siderophore acquisition systems. Siderophores are the small organic chelating compounds having a molecular weight between 150 and 2000 Da with a very high affinity for iron (Jones *et al.*, 1980). The direct way to capture host iron is either from free heme or from heme-containing proteins, such as hemoglobin. The presence of heme uptake systems in UPEC helps them to acquire a readily available iron source *in vivo,* heme. Iron binding receptors Hma and ChuA bind to the heme and the coordinated molecule is transported into the periplasm (Hagan & Mobley, 2009); ChuT mediates further transfer to the cytoplasm through an ATP- binding cassette (ABC) transporter (Stojiljkovic & Perkins-Balding, 2002). In addition, UPEC can purloin host iron through high-affinity siderophores including salmochelins, C-glycosylated derivatives of enterobactin, and other siderophores, such as aerobactin, and yersiniabactin (Henderson *et al.*, 2009). Salmochelins are encoded by the *iroBCDEN* gene cluster. This siderophore contributes to the virulence of extraintestinal pathogenic *E. coli* strains by escaping the action of Lipocalin-2 isolated from neonatal meningitis, UTIs, prostatitis and

APEC isolates (Raffatellu *et al.*, 2009). Aerobactin is highly expressed and stable at low pH and displays a higher affinity than enterobactin (Valdebenito *et al.*, 2006). Interestingly, yersiniabactin has been found to also contribute to UPEC resistance to copper toxicity in urine (Chaturvedi *et al.*, 2012). Like iron, zinc is also an essential element for bacterial growth. The high-affinity zinc transport system ZnuACB has been expressed during UTI to acquire zinc in the host (Sabri *et al.*, 2009). Polysaccharidic capsules and serum resistance are also important traits associated with UPEC strains especially those which can infect the kidney and develop into more systemic infection and septicemia (Cross *et al.*, 1986). Antiphagocytic capsules can reduce the uptake of bacteria by host phagocytes and promote dissemination in blood and extra-intestinal tissues.

Intracellular Bacterial Communities

Uropathogenic *E. coli* can sometimes develop into intracellular bacterial communities (IBCs) (Figure 2.4) and Quiescent Intracellular Reservoirs (QIRs) (Kerrn *et al.*, 2005; Mulvey *et al.*, 2001). IBCs have been noted for their resistance to host immune clearing and quiescent intracellular reservoirs composed of small rosettes of bacteria within Lamp-1–positive endocytic vesicles that can persist for several weeks protected from antibiotics and can be considered another potential source of infection (Mysorekar & Hultgren, 2006). Invasion of urothelium by UPEC can be dependent or independent of Type 1 fimbriae-mediated uroplakin binding to cells that trigger a signal transduction cascade that activates the Rho family of GTP binding proteins. This results in cytoskeleton rearrangements in host cells and internalization of UPEC by a zippering mechanism in which the plasma membrane engulfs the bacterium (Martinez *et al.*, 2000). After IBC development, bacteria can be released from the facet cells but can have altered cell morphology, as peripheral bacteria of IBC include motile rod-shaped bacteria and some other bacterial cells are in a filamentous state (Mulvey *et al.*, 2001). Bacteria released from host cells are capable of restarting the IBC development cascade in neighboring cells to generate new IBC intracellular populations; and in the case of exfoliation of urothelial cells, the released bacteria can invade the underlying transitional urothelial cells (Justice *et al.*, 2004). This phenomenon supports the potential for recurrence of UTI by the same strain without a need for recurring exogenous source contamination.

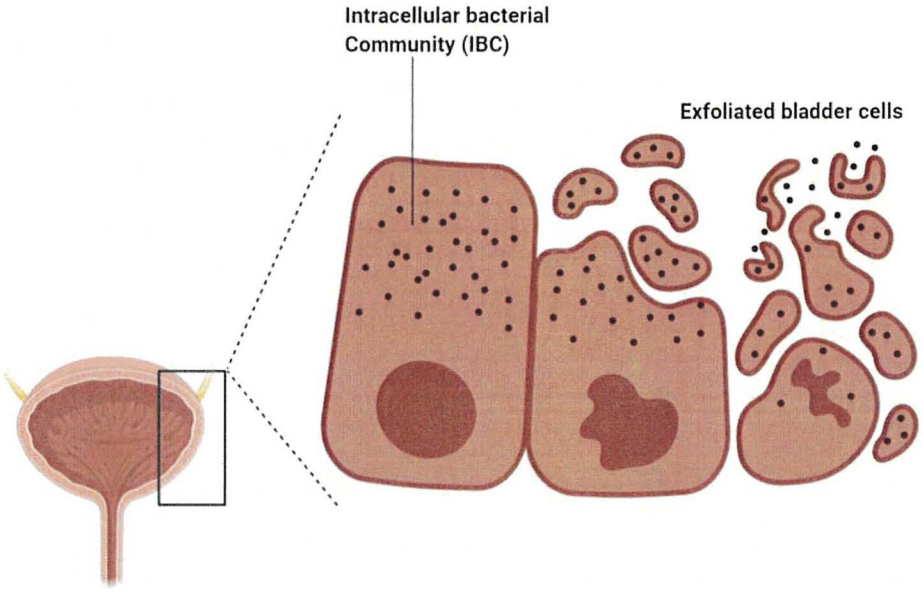

Figure 2.4 Intracellular Bacterial Communities (IBCs)

Transitional epithelium is found lining the urinary bladder. UPEC express adhesive structures known as type 1 fimbriae containing the FimH adhesin that mediates binding to mannosylated uroplakins and integrins that coat the surface of umbrella cells. Uroplakin binding by FimH induces actin rearrangement and bacterial internalization and multiplies inside the cytoplasm to form biofilm-like IBCs. Upon infection, the host triggers exfoliation and expels epithelial cells into the urine. The bacteria can flux out of their intracellular niche and can infect neighboring cells to start a new IBC cycle. Adapted from (Kaper *et al.*, 2004).

Host Inflammatory Response to UPEC

UPEC attachment to the uroepithelium is first inhibited by mechanical and physical stresses including the flow of urine, the mucociliary escalator, low pH, high osmolarity, and exposure to antimicrobial peptides like β defensin-1 and cathelicidin LL-37 (Becknell *et al.*, 2013; Chromek *et al.*, 2006). A number of soluble factors are produced by the host to limit bacteria from binding to urothelial receptors or to impede colonization such as lactoferrin, transferrin, and lipocalin-2 which are produced by the host to sequester iron and limit iron availability, and the mannosylated uromodulin (Tamm-Horsfall protein) that binds to type 1 fimbriae of UPEC to limit adherence to bladder epithelium (Pak *et al.*, 2001).

Furthermore, UPEC infection activates the innate immune response. UPEC components like LPS and fimbriae, ligate Toll-like receptor (mainly TLR4) on host epithelium (Bäckhed *et al.*, 2001) and elicit localized production of proinflammatory cytokines (IL-1, IL-6, IL-8) (Spencer *et al.*, 2014). TLR4 is important for clearance and the inflammatory response in the bladder and in the kidney,

as TLR4 knockout mice infected with UPEC have higher bacterial burdens (Ashkar *et al.*, 2008). TLR4 signaling is also induced by P - fimbriae through LPS-independent (Frendéus *et al.*, 2001) or LPS and type-1 fimbriae dependent pathways (Hedlund *et al.*, 2001). However, UPEC can also attenuate innate responses to epithelial infection by blocking the activation of the NF-κB pathway (Klumpp *et al.*, 2001).

Information regarding the adaptive immune response to UTI is limited. There has been some evidence of the antibody-mediated clearance of *E. coli* (Thumbikat *et al.*, 2006). They found $CD4^+$ and $CD8^+$ cells were infiltrated into the bladder and the CD69 activation marker was expressed in the spleen as well as serum antibodies from previously infected donor mice protected the wild-type naive recipient mice against UPEC challenge (Thumbikat *et al.*, 2006).

Meningitis/sepsis-associated *Escherichia coli* (MNEC)

This pathotype is associated with cases of meningitis particularly in neonates (Dietzman *et al.*, 1974). It has been found that 80% of isolates from neonatal meningitis harbor antiphagocytic K1 capsular polysaccharide (Kim *et al.*, 1992; Robbins *et al.*, 1974) and most of these K1 isolates are present in the serogroups like O18, O7, O16, O1, and O45 (Bonacorsi *et al.*, 2003; Sarff *et al.*). Inflammation of the meninges by MNEC comprises various stages of infection - the first translocation of bacteria into the circulatory system and upon reaching a threshold of greater than 10^3 CFU/ml in the blood, MNEC can breach the blood-brain barrier (BBB). The meninges which form a structural and functional blood-brain barrier are composed of endothelial cells called brain microvascular endothelial cells (BMECs). MNEC express adhesins - S fimbrial adhesins involved in BMEC binding with NeuAc α2,3-galactose receptor (Prasadarao *et al.*, 1993), type 1 fimbriae and OmpA (Khan *et al.*, 2003; Teng *et al.*, 2005), which contribute to adherence and invasion of brain endothelial cells. Furthermore, an outer membrane protein NlpI can also mediate binding/invasion of MNEC to brain endothelial cells (Teng *et al.*, 2010). The toxin CNF1 through activation of the RhoA pathway may also contribute to MNEC invasion of BMECs *in vitro* and penetration into the brain *in vivo* (Khan *et al.*, 2002). IbeA has also been associated with the invasion of BMEC (Huang *et al.*, 2001). In addition to the role of IbeA in invasion and in the crossing of BBB, it has been linked to an effect on the level of expression of type 1 fimbriae (Cortes *et al.*, 2008) and hence could play a role in the endothelial cell colonization. Further, IbeA contributed to oxidative stress resistance (Fléchard *et al.*, 2012) and therefore could play a role in the protection of bacteria against the H_2O_2 stress exposure response by the host immune system. The K1 polysaccharide capsule can contribute to serum resistance, antiphagocytic

properties and intracellular survival within vacuoles (Cross *et al.*, 1986; Kim *et al.*, 2003) and as such an important virulence factor of MNEC strains.

Avian Pathogenic *Escherichia coli* (APEC)

Avian colibacillosis is a major bacterial infectious disease in the poultry industry worldwide. So, APEC is regarded as the major cause of morbidity and mortality in chickens of all ages, as a primary or secondary pathogen in localized or systemic infection which results in heavy economic losses to the poultry industry (Saif *et al.*, 2003). APEC also infects other avian species including turkeys and ducks (Emery *et al.*, 1992; Olsen *et al.*, 2011; Wei *et al.*, 2013). A variety of disease types have been observed: including yolk sac infection, omphalitis, swollen head syndrome, respiratory tract infection, septicemia, enteritis, and cellulitis. Colibacillosis in chickens results in death by septicemia in acute infection whereas subacute infections can result in pericarditis, airsacculitis and perihepatitis (Norton *et al.*, 2000). APEC strains commonly belong to three serogroups, O1, O2, and O78 although many different serogroups have been identified in APEC and O1, O2, and O78 are not always predominant in certain studies (Ewers *et al.*, 2004). Several virulence factors have been associated with APEC strains. These include fimbrial adhesins (type 1 fimbriae (La Ragione *et al.*, 2000), P fimbriae (Kariyawasam & Nolan, 2009), and Stg fimbriae (Lymberopoulos *et al.*, 2006), curli (La Ragione *et al.*, 2000), Yqi (Antão *et al.*, 2009), outer membrane proteins and other surface molecules contributing to serum resistance or antiphagocytic properties (Increased serum survival (Iss) (Foley *et al.*, 2000; Nolan *et al.*, 2003), two-component signal transduction systems (RstA/RstB (Gao *et al.*, 2015b), PhoB/PhoR (Bertrand *et al.*, 2010), BarA/UvrY (Herren *et al.*, 2006)), O78 lipopolysaccharide (Mellata *et al.*, 2010), and K1 (Mellata *et al.*, 2003)), iron and metal acquisition systems (aerobactin (Gao *et al.*, 2015a), salmochelin (Caza *et al.*, 2008), yersiniabactin (Li *et al.*, 2011), heme utilization/transport protein ChuA (Gao *et al.*, 2012) and the Sit iron acquisition locus) (Sabri *et al.*, 2008)), autotransporters (Tsh, Vat, AatA (Li *et al.*, 2010; Dozois *et al.*, 2000; Parreira & Gyles, 2003)), metabolism (the phosphate transport system (Lamarche *et al.*, 2005), sugar metabolism (Chouikha *et al.*, 2006), and nitrite transporter NirC (de Paiva *et al.*, 2015)). Specific virulence genes including *iss*, *iroN*, *ompT, iutA* and *hlyF* are commonly present in APEC and are frequently encoded on large plasmids such as Colicin V (ColV) plasmids (Johnson *et al.*, 2006). In addition, other factors such as IbeA, and type VI secretion system, which are known to affect expression of type I fimbriae, are involved in colonization of the respiratory tract (Germon *et al.*, 2005). However, no single common virulence factor has been identified in all strains.

Avian Colibacillosis

E. coli is an intestinal commensal of poultry, but some of these fecal isolates when inhaled by poultry can colonize the respiratory tract and then cause colibacillosis which can include respiratory infection as well as systemic fatal disease (Dho-Moulin & Fairbrother, 1999). Isolates of serotypes O78: K80, O1: K1 and O2: K1 are prevalent among *E. coli* causing infection of extraintestinal tissues in chicken, turkey and ducks (Dozois *et al.*, 1992; McPeake *et al.*, 2005; Wang *et al.*, 2010), although many other serotypes are associated with APEC infections.

Colonization in the trachea and the air sacs is considered the first step of systemic infection for APEC (Figure 2.5). Airsacculitis is a common type of infection in poultry of all ages. In addition to the aerogenic route, various other infection routes have been described: neonatal infections, infections through dermal lesions, infection of the reproductive organs. Once in the blood, APEC can then disseminate to the liver and pericardium, and the infection may also lead to bacteremia and septicemia (Dho-Moulin & Fairbrother, 1999). A laying hen having *E. coli* induced salpingitis can have an infected egg before shell formation or fecal contamination of eggshell is possible when the egg passes through the cloaca (Saif *et al.*, 2003). This can lead to a high mortality rate among young chicks during the first few days or weeks after hatching by APEC which can cause yolk sac infection and embryo mortality (Saif *et al.*, 2003).

Adhesins such as fimbriae, Stg, Tsh, Yqi can contribute to APEC colonization of the respiratory tract: the trachea and the lungs (Dozois *et al.*, 2000). Carbohydrate metabolism may also contribute to the colonization of the lung or air sacs (Chouikha *et al.*, 2006). In order to disseminate in the bloodstream, bacteria need to translocate through the lungs and air sac interstitium. K1 capsule was shown to facilitate the translocation of APEC into the blood vascular system (Ewers *et al.*, 2004; McPeake *et al.*, 2005). When APEC disseminate in the blood, they encounter avian innate immune defenses and nutrient limitation. In this context, siderophores like aerobactin and salmochelins, the ChuA heme uptake and Sit metal transporter help to sequester iron and other metals from the host environment (Caza *et al.*, 2008). In addition, protectin structures which help to evade the host immune system like K1 capsule, Iss, Type III secretion system, and specific O antigens such as O78 can contribute to survival and virulence through resistance of the avian immune response and the serum complement system (Mellata *et al.*, 2003).

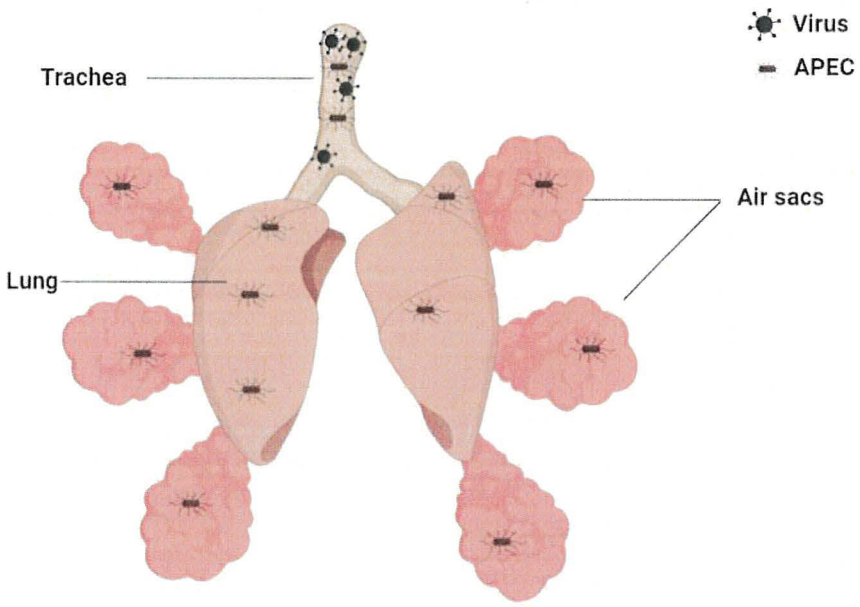

Figure 2.5 Colonization in the trachea and air sac is the first step in systemic infection of APEC

APEC can reach trachea by inhalation of contaminated aerosol particles. APEC infection in the upper respiratory tract is sometimes followed by a primary mycoplasmal or viral infection. Once inside the lung and airsac of poultry, APEC can enter the blood and internal organs leading to the development of airsacculitis, pericarditis, perihepatitis and salpingitis.

2.1.3 Functional overlap of virulence factors of extraintestinal pathogenic *E. coli*

When considering the virulence factors identified with ExPEC from different host species or tissues it is clear that there are certain commonalities. Virulence factors of ExPEC can be grouped into the following major classes: adhesins, iron/metal acquisition, structures to prevent phagocytosis or serum resistance and toxins (Table 2.1). It is interesting that many ExPEC strains share the same virulence factors, and this suggests that such systems may provide a broad-host-range infection capacity. However, despite the presence of some commonly shared virulence traits, there is considerable genetic diversity among ExPEC, and it is likely that certain groups of strains have distinct means of causing infection in different hosts. Due to overlap in serogroups, phylogenetic groups and virulence attributes APEC strains are also associated with extraintestinal infections, such as UTIs or neonatal meningitis in humans (Bélanger *et al.*, 2011; Danzeisen *et al.*, 2013; Rodriguez-Siek *et al.*, 2005). From this standpoint, APEC has been described to also represent a zoonotic/food-borne risk for human infections. This possibility seems further substantiated by analyses of genomes of different APEC and human ExPEC strains which were shown to share many common features (Brzuszkiewicz *et al.*, 2006; Xie *et al.*, 2006). Further, in rodent models, APEC strains have also been shown to cause UTI in mice (Jakobsen *et al.*, 2010)

or neonatal meningitis in rat pups (Tivendale *et al.*, 2010). Conversely, some human ExPEC strains were also found to be virulent in chickens (Moulin-Schouleur *et al.*, 2007). Despite the potential for cross-species infection by ExPEC, more epidemiological evidence concerning transmission events of ExPEC is needed to more strongly support whether or not *E. coli* from food animals particularly poultry may be a source for ExPEC infections such UTIs or neonatal meningitis in humans.

Table 2.1 Some examples of virulence factors that have been identified from ExPEC in humans and APEC from poultry

Virulence factors	Genes	Actions	ExPEC pathotype
Adhesins			
Type 1 fimbriae	*fim*	Initial colonization in the site of infection (Connell *et al.*, 1996; Teng *et al.*, 2005)	UPEC, APEC, MNEC
Afimbrial adhesion	*afa*	Responsible for P-blood group independent mannose-resistant hemagglutination and epithelial adhesion (Labigne-Roussel *et al.*, 1984)	UPEC
P fimbriae	*pap*	Adhesin (Wullt *et al.*, 2000), induces cytokine expression (Hedlund *et al.*, 1999)	UPEC, APEC, MNEC
Dr fimbriae	*dra*	Mediates the recognition of DAF (decay-accelerating factor) receptors in kidney (Goluszko *et al.*, 1997)	UPEC
S fimbriae	*sfa*	Adhesion to kidney and bladder epithelium (Korhonen *et al.*, 1984; Korhonen *et al.*, 1986)	UPEC, MNEC
F1C fimbriae	*foc*	Adhesion to renal epithelial cells (Backhed *et al.*, 2002)	UPEC

Curli	*crl, csg*	Biofilm formation and adhesion to chicken trachea (La Ragione *et al.*, 2000; Nhu *et al.*, 2018)	UPEC, APEC
Mat	*mat*	Temperature regulated fimbriae involved in biofilm formation (Lehti *et al.*, 2010)	MNEC
Antigen 43	*flu*	Adhesion and biofilm development (Zalewska-Pia *et al.*, 2015)	UPEC
Iha	*iha*	IrgA homologue adhesion (Johnson *et al.*, 2005a)	UPEC
Temperature sensitive haemagglutinin (Tsh)	*tsh*	Adhesion to chicken erythrocytes (Kostakioti & Stathopoulos, 2004)	APEC
UPEC trimeric autotransporter adhesin	*upa*	Adhesion to human bladder epithelial cells (Valle *et al.*, 2008)	UPEC
Iron acquisition system			
Salmochelin	*iroN*	Siderophore receptor (Hantke *et al.*, 2003)	UPEC, APEC, MNEC
Aerobactin	*iuc, aer*	Siderophore (Gao *et al.*, 2012)	UPEC, APEC
Iron repressible protein	*irp2*	Synthesis of yersiniabactin (Chaturvedi *et al.*, 2012)	UPEC, MNEC
ChuA, Hma	*chuA, hma*	Iron uptake from heme (Garénaux *et al.*, 2011)	UPEC, MNEC
SitABC	*sitA, B, C*	Mn, Fe transport (Sabri *et al.*, 2008)	UPEC, APEC

Protectins/Serum resistance/Invasins			
Capsule	*KpsMI-neuA, KpsMII*	Protection from phagocytosis (Kim *et al.*, 1992)	MNEC
Transfer protein	*traT*	Evade complement activity (Moll *et al.*, 1980)	APEC, MNEC
Outer membrane protein	*omp*	Resistance to complement (Chaffer *et al.*, 1999)	UPEC, MNEC, APEC
Increased serum survival	*iss*	Protection from phagocytosis (Foley *et al.*, 2000)	UPEC, MNEC, APEC
ColV	*cvaC*	Facilitate colonization (Yang & Konisky, 1984)	UPEC, MNEC, APEC
IbeA	*ibeA*	Spread into and through brain endothelium, expression of type-1 fimbriae (Germon *et al.*, 2005; Huang *et al.*, 2001)	MNEC, APEC
Toxins			
Pic	*pic*	Mucinase, hemagglutination, cleavage of O glycans (Heimer *et al.*, 2004; Parham *et al.*, 2004)	UPEC
Sat	*sat*	Vacuolating cytotoxin (Guyer *et al.*, 2002)	UPEC
Vat	*vat*	Vacuolating cytotoxin (Parreira & Gyles, 2003)	APEC, UPEC
Hemolysin	*hlyA*	Pore forming toxin (Dhakal & Mulvey, 2012)	UPEC
Cytotoxic necrotizing factor	*cnf*	Responsible for apoptosis and modification of dynamic of actin cytoskeleton (Khan *et al.*, 2003; Mills *et al.*, 2000)	UPEC, MNEC

Cytolethal distending toxin	*cdt*	Inhibits G2/M cell cycle (Tóth *et al.*, 2003)	UPEC, MNEC

Among the above-mentioned virulence factors of ExPEC, this thesis is focused only on the study of some of the new members of SPATEs (serine protease autotransporters of *Enterobacteriaceae*). SPATEs are secreted proteins that contribute to virulence and function as proteases, toxins, adhesins, and/or immunomodulators (Dutta *et al.*, 2002). The availability of the complete genome sequence of APEC O1:K1 strain QT598, isolated from a 4-day-old turkey has drawn our attention to a number of predicted virulence genes having unknown functions. APEC O1 was the strain of choice because it contained traits of both APEC and UPEC (Rodriguez-Siek *et al.*, 2005). *In silico* studies found that QT598 has the potential to produce a total of 5 serine protease autotransporters (SPATEs). Three of these, two chromosomally encoded SPATE genes (we named *tagB* and *tagC)* and a novel plasmid-encoded SPATE gene *(sha*) have not been previously characterized. The remaining two SPATEs were the previously characterized Vat and Tsh proteins. In addition, these new autotransporter genes are present in some APEC and some human uropathogenic *E. coli* (UPEC) strains. Hence, we hypothesize that these SPATEs could play an important role in colonization and dissemination of the bacteria inside the host. Given that, ATs are found in UPEC strains, we hypothesize that not only these systems can play a role in the development of colibacillosis but may also contribute to other extra-intestinal infections such as urinary tract infections. The possible function and roles of these new SPATES in the pathogenesis of extraintestinal pathogenic *E. coli* were investigated, including hemagglutination, autoaggregation, biofilm and cytotoxicity when expressed in *E. coli* K-12. Before going into the findings of these new SPATEs, understanding the biology of SPATEs is necessary. In the following chapter, different aspects of SPATEs – secretion pathways, biological activities of its members and its regulation are discussed.

3 REVIEW ARTICLE ON SPATES

Serine Protease Autotransporters of the *Enterobacteriaceae* (SPATEs): Out and about and chopping it up

Authors: Pravil Pokharel[1,2#], Hajer Habouria[1,2#], Hicham Bessaiah[1,2], and Charles M. Dozois[1,2,3]

[1] Institut national de recherche scientifique (INRS) - Centre Armand-Frappier Santé Biotechnologie, Laval, Quebec, Canada
[2] Centre de recherche en infectiologie porcine et avicole (CRIPA), Saint-Hyacinthe, Quebec, Canada
[3] Institut Pasteur International Network

[#] These two authors contributed equally as primary authors of this research

Title of Journal: Microorganisms

2019, *7*(12), 594| **Received:** 25 October 2019 / **Accepted:** 13 November 2019 / **Published:** 21 November 2019

DOI **https://doi.org/10.3390/microorganisms7120594**

Contribution of authors:

The concept was formulated by **P.P.** and **H.H.** and supervised by **C.M.D.** The manuscript covering the section of Introduction, The Autotransporter secretion pathway, SPATEs and the details of EspC, EspP, Pic/PicU, EatA, Pet, EaaA, TagBC and Sha was written by **P.P.** Immunogold staining of *E. coli* BL21 expressing Sha was performed by **P.P.** Figure 1, 3 and 4 was made by **P.P.** while Figure 2 was made by **H.H.** Sections of Tsh/Hbp, Vat, Sat, SepA, SigA, Boa and Regulation of expression of SPATEs was written by **H.H.** The manuscript was reviewed and edited by **P.P., H.H., H.B., and C.M.D.** Funding acquired by **C.M.D.**

3.1 Abstract

Autotransporters are secreted proteins with multiple functions produced by a variety of Gram-negative bacteria. In *Enterobacteriaceae*, a subgroup of these autotransporters is the SPATEs (Serine Protease Autotransporters of *Enterobacteriaceae*). SPATEs play a crucial role in survival and virulence of pathogens such as *Escherichia coli* and *Shigella* spp. and contribute to intestinal and extra-intestinal infections. These high molecular weight proteases are transported to the external milieu by the type Va secretion system and function as proteases with diverse substrate specificities and biological functions including adherence, mucosal colonization, immune modulation and cytotoxicity. Herein, we overview SPATEs and discuss recent findings on the biological roles of these secreted proteins including proteolysis of substrates, adherence to cells, modulation of the immune response, and virulence in host models. In closing, we highlight recent insights into the regulation of expression of SPATEs that could be exploited to understand fundamental SPATE biology.

3.2 Introduction

Bacteria have acquired a capacity to export and secrete proteins and other molecules to the cell surface in order to interact with the extracellular environment. The transport of proteins to the cell surface is achieved through several highly specialized protein secretion systems that release them into the extracellular milieu. In Gram-negative bacteria, which have an inner and outer membrane that contains a periplasmic space, secretion can be a two-step process involving export to the periplasmic space, and in some cases subsequent secretion through the outer membrane. Autotransporter (AT) proteins comprise a large family with more than 1000 members that have been characterized [1]. AT proteins represent the largest family of secreted polypeptides in Gram-negative bacteria and Serine Protease Autotransporters of *Enterobacteriaceae* (SPATEs) are a subclass of AT proteins that contain a protease domain belonging to the trypsin-like family which typically contains a serine in the catalytic motif [1]. In recent years, considerable information has been obtained about how these proteins are assembled and secreted. Here, we review the latest findings on the AT secretion system with a recent model for transporting SPATE cargo out of the bacterial cell and in-depth updates of members of SPATEs including studies on genomic distribution, gene regulation, classification, and fate of the protein during *in vitro* or *in vivo* host interaction.

3.2.1 The Autotransporter Secretion Pathway

AT secretion through the outer membrane is mediated by the type V secretion system (T5SS) or AT secretion pathway. The T5SS pathway has been subdivided into five subtypes: (i) T5SS of monomeric ATs is classed as type Va secretion (ii) two-partner secretion is classed as type Vb secretion (iii) trimeric AT secretion is classed as type Vc secretion [2], (iv) secretion of ATs homologous to both type Va and type Vb is described as type Vd [3], and (v) secretion of intimins and invasins is classed as subtype Ve [4]. SPATEs are monomeric ATs that are secreted by the type Va secretion pathway.

The figure below depicts the major differences between these subtypes which include the variations in alignments of different domains (Figure 3.1). In type Va ATs, release of the N-terminal passenger domain is assisted by a C-terminal translocation domain or auto processed and liberated into the external milieu (explained in detail below) [1]. Type Vb, is a split variant of the type Va system as the passenger domain and translocation domain are located in different polypeptide chains, and the translocated domain contains periplasmic polypeptide transport associated (POTRA) motifs. As such, the type Vb class has also been described as a two-partner

secretion system [5]. The type Vc class are also called trimeric autotransporter adhesins because they have ATs proteins arranged in trimeric forms [2]. Type Vd ATs differ from type Va due to the presence of additional periplasmic domains between the passenger domain and the translocation domain, which is homologous to the periplasmic domains present in type Vb proteins [3]. Likewise, in type Ve ATs , the domains have a reverse order, wherein the passenger domain is at the C-terminal and translocation domain is N-terminal [4].

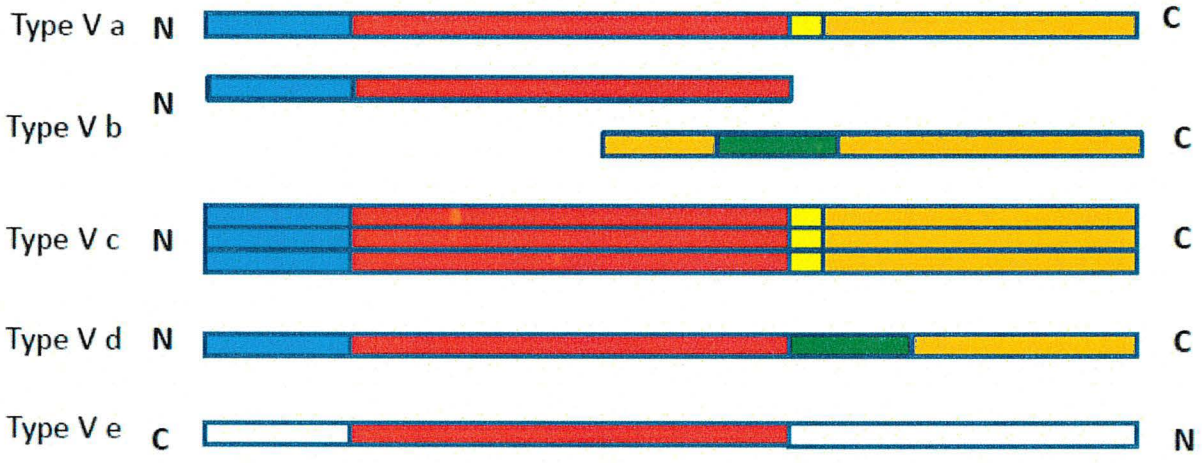

Figure 3.1 Scheme presenting domain organization among the subclasses of type V bacterial autotransporter proteins

The labeling includes the conserved domains, colored blocks correspond to: Signal peptide (blue), passenger domain (red), POTRA domain (green), linker domain (yellow) and translocation domain (orange). Adapted from [1, 4].

Understanding the biogenesis of the SPATEs is of great interest for the isolation, purification, and characterization of these proteins. Over the last two decades, a diversity of predicted AT proteins including SPATES, has been identified through the sequencing of many bacterial genomes and through bioinformatics analysis. However, there is a paucity of information regarding to their biological functions and structural characterization. The crystal structure of the passenger domain of three SPATEs has been determined: EspP from an *Escherichia coli* O157:H7 strain [6], Hbp (also called Tsh) from an extra-intestinal pathogenic *E. coli* (ExPEC) strain [7] and Pet from enteroaggregative *E. coli* (EAEC) strains [8]. Based upon these crystal structures, general models of structure and translocation have been proposed, although, whether such models derived from only a few SPATE structures collectively represent all other SPATEs remains to be determined.

The general structure of AT proteins, including SPATES, comprises three functional domains: the signal peptide, which mediates the Sec-dependent transport of the protein into the periplasm; the N-terminal passenger domain (also called the α-domain), which is the mature protein that is

exposed at the surface of the outer membrane and/or released extracellularly; and the pore-forming carboxyl-terminal translocator domain (also called as β-barrel), which provides the channel through which the passenger domain is translocated to the surface of the outer membrane [9]. Initial proposals of ATs as autonomously secreted proteins have been rejected due to recent findings indicating a role for accessory proteins located in the inner membrane [10], the periplasm [11] and the outer membrane [10] which facilitate or mediate translocation of AT proteins to the cell surface.

ATs are exported into the periplasmic space through the Sec-dependent pathway [1], and export can occur co-translationally or follow autotransporter synthesis into the cytoplasm [12]. Immediate export following translation could improve export by preventing nonproductive interaction like misfolding, aggregation and degradation of nascent protein in the cytoplasm. Upon reaching the periplasm via the Sec-translocon and cleavage of the signal sequence, AT proteins are then protected by conserved periplasmic chaperones such as Skp, SurA, and DegP and directed toward the β-barrel assembly machinery (Bam) complex which catalyzes the insertion and assembly of the outer membrane protein (Figure 3.2) [13, 14]. A "Hybrid barrel-model" (Figure 3.2) has been proposed to explain the translocation of the passenger domain through the outer membrane. It has been shown that passenger domain secretion does not appear to use ATP, but that vectorial folding of the C-terminal of the passenger domain may contribute the necessary energy required for transmembrane passage and folding [15].

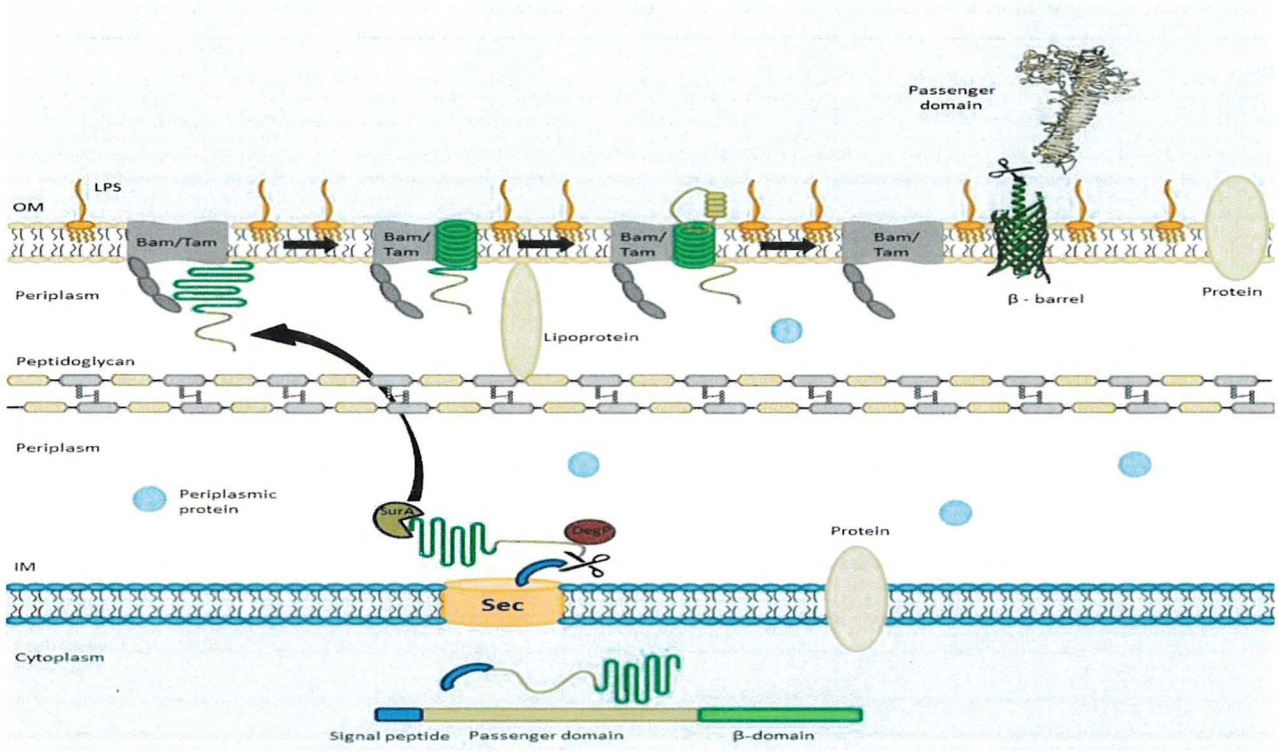

Figure 3.2 Schematic overview of Autotransporter (AT) processing, export, and secretion

The Signal peptide (SP) mediated by the Sec apparatus, guides translocation of the autotransporter to the periplasmic space. In the periplasm, the AT is kept in a "translocation competent state" by recruiting chaperones such as Skp, SurA, and DegP. Further, the Bam complex assists in the integration of the β-domain into the outer membrane and promotes the translocation of the passenger domain across the outer membrane through a hybrid-barrel mechanism wherein the AT β-barrel and Bam/Tam protein domains interact. Periplasmic chaperones such as SurA and DegP deliver an unfolded autotransporter to BamA/TamA. POTRA domains (gray in beaded structure) are contact sites for the AT protein to be transported. A hybrid-barrel is then formed by insertion of the AT β-strand through the gate region between strands 1 and 16 of the BamA/TamA barrel. Barrel expansion results in pore opening and the passenger domain can then protrude through the hybrid barrel. Subsequently, the passenger domain is released from the hybrid structure and may remain on the bacterial cell surface or can be cleaved for release from the bacterial cell. Adapted from [13] and [14].

Sec-dependent export of AT proteins through the inner membrane

The N-terminal signal peptide of all autotransporters mediates insertion through the inner membrane through a Sec-dependent mechanism that is common to many other exported or secreted proteins. Generally, the N-terminal signal sequences in proteins show a tripartite organization of n, h, and c regions which correspond to N-terminal, hydrophobic, and cleavage sites [16, 17]. Analysis of signal sequence mutants revealed that a hydrophobic, H region is an essential part for targeting and membrane insertion [16].

The signal peptide sequence has the function of targeting or protein translocation to the inner membrane. In *E. coli*, protein export through the Sec pathway can involve two distinct pathways:

i) The SecB/SecA pathway wherein the chaperone SecB, prevents premature aggregation or folding, keeping the protein in a "translocation – competent state" and leads to transfer to Sec A [18], ii) The SRP (Signal Recognition Particle) pathway in which the SRP nucleoprotein complex mediates co-translational targeting by interacting with a highly hydrophobic signal sequence following translation from ribosome towards the translocon [19].

AT protein transit through the Periplasm

The mechanism of secretion from the periplasm and the transitional state of ATs while localized in the periplasm is still debated. In fact, in the periplasmic space, these proteins are prone to immature folding or aggregation and degradation by periplasmic proteases. Misfolding or degradation of ATs can be prevented apparently either by prolonged interaction with the Sec-translocon or by interaction with periplasmic chaperones [**11**], or both. The periplasmic localization of ATs is likely to be very transient, and translocation to the outer membrane may occur rapidly following export and processing of the signal peptide through the cytoplasmic membrane.

Transport of ATs through the outer membrane (The Hybrid-Barrel model)

Proteins of the Omp85 superfamily such as BamA promote the insertion and folding of β-barrel outer-membrane proteins (OMPs) including AT proteins across the bacterial outer membrane [**14**, **20**]. BamA possesses five periplasmic POTRA domains which are believed to recognize substrates mediated by β-strand augmentation [**21**, **22**]. In addition to BamA, TamA has been involved in the translocation of autotransporters [**10**]. TamA is a homologue of BamA and shares common mechanisms associated with catalytic functions like insertase and chaperone foldase activity [**23**]. Thus, a similar model of AT translocation has been proposed for both the BamA and TamA translocation systems.

Despite the lack of a satisfactory model for autotransporter delivery at the outer membrane, the hybrid barrel model (Figure 3.2) provides a plausible mechanistic model that is based on interactions with the open 16-stranded BamA and TamA barrels. The unzipped strands of these proteins can incorporate β-strands of autotransporter by β-augmentation, creating a hybrid-barrel of the AT protein with BamA/TamA. The resulting hybrid-barrel would form a pore through which the passenger domain would be translocated outside the outer membrane. Subsequent to passenger domain translocation through the outer membrane, the hybrid-complex would disassociate releasing the assembled autotransporter laterally into the outer membrane and returning BamA/ TamA to its free, uncoupled state [**23**, **24**].

Passenger domain cleavage

At the bacterial surface, the fate of AT proteins can be dependent on the specific proteins themselves as well as the physiological conditions or the environmental niche. Some ATs remain associated with the outer membrane surface whereas others, such as the Pet and EspP SPATEs, show autocatalytic activity within the β-barrel leading to cleavage of the linker and release of the passenger domain from the bacterial cell surface [**25**, **26**]. Cleavage of the passenger domain from the β - domain can take place by various mechanisms. In the case of the SPATES, the cleavage site is generally conserved.

A cleavage site is located in the "Linker Domain" of SPATE proteins

The linker domain encompasses an conserved 14-residue segment that bridge the passenger domain and translocation domain junction in the SPATEs, and studies have shown that the cleavage site is conserved in this domain. Analysis of the (^{1021}EVNNLNKRMGDL^{1032}) sequence motif of EspP showed that the passenger domain is cleaved after the first asparagine residue [**27**, **28**]. The mutation in the linker peptide resulted in impaired passenger domain cleavage of EspP [**28**]. Similar mutations impaired passenger domain cleavage and passenger domain translocation of another SPATE, Tsh [**29**]. These findings suggest that the linker domain and sequence play an important role in the processing of the passenger domain. However, some SPATEs lack a twin asparagine sequence. For example, RpeA from a rabbit enteropathogenic *E. coli* (EPEC) strain lacks the twin asparagine residues within its linker domain and it was shown that this protein was not released into the supernatant [**30**]. By contrast, a recently identified SPATE called Sha (Serine protease hemagglutinin autotransporter) lacks the twin asparagine residues but was released into the culture supernatant [**31**], suggesting motifs other than the twin asparagine site may be recognized for cleavage of certain SPATEs.

3.2.2 SPATEs

Members of the SPATE family are autotransporter proteins from a variety of enterobacterial species, that all contain a consensus serine protease motif, and they have most notably been described from pathogenic *Escherichia coli and Shigella* spp. Although some other SPATEs have also been described in other enterobacteria including *Serratia marcescens* [32], *Salmonella bongori* [33], *Citrobacter rodentium* [34], and *Edwardsiella tarda* [35].

Other conserved architectures in SPATEs include: 1) A highly conserved secretion domain/translocation domain called a β-domain. Overall, protein homology ranges from 25 to 55%

but in the case of the β-domain, homology ranges from 60 to 90% identity [36]; 2) A conserved serine protease motif (consensus GD**S**GSP where **S** is the catalytic serine) at similar positions in their N-terminal passenger domain between residues 250-270 [25, 26, 37, 38]; 3) The serine protease motif of SPATEs does not have a role in the cleavage of the passenger domain from the β-domain [33]; 4) The passenger domain of the SPATEs are cleaved from the β-domain from a conserved cleavage site between the two asparagines [25, 39]; 5) All SPATEs have unusually long signal sequences (>50 amino acids) that have been shown to facilitate post-translational targeting [40]; 6) In contrast to the classical autotransporter IgA1protease, none of the SPATEs can cleave IgA1; 7) SPATEs are highly immunogenic proteins having specific phenotypes [41].

Classification of SPATES

SPATEs are subdivided into class 1 and class 2 based on structural and functional properties. The class 1 SPATEs are cytopathic/cytotoxic toxins (eliciting cellular changes such as cytoplasmic shrinkage, loss of membrane integrity and activation of apoptosis), likely caused by cleavage of cytoskeletal proteins such as spectrin/fodrin [**41**]. Further, class 1 SPATEs are believed to show cytotoxic activity primarily through targeting of intracellular substrates. On the other hand, class 2 SPATEs, the larger phylogenetic cluster, comprises O-glycoproteases that cleave mucin and other O-glycoproteins present not only on epithelial cells but also on the surface of hematopoietic cells [**42**]. Thus, due to mucinolytic activity, class 2 SPATEs can impart a subtle competitive advantage in mucosal colonization [**41**]. Sat, Pet, EspP, EspC, and SigA SPATEs belong to class 1 whereas Pic, PicU, Tsh/Hbp, Vat, EatA, and SepA belong to class 2 SPATEs.

Distribution of SPATEs among intestinal and extra-intestinal pathogenic *E. coli*

Some SPATEs are present in one or more pathotypes of *E. coli* (Figure 3.3). Generally, the following SPATES are found in various groups: EspP (extracellular serine protease plasmid (pO157-encoded) from enterohemorrhagic *E. coli* (EHEC) [**26**], Pet (plasmid-encoded toxin) from enteroaggregative *E. coli* (EAEC) [**25**], Pic (protein involved in intestinal colonization) from EAEC and uropathogenic *E. coli* (UPEC) and *Shigella* [**39**], EspC (EPEC secreted protein C) from enteropathogenic *E. coli* (EPEC), EatA (ETEC autotransporter A) from enterotoxigenic *E. coli* (ETEC) [**43**], Tsh (temperature-sensitive hemagglutinin)/ Hbp (hemoglobin protease) mainly in avian pathogenic *E. coli* (APEC) and some ExPEC (MNEC, UPEC) [**37**, **44**], Sat (secreted autotransporter toxin) from UPEC [**45**], and Vat (vacuolating autotransporter toxin), TagBC (Tandem autotransporter genes B and C), and Sha (Serine-protease hemagglutinin autotransporter) from APEC and UPEC strains [**46**] [**31**].

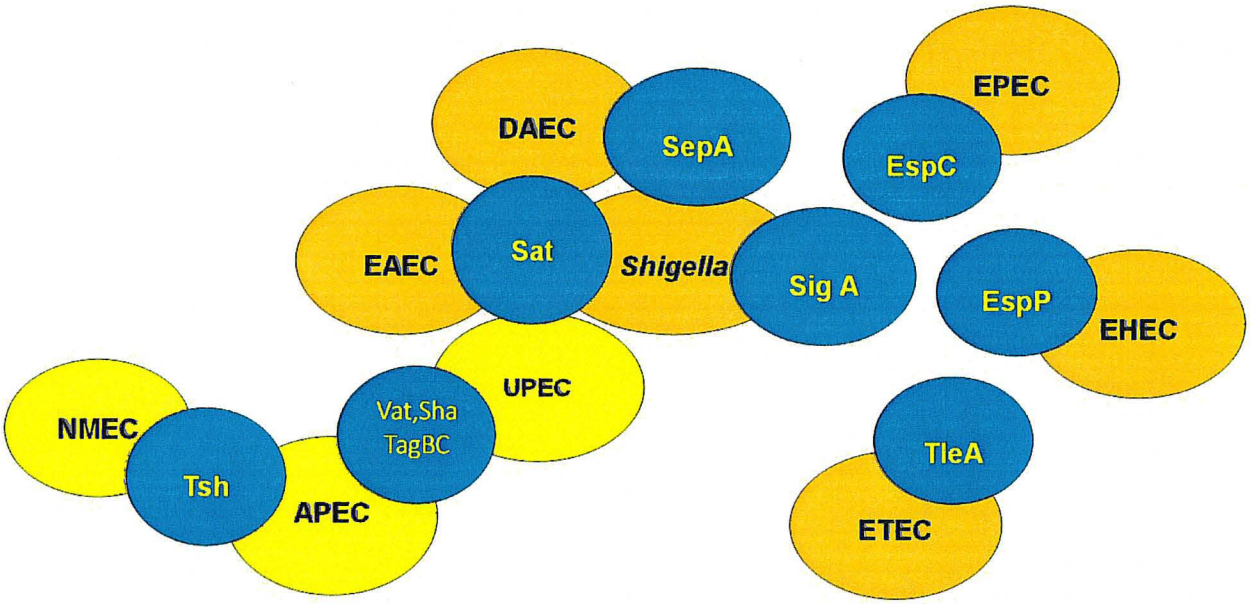

Figure 3.3 Distribution of SPATEs among intestinal and extra-intestinal pathogenic *E. coli*

SPATEs have been found not only in all recognized intestinal *E. coli* pathotypes (highlighted in orange) but also in extra-intestinal *E. coli* pathotypes (highlighted in yellow). The recent availability of many more bacterial genome sequences has led to identification of new and previously described SPATE proteins among both human and animal pathogens, including *Salmonella, Citrobacter,* and *Edwarsiella*, as well as some commensal *E. coli* strains. (APEC, Avian pathogenic *E. coli;* DAEC, Diffuse Adhering *E. coli;* UPEC, Uropathogenic *E. coli;* NMEC, Neonatal meningitis *E. coli;* EAEC, Enteroaggregative *E. coli;* EHEC, Enterohemorrhagic *E. coli;* EPEC; Enteropathogenic *E. coli,* ETEC, Enterotoxigenic *E. coli*).

Allelic variation

Phylogenetic comparisons of SPATE sequences available in the NCBI databases demonstrate that these proteins share high homology among their fellow members because of the high degree of amino acid identity in the C-terminal β – domains [**47**]. If we consider only the passenger domain, the percentage of homology drops considerably and signifies that different members contain distinct regions and have different biological functions (Figure 3.4). In addition, some predicted SPATEs are related allelic variants of some of the characterized SPATEs. Despite demonstrating some closer identity to some of the characterized SPATEs, only functional testing of these proteins can confirm their specific bioactivities.

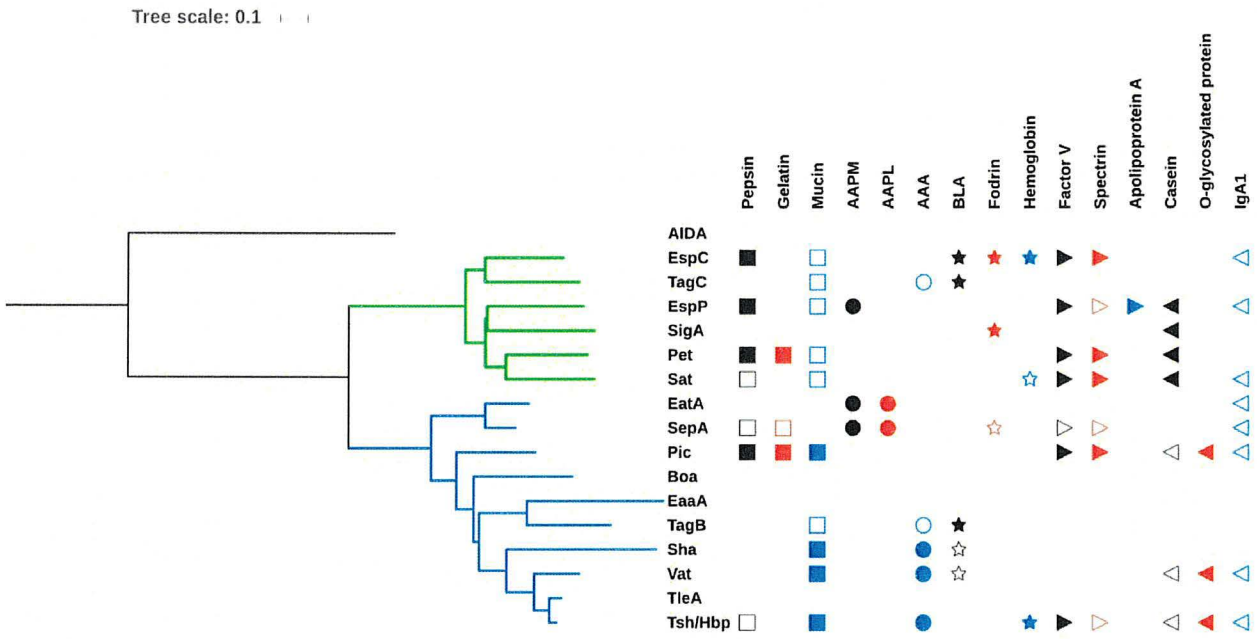

Figure 3.4 Evolutionary relationships of SPATEs based on passenger domain sequences and presentation of known protease substrates

The evolutionary history of passenger domains of characterized SPATEs was inferred using the Neighbour-Joining method [48]. The tree is drawn to scale, with branch lengths in the same units as those of the evolutionary distances used to infer the phylogenetic tree. The evolutionary distances were computed using the JTT matrix-based method [49] and are in the units of the number of amino acid substitutions per site. The analysis involved 17 protein sequences. All positions containing gaps and missing data were eliminated. Evolutionary analyses were conducted in MEGA6 [50]. Multiple sequence alignment was performed by Clustal W and the tree was constructed using the Mega6 software with PhyML/bootstrapping and iTOL [51]. The cluster of cytotoxic SPATEs (class 1) is in green branches while immunomodulator SPATEs (class 2) are in blue branches. SPATE protein sequences are available in NCBI database as follows: EspC, GenBank Accession No. AAC44731; EspP, NP_052685; SigA, AF200692; Pet, SJK83553; Sat, AAG30168; EatA, CAI79539, SepA , Z48219; Sha, MH899684; Pic, ALT57188; Boa, AAW66606; TagB and TagC, MH899681; EaaA, AAF63237; Vat, AY151282; TleA, KF494347; Tsh/Hbp, AF218073; AIDA, ABS20376; AAPM: MeOSuc-Ala-Ala-Pro-Met-pNA, AAPL: Suc-Ala-Ala-Pro-Leu-pNA, AAA: N-Succinyl-Ala-Ala-Ala-p-nitroanilide, BLA: N-Benzoyl-L-arginine 4-nitroanilide. The cleaved substrates, substrates that were negative for cleavage and those untested substrates are represented by filled symbol, unfilled symbol and no symbol respectively. This comparison shows that some of the activities are phylogenetically distributed.

3.2.3 Confusion due to improper annotation of uncharacterized SPATE encoding proteins

Due to the presence of conserved domains and similarities in protein sequences among SPATEs, there are some cases where SPATE protein sequences were misnamed or given the name of a related, but distinct SPATE. For example, Vat (GeneBank Accession No. AAN78874) was annotated as Tsh/Hbp in the UPEC CFT073 genome although this protein shares 78% identity with Tsh/Hbp [33, 52, 53]. Similarly, in the genome of *E. coli* PCN033 which was isolated from a pig with meningitis, a putative SPATE gene (GeneBank Accession No. AKK51062) is named as EspC, despite this protein only having 59% identity with EspC (GeneBank Accession No.

WP_109867760). So, for annotations in some enterobacterial genomes, it is unfortunate that numerous uncharacterized SPATEs are incorrectly labeled as specific characterized SPATEs, despite sharing a limited degree of identity, particularly in the absence of demonstration of any biological or experimentally confirmed activities.

3.2.4 SPATEs demonstrate a diversity of biological activities associated with virulence

Since the discovery of the first SPATE, Tsh, two decades ago, research has focused on characterizing SPATEs by determining their biological activities and substrate specificities and in some cases, structural properties have been studied through crystallography. Serine protease activity is due to the GD**S**GS motif and this activity is inhibited by phenylmethane sulfonyl fluoride (PMSF), but not by the metalloprotease inhibitor, Ethylene diamine tetraacetic acid (EDTA) [26]. The virulence properties of SPATEs may in part be attributed to proteolytic activity. However, it is now clear that there is a staggering diversity in biological substrates and modes of action. In the next sections, we focus on specific characteristics and functions of various SPATEs (summarized in Table 3.1) and their possible roles in enterobacterial pathogenesis.

Table 3.1 Summary of characteristics of different SPATEs

SPATEs	Organism[a]	Biological functions	References
EatA	ETEC	Enterotoxin	[54]
EspC	EPEC	Cytotoxin, Enterotoxin Cleavage of fodrin, hemoglobin, pepsin, coagulation factor V, translocator components (EspA/EspD) of T3SS Cell rounding and cell detachment	[55] [56] [41] [57] [58]
Pet	EAEC	Mucosal cytoxicity, Cleavage of spectrin, pepsin, factor V	[59] [25] [60] [61] [41]
Pic	Shigella, EAEC	Serum resistance	[39] [62] [52] [42] [63]

		Mucinase, Hemagglutination Colonization, Cleavage of gelatin, factor V, O – glycans: PSGL-1, CD44, CD45, CD93 and CX3CL1	[41]
EspP	EHEC, STEC	Cleaved pepsin, factor V, apolipoprotein, complement factors: C3/C3b and C5	[41] [64] [26] [65] [66]
Tsh/Hbp	APEC	Hemagglutinin, Binding to Caco-2 cells and to EMPs (laminin, fibronectin, and collagen IV) and heme Cleavage of mucin, factor V and O-glycosylated proteins in leukocyte	[37, 41, 63, 67]
Sha	APEC, UPEC	Autoaggregation, hemagglutination, biofilm formation, proteolytic activity on synthetic peptide: N-Succinyl-Ala-Ala-Ala-p-nitroanilide, adherence and cytopathic effects on bladder epithelial cell line	[31]
TleA	ETEC	Binding to Caco-2 cells Cleavage of bovine submaxillary mucin, leukocyte surface glycoproteins CD45 and P-selectin glycoprotein ligand 1	[68]
Vat	APEC, UPEC	Vacuolating cytotoxin, Agglutinate leukocyte Cleavage of O-glycosylated proteins in leukocyte	[46, 63]
Sat	UPEC	Vacuolating cytotoxin on HK-2, HEp-2 and Vero monkey kidney cells Cleavage of casein, factor V and spectrin	[41, 45, 69]

SepA	*Shigella flexneri*	Intestinal inflammation, proteolytic activity toward synthetic peptides: Suc-Ala-Ala-Pro-Phe-pNA, Suc-Val-Pro-Phe-pNA and Suc-Phe-Leu-Phe-pNA	[70] [71]
SigA	*Shigella flexneri*	Cytotoxin, Cleavage of casein, recombinant human α II spectrin Cell rounding and cell detachment	[72, 73]
Boa	*Salmonella bongori*	Unknown	[74]
TagBC	UPEC, APEC	Autoaggregation, proteolytic effect on synthetic peptide: N-Benzoyl-L-arginine 4-nitroanilide cytopathic effect on human bladder cell lines	[31]

[a] Bacteria known to produce these SPATEs. APEC, Avian pathogenic *E. coli;* DAEC, Diffuse Adhering *E. coli;* STEC, Shiga toxin-producing *E. coli*; UPEC, Uropathogenic *E. coli;* NMEC, Neonatal meningitis *E. coli;* EAEC, Enteroaggregative *E. coli;* EHEC, Enterohemorrhagic *E. coli;* EPEC; Enteropathogenic *E. coli,* ETEC, Enterotoxigenic *E. coli*)

EaaA/ EaaC

The EaaA and EaaC SPATEs (GenBank Accession No. Protein AAF63237.1, Nucleotide AF151091) were first identified from *Escherichia coli* reference strain ECOR-9, a human commensal intestinal isolate. These two SPATE encoding genes were found to be associated with genes encoding non-immune immunoglobulin binding proteins that were also associated with prophages [75]. The EaaA and EaaC SPATEs are very similar 1335 aa proteins sharing 99% identity (only 8 aa substitutions). Other than identification of these genes in ECOR-9, *eaa* gene sequences were also shown to be present in other ECOR strains (ECOR-2, ECOR-5, and ECOR-12) belonging to phylogenetic group A, but these SPATE sequences were not identified in a variety of clinical isolates [76]. However, screening of genomic sequence databases indicates EaaA/EaaC sequences are present in a diversity of *E. coli* strains (at least 50 entries of highly similar proteins identified from uniprot.org). Other than identification of the sequences in different strains, no phenotypic or biochemical properties of Eaa SPATEs have been investigated thus far.

EatA

EatA for ETEC autotransporter A (GenBank Accession No. CAI79539, Q84GK0; AY163491.2) is secreted by some ETEC strains and has been shown to contribute to virulence in the rabbit ileal loop model of infection since an *eatA* mutant demonstrated less marked and slowed fluid accumulation [43]. The *eatA* sequence was identified on a plasmid, pCS1, in *E. coli* strain H10407. The EatA protein shares over 80% identity to the SepA SPATE from *Shigella flexneri.* EatA was found to degrade a bacterial adhesin EtpA which could reduce intestinal colonization, but in parallel increased access of ETEC toxins at the host cell surface [54]. EatA was also shown to be highly immunogenic and could contribute to ETEC virulence by degrading the MUC2 protein at the small intestinal mucous layer, which could further promote access to ETEC toxins to epithelial cell surfaces [77]. The EatA protein was also shown to be present in most ETEC (over 70%) [78] and has been identified less commonly in some EAEC strains (4.1% of isolates) [79]. EatA has vaccine potential for prevention of ETEC, as it generated a high antibody response and protection against ETEC intestinal infection [77].

EspC

The EspC (EPEC secreted protein C) passenger domain is a 110 kDa protein (GenBank Accession No. AAC44731, U69128.1), and one of the first proteins reported to be secreted by EPEC [38]. As with other SPATEs, although EspC shares some sequence homology to IgA proteases, it cannot cleave IgA nor is the catalytic serine GD**S**GS motif required for release of the passenger domain from the β-domain into the external milieu [38]. It was also shown that EspC is not involved in EPEC generation of attaching and effacing (A/E) lesions, nor is it required for adherence or invasion of tissue culture cells. EspC showed enterotoxic activity and increased tissue PD (potential difference) and Isc (short circuit current) of rat jejunum mounted in Ussing chambers [80]. EspC enterotoxic activity was nullified by pre-incubation with an antiserum against another SPATE, Pet [80]. Like Pet, EspC produced cytotoxic effects on cultured epithelial cells but with three times higher dose (120 μg/ml) than Pet. The actin cytoskeleton was disrupted, resulting in cell contraction, loss of actin stress fibers and cell detachment. This overall effect was due to the serine protease motif of EspC [55]. Also, like Pet, EspC cleaved an intracellular target, α-fodrin but the cleavage sites were different. Pet cleaves fodrin within the calmodulin-binding domain between M^{1198} and V^{1199} [61]. EspC cleavage of fodrin occured outside of the calmodulin binding domain [55]. Once inside the cells, kinetics of protein degradation indicate that purified EspC cleaves fodrin at two sites (within the 11^{th} repetitive unit between Q^{1219} and ^{L1220} and within the 9^{th} repetitive unit between D^{938} and L^{939}) which then results in disruption of focal adhesion

including dephosphorylation and degradation of paxillin and FAK; leading to cell rounding and detachment [58]. However, entry to a target cell (cytosol) is critical for EspC cytotoxicity. Though internalization of purified EspC by pinocytosis was shown by [81], it cannot be considered as a natural pathophysiological phenomenon for enteric infection, as it took 8 hours of incubation for insertion while EPEC infection delivers EspC into the cells after 30 minutes. Interestingly, EspC is secreted into the milieu by the T5SS and then incorporated into the T3SS translocon for entry into host cells [82]. Further, EspC has a relevant role in cell death induced by EPEC. EspC is able to induce apoptosis and necrosis in epithelial cells [56] and apoptosis could be the first event which can manifest to increased necrosis. Also, EspC was shown to interfere with the caspase cascade required for induction of apoptosis which was partially dependent on serine protease activity.

Several biological targets recognized by EspC which are relevant to its diarrheagenic activity have been identified. Purified EspC cleaved human hemoglobin at an optimum pH between 5 and 6 [57]; although correlation of this biological property for EPEC virulence is yet to be established. EspC has also been shown to cleave other substrates like pepsin, glycoprotein coagulation factor V, and spectrin [41]. Apart from cleaving different biological substrates, EspC also cleaves bacterial components of the secretion system. EspC was found to target EspA/EspD which are translocator components of the Type III secretion system (T3SS) and control of pore formation and cytotoxicity by T3SS for the host cell [83]. The T3SS acts as a molecular syringe, comprised of pore-forming translocator proteins EspB and EspD which insert into the host cell plasma membrane and EspA which forms a hollow structure connecting the T3SS needle into the cell [84]. This result indicates that control of pore formation by EspC can support bacterial colonization, by mediating a controlled release of effector proteins from the T3SS to limit host cell death, since this could increase the immune response and potential clearance of EPEC at an early stage of infection.

Pet

Pet (Plasmid encoded toxin) is a 104 kDa enterotoxin produced by EAEC (GenBank Accession No. SJK83553), which has been found to increase jejunal potential difference (PD) and Isc (short circuit currents) accompanied by mucosal damage, exfoliation of cells and development of crypt abscesses [25]. Pet is encoded on the pAA plasmid and comprises a 52 aa *N*-terminal signal peptide and the secreted passenger domain (amino acids 53-1018) which cleaves from the β-domain between N^{1018} and N^{1019} [25].

A host-specific factor is essential for proper folding of the Pet autotransporter because clones of *E. coli* HB101 produced both folded and misfolded variants of Pet but the wild-type EAEC only produced the properly folded active Pet, suggesting that the accessory protein from EAEC may be absent or non-functional in strain HB101 [85]. This observation shows that correct protein folding is not required for AT secretion but that accessory proteins are necessary for folding ATs in the right conformation [11, 13, 86]. X-ray structure of the Pet passenger domain was resolved and when compared with the most similar SPATE, EspP (50% sequence identity); Pet harbors a β-pleated sheet from residues 181-1900 whereas EspP has a coiled loop. Further, the Pet passenger domain showed more β-sheets between residues 135-143 compared to EspP [8]. These β-helices are presumed to confer functionality to the protein.

Pet produced changes in host cytoskeletal architecture in both HEp-2 and HT29 epithelial cells characterized by time and dose-dependent cell elongation followed by cell rounding and detachment from the substrate, which was dependent on serine protease activity [60]. Cellular morphological changes were visible after 2 hours of incubation with Pet (25μg/ml). Pet also contributes to pathology at the mucosa which is characterized by dilation of crypt opening, extrusion of colonic enterocytes, development of intercrypt cervices and loss of apical mucus from goblet cells as a result of contraction of interlinking cytoskeleton integrity and loss of actin stress fibers and focal contacts [59]. These cytopathic effects may be due to internalization in host cells by the vesicular system as Pet activity completely vanished following incubation with brefeldin A [87]. Pet interaction with host cells requires a two-hour time lag leading to cell damage and requires a sequence of events: 1. Binding to cell 2. Entry into the cell by clathrin-dependent receptor-mediated endocytosis 3. Entry into early endosomes 4. Passage to the Golgi apparatus from endosomes 5. Retrograde vesicular transport from the Golgi complex to the ER 6. Delivery to the cytosol through the ER-associated degradation (ERAD) pathway [61, 88]. Once internalized, loss of actin microfilaments takes place due to the breakdown of cellular spectrin [60, 89]. Similar to Pet, EspC also produces cytotoxic activities on epithelial cells, although the dose of EspC was three times higher and a longer incubation time was required to produce a similar result [55]. Subsequently, it was shown that the d2 subdomain of the passenger domain is required for Pet internalization by recognizing the Pet host cell receptor, cytokeratin 8 [90]; the d1 subdomain is the largest domain having a serine protease motif and was incapable of binding the cell surface without the aid of d2 subdomain [90, 91]. Pet preferentially cleaves α-fodrin between M^{1198} and V^{1199} residues within the calmodulin-binding domain of fodrin's 11^{th} repetitive unit [61, 92]. Pet-mediated cleavage of α-fodrin (spectrin) has been suggested to induce enterocyte death via apoptosis [93, 94]. Together, this phenotype of Pet could explain the cellular alteration during

EAEC pathogenesis [92]. Recent studies have shown that the spice, curcumin, can also affect the secretion of Pet on the bacterial surface and subsequent internalization into the epithelial cells [95].

Pic

Protein involved in colonization (Pic) is a 109.8 kDa extracellular protein secreted by both EAEC (GenBank Accession No. ALT57188, AF097644.1), and *Shigella flexneri* 2a [39] and also atypical EPEC [96]. Pic catalyzed mucin degradation and has also been shown to confer serum resistance and hemagglutination [39]. Further, Pic also cleaved gelatin but did not demonstrate any activity against human immunoglobulins. In addition to Pic identified in diarrheagenic *E. coli*, another highly similar SPATE named PicU (96% amino acid identity to Pic) has been identified in some uropathogenic isolates. PicU was functionally similar to Pic from EAEC, degraded mucin and contributed to colonization during UTI [52, 62]. Interestingly, mucinase activity was not only important as a virulence factor but also may contribute to nutrient availability, since the *pic* mutant was less able to grow when compared to the wild-type strain [97]. The Pic mucinase (from all groups EAEC, UPEC, and *Shigella flexneri*) is responsible for increased secretion of mucus in the intestinal lumina of rat ileal loops by increasing mucus production in goblet cells even though this activity was independent of the serine protease motif [98]. This secretory activity of Pic favors the formation of biofilm by EAEC, a hallmark of EAEC infection. The mucolytic activity of Pic not only contributed to damage to the intestinal mucosal layer, but also cleaved mucin-type O-glycans of the immune system, including PSGL-1, CD44, CD45, CD93, and CX3CL1 [42, 63]. Further, Pic significantly reduced complement activation by cleaving complement cascade factors- C3, C4 and C2 [99]. Downregulation of complement activation by Pic may contribute to EAEC, *Shigella* and UPEC infections. To add to its virulence potential, Pic was also shown to induce PMN activation and programmed T-cell death [42].

PicU was identified in a UPEC strain and also demonstrates mucinase activity that may contribute to UTI pathogenesis [62]. To support this observation, a *picU* mutant of *E. coli* CFT073 was less able to colonize compared to wild-type parent although differences were not statistically significant. In addition, pepsin and coagulation factor V are other cleavage substrates for PicU [62]

Interestingly, a SPATE in *Citrobacter rodentium* similar to Pic and PicU, named PicC (79% identity at amino acid level), showed mucinase activity [100]. The *picC* mutant outcompeted the wild-type and elicited more colitis. The PicC protease may, therefore, be an important immune regulator that could function to decrease stimulation of the host immune system during infection [100].

EspP

The extracellular serine protease plasmid (pO157-encoded) (EspP) was isolated from the culture supernatant of EHEC O157: H7 EDL933 associated with hemolytic uremic syndrome (HUS) (GenBank Accession No. NP_052685; CAA66144, X97542.1) [26] and Shiga toxin producing *Escherichia coli* (STEC) [64, 101]. PssA (protease secreted by STEC) is the homolog of EspP which differs by a single amino acid change and was found to be cytotoxic for Vero cells [102]. EspP is generally associated with STEC, EHEC and atypical EPEC [103]. *In silico* analysis suggests that the signal sequence of EspP is cleaved between residues A^{55} and A^{56} [26] and the 104 kDa passenger domain contains a chaperone motif and a 30 AA linker domain that connects the β-domain and the passenger domain [104]. It was later shown that biogenesis and export of EspP were not self-mediated but also required additional periplasmic chaperones SurA and DegP, which aided in the proper folding of the AT passenger domain during translocation through the Bam complex [105].

EspP proteins have been classified as four distinct alleles namely EspPα, EspPβ, EspPγ, and EspPδ; where EspPα is associated with highly virulent EHEC O157: H7 and major non-O157 EHEC and can contribute to biofilm formation by forming macroscopic rope-like polymers which were refractory to antibiotics and showed adhesive and cytopathic effects [106]; EspPγ cleaved pepsin and human coagulation factor V, although EspPβ and EspPδ were either not secreted or proteolytically inactive [64]. Interestingly, EspPα was more prevalent in human isolates (84%) than in environmental isolates (47%) but EspPγ was more prevalent in the environment (40%) than from human sources (11%) [64, 107]. The genetic diversity of EspP alleles with divergent biological activities warrant specific subtyping for the screening of *espP* genes. The crystal structure of the EspP passenger domain was solved at 2.5˚A, and revealed a large β-helical stalk and a globular subdomain with the catalytic triad [6] and shared overall structure to the previously crystallized Hbp protein [7]. However, in contrast to Hbp, the active site of EspPα is slightly wider, deeper and more exposed, suggesting that it likely interacts with larger substrates [6].

EspP was shown to cleave substrates such as coagulation factor V [26], porcine pepsin A [26], apolipoprotein [65], major complement factor proteins C3/C3b but not factors H and I [66]. A valid argument for prolonged hemorrhage due to EspPα is strengthened by the ability of EspPα to cleave various serpins (serine protease inhibitors) from human plasma which are involved in blood coagulation [108]. Cleavage was specific, targeting only procoagulatory serpins such as α2-AP and α1-PI [108]. Like EspPα, EspI, another SPATE from STEC also cleaved α2-AP and α1-PI, [65], but unlike EspPα, EspI mediated cleavage was not complete due to the formation of an

inhibitory serpin-enzyme-complex [108]. Further, EspP was found to stimulate electrogenic ion transport in human colonoid monolayers, although this activity was Ca^{+2} dependent but independent of serine protease activity [109]. Taken together, the role of EspP in blood coagulation, pathophysiology and immunomodulation can contribute to pathogenesis of EHEC.

Tsh/Hbp

The first characterized SPATE, temperature-sensitive hemagglutinin (Tsh) was identified on a ColV-type plasmid in APEC strain χ7122 [37, 110]. The *tsh* gene (GenBank Accession No. AF218073) encodes a protein of 1,377 amino acids with a molecular weight of approximately 148-kDa. It is composed of a leader sequence which is cleaved between residues A^{52} and A^{53}, a 106-kDa passenger domain which encompasses the serine protease motif (S_{259}) extending from residues 53 to 1,100, and a β-barrel domain of 33-kDa which extends from residues 1,101 to 1,377 [37]. Based on the sequence homology, Tsh was also reported in some UPEC strains [52]. However, Heimer et al. were screening for *vat,* not *tsh*, and they erroneously named the *vat* gene in CFT073 and other UPEC as *tsh*. However, it has been reported in one study that some human ExPEC strains from newborn meningitis (11 to 50 percent) also contain *tsh* located on large plasmids similar to ColV plasmids [111]. A Tsh-like protein sharing 60 % aa identity with *E. coli* Tsh was also reported in *Edwardsiella tarda*, a fish pathogen [35]. Despite the 60% identity of this SPATE from *Edwardsiella tarda* to Tsh, the biological functions of this protein and its role in virulence of fish may be different.

The production of Tsh in *E. coli* K-12 was found to be higher at low temperature (26°C) and it conferred the capacity to agglutinate chicken erythrocytes in a mannose resistant manner. However, at higher temperatures, Tsh was released into the supernatant medium and this agglutination activity was lost leading the name, temperature-sensitive hemagglutinin [37]. Interestingly, the hemagglutination phenotype was also observed for Tsh with sheep [112], bovine, pig, turkey, rabbit, horse, and dog [31] and human erythrocytes [63], further Tsh promoted adherence to Caco-2 cells and to extracellular matrix proteins such as laminin, fibronectin, and collagen IV [112]. Sequence analyses indicated that Tsh is a homolog to IgA proteases (56% of similarity) of *Hemophilus influenzae* and *Neisseria gonorrhoea* [113], but was unable to cleave IgA. Tsh was shown to cleave mucin, factor V [41] and O-glycosylated proteins such as CD43, CD44, CD45, CD93, CD162, and CX3CL1 *in vitro* [42, 63], suggesting diverse roles in cellular and immune functions. Tsh seems to also contribute directly to APEC infection as its presence accelerates the progression of the infection and could lead to the development of lesions and deposition of fibrin in avian air sacs [37, 112]. In addition to these functions, Tsh was shown to

have potential enterotoxin function to induce fluid accumulation in a rabbit ligated illeal loop assay [114], although the significance of this role for Tsh in mammalian enteric disease is unknown.

Hbp (hemoglobin protease) is a near-identical variant of Tsh that was isolated from a patient with an intra-abdominal wound infection, and only differs by two amino acids (Q209K and A842T) (GenBank Accession No. AJ223631) [44]. Like *tsh*, the *hbp* gene is located on a virulence plasmid, pColV-K30. Hbp was shown to cleave hemoglobin and acquire heme in an iron-depleted host niche [44]. Heme captured by Hbp could help in the growth of *Bacteroides fragilis* since *B. fragilis* was shown to contain a specific receptor for the heme-Hbp complex and it is capable of exploiting rarer heme available from host complexes and cause intra-abdominal abscesses in patients [67].

TleA

Tsh-like ETEC autotransporter or TleA (GenBank Accession No. KF494347) is an AT that was identified in an ETEC strain [68]. It is a 4,110-bp gene that encodes a 1,369-amino-acid precursor. Sequence analyses have shown that TleA contains a signal peptide from residues 1 to 52, a passenger domain from residues 53 to 1,092 with a serine protease motif GD**S**GS from residues 257 to 261 and a β-barrel domain from residues 1,093 to 1,369. The alignment of the passenger domain sequences of the other members of SPATEs indicated that TleA is a class 2 SPATE and shares 97% identity with the Tsh autotransporter [68]. TleA may have a role in intestinal colonization and immunomodulation as it was shown to degrade bovine submaxillary mucin and leukocyte surface glycoproteins CD45 and P-selectin glycoprotein ligand 1. Further, nonadherent *E. coli* HB101 expressing TleA conferred the capacity to adhere to Caco-2 cells, while such adherence was not observed in the wild-type ETEC strain 1766a [68].

Vat

Vacuolating autotransporter toxin (Vat) is a 140 kDa class II SPATE that was found to be encoded on a pathogenicity island from APEC *E. coli* Ec222, and was shown to contribute to respiratory tract infection, cellulitis and septicemia in poultry [46]. The *vat* gene is located on a pathogenicity island (VAT-PAI) between the *proA* and *yagU* genes (GenBank Accession No. AY151282). The *vat* pathogenicity island in Ec222 contains 33 ORFs wherein *vat* is ORF27. Interestingly, ORF26 shares 44% aa identity with the PapX regulator from UPEC strains [46]. The *vat* predicted gene product also shares 97% identity with an AT present in UPEC strain CFT073 which was annotated mistakenly as Tsh/Hbp. However, the new annotation has been corrected as Vat-ExPEC [33, 52,

53]. Vat shares 77.5% identity to Tsh/Hbp of APEC [44, 110], which explains why Vat has sometimes been mislabeled as Tsh for certain strains or genome sequences.

Unlike Tsh/Hbp, the secreted 111.8-kDa Vat passenger domain was unable to cleave the casein-based substrate [46]. Compared to the *vat* mutant, APEC Ec222 exhibited a robust cytotoxic effect on chicken embryonic fibroblast (CEF) cells. Cytotoxic activity involved vacuole formation in cells which was visualized from 2-24 h after exposure [46]. In a cellulitis infection model, chickens challenged with *E. coli* Ec222 developed cellulitis, whereas none of the chickens developed cellulitis when infected with the *vat* mutant [46]. In UPEC, Vat elicits an antibody response in some urosepsis patients, and the titer of Vat-specific IgG was higher in the plasma of patients compared to the titer found in controls and patients infected with *vat*-negative UPEC strains [115]. Vat also has a role in fitness of UPEC colonization during murine systemic infection [116]. Further, a role for Vat in combination with other SPATEs was demonstrated for fitness in murine kidney colonization and cytotoxicity [31]. Vat has also been shown to mediate agglutination of erythrocytes and cleavage of O-glycoproteins *in vitro* [63].

Vat (Vat-AIEC) present in Adherent Invasive *E. coli* (AIEC) associated with Crohn's disease, showed 97% similarity to Vat identified from APEC Ec222 with a modification in the conserved serine catalytic domain to GD**S**GSP instead of the conserved AT**S**GSP motif present in Vat [117]. Vat-AIEC acts as a mucinase and inactivation of *vat* reduced gut colonization by one-log in a mouse model [117].

Sha

A recently identified SPATE-encoding gene *sha* (serine-protease hemaglutinin autotransporter) is located on a distinct region of a ColV-type plasmid [31]. The *sha* gene (GenBank Accession No. MH899684) was more common among APEC (present in 20% of 299 APEC strains) than in UPEC (0.9% of 697 strains). Sha is more closely related to Tsh (43% identity) and Vat proteins (38% identity) than to other SPATEs. Like Vat and Tsh, Sha showed elastase-like activity by cleaving N-Succinyl-Ala-Ala-Ala-p-nitroanilide. In addition, Sha increased adherence to both human and avian epithelial cells, whereas Tsh only increased adherence to bladder cells, and Vat only increased adherence to kidney cells. Sha also demonstrated hemagglutation for erythrocytes of a variety of animal species (sheep, bovine, pig, dog, chicken, turkey, rabbit, horse, and human), contributed to increased biofilm formation, and delayed cytotoxicity (release of LDH after 12 h from bladder epithelial cells). As similar carbohydrates may be present on erythrocyte surfaces, it is not surprising that Sha as well as Tsh and Vat autotransporters demonstrated extensive hemagglutination activity for a variety of erythrocytes. We believe that the contrasting

phenotype when Sha is expressed in high copy vector – agglutination with erythrocytes by the protein present on the bacterial surface as well as the cytopathic effects of released protein in culture supernatant could be explained by the presence of protein both in the bacterial surface and released in the supernatant (Figure 3.5). Although loss of *sha* didn't affect competitive fitness during colonization of the urinary tract of female mice, *sha* expression was upregulated six-fold in infected bladder compared to culture in LB broth [31].

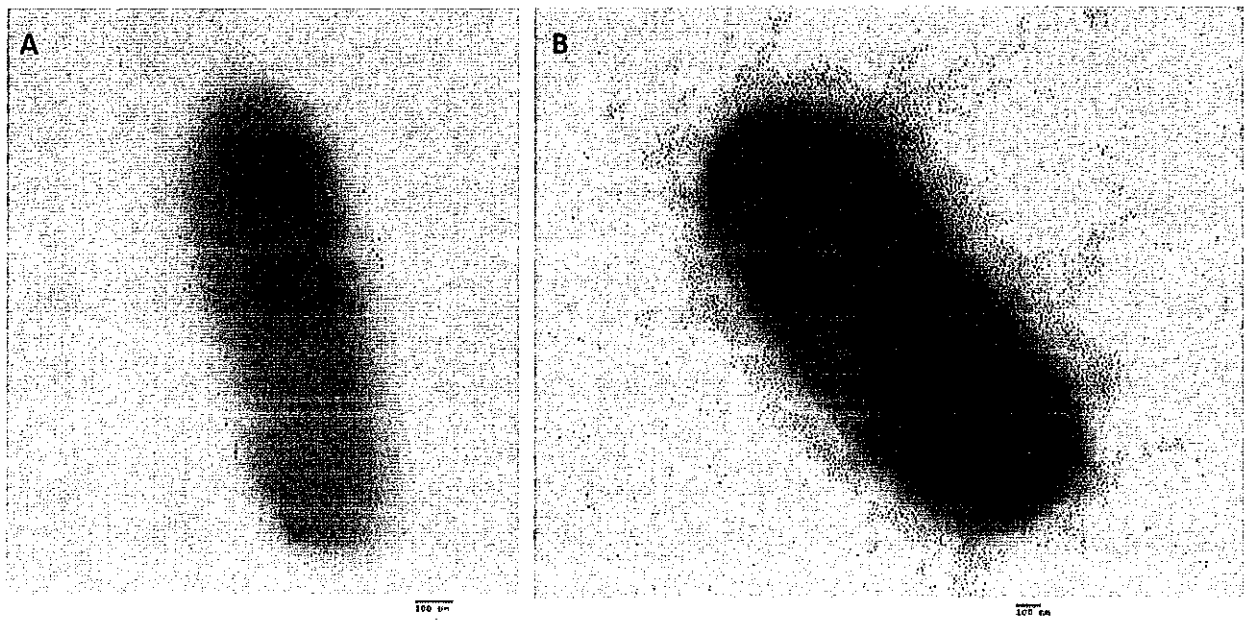

Figure 3.5 Transmission electron micrographs of *E. coli* BL21 expressing the Sha autotransporter [31] immunolabelled with 10-nm-diameter gold particles

(A) The negative control, adsorbed serum was used for the primary incubation with *E. coli* BL21 empty vector and shows a very low background of gold particles. (B) Gold-labelling with AT-specific antibodies shows that when Sha is constitutively expressed, proteins are localized on the surface as well as released in the supernatant. So, the protein released can gain access to host cell targets, whereas the protein associated with bacterial cells can mediate agglutination, autoaggregation, and adherence to host cells. Bar 100 nm

Sat

A Secreted autotransporter toxin (Sat) was identified in UPEC strain CFT073 [45] and later also described in *Shigella*, EAEC, DEAC and neonatal septicemia *E. coli* strains [118]. The 3,885-bp *sat* gene (GenBank Accession No. AAG30168) is located on a pathogenicity island that also carries a *pap* fimbrial gene cluster. The *sat* gene product is a 1,295-amino-acid precursor with a molecular weight of 142-kDa [45]. Sat was unable to agglutinate human erythrocytes, did not cleave glycoproteins CD43 and CD162 from Jurkat cells [63]. Sat was also shown to cleave casein, coagulation factor V and nonerythroid spectrin, but not pepsin or mucin [41, 45]. Like Vat, Sat also exhibited cytotoxicity on epithelial cells, including HK-2, HEp-2 and Vero cells,

characterized by vacuole formation, autophagy and cell detachment [45, 69, 119]. Cytotoxicity included disruption of actin and other cytoskeletal and nuclear proteins and was dependent on the serine protease active site [120]. Mechanism of internalization of Sat inside the cell is unknown and was found to be localized specifically to the cytoskeletal fraction of bladder and kidney epithelial cells [120].

The autophagy in HeLa epithelial cells triggered by Sat led to disruption of the F-actin cytoskeleton [119]. Sat also modified tight junction-associated proteins ZO-1, ZO-2 and occludins in human polarized epithelial intestinal Caco-2 and TC7 cells, resulting in increased paracellular permeability [121]. In addition, Sat induced a strong immune response in a murine model of ascending urinary tract infection, although a *sat* mutant colonized urine, bladder and kidneys as well as the wild-type strain [45]. However, kidneys of mice infected with the wild-type strain showed dissolution of the glomerular membrane and vacuolation of proximal tubules and these lesions were absent in kidneys infected with the *sat* mutant [69]. In addition, Sat from a Diffusely adhering *E. coli* (DAEC) strain triggered pronounced fluid accumulation and villous necrosis in rabbit ileal tissue [122]. Taken together, Sat plays an important role as a cytotoxin in the pathogenicity of urinary tract infection as well as in intestinal infections. To define the role of Sat as an enterotoxin in the probiotic strain *Escherichia coli* Nissle 1917 is enigmatic because Nissle 1917 is expected to show beneficial effect but it produced cytopathic Sat which was functional during colonization of the mouse intestine [123].

SepA

Shigella extracellular protein A (SepA) was identified in *Shigella flexneri,* which causes diarrhea (shigellosis) in humans [70] and also in some enteroaggregative *E. coli* (EAEC) strains [103]. The *sepA* gene (GenBank Accession No. Z48219) is located on the 200 kb virulence plasmid pWR100 and encodes a 1366 aa precursor of 146 kDa [70]. SepA exhibited protease activity of some synthetic peptides such as Suc-Val-Pro-Phe-pNA [71], although no protease activity was found on natural substrates such as gelatin, IgA1 [70], angiotensin-I, egg lysozyme [71], fibronectin, mucin, pepsin, factor V, spectrin, or fodrin [41]. Unlike other class-2 SPATEs, SepA did not cleave O-linked glycoproteins from leucocytes such as CD43, CD44, CD45, CD93, CD162, and CX3CL1 [63]. Deletion of *sepA* did not affect entry of *S. flexneri* into epithelial cells, or cell to cell spread, however the *sepA* mutant showed a decrease in fluid accumulation and inflammation in the rabbit ileal loop model compared to the wild-type [70]. Further, in a human explant model, the *sepA* mutant demonstrated reduced mucosal damage and a significant reduction in desquamation of intestinal epithelial barrier [124]. SepA also induced disruption of the apical pole of a polarized

epithelial barrier and facilitated invasion of intestinal cells by *Shigella* [125]. This was associated with a decrease in LIMK1 leading to increased accumulation of cofilin, a protein involved in actin dynamics [125, 126].

SigA

Shigella IgA-like protease homologue or SigA is another SPATE identified in *Shigella flexneri* 2a [72] (GenBank Accession No. AF200692). The *sigA* gene is located on the *she* pathogenicity island and encodes a 103 kDa protein [72, 74]. SigA confers cytotoxic and enterotoxic effects and was shown to cleave casein [72] and recombinant human α II spectrin (α-fodrin) [73], indicating that it might contribute to pathophysiological manifestation of *Shigella*. SigA shares 56% identity to the Pet. It was shown that a *S. flexneri* 2a *sigA* mutant had 30% reduction in fluid accumulation in a rabbit ileal loop model and immunogenic SigA can bind to HEp-2 cells to induce cell rounding and detachment; phenotypes similar to purified Pet toxin from enteroaggregative *E. coli,* suggesting that SigA could play a key role in the virulence of *S. flexneri* [72, 73]. Owing to the immunogenic properties of SigA [127], a computational approach has been used to identify potential epitopes for generation of a peptide vaccine against *Shigella* [128]. Due to their high immunogenicity the potential of SigA and other SPATEs could be exploited as vaccine targets.

Boa

Although most SPATEs identified to date were characterized from different pathotypes of *E. coli* and *Shigella* spp., Boa represents the only SPATE identified in *Salmonella* spp. Boa is present in *Salmonella bongori*, a *Salmonella* species associated mainly with reptiles, but which have been reported to infect some animals and humans. Surprisingly, no other SPATEs have been identified in all other *Salmonella enterica* serovars. It has been suggested that Boa may have been acquired by horizontal gene transfer from another Enterobacteria such as *E. coli* [74]. The *boa* gene encodes a 1,384 protein (GenBank Accession No. AAW66606, FR877557) predicted to have a long signal peptide of 57 residues, a passenger domain of 1,050 residues containing a serine protease GDSGS motif from residues 262 to 266 and a β-barrel domain of 277 residues [74, 129]. So far, the functions of the Boa protein or its potential role for *Salmonella bongori* pathogenesis has not been determined.

TagBC

Recently, two new SPATEs referred to as "tandem autotransporter genes, *tagB* and *tagC,* located adjacent to each other on a genomic island between the conserved *E. coli* genes *yjdI* and *yjdK* in an APEC O1: K1 strain were identified [31]. Genome analysis and screening for *tagB* and *tagC*

(GeneBank Accession No. MH899681) indicate that these SPATE genes are present in APEC as well as UPEC strains [31]. Among 697 UPEC isolates, *tagB* sequences were present in 70 isolates (10%), whereas *tagC* sequences were present in 80 isolates. While amongst 299 APEC strains, *tagB* sequences were present in 14 isolates (4.7%) and *tagC* sequences were present in 21 isolates (7%). Interestingly, all the *tagB* or *tagC*-positive APEC isolates were exclusively from infections in turkeys. Both proteins showed trypsin-like activity and efficiently cleaved N-Benzoyl-L-arginine 4-nitroanilide, similarly to the activity of EspC protein. Further, TagB and TagC were autoaggregating, hemagglutinating, could promote adherence to the HEK 293 renal and 5637 bladder cell lines as well as cytotoxic to human bladder cell lines when expressed in *E. coli* K-12 (with early release of LDH after 5 hours). Neither of them required a functional serine protease motif for secretion [31]. Inspite of these *in vitro* phenotypes, loss of TagBC did not have any appreciable effect on virulence or fitness of the mutant in bladder and kidneys of infected mice.

3.2.5 Regulation of expression of SPATEs

Although numerous SPATEs have been characterized and their roles in infection and cell toxicity have been reported, determination of the mechanisms of regulation of SPATEs has been limited. In general, most SPATEs are thermally regulated and are better expressed under conditions like the host infection sites and upon contact with host cells, in tissue culture medium and at neutral to alkaline pH (7 to 9). EspP, EspC, Tsh, Pic, SigA, SepA are thermoregulated, although mechanisms of regulation remain to be elucidated [26, 37, 39, 57, 113]. Expression of the *vat-AIEC* gene was upregulated when grown at pH 7.5 with bile salts and mucin, which are similar to conditions in the distal ileal segment of the GI tract [117]. Expression of EspP in culture supernatant was higher in lysogeny broth (LB) than in minimal essential medium (MEM) as well as higher at 37°C than at 20°C [26, 130]. Further, when EHEC 5236/96 (O26 : H11) was grown in contact with human intestinal epithelial HCT-8 cells, *espP* expression was upregulated more than 35-fold [131]. Likewise, transcription of *pet* expression was increased in tryptone-containing medium which might be of clinical significance for the milk-drinking pediatric population that can be infected with EAEC. Similarly, *tsh* and *vat* expression was shown to be upregulated in minimal medium when compared to rich LB medium [31]. Despite determining what conditions increase expression of some SPATEs, defining which regulatory mechanisms control SPATE expression has been limited. Specific aspects of regulation of expression of some SPATEs are presented below.

Regulation by LER

The locus of enterocyte effacement (LEE) encoded regulator (Ler) regulates the LEE pathogenicity island of EPEC and EHEC which produce attaching and effacing lesions on host intestinal epithelial cells. Ler activates the transcription of various LEE operons [132]. Apart from regulating operons associated with the LEE and its Type 3 secretion system, Ler also strongly activates the *espC* promoter (by 31-fold) and hence increases the production of the EspC SPATE in EPEC [133].

Regulation by H-NS

Histones are small, abundant, highly conserved proteins that have been recognized as DNA binding proteins. They play a role in compacting DNA into the nucleosome, the main structures to form chromosomes, in eukaryotic cell nuclei [134, 135]. In bacteria, such as *E. coli*, some proteins have been described as histone-like proteins. They may not share the same functions as compacting prokaryotic DNA but it was shown that they play a role in the regulation of genes by competing for binding to their promoter, and these genes could be associated with virulence, osmoregulation, pH and temperature sensing [136]. Based on sequence homology, four major groups of histone-like proteins were described: histone-like proteins *Escherichia coli* U93 (HU), histone-like nucleoid structuring proteins (H-NS), integration host factors (IHF), and factors for inversion stimulation (FIS). Among these, a role for H-NS has been reported for the regulation of different AT encoding genes including regulation of the SPATE Vat.

H-NS has been shown to regulate different trimeric autotransporters [137-139]. Further, H-NS repressed the expression of *vat*; in UPEC strain CFT073, as a Δ*hns* mutant was shown to secrete a significantly higher level of Vat than the wild type strain [115]. Further, sequence analysis of the *vat* promoter region predicted the presence of three potential H-NS binding sites in the *vat* promoter region [115]. It seems H-NS could also potentially directly regulate other SPATE genes, as there are predicted putative H-NS binding sites present in SPATE gene promoter regions (Table 3.2). However, further experimental evidence will be required to confirm whether regulation of expression of SPATEs by H-NS is a common phenomenon.

Table 3.2 The potential H-NS binding sites on the promoter region of SPATEs as predicted by Virtual Footprint Software[a]

SPATEs	Potential H-NS binding sites
boa	$^{-97}$GCAATAAACC^{-88} (-), $^{-96}$GCAATAAAAT^{-87} (-),$^{-80}$GCTATAAAAA^{-71} (-)
sigA	$^{-179}$TGGTTAGATA^{-170} (-),$^{-170}$GTGATTGATT^{-161} (-), $^{-19}$CCGATATTTC^{-10} (-)
pic	$^{-159}$CAGATAAAAC^{-150} (+), $^{-109}$TGCATTAATG^{-100} (-), $^{-35}$GGGATATAAA^{-26} (-)
sepA	$^{-176}$ATGATAAAAA^{-167}(+), $^{-35}$AAGATTAATT^{-26} (-)
tsh/hbp	$^{-164}$CACATAAAGT^{-155} (-), $^{-28}$AAAATAAAAT^{-19} (-), $^{-10}$GTAATTAAAA^{-1} (+)
espC	$^{-300}$ACCATTAAAA^{-291} (+), $^{-299}$CCATTAAAAT^{-290} (+), $^{-111}$GCCACAAACT^{-102} (-)
espP	$^{-280}$TCGATTGTTA^{-271} (-), $^{-96}$CAGATAAATG^{-87} (-), $^{-46}$CTGATACATT^{-37} (+)
pet	$^{-177}$ATGATTAATT^{-168} (+),$^{-42}$AGGATTAAGA^{-33} (-),$^{-24}$TCAATAAATG^{-15} (+)
sat	$^{-177}$ACGATCAATT^{-168} (+),$^{-166}$ACGATCAATT^{-157} (+),$^{-24}$TCAATAAATG^{-15} (+)
eatA	$^{-88}$GCTATCTATT^{-79} (+),$^{-71}$ACAATAAATG^{-62} (+),$^{-40}$TCCACACAAC^{-31} (-)
eaaA	$^{-314}$ACCATACAGC^{-305} (-),$^{-124}$GCGGTAAAAA^{-115} (-)
tagB	$^{-304}$ACGAAAAAAA^{-295} (-),$^{-161}$CTGATAAATA^{-152} (-),$^{-128}$TCGATAAATG^{-119} (+)
tagC	$^{-256}$GCAATTAATA^{-247} (+),$^{-62}$TCGCTATATT^{-53} (+),$^{-56}$ACTATAAATA^{-47} (-)
sha	$^{-187}$CCCACAAATC^{-178} (-),$^{-48}$TCCTTATATT^{-39} (+),$^{-32}$TCAATAGATA^{-23} (-)
vat	$^{-296}$TCCATATATC^{-287} (+),$^{-295}$TGGATATATG^{-286} (-),$^{-107}$GCTATATAAT^{-98} (-)

[a] **Virtual Footprint software [140] was used for *in silico* analysis of different SPATEs promoter regions for putative regulatory H-NS binding sites and additional experimentation is required to confirm a role for H-NS in regulation of SPATE gene regulation. Pattern matching tool Virtual Footprint used specific position weight matrices (PWMs) to generate the top 3 potential binding sites upstream to the start codon with high scoring matches.**

Regulation of Vat by the MarR-related protein VatX

The Multiple Antibiotic Resistance Regulator (MarR) family are proteins that regulate the expression of many genes involved in resistance to multiple antibiotics including tetracycline, chloramphenicol, β-lactams, nalidixic acid, penicillins, fluoroquinolones, toxic substances, organic solvents, oxidative stress agents and pathogenic factors [115, 141-145]. In *E. coli*, MarR is located in the chromosome in the *mar* locus and consists of an operator marO and two divergent transcriptional units marC and marRAB [146]. Besides, the possible role of H-NS as a negative regulator of Vat, an open reading frame was located downstream of the *vat* gene designated as ORF26 in the VAT-PAI from Ec222 [46] and c0392 in CFT073 [53]. This ORF shares 44% amino acid identity to the protein PapX (P pilus-associated transcriptional regulator) from CFT073 [115, 147]. PapX has been described as a member of the MarR family, it regulates flagella by binding to the *flhDC* promoter region [115, 147]. Considering identity to PapX, the ORF was named VatX. The *vatX* gene is present and adjacent to the *vat* gene in many strains. The VatX protein contains a MarR PFAM domain (PF01047) and a helix-turn-helix motif that is characteristic of DNA binding proteins and was classified in a different clade of MarR family regulators and is more closely related to the PapX, SfaX, and FocX fimbria-associated regulators. In UPEC strain CFT073, overexpression of VatX increased expression of Vat 3-fold compared to wild-type levels. Interestingly, in the absence of H-NS, the *vat* and *vatX* genes were both co-transcribed, suggesting VatX may compete with H-NS to promote expression of *vat* [115].

Co-regulation of SPATEs by CRP and FIS proteins

The cyclic AMP receptor protein (CRP) is a global transcription factor that is required by *E. coli* in carbon metabolism [148, 149]. CRP binds as a homodimer to a 16-bp DNA binding site, is allosterically activated by cAMP binding and interacts with RNA polymerase as either an activator or a repressor of transcription initiation [150]. CRP has been identified as a key transcription factor for the *pet* gene in EAEC strain 042 [151]. In addition, transcription from the *pet* promoter was found to be co-dependent on CRP and Fis regulators and the synergy between these regulators was due to the non-optimal position for transcription initiation of CRP and the additional required binding of the Fis regulator [151]. Fis is a versatile transcription factor and is involved in site-specific recombination events, organization of local DNA topology in bacterial chromosomes, and as a global transcription factor [152, 153]. It binds DNA as a homodimer that recognizes a degenerate 15-bp binding sequence often found in many promoter regions [154]. Through a co-activation mechanism, Fis was also shown to co-regulate SPATE genes with CRP including the *sat* gene from UPEC and *sigA* from *Shigella sonnei* [155].

Clearly, further investigation of regulation of SPATE expression by either DNA-binding proteins, transcriptional factors and mechanisms controlling expression of different SPATE proteins is needed. Further, potential crosstalk or hierarchical production of different SPATES needs to be considered and to what extent other virulence proteins affect the trafficking and secretion of SPATEs, if they are using the same secretion machinery such as BAM/TAM systems for their export and biogenesis at the bacterial cell surface.

3.2.6 Some SPATEs can also mediate degradation of bacterial protein targets

The perspective of considering SPATEs uniquely as virulence proteins specifically produced to damage host cells and promote infection has been called into question in recent years. A newly described role for some SPATEs has been identified to be the degradation of bacterial proteins and secretion systems. Protease activity of SPATEs has mainly been determined for host proteins, however, importantly some SPATEs can play an important role in infection through targeting of other bacterial substrates. The EatA SPATE from ETEC degrades the ETEC EtpA adhesin which can lead to reduced intestinal colonization [54]. Reduced colonization may be an advantage for ETEC to quickly deliver enterotoxin without causing extensive damage and may reduce inflammation and decrease the host immune response – acting as hit and run strategy of the bacteria. Similar activity was shown by EspC, wherein EspC reduced secretion of EspA and EspD, which are effector proteins of the EPEC T3SS involved in pore formation on host cell [83]. In this case, EspC reduced pore formation and cytotoxicity by degrading EspA and EspD. A similar interchangeable activity was seen with EspP as well [83]. Therefore, these SPATEs can also contribute to EPEC/EHEC infections by degrading other bacterial secreted proteins secreted by the T3SS before they contact the host cell. Another example of SPATE influence on other bacterial virulence factors is EspPα present in EHEC which has been shown to degrade the pore-forming RTX-toxin hemolysin Ehx (EHEC- Hly) [156] in its free and vesicle-bound form [131]. EspP mediated cleavage was specific to the Ehx hydrophobic domain, which is crucial for interaction with the host cell membrane and pore formation [157]. Similarly, the reduction in the level of active pore-forming toxin may also alter the host immune response and contribute to intestinal colonization and pathogenesis.

3.3 Conclusion

Improved technologies and affordability of DNA sequencing and other methods to investigate bacterial/host interactions has greatly advanced our understanding of many aspects of bacterial pathogenesis in recent years. The large amount of data from genome sequences has also resulted in determination of new putative SPATEs which may also contribute to host colonization and infection. Two decades after the characterization of the first SPATE, much progress has been made in the study of SPATEs by combining *in silico* bioinformatics, bacteriology, molecular biology, biochemistry and cellular biology and pathogenesis studies. Within the SPATE family, all members may share a similar global structure, but each SPATE may mediate distinct functional properties and substrate specificities and be associated with certain bacterial pathotypes, the type of the disease they cause, and host animal species they infect. One would expect that the variety of host and tissues niches could result in diversification of SPATE functions. Further, these pathogens can also differ in their interactions with the host, with some SPATE producing pathogens remaining extracellular during infection, whereas others may invade cells or survive in host phagocytes. Many questions remain to be answered about the molecular basis for substrate recognition and specificity of SPATEs and fundamentally understanding how these proteins are regulated. It is also unclear to what extent these SPATEs may modulate or alter proteins and the bacterial surface and affect pathogenesis. Moreover, the SPATE proteins are also frequently present in certain enterobacterial pathogens commonly associated with both enteric and systemic diseases in humans and animal hosts. As these proteins are highly immunogenic, it stands to reason that the SPATEs or their conserved epitopes can be targeted for potential approaches to develop vaccines to prevent such diseases.

3.4 References

1. Henderson, I.R., et al., *Type V protein secretion pathway: the autotransporter story.* Microbiology and molecular biology reviews, 2004. **68**(4): p. 692-744.
2. Linke, D., et al., *Trimeric autotransporter adhesins: variable structure, common function.* Trends in microbiology, 2006. **14**(6): p. 264-270.
3. Salacha, R., et al., *The Pseudomonas aeruginosa patatin-like protein PlpD is the archetype of a novel Type V secretion system.* Environmental microbiology, 2010. **12**(6): p. 1498-1512.
4. Leo, J.C., I. Grin, and D. Linke, *Type V secretion: mechanism (s) of autotransport through the bacterial outer membrane.* Phil. Trans. R. Soc. B, 2012. **367**(1592): p. 1088-1101.
5. Jacob-Dubuisson, F., C. Locht, and R. Antoine, *Two-partner secretion in Gram-negative bacteria: a thrifty, specific pathway for large virulence proteins.* Molecular microbiology, 2001. **40**(2): p. 306-313.
6. Khan, S., et al., *Crystal structure of the passenger domain of the Escherichia coli autotransporter EspP.* Journal of molecular biology, 2011. **413**(5): p. 985-1000.
7. Otto, B.R., et al., *Crystal structure of hemoglobin protease, a heme binding autotransporter protein from pathogenic Escherichia coli.* Journal of Biological Chemistry, 2005. **280**(17): p. 17339-17345.
8. Meza-Aguilar, J.D., et al., *X-ray crystal structure of the passenger domain of plasmid encoded toxin (Pet), an autotransporter enterotoxin from enteroaggregative Escherichia coli (EAEC).* Biochemical and biophysical research communications, 2014. **445**(2): p. 439-444.
9. Veiga, E., et al., *Export of autotransported proteins proceeds through an oligomeric ring shaped by C-terminal domains.* The EMBO journal, 2002. **21**(9): p. 2122-2131.
10. Selkrig, J., et al., *Discovery of an archetypal protein transport system in bacterial outer membranes.* Nature Structural and Molecular Biology, 2012. **19**(5): p. 506.
11. Ruiz-Perez, F., et al., *Roles of periplasmic chaperone proteins in the biogenesis of serine protease autotransporters of Enterobacteriaceae.* Journal of bacteriology, 2009. **191**(21): p. 6571-6583.
12. Sijbrandi, R., et al., *Signal recognition particle (SRP)-mediated targeting and Sec-dependent translocation of an extracellular Escherichia coli protein.* Journal of Biological Chemistry, 2003. **278**(7): p. 4654-4659.
13. Purdy, G.E., C.R. Fisher, and S.M. Payne, *IcsA surface presentation in Shigella flexneri requires the periplasmic chaperones DegP, Skp, and SurA.* Journal of bacteriology, 2007. **189**(15): p. 5566-5573.
14. Sauri, A., et al., *The Bam (Omp85) complex is involved in secretion of the autotransporter haemoglobin protease.* Microbiology, 2009. **155**(12): p. 3982-3991.
15. Peterson, J.H., et al., *Secretion of a bacterial virulence factor is driven by the folding of a C-terminal segment.* Proceedings of the National Academy of Sciences, 2010. **107**(41): p. 17739-17744.
16. Michaelis, S., J. Hunt, and J. Beckwith, *Effects of signal sequence mutations on the kinetics of alkaline phosphatase export to the periplasm in Escherichia coli.* Journal of bacteriology, 1986. **167**(1): p. 160-167.
17. Martoglio, B. and B. Dobberstein, *Signal sequences: more than just greasy peptides.* Trends in cell biology, 1998. **8**(10): p. 410-415.
18. Randall, L. and S. Hardy, *SecB, one small chaperone in the complex milieu of the cell.* Cellular and Molecular Life Sciences CMLS, 2002. **59**(10): p. 1617-1623.
19. Valent, Q.A., et al., *The Escherichia coli SRP and SecB targeting pathways converge at the translocon.* The EMBO journal, 1998. **17**(9): p. 2504-2512.

20. Bredemeier, R., et al., *Functional and phylogenetic properties of the pore-forming β-barrel transporters of the Omp85 family.* Journal of Biological Chemistry, 2007. **282**(3): p. 1882-1890.
21. Fleming, P.J., et al., *BamA POTRA domain interacts with a native lipid membrane surface.* Biophysical journal, 2016. **110**(12): p. 2698-2709.
22. Albrecht, R., et al., *Structure of BamA, an essential factor in outer membrane protein biogenesis.* Acta Crystallographica Section D: Biological Crystallography, 2014. **70**(6): p. 1779-1789.
23. Gruss, F., et al., *The structural basis of autotransporter translocation by TamA.* Nature Structural and Molecular Biology, 2013. **20**(11): p. 1318.
24. Noinaj, N., et al., *Lateral opening and exit pore formation are required for BamA function.* Structure, 2014. **22**(7): p. 1055-1062.
25. Eslava, C., et al., *Pet, an autotransporter enterotoxin from enteroaggregative Escherichia coli.* Infection and immunity, 1998. **66**(7): p. 3155-3163.
26. Brunder, W., H. Schmidt, and H. Karch, *EspP, a novel extracellular serine protease of enterohaemorrhagic Escherichia coli O157: H7 cleaves human coagulation factor V.* Molecular microbiology, 1997. **24**(4): p. 767-778.
27. Dautin, N., et al., *Cleavage of a bacterial autotransporter by an evolutionarily convergent autocatalytic mechanism.* The EMBO journal, 2007. **26**(7): p. 1942-1952.
28. Dautin, N. and H.D. Bernstein, *Residues in a conserved α-helical segment are required for cleavage but not secretion of an Escherichia coli serine protease autotransporter passenger domain.* Journal of bacteriology, 2011. **193**(15): p. 3748-3756.
29. Kostakioti, M. and C. Stathopoulos, *Role of the α-helical linker of the C-terminal translocator in the biogenesis of the serine protease subfamily of autotransporters.* Infection and immunity, 2006. **74**(9): p. 4961-4969.
30. Leyton, D.L., et al., *Contribution of a novel gene, rpeA, encoding a putative autotransporter adhesin to intestinal colonization by rabbit-specific enteropathogenic Escherichia coli.* Infection and immunity, 2007. **75**(9): p. 4664-4669.
31. Habouria, H., et al., *Three new serine-protease autotransporters of Enterobacteriaceae (SPATEs) from extra-intestinal pathogenic Escherichia coli and combined role of SPATEs for cytotoxicity and colonization of the mouse kidney.* Virulence, 2019. **10**(1): p. 568-587.
32. Ohnishi, Y., T. Beppu, and S. Horinouchi, *Two genes encoding serine protease homologues in Serratia marcescens and characterization of their products in Escherichia coli.* The Journal of Biochemistry, 1997. **121**(5): p. 902-913.
33. Parham, N.J., et al., *Distribution of the serine protease autotransporters of the Enterobacteriaceae among extraintestinal clinical isolates of Escherichia coli.* Journal of clinical microbiology, 2005. **43**(8): p. 4076-4082.
34. Vijayakumar, V., et al., *Role of class 1 serine protease autotransporter in the pathogenesis of Citrobacter rodentium colitis.* Infection and immunity, 2014. **82**(6): p. 2626-2636.
35. Hu, Y.-h., et al., *The serine protease autotransporter Tsh contributes to the virulence of Edwardsiella tarda.* Veterinary microbiology, 2016. **189**: p. 68-74.
36. Dautin, N., *Serine protease autotransporters of enterobacteriaceae (SPATEs): biogenesis and function.* Toxins, 2010. **2**(6): p. 1179-1206.
37. Dozois, C.M., et al., *Relationship between the Tsh autotransporter and pathogenicity of avian Escherichia coli and localization and analysis of the Tsh genetic region.* Infection and immunity, 2000. **68**(7): p. 4145-4154.
38. Stein, M., et al., *Characterization of EspC, a 110-kilodalton protein secreted by enteropathogenic Escherichia coli which is homologous to members of the immunoglobulin A protease-like family of secreted proteins.* Journal of bacteriology, 1996. **178**(22): p. 6546-6554.

39. Henderson, I.R., et al., *Characterization of Pic, a Secreted Protease ofShigella flexneri and EnteroaggregativeEscherichia coli.* Infection and immunity, 1999. **67**(11): p. 5587-5596.
40. Peterson, J.H., R.L. Szabady, and H.D. Bernstein, *An unusual signal peptide extension inhibits the binding of bacterial presecretory proteins to the signal recognition particle, trigger factor, and the SecYEG complex.* Journal of Biological Chemistry, 2006. **281**(14): p. 9038-9048.
41. Dutta, P.R., et al., *Functional comparison of serine protease autotransporters of Enterobacteriaceae.* Infection and immunity, 2002. **70**(12): p. 7105-7113.
42. Ruiz-Perez, F., et al., *Serine protease autotransporters from Shigella flexneri and pathogenic Escherichia coli target a broad range of leukocyte glycoproteins.* Proceedings of the National Academy of Sciences, 2011. **108**(31): p. 12881-12886.
43. Patel, S.K., et al., *Identification and molecular characterization of EatA, an autotransporter protein of enterotoxigenic Escherichia coli.* Infection and immunity, 2004. **72**(3): p. 1786-1794.
44. Otto, B.R., et al., *Characterization of a hemoglobin protease secreted by the pathogenic Escherichia coli strain EB1.* The Journal of experimental medicine, 1998. **188**(6): p. 1091-1103.
45. Guyer, D.M., et al., *Identification of sat, an autotransporter toxin produced by uropathogenic Escherichia coli.* Molecular microbiology, 2000. **38**(1): p. 53-66.
46. Parreira, V. and C. Gyles, *A novel pathogenicity island integrated adjacent to the thrW tRNA gene of avian pathogenic Escherichia coli encodes a vacuolating autotransporter toxin.* Infection and immunity, 2003. **71**(9): p. 5087-5096.
47. Ruiz-Perez, F. and J.P. Nataro, *Bacterial serine proteases secreted by the autotransporter pathway: classification, specificity, and role in virulence.* Cellular and molecular life sciences, 2014. **71**(5): p. 745-770.
48. Saitou, N. and M. Nei, *The neighbor-joining method: a new method for reconstructing phylogenetic trees.* Molecular biology and evolution, 1987. **4**(4): p. 406-425.
49. Jones, D.T., W.R. Taylor, and J.M. Thornton, *The rapid generation of mutation data matrices from protein sequences.* Bioinformatics, 1992. **8**(3): p. 275-282.
50. Tamura, K., et al., *MEGA6: molecular evolutionary genetics analysis version 6.0.* Molecular biology and evolution, 2013. **30**(12): p. 2725-2729.
51. Ciccarelli, F.D., et al., *Toward automatic reconstruction of a highly resolved tree of life.* science, 2006. **311**(5765): p. 1283-1287.
52. Heimer, S.R., et al., *Autotransporter genes pic and tsh are associated with Escherichia coli strains that cause acute pyelonephritis and are expressed during urinary tract infection.* Infection and immunity, 2004. **72**(1): p. 593-597.
53. Welch, R.A., et al., *Extensive mosaic structure revealed by the complete genome sequence of uropathogenic Escherichia coli.* Proceedings of the National Academy of Sciences, 2002. **99**(26): p. 17020-17024.
54. Roy, K., et al., *Adhesin degradation accelerates delivery of heat-labile toxin by enterotoxigenic E. coli.* Journal of Biological Chemistry, 2011: p. jbc. M111. 251546.
55. Navarro-García, F., et al., *The serine protease motif of EspC from enteropathogenic Escherichia coli produces epithelial damage by a mechanism different from that of Pet toxin from enteroaggregative E. coli.* Infection and immunity, 2004. **72**(6): p. 3609-3621.
56. Serapio-Palacios, A. and F. Navarro-Garcia, *EspC, an autotransporter protein secreted by enteropathogenic Escherichia coli, causes apoptosis and necrosis through caspase and calpain activation, including direct procaspase-3 cleavage.* MBio, 2016. **7**(3): p. e00479-16.
57. Elisa Drago-Serrano, M., S. Gavilanes Parra, and H. Angel Manjarrez-Hernández, *EspC, an autotransporter protein secreted by enteropathogenic Escherichia coli (EPEC),*

displays protease activity on human hemoglobin. FEMS microbiology letters, 2006. **265**(1): p. 35-40.
58. Navarro-Garcia, F., et al., *EspC promotes epithelial cell detachment by enteropathogenic Escherichia coli via sequential cleavages of a cytoskeletal protein and then focal adhesion proteins.* Infection and immunity, 2014. **82**(6): p. 2255-2265.
59. Henderson, I.R., et al., *Involvement of the EnteroaggregativeEscherichia coli Plasmid-Encoded Toxin in Causing Human Intestinal Damage.* Infection and immunity, 1999. **67**(10): p. 5338-5344.
60. Navarro-García, F., et al., *Cytoskeletal effects induced by pet, the serine protease enterotoxin of enteroaggregative Escherichia coli.* Infection and immunity, 1999. **67**(5): p. 2184-2192.
61. Canizalez-Roman, A. and F. Navarro-García, *Fodrin CaM-binding domain cleavage by Pet from enteroaggregative Escherichia coli leads to actin cytoskeletal disruption.* Molecular microbiology, 2003. **48**(4): p. 947-958.
62. Parham, N.J., et al., *PicU, a second serine protease autotransporter of uropathogenic Escherichia coli.* FEMS microbiology letters, 2004. **230**(1): p. 73-83.
63. Ayala-Lujan, J.L., et al., *Broad spectrum activity of a lectin-like bacterial serine protease family on human leukocytes.* PLoS One, 2014. **9**(9): p. e107920.
64. Brockmeyer, J., et al., *Subtypes of the plasmid-encoded serine protease EspP in Shiga toxin-producing Escherichia coli: distribution, secretion, and proteolytic activity.* Applied and environmental microbiology, 2007. **73**(20): p. 6351-6359.
65. Schmidt, H., et al., *Identification and characterization of a novel genomic island integrated at selC in locus of enterocyte effacement-negative, Shiga toxin-producing Escherichia coli.* Infection and immunity, 2001. **69**(11): p. 6863-6873.
66. Orth, D., et al., *EspP, a serine protease of enterohemorrhagic Escherichia coli, impairs complement activation by cleaving complement factors C3/C3b and C5.* Infection and immunity, 2010. **78**(10): p. 4294-4301.
67. Otto, B.R., et al., *Escherichia coli hemoglobin protease autotransporter contributes to synergistic abscess formation and heme-dependent growth of Bacteroides fragilis.* Infection and immunity, 2002. **70**(1): p. 5-10.
68. Gutiérrez, D., et al., *TleA, a Tsh-like autotransporter identified in a human enterotoxigenic Escherichia coli strain.* Infection and immunity, 2015. **83**(5): p. 1893-1903.
69. Guyer, D.M., et al., *Sat, the secreted autotransporter toxin of uropathogenic Escherichia coli, is a vacuolating cytotoxin for bladder and kidney epithelial cells.* Infection and immunity, 2002. **70**(8): p. 4539-4546.
70. Benjelloun-Touimi, Z., P.J. Sansonetti, and C. Parsot, *SepA, the major extracellular protein of Shigella flexneri: autonomous secretion and involvement in tissue invasion.* Molecular microbiology, 1995. **17**(1): p. 123-135.
71. Benjelloun-Touimi, Z., et al., *SepA, the 110 kDa protein secreted by Shigella flexneri: two-domain structure and proteolytic activity.* Microbiology, 1998. **144**(7): p. 1815-1822.
72. Al-Hasani, K., et al., *The sigA gene which is borne on the shepathogenicity island of Shigella flexneri 2a encodes an exported cytopathic protease involved in intestinal fluid accumulation.* Infection and immunity, 2000. **68**(5): p. 2457-2463.
73. Al-Hasani, K., et al., *The immunogenic SigA enterotoxin of Shigella flexneri 2a binds to HEp-2 cells and induces fodrin redistribution in intoxicated epithelial cells.* PloS one, 2009. **4**(12): p. e8223.
74. Yen, Y.T., et al., *Common themes and variations in serine protease autotransporters.* Trends in microbiology, 2008. **16**(8): p. 370-379.
75. Sandt, C.H. and C.W. Hill, *Four Different Genes Responsible for Nonimmune Immunoglobulin-Binding Activities within a Single Strain of Escherichia coli.* Infection and immunity, 2000. **68**(4): p. 2205-2214.

76. Restieri, C., et al., *Autotransporter-encoding sequences are phylogenetically distributed among Escherichia coli clinical isolates and reference strains.* Appl. Environ. Microbiol., 2007. **73**(5): p. 1553-1562.
77. Kumar, P., et al., *EatA, an immunogenic protective antigen of enterotoxigenic Escherichia coli, degrades intestinal mucin.* Infection and immunity, 2014. **82**(2): p. 500-508.
78. Del Canto, F., et al., *Distribution of classical and nonclassical virulence genes in enterotoxigenic Escherichia coli isolates from Chilean children and tRNA gene screening for putative insertion sites for genomic islands.* Journal of clinical microbiology, 2011. **49**(9): p. 3198-3203.
79. Andrade, F.B., et al., *Distribution of serine protease autotransporters of Enterobacteriaceae in typical and atypical enteroaggregative Escherichia coli.* Infection, Genetics and Evolution, 2017. **50**: p. 83-86.
80. Mellies, J.L., et al., *espC pathogenicity island of enteropathogenic Escherichia coli encodes an enterotoxin.* Infection and immunity, 2001. **69**(1): p. 315-324.
81. Vidal, J.E. and F. Navarro-García, *Efficient translocation of EspC into epithelial cells depends on enteropathogenic Escherichia coli and host cell contact.* Infection and immunity, 2006. **74**(4): p. 2293-2303.
82. Vidal, J.E. and F. Navarro-García, *EspC translocation into epithelial cells by enteropathogenic Escherichia coli requires a concerted participation of type V and III secretion systems.* Cellular microbiology, 2008. **10**(10): p. 1975-1986.
83. Guignot, J., A. Segura, and G.T. Van Nhieu, *The serine protease EspC from enteropathogenic Escherichia coli regulates pore formation and cytotoxicity mediated by the type III secretion system.* PLoS pathogens, 2015. **11**(7): p. e1005013.
84. Garmendia, J., G. Frankel, and V.F. Crepin, *Enteropathogenic and enterohemorrhagic Escherichia coli infections: translocation, translocation, translocation.* Infection and immunity, 2005. **73**(5): p. 2573-2585.
85. Nemec, K.N., et al., *A host-specific factor is necessary for efficient folding of the autotransporter plasmid-encoded toxin.* Biochimie, 2010. **92**(2): p. 171-177.
86. Wagner, J.K., et al., *Contribution of the periplasmic chaperone Skp to efficient presentation of the autotransporter IcsA on the surface of Shigella flexneri.* Journal of bacteriology, 2009. **191**(3): p. 815-821.
87. Navarro-García, F., et al., *Plasmid-Encoded Toxin of EnteroaggregativeEscherichia coli is Internalized by Epithelial Cells.* Infection and immunity, 2001. **69**(2): p. 1053-1060.
88. Navarro-García, F., et al., *Pet, a non-AB toxin, is transported and translocated into epithelial cells by a retrograde trafficking pathway.* Infection and immunity, 2007. **75**(5): p. 2101-2109.
89. Dutta, P.R., B.Q. Sui, and J.P. Nataro, *Structure-function analysis of the enteroaggregative Escherichia coli plasmid-encoded toxin autotransporter using scanning linker mutagenesis.* Journal of Biological Chemistry, 2003. **278**(41): p. 39912-39920.
90. Nava-Acosta, R. and F. Navarro-Garcia, *Cytokeratin 8 is an epithelial cell receptor for Pet, a cytotoxic serine protease autotransporter of Enterobacteriaceae.* MBio, 2013. **4**(6): p. e00838-13.
91. Chavez-Dueñas, L., et al., *The subdomain 2 of the autotransporter Pet is the ligand site for recognizing Pet receptor on the epithelial cell surface.* Infection and immunity, 2016: p. IAI. 01528-15.
92. Villaseca, J.M., et al., *Pet toxin from enteroaggregative Escherichia coli produces cellular damage associated with fodrin disruption.* Infection and immunity, 2000. **68**(10): p. 5920-5927.
93. Martin, S.J., et al., *Proteolysis of fodrin (non-erythroid spectrin) during apoptosis.* Journal of Biological Chemistry, 1995. **270**(12): p. 6425-6428.

94. Wang, K.K., et al., *Simultaneous degradation of αII-and βII-spectrin by caspase 3 (CPP32) in apoptotic cells.* Journal of Biological Chemistry, 1998. **273**(35): p. 22490-22497.
95. Sanchez-Villamil, J.I., et al., *Curcumin blocks cytotoxicity of enteroaggregative and enteropathogenic Escherichia coli by blocking Pet and EspC proteolytic release from bacterial outer membrane.* Frontiers in Cellular and Infection Microbiology, 2019. **9**: p. 334.
96. Abreu, A.G., et al., *The serine protease Pic as a virulence factor of atypical enteropathogenic Escherichia coli.* Gut microbes, 2016. **7**(2): p. 115-125.
97. Harrington, S.M., et al., *The Pic protease of enteroaggregative Escherichia coli promotes intestinal colonization and growth in the presence of mucin.* Infection and immunity, 2009. **77**(6): p. 2465-2473.
98. Navarro-Garcia, F., et al., *Pic, an autotransporter protein secreted by different pathogens in the Enterobacteriaceae family, is a potent mucus secretagogue.* Infection and immunity, 2010. **78**(10): p. 4101-4109.
99. Abreu, A.G., et al., *The serine protease Pic from enteroaggregative Escherichia coli mediates immune evasion by the direct cleavage of complement proteins.* The Journal of infectious diseases, 2015. **212**(1): p. 106-115.
100. Bhullar, K., et al., *The serine protease autotransporter pic modulates citrobacter rodentium pathogenesis and its innate recognition by the host.* Infection and immunity, 2015: p. IAI. 00025-15.
101. Brockmeyer, J., et al., *Structure and function relationship of the autotransport and proteolytic activity of EspP from Shiga toxin-producing Escherichia coli.* PloS one, 2009. **4**(7): p. e6100.
102. Djafari, S., et al., *Characterization of an exported protease from Shiga toxin-producing Escherichia coli.* Molecular microbiology, 1997. **25**(4): p. 771-784.
103. Boisen, N., et al., *High prevalence of serine protease autotransporter cytotoxins among strains of enteroaggregative Escherichia coli.* The American journal of tropical medicine and hygiene, 2009. **80**(2): p. 294-301.
104. Velarde, J.J. and J.P. Nataro, *Hydrophobic residues of the autotransporter EspP linker domain are important for outer membrane translocation of its passenger.* Journal of Biological Chemistry, 2004. **279**(30): p. 31495-31504.
105. Ruiz-Perez, F., I.R. Henderson, and J.P. Nataro, *Interaction of FkpA, a peptidyl-prolyl cis/trans isomerase with EspP autotransporter protein.* Gut microbes, 2010. **1**(5): p. 339-344.
106. Xicohtencatl-Cortes, J., et al., *Bacterial macroscopic rope-like fibers with cytopathic and adhesive properties.* Journal of Biological Chemistry, 2010. **285**(42): p. 32336-32342.
107. Khan, A.B., et al., *Serine protease espP subtype α, but not β or γ, of Shiga toxin-producing Escherichia coli is associated with highly pathogenic serogroups.* International Journal of Medical Microbiology, 2009. **299**(4): p. 247-254.
108. Weiss, A., H. Joerss, and J. Brockmeyer, *Structural and functional characterization of cleavage and inactivation of human serine protease inhibitors by the bacterial SPATE protease EspPα from enterohemorrhagic E. coli.* PloS one, 2014. **9**(10): p. e111363.
109. Tse, C., et al., *Enterohemorrhagic E. coli (EHEC)—Secreted Serine Protease EspP Stimulates Electrogenic Ion Transport in Human Colonoid Monolayers.* Toxins, 2018. **10**(9): p. 351.
110. Provence, D.L. and R. Curtiss, *Isolation and characterization of a gene involved in hemagglutination by an avian pathogenic Escherichia coli strain.* Infection and immunity, 1994. **62**(4): p. 1369-1380.
111. Nicholson, B.A., et al., *Genetic characterization of ExPEC-like virulence plasmids among a subset of NMEC.* PloS one, 2016. **11**(1): p. e0147757.

112. Kostakioti, M. and C. Stathopoulos, *Functional analysis of the Tsh autotransporter from an avian pathogenic Escherichia coli strain.* Infection and immunity, 2004. **72**(10): p. 5548-5554.
113. Stathopoulos, C., D.L. Provence, and R. Curtiss, *Characterization of the Avian PathogenicEscherichia coli Hemagglutinin Tsh, a Member of the Immunoglobulin A Protease-Type Family of Autotransporters.* Infection and immunity, 1999. **67**(2): p. 772-781.
114. Maluta, R.P., et al., *Avian extraintestinal Escherichia coli exhibits enterotoxigenic-like activity in the in vivo rabbit ligated ileal loop assay.* Foodborne pathogens and disease, 2014. **11**(6): p. 484-489.
115. Nichols, K.B., et al., *Molecular characterization of the vacuolating autotransporter toxin in uropathogenic Escherichia coli.* Journal of bacteriology, 2016. **198**(10): p. 1487-1498.
116. Subashchandrabose, S., et al., *Genome-wide detection of fitness genes in uropathogenic Escherichia coli during systemic infection.* PLoS pathogens, 2013. **9**(12): p. e1003788.
117. Gibold, L., et al., *The Vat-AIEC protease promotes crossing of the intestinal mucus layer by Crohn's disease-associated Escherichia coli.* Cellular microbiology, 2016. **18**(5): p. 617-631.
118. Tapader, R., et al., *The high prevalence of serine protease autotransporters of Enterobacteriaceae (SPATEs) in Escherichia coli causing neonatal septicemia.* European journal of clinical microbiology & infectious diseases, 2014. **33**(11): p. 2015-2024.
119. Liévin-Le Moal, V., et al., *Secreted autotransporter toxin (Sat) triggers autophagy in epithelial cells that relies on cell detachment.* Cellular microbiology, 2011. **13**(7): p. 992-1013.
120. Maroncle, N.M., et al., *Protease activity, secretion, cell entry, cytotoxicity, and cellular targets of secreted autotransporter toxin of uropathogenic Escherichia coli.* Infection and immunity, 2006. **74**(11): p. 6124-6134.
121. Guignot, J., et al., *The secreted autotransporter toxin, Sat, functions as a virulence factor in Afa/Dr diffusely adhering Escherichia coli by promoting lesions in tight junction of polarized epithelial cells.* Cellular microbiology, 2007. **9**(1): p. 204-221.
122. Taddei, C.R., et al., *Secreted autotransporter toxin produced by a diffusely adhering Escherichia coli strain causes intestinal damage in animal model assays.* FEMS microbiology letters, 2005. **250**(2): p. 263-269.
123. Toloza, L., et al., *The secreted autotransporter toxin (Sat) does not act as a virulence factor in the probiotic Escherichia coli strain Nissle 1917.* BMC microbiology, 2015. **15**(1): p. 250.
124. Coron, E., et al., *Characterisation of early mucosal and neuronal lesions following Shigella flexneri infection in human colon.* PloS one, 2009. **4**(3): p. e4713.
125. Maldonado-Contreras, A., et al., *Shigella depends on SepA to destabilize the intestinal epithelial integrity via cofilin activation.* Gut microbes, 2017. **8**(6): p. 544-560.
126. Huang, T.Y., C. DerMardirossian, and G.M. Bokoch, *Cofilin phosphatases and regulation of actin dynamics.* Current opinion in cell biology, 2006. **18**(1): p. 26-31.
127. Scorza, F.B., et al., *High yield production process for Shigella outer membrane particles.* PloS one, 2012. **7**(6): p. e35616.
128. Oany, A.R., et al., *Vaccinomics approach for designing potential peptide vaccine by targeting Shigella spp. serine protease autotransporter subfamily protein SigA.* Journal of immunology research, 2017. **2017**.
129. Fookes, M., et al., *Salmonella bongori provides insights into the evolution of the Salmonellae.* PLoS pathogens, 2011. **7**(8): p. e1002191.
130. Ebel, F., et al., *Temperature-and medium-dependent secretion of proteins by Shiga toxin-producing Escherichia coli.* Infection and Immunity, 1996. **64**(11): p. 4472-4479.

131. Brockmeyer, J., et al., *Enterohaemorrhagic Escherichia coli haemolysin is cleaved and inactivated by serine protease EspPα.* Environmental microbiology, 2011. **13**(5): p. 1327-1341.
132. Friedberg, D., et al., *Hierarchy in the expression of the locus of enterocyte effacement genes of enteropathogenic Escherichia coli.* Molecular microbiology, 1999. **34**(5): p. 941-952.
133. Elliott, S.J., et al., *The Locus of enterocyte effacement (LEE)-encoded regulator controls expression of both LEE-and non-LEE-encoded virulence factors in enteropathogenic and enterohemorrhagicEscherichia coli.* Infection and immunity, 2000. **68**(11): p. 6115-6126.
134. Drlica, K. and J. Rouviere-Yaniv, *Histonelike proteins of bacteria.* Microbiological reviews, 1987. **51**(3): p. 301.
135. Workman, J. and R. Kingston, *Alteration of nucleosome structure as a mechanism of transcriptional regulation.* Annual review of biochemistry, 1998. **67**(1): p. 545-579.
136. Anuchin, A., et al., *Histone-like proteins of bacteria (review).* Applied biochemistry and microbiology, 2011. **47**(6): p. 580-585.
137. Allsopp, L.P., et al., *Molecular characterization of UpaB and UpaC, two new autotransporter proteins of uropathogenic Escherichia coli CFT073.* Infection and immunity, 2012. **80**(1): p. 321-332.
138. Allsopp, L.P., et al., *Functional heterogeneity of the UpaH autotransporter protein from uropathogenic Escherichia coli.* Journal of bacteriology, 2012. **194**(21): p. 5769-5782.
139. Totsika, M., et al., *Molecular characterization of the EhaG and UpaG trimeric autotransporter proteins from pathogenic Escherichia coli.* Applied and environmental microbiology, 2012. **78**(7): p. 2179-2189.
140. Münch, R., et al., *Virtual Footprint and PRODORIC: an integrative framework for regulon prediction in prokaryotes.* Bioinformatics, 2005. **21**(22): p. 4187-4189.
141. George, A. and S. Levy, *Gene in the major cotransduction gap of the Escherichia coli K-12 linkage map required for the expression of chromosomal resistance to tetracycline and other antibiotics.* Journal of bacteriology, 1983. **155**(2): p. 541-548.
142. Cohen, S.P., et al., *Cross-resistance to fluoroquinolones in multiple-antibiotic-resistant (Mar) Escherichia coli selected by tetracycline or chloramphenicol: decreased drug accumulation associated with membrane changes in addition to OmpF reduction.* Antimicrobial agents and chemotherapy, 1989. **33**(8): p. 1318-1325.
143. George, A.M. and S.B. Levy, *Amplifiable resistance to tetracycline, chloramphenicol, and other antibiotics in Escherichia coli: involvement of a non-plasmid-determined efflux of tetracycline.* Journal of Bacteriology, 1983. **155**(2): p. 531-540.
144. Asako, H., et al., *Organic solvent tolerance and antibiotic resistance increased by overexpression of marA in Escherichia coli.* Applied and environmental microbiology, 1997. **63**(4): p. 1428-1433.
145. Ariza, R., et al., *Repressor mutations in the marRAB operon that activate oxidative stress genes and multiple antibiotic resistance in Escherichia coli.* Journal of bacteriology, 1994. **176**(1): p. 143-148.
146. Cohen, S.P., H. Hächler, and S. Levy, *Genetic and functional analysis of the multiple antibiotic resistance (mar) locus in Escherichia coli.* Journal of bacteriology, 1993. **175**(5): p. 1484-1492.
147. Simms, A.N. and H.L. Mobley, *PapX, a P fimbrial operon-encoded inhibitor of motility in uropathogenic Escherichia coli.* Infection and immunity, 2008. **76**(11): p. 4833-4841.
148. Gosset, G., et al., *Transcriptome analysis of Crp-dependent catabolite control of gene expression in Escherichia coli.* Journal of bacteriology, 2004. **186**(11): p. 3516-3524.
149. Green, J., et al., *Cyclic-AMP and bacterial cyclic-AMP receptor proteins revisited: adaptation for different ecological niches.* Current opinion in microbiology, 2014. **18**: p. 1-7.

150. Won, H.-S., et al., *Structural overview on the allosteric activation of cyclic AMP receptor protein.* Biochimica et Biophysica Acta (BBA)-Proteins and Proteomics, 2009. **1794**(9): p. 1299-1308.
151. Rossiter, A.E., et al., *Transcription of the plasmid-encoded toxin gene from Enteroaggregative Escherichia coli is regulated by a novel co-activation mechanism involving CRP and Fis.* Molecular microbiology, 2011. **81**(1): p. 179-191.
152. Koch, C. and R. Kahmann, *Purification and properties of the Escherichia coli host factor required for inversion of the G segment in bacteriophage Mu.* Journal of Biological Chemistry, 1986. **261**(33): p. 15673-15678.
153. Travers, A., R. Schneider, and G. Muskhelishvili, *DNA supercoiling and transcription in Escherichia coli: The FIS connection.* Biochimie, 2001. **83**(2): p. 213-217.
154. Kahramanoglou, C., et al., *Direct and indirect effects of H-NS and Fis on global gene expression control in Escherichia coli.* Nucleic acids research, 2010. **39**(6): p. 2073-2091.
155. Rossiter, A.E., et al., *Expression of different bacterial cytotoxins is controlled by two global transcription factors, CRP and Fis, that co-operate in a shared-recruitment mechanism.* Biochemical Journal, 2015. **466**(2): p. 323-335.
156. Schmidt, H., L. Beutin, and H. Karch, *Molecular analysis of the plasmid-encoded hemolysin of Escherichia coli O157: H7 strain EDL 933.* Infection and immunity, 1995. **63**(3): p. 1055-1061.
157. Welch, R., *RTX toxin structure and function: a story of numerous anomalies and few analogies in toxin biology*, in *Pore-Forming Toxins.* 2001, Springer. p. 85-111.

4 OBJECTIVES

As mentioned earlier, ExPEC cause a variety of diseases in humans and livestock, including avian colibacillosis, a major infectious disease in poultry, caused by APEC, and urinary tract infections (UTI) in humans, particularly women. With the identification of the *tagBC* genomic island in APEC and UPEC strains from our lab collection as well as in the published genomes of ExPEC, one could speculate they could contribute to virulence in different hosts. *In silico* analysis of TagB and TagC also shows that they belong to the SPATE family which display different virulence functions in *E. coli* and *Shigella.* Thus, major objectives of this thesis were to characterize these novel SPATEs.

I. To understand the role of novel SPATEs in the pathogenesis of extraintestinal infection of *E. coli* (Article 1)

We used cell culture and murine infection models to determine the contribution of these novel SPATEs in the pathogenesis of ExPEC infection. We checked the phenotypes of these proteins using *in vitro* assays like toxicity, biofilm formation, resistance to serum, hemagglutination capacity and cell adherence.

II. To investigate the role of serine catalytic motif in biological activity (Article 2)

Based upon data from the first article showing the functional role of these SPATEs in adherence, protease activity, and cytopathic effects, we investigated the role of the conserved serine catalytic motif of SPATEs by using site-directed mutagenesis to understand involvement of the serine site in these activities. This provided us with insights into the role of serine catalytic site for the processing of the SPATEs as well as other biological activities.

5 ARTICLE 1: COMBINED ROLE OF SPATES DURING INFECTION

Three new serine-protease autotransporters (SPATEs) from extra-intestinal pathogenic *Escherichia coli* and combined role of SPATEs for cytotoxicity and colonization of the mouse kidney

Authors: Hajer Habouria[1,2#] **Pravil Pokharel**[1,2#], Segolène Maris[1,2], Amélie Garénaux[1,2], Hicham Bessaiah[1,2], Sébastien Houle[1,2], Frédéric J. Veyrier[1,4], Stéphanie Guyomard-Rabenirina[3,4], Antoine Talarmin[3,4], and Charles M. Dozois[1,2,4]

[1] Institut national de recherche scientifique (INRS)-Institut Armand Frappier

[2] Centre de recherche en infectiologie porcine et avicole (CRIPA)

[3] Institut Pasteur de Guadeloupe, Les Abymes, Guadeloupe, France.

[4] Institut Pasteur International Network

[#] These two authors contributed equally as primary authors of this research

Title of Journal: Virulence

Volume 10, 2019 - Issue 1 Pages 568-587 | **Received** 07 Feb 2019, **Accepted** 17 May 2019, **Published online**: 14 Jun 2019

DOI https://doi.org/10.1080/21505594.2019.1624102

Contribution of authors:

P.P. wrote the manuscript for the results of TagB and TagC proteins while **H.H.** wrote the section of Sha protein results. **P.P.** cloned TagB, TagC and EspC while **H.H.** cloned Tsh, Vat and Sha. **C.M.D.** generated Figure 1, ST1, ST2, **P.P.** generated Figure 2, S1, S3, S5 and **H.H.** generated Figure 5, S2 and S4. Deletion of *tagB*, *tagC* and *vat* of QT598 was done by **P.P.** while **H.H.** deleted *tsh* and *sha* genes. All the experiments, data analysis and curation related to TagB and TagC proteins were done by **P.P.** and related to Sha was done by **H.H.** and later results were compiled together. **S.M.** carried out screening of UPEC strains and **P.P.** and **H.H.** did screen of APEC strains for SPATE gene **A.G.** analyzed the PacBio sequencing data of QT598. **F.J.V.** sequenced QT598. **S.G.R.** and **A.T.** provided clinical strains. Animal infections were done by **P.P., H.H., H.B.,** and **S.H.** The manuscript was reviewed and edited by **P.P., H.H., H.B., S.H.** and **C.M.D.**

5.1 Abstract

Serine protease autotransporters of *Enterobacteriaciae* (SPATEs) are secreted proteins that contribute to virulence and function as proteases, toxins, adhesins, and/or immunomodulators. An extra-intestinal pathogenic *E. coli* (ExPEC) O1:K1 strain, QT598, isolated from a turkey, was shown to contain *vat*, *tsh*, and three uncharacterized SPATE-encoding genes. Uncharacterized SPATEs: Sha (*S*erine-protease *h*emagglutinin *a*utotransporter), TagB and TagC (*t*andem *a*utotransporter *g*enes *B* and *C*) were tested for activities including hemagglutination, autoaggregation, and cytotoxicity when expressed in *E. coli* K-12. Sha and TagB conferred autoaggregation and hemagglutination activities. TagB, TagC, and Sha all exhibited cytopathic effects on a bladder epithelial cell line. In QT598, *tagB* and *tagC* are tandemly encoded on a genomic island and were present in 10% of UTI isolates and 4.7% of avian *E. coli*. Sha is encoded on a virulence plasmid and was present in 1% of UTI isolates and 20% of avian *E. coli*. To specifically examine the role of SPATEs for infection, the 5 SPATE genes were deleted from strain QT598 and tested for cytotoxicity. Loss of all five SPATEs abrogated the cytopathic effect on bladder epithelial cells, although derivatives producing any of the 5 SPATEs retained cytopathic activity. In mouse infections, *sha* gene-expression was up regulated by a mean of 6-fold in the bladder compared to growth *in vitro*. Loss of either *tagBC* or *sha* did not reduce urinary tract colonization. Deletion of all 5 SPATEs, however, significantly reduced competitive colonization of the kidney supporting a cumulative role of SPATEs for QT598 in the mouse UTI model.

5.2 Introduction

Escherichia coli is a common commensal of the gastrointestinal tract of mammals and birds and is also a versatile pathogen associated with a variety of intestinal and extra-intestinal infections. Pathogenic *E. coli* belong to two main groups: intestinal pathogenic *E. coli*, and extra-intestinal pathogenic *E. coli* (ExPEC) [1,2]. Among ExPEC, the strains have been classified into pathotypes based on the sites of infection or the animal species they have infected, although these different ExPEC subgroups often share certain traits [3–8]. Such pathotypes include neonatal meningitis *E. coli* (NMEC), uropathogenic *E. coli* (UPEC), and avian pathogenic *E. coli* (APEC) [2,9,10]. Avian pathogenic *E. coli* (APEC) is a subset of ExPEC that causes respiratory infections and septicemia in poultry [4,10–12]. The genomes of a number of APEC strains and their virulence plasmids have been sequenced and share similarities to some human ExPEC isolates and their plasmids [13–18]. The plasticity of the *E. coli* genome has led to the emergence of numerous combinations of genes that can be encoded on genomic islands or harbored on plasmids that can contribute to fitness, adaptability, and virulence of a variety of ExPEC strains [19–21].

APEC and human ExPEC strains share multiple virulence factors that promote survival and colonization of the host during extraintestinal infections. These include fimbriae, iron acquisition systems, autotransporter (AT) proteins, capsular polysaccharides, O-antigens, toxins and secretion systems [1,2,9,11,12]. Most APEC strains also contain conjugative colicin V (ColV) or similar plasmids that encode multiple virulence genes that have been shown to contribute to virulence in poultry [11,22,23], and also to urinary tract infection or systemic infection in rodent models [6,24,25]. The shared battery of virulence genes and the close phylogenetic relatedness of some APEC and human ExPEC strains suggest that some APEC may be potential zoonotic pathogens for humans [6,7,25–28].

Among pathogenic *E. coli* virulence factors, AT proteins comprise a large family that falls into three main categories: SPATEs (Serine Protease Autotransporters of *Enterobacteriaceae*), trimeric AT proteins, and the self-associating autotransporters (SAATs), such as AIDA-1 and Antigen43 (Ag43) [29–31]. AT proteins are exported by the type V secretion system, which can be classified into 5 subgroups: Va for the monomeric autotransporters which includes SPATEs, Vb for the two-partner secretion system, Vc for the trimeric AT, Vd for the ATs that are homologous to both type Va and type Vb, and Ve for the intimins and invasins which have a reverse order of domains [32]. The export process of the AT may also require additional proteins such as the BAM and TAM assembly systems [33,34]. SPATEs consist of three specific domains: (i) a signal peptide which translocates the protein from cytoplasm to periplasm by the Sec-

dependant pathway (ii) a functional passenger domain which contains a conserved serine protease motif (GDSGS), and (iii) a β-barrel domain which is localized in the outer membrane acting as a pore-forming domain that translocates the passenger domain [35]. SPATEs have been grouped into two main classes; class 1 SPATEs consist of cytotoxic proteins, whereas class 2 SPATEs represent immunomodulator proteins [32]. Certain SPATEs including the secreted autotransporter toxin (Sat), vacuolating autotransporter protein (Vat), temperature-sensitive hemagglutinin (Tsh), which has also been called hemoglobin protease (Hbp) [36], and protein involved in colonization (Pic) [37] have been previously reported in APEC and human ExPEC.

The SPATEs comprise a diverse group of autotransporter proteins that contribute to the virulence of pathogenic *E. coli* and *Shigella* spp., and other Enterobacteria [2,22,32,37–43]. Some SPATEs were shown to be important virulence factors in disseminated infection of ExPEC due to their proteolytic activity, which can promote the degradation of host cell substrates and elicit an inflammatory response [32,44]. In ExPEC, SPATE proteins have previously been characterized and have been shown to be associated with infections of both humans and other animals including poultry. SPATEs identified in uropathogenic *E. coli* include Sat [44], Vat [45,46] and PicU [41]. The *sat* gene encodes a vacuolating toxin and *sat* sequences were present in 55% of UPEC strains [40] but were not identified in a collection of APEC isolates [47]. PicU is homologous to the Pic protein identified in *Shigella* and enteroaggregative *E. coli* (EAEC) [37]. *PicU* was found in 22% of UPEC isolates [41] and 9% of APEC strains [47]. The Vat autotransporter was first discovered in APEC [45], was present in 60–70% of ExPEC from human infections [46,48] and 33% of APEC strains [47]. The Vat toxin was shown to contribute to virulence, respiratory infection, and cellulitis in broiler chickens [45]. Both *pic* and *vat* were shown to contribute to the fitness of UPEC in a mouse model of systemic infection [43]. Tsh was the first SPATE identified in *E. coli* [49] and was shown to contribute to the development of respiratory lesions in the air sacs of chickens [22]. The *tsh* gene is located on ColV-type plasmids, was present in 50% of APEC strains [47], is less commonly associated with human ExPEC, but can be associated with certain human ExPEC strains [18,50–52].

In this report, analysis of the genome sequence of an APEC O1 strain, QT598, revealed that it contained 5 distinct SPATEs. Three of these, two chromosomally encoded SPATE genes (we name *tagB* and *tagC*) and a novel plasmid-encoded SPATE gene *(sha)* have not been previously characterized. The remaining two SPATEs were the previously characterized Vat and Tsh proteins. Herein, we have characterized the three novel SPATEs, determined their prevalence

among avian and human urinary tract isolates, and investigated the role of these SPATEs for cytotoxicity and in the colonization of the murine urinary tract.

5.3 Results

5.3.1 Genomic analysis identifies five predicted SPATEs encoded by *E. coli* strain QT598

Strain QT598 was initially isolated from an infected turkey poult in France as MT156 [53]. It is a phylogenetic group B2 strain belonging to serogroup O1, a common serogroup among ExPEC strains causing infections in both poultry and humans. This APEC strain was sequenced initially because it contains most of the known APEC-associated virulence genes and was previously found to be virulent in one-day-old chicks [54]. QT598 belongs to sequence type (ST) 1385. Other strains belonging to ST1385 include other APEC O1 isolates, a canine urinary isolate, and environmental isolates (http://enterobase.warwick.ac.uk/). Interestingly, ST1385 strains are related to other STs including ST91, which contains some strains from human extraintestinal infections and *E. coli* F54, an O18: K1 human fecal isolate sharing many virulence genes found in ExPEC from neonatal meningitis [55].

The genome of QT598 contains five SPATE-encoding sequences (Figure 5.1). The SPATEs were identified by blasting the Tsh protein sequence against the contigs using TBlastN. Two of the SPATE genes, *tsh* and a novel SPATE which we have called *sha* (for **s**erine-protease ***h***emaglutinin ***a***utotransporter), are located on a ColV-type plasmid (pEC598). The *vat* gene was also identified on a genomic island. Finally, a genomic region was identified containing two distinct SPATE-encoding sequences near each other, which we have named *tagB* and *tagC* (for ***t***andem ***a***utotransporter ***g***enes *B* and *C*).

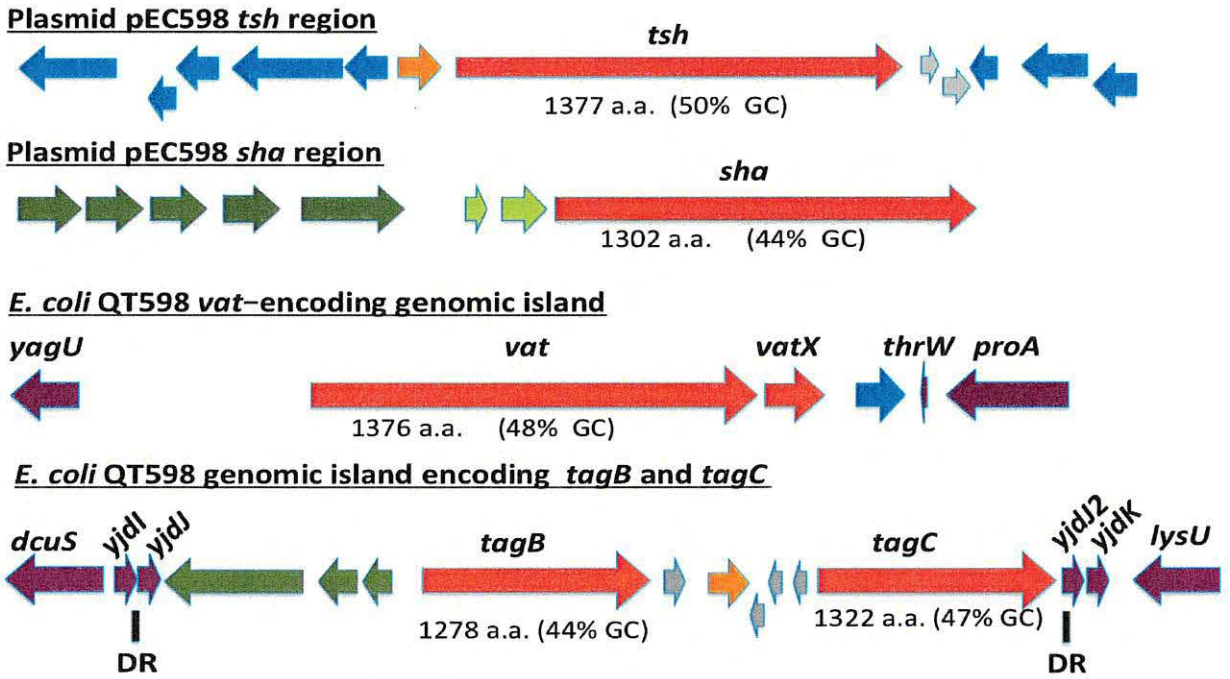

Figure 5.1 Regions containing the five SPATE-encoding genes in *E. coli* QT598

The *tsh* and *sha* genes are located on a ColV-type plasmid (pEC598). The *vat*, *tagB*, and *tagC* genes are located on genomic islands. Arrows indicate open reading frames (ORFs). SPATE encoding ORFs and regulatory gene *vatX* are in red. Predicted full amino acid lengths and GC content of the SPATE ORFs are indicated below arrows. Blue ORFs are related to insertion elements, integrases, or mobile elements. Dark green ORFs are predicted fimbrial proteins. Light green ORFs are predicted EAL-domain proteins. Grey ORFs are hypothetical uncharacterized ORFs. Orange ORFs are hypothetical regulatory proteins. Purple ORFs are genes conserved in *E. coli* K-12 that border the SPATE-encoding genomic regions. Direct repeats (DR) are indicated for the region containing the tag AT genes.

The *tsh* open reading frame on plasmid pEC598 shares the highest identity to *tsh* from plasmid pACN001-B (accession number KC853435.1) [56] and similar sequences in the NCBI database, differing in only 1 nucleotide, a Gly_{1177}- Ser_{1177} substitution. Compared to the characterized Tsh (Hbp) proteins, Tsh from APEC strain χ7122 [22] and hemoglobin protease (Hbp) from ExPEC strain EB1 [36], Tsh_{QT598} contains 4 and 2 amino acid differences, respectively. In QT598, *tsh* is also flanked by sequences related to transposases and insertional sequences (Figure 5.1) that also flank *tsh* on other IncFII plasmids [22,36]. The *sha* gene is also located on pEC598 and has a 44% GC content. Sequence analysis of the *sha* gene revealed an open reading frame (ORF) of 3909 bp encoding a predicted precursor protein of 1302 amino acids with an N-terminal domain signal peptide (residues 1–51), a passenger domain (residues 52–1026) (predicted molecular mass of 105.7 kDa) containing a consensus serine protease motif ^{256}GD**S**GS, and β-barrel domain (residues 1027–1302). Interestingly, the highly conserved SPATE cleavage site of two consecutive asparagines "EV**NN**LNK", found between the passenger domain and the β-barrel of

most SPATEs has a role in the release of the passenger domain from the bacterial cell surface [57], is absent in Sha. Sha is more closely related to Tsh and Vat proteins than to other SPATEs (Figure 5.2). The global alignment of Sha with Tsh_{QT598} has 43% identity/56% similarity with 237 gaps, whereas the global alignment of Sha with Vat_{QT598} is 38% identity/52% similarity with 252 gaps.

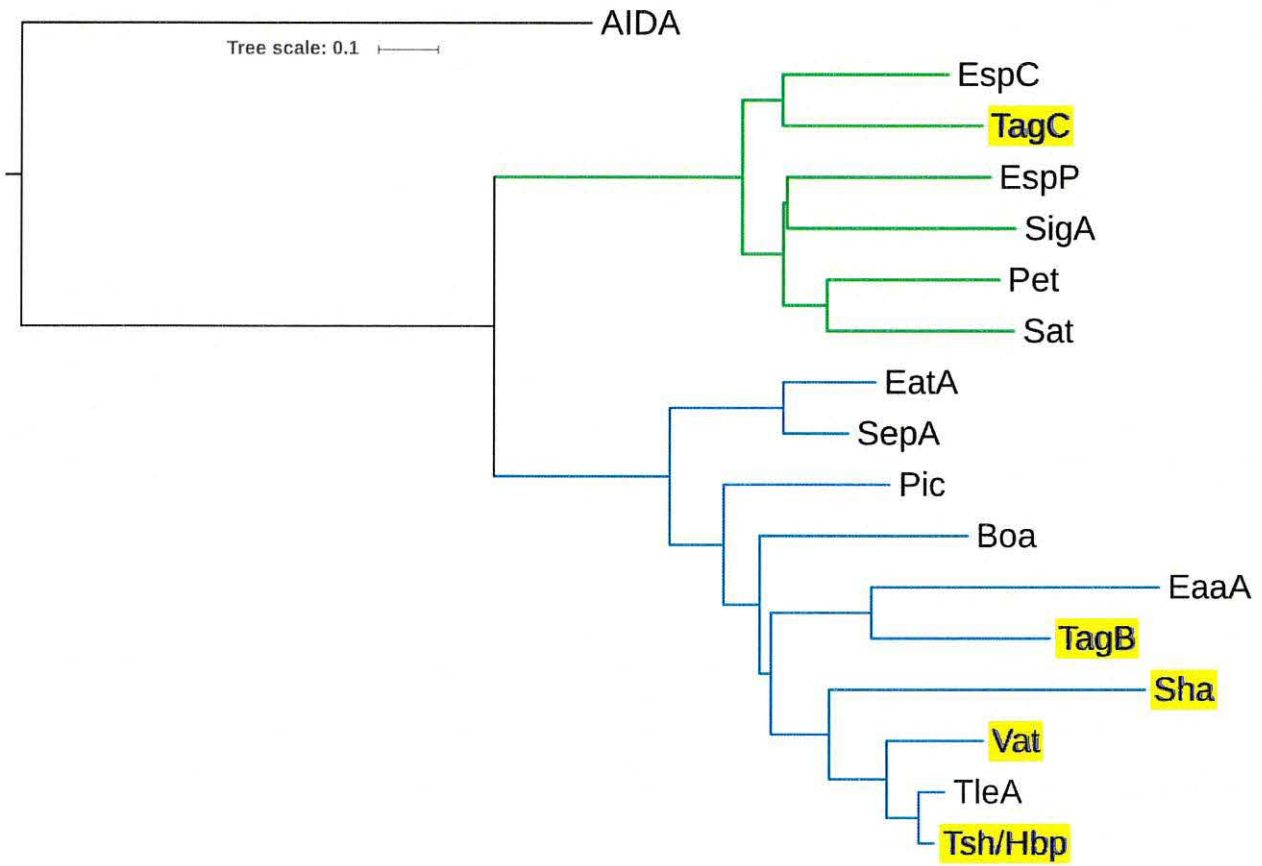

Figure 5.2 Phylogenetic analysis of new SPATEs identified in the QT598 genome

The evolutionary history of passenger domains of QT598 SPATEs (highlighted in yellow) as well as other characterized SPATEs was inferred using the Neighbor-Joining method [98]. The optimal tree with the sum of branch length = 8.78918031 is shown. The tree is drawn to scale, with branch lengths in the same units as those of the evolutionary distances used to infer the phylogenetic tree. The evolutionary distances were computed using the JTT matrix-based method [99] and are in the units of the number of amino acid substitutions per site. The analysis involved 17 amino acid sequences. All positions containing gaps and missing data were eliminated. There were a total of 723 positions in the final dataset. Evolutionary analyses were conducted in MEGA6 [85]. Multiple sequence alignment was performed by Clustal W, and the tree was constructed using the Mega6 software with PhyML/bootstrapping. A cluster of cytotoxic SPATEs (class 1) comprise the green branches, while immunomodulator SPATEs (class 2) are in blue branches. DNA regions encoding SPATE protein sequences are available in NCBI database as follows: EspC, GenBank Accession No. AAC44731, TagB and TagC, MH899681; EspP, NP_052685; SigA, AF200692; Pet, SJK83553; Sat, AAG30168; EatA, CAI79539, SepA, Z48219; Pic, ALT57188; Boa, AAW66606; EaaA, AAF63237; Sha, MH899684; Vat, MH899682; TleA, KF494347; Tsh/Hbp, MH899683.

The *vat* gene from QT598 is present on a genomic island that includes the *vatX* regulatory gene and is located between the *E. coli* conserved genes *yagU* and *proA* adjacent to the *thrW*-tRNA gene (Figure 5.1). This is a conserved insertion site for *vat*-encoding genomic islands [58]. Vat_{QT598} is a predicted 1376 aa precursor with a single substitution (His_{534}-Arg_{534}) compared to Vat from UPEC strain CFT073 (accession number AAN78874.1). At least 41 predicted Vat protein sequences from different *E. coli* strains share an identical predicted Vat_{QT598} sequence, indicating it is a common allelic variant of Vat (Supplemental Table 1). These entries include sequences from strains isolated from fecal samples and infections of poultry and two human UTIs that are labeled as "Hbp" or "SepA" proteins in the databank.

The two new chromosomal encoded SPATE genes were named *tagB* and *tagC*, **T**andem **a**utotransporter **g**enes (Tag) because of their tandem co-localization in the genome of QT598 as well as in various other *E. coli* strains such as multidrug-resistant CTX-M-15-producing ST131 isolate *E. coli* JJ1886 (Accession number CP006784), porcine *E. coli* PCN033 (Accession number CP006632), and *E. coli* CI5 (Accession number CP011018). The *tagB* and *tagC* SPATE-encoding genes from QT598 are located on a genomic island between the *E. coli* conserved genes *yjdI* and *yjdK* (Figure 5.1). Given the TagBC genomic region is absent in *E. coli* K-12 strains, flanked by direct repeat (DR) sequences that correspond to duplication of *yjdJ* sequences bordering each side of the genomic island (Figure 5.1) and the genomic island has a mean GC content of 41%, which is considerably lower than the 50% GC of *E. coli*, it appears that this island was acquired via horizontal gene transfer. Related genomic islands containing similar SPATE encoding genes at this insertion site are present in other *E. coli* genome sequences including antibiotic-resistant strains isolated from the urinary tract and other infections in humans (Supplemental Table 2). The predicted TagB and TagC proteins share the closest identity to the EaaA [59] and EspC [60], respectively (Figure 5.2). TagB shares 46% identity/63% similarity to EaaA with 84 gaps over its full length. TagC shares 60% identity/74% similarity to EspC with 22 gaps. TagB comprises a predicted signal peptide (residues 1–58), a passenger domain from residues 59–1006 (predicted molecular mass of 101 kDa) containing a consensus serine protease motif ^{253}GDSGS, and a β-barrel domain from residues 1007–1283. TagC comprises a predicted signal peptide (residue 1–53), a passenger domain from residues 55–1032 (predicted molecular mass of 105.14 kDa) with a consensus serine protease motif ^{250}GD**S**GS, and β-barrel domain ranging between 1033 and 1309 residues. Both TagB and TagC contain the conserved twin asparagine (N-N) residues in the linker domain connecting passenger and β-barrel domains, EIN^{1006}NLNDRM and EVN^{1032}NLNKRM, respectively.

5.3.2 Prevalence of new SPATE genes in human uropathogenic and avian pathogenic *E. coli*

To determine the distribution of the SPATE sequences among *E. coli* clinical isolates, the presence of these three new SPATE sequences as well as *vat* and *tsh* were detected by PCR in a collection of UPEC isolates from Guadeloupe (697 isolates) [61] and from avian pathogenic *E. coli* (299 isolates) [22]. For the UPEC isolates, *tagB* sequences were present in 70 isolates (10%), whereas *tagC* sequences were present in 80 isolates (11.5%). Interestingly, 96.8% (69/70) of the *tagB*-positive isolates were also *tagC*-positive. Furthermore, 68 of the *tagB* isolates belonged to phylogenetic group B2, with one isolate from group B1 and one untypable isolate. The 11 isolates that contained *tagC* but not *tagB* sequences belonged to groups other than B2: B1 (3 isolates), D (3 isolates), F (4 isolates), or A (1 isolate). *Sha* was the least common sequence and was present in only 6 UTI isolates (0.9%), all of which belonged to group B2 and were also *vat*-positive. Five of the *sha*-positive strains also contained *tagB* and *tagC*, whereas *vat* and *sat* sequences were more common and found in 333 isolates (47.8%) and 217 isolates (31.1%), respectively. The *tsh* gene was present in 41 UPEC isolates (5.9%). In summary, in UPEC, *tagB* and *tagC* were found together in a subset of strains belonging to phylogenetic group B2, although some strains belonging to other phylogenetic groups were only *tagC* positive.

With regards to the APEC strains, *tagB* sequences were present in 14 isolates (4.7%) and *tagC* sequences were present in 21 isolates (7%). All 14 *tagB*-positive APEC were also *tagC*-positive, and 13/14 of these belonged to phylogenetic group B2. Among these, 10 strains belonged to serogroup O1, 1 was serogroup O78, and 3 were of undetermined serogroup. Interestingly, among the 299 APEC strains that were screened, comprised of 109 from chickens, 175 from turkeys, and 15 from ducks, all the *tagB* or *tagC*-positive isolates were exclusively from infections in turkeys. Overall, like UPEC, *tagB*, and *tagC* were specifically present in a subset of APEC strains, mainly belonging to group B2, although some strains belonging to other phylogenetic groups only contained *tagC* sequences.

The *sha* sequences were present in 61 APEC strains (20%). The majority, 42 strains, belonged to phylogenetic group A, 11 strains belonged to group B1, 5 strains belonged to group B2, and 3 strains belonged to group D. Among these *sha*-containing strains, 35 belonged to serogroup O78, 3 were from serogroup O1, 2 strains each belonged to serogroups O11, O54, O21, and O8, and

one belonged to serogroup O55. The remaining 12 strains were from undetermined serogroups. The *sha* gene is, therefore, clearly more prevalent among APEC than UPEC in the subset of strains we analyzed. This could be due to the association of the *sha* gene with the ColV plasmid.

5.3.3 Cloning and production of SPATEs in culture supernatants

All five of the predicted SPATE-encoding genes and promoter regions were cloned to determine their expression and for use in a variety of phenotypic tests. Each of the five SPATE genes, when cloned into *E. coli* BL21, produced a high-molecular-weight protein (>100 kDa) in culture supernatants that corresponded to the expected product (Figure 5.3). In addition, derivatives of strain QT598 wherein these SPATE-encoding genes were inactivated were generated. Analysis of supernatant fractions of QT598, by SDS-PAGE, revealed the presence of SPATE proteins expressed under laboratory conditions, as demonstrated by visualization of bands with a high molecular mass (>100 kDa) secreted in the external milieu. By contrast, no such bands were observed in the supernatant extracts of the SPATE-free, Δ*5ATs*, derivative of QT598 (Figure 5.3). The purity of concentrated supernatant filtrate was also evaluated by silver staining (Supplemental Figure S1). Protein bands of the newly identified SPATEs were extracted from gels and sampled by mass spectrometry for peptide analysis following trypsin digestion (Supplemental Figure S2). For Sha, peptides corresponding to the mature secreted protein spanned from amino acids 52 to 1009. Despite not containing the twin asparagine (N-N) cleavage site present in most SPATEs, peptide profiles suggest the cleavage site from the β-barrel domain likely resides within the 1010–1020 region. This region contains two adjacent polar amino acids, Ser1015, and Asp1016, that may serve as the cleavage site. For TagB, peptide scans suggest that the mature secreted protein spans from amino acids 54 to 1006 based on the twin Asp1006-Asp1007 location. For TagC, peptide scans suggest that the mature secreted protein spans from at least amino acid 60 to 1026 with a predicted twin Asp1032-Asp1033 cleavage site. As expected, peptides corresponding to the predicted amino-terminal signal peptides and the carboxy-terminal predicted β-barrel domains of the Sha, TagB, and TagC SPATEs were not identified from peptide analysis of the secreted proteins (Supplemental Figure S2).

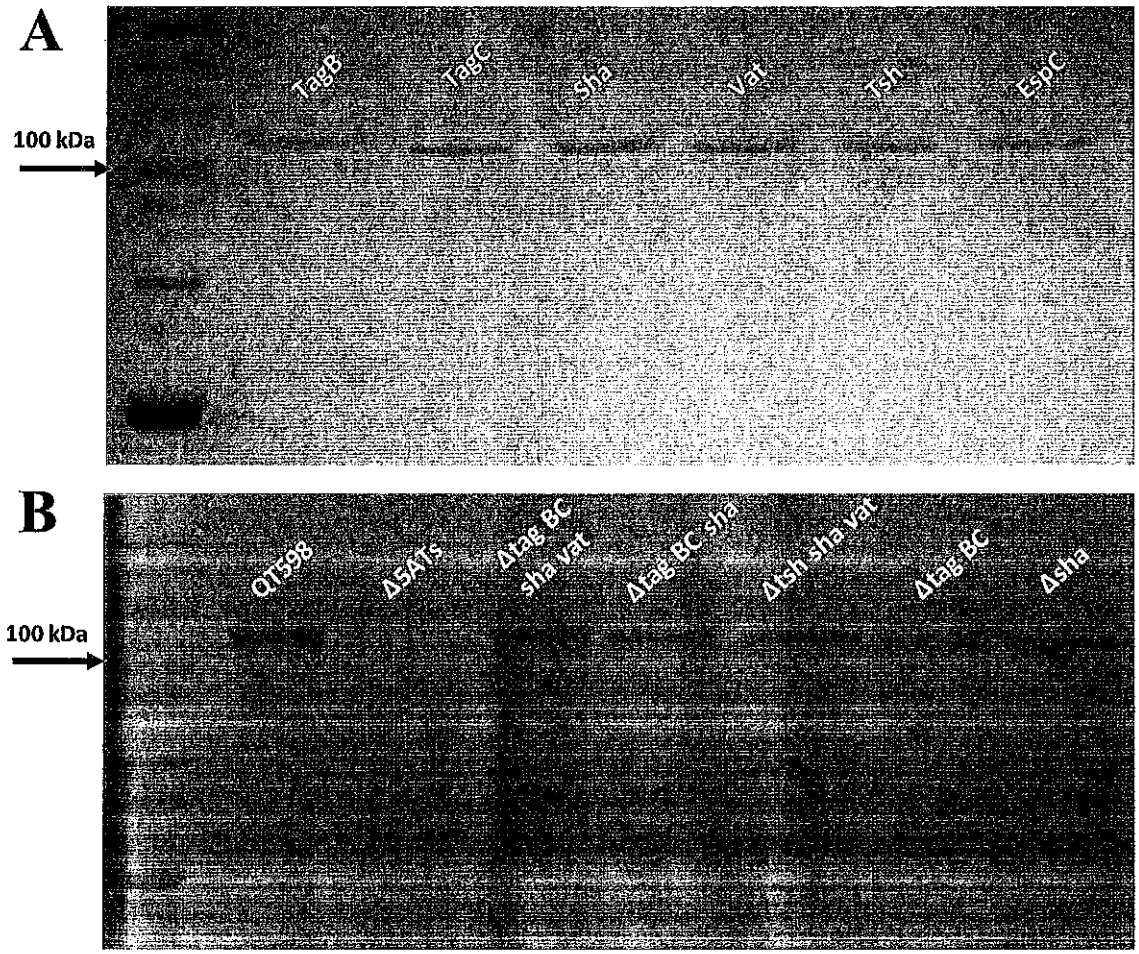

Figure 5.3 Detection of SPATE proteins by SDS-PAGE

A. SDS-PAGE analysis of cloned SPATE genes. Clones expressing SPATE proteins were produced in the BL21 background with high-copy plasmid pBCsk+. Supernatants were filtered then concentrated through Amicon filters with 50 kDa cutoff. Samples containing 5 µg protein were migrated with protein marker (10–200 kDa) and stained with Coomassie blue (arrow represents 100 kDa size marker). B. Detection of SPATEs from supernatants of strain QT598 and various SPATE gene mutant derivatives. Supernatants from an overnight culture of the respective mutants were filtered, concentrated and run on SDS-polyacrylamide gels and stained with Coomassie blue to visualize proteins.

5.3.4 Cleavage of oligopeptides by SPATE proteins

To determine the protease substrate cleavage specificity of the new SPATEs, we used synthetic polypeptides conjugated with *p*NA at the C-terminus. Purified proteins from supernatants of each SPATE were incubated with N-Succinyl-Ala-Ala-Ala-p-nitroanilide (elastase substrate), N-Benzoyl-L-arginine 4-nitroanilide (trypsin substrate) and N-succinyl-ala-ala-pro-phe-p-nitroanilide (chymotrypsin substrate) (Sigma-Aldrich, St. Louis, MO, USA). TagB and TagC demonstrated trypsin-like activity and efficiently cleaved N-Benzoyl-L-arginine 4-nitroanilide, similarly to the EspC protein (Figure 5.4). By contrast, Sha demonstrated significant elastase-like activity toward

N-Succinyl-Ala-Ala-Ala-p-nitroanilide, as did the Vat and Tsh proteins (Figure 5.4). The cleavage activity of high-molecular-weight supernatant fractions from WT strain QT598 and SPATE mutant derivatives was also determined (Figure 5.4). QT598 demonstrated both trypsin-like and elastase-like activity, whereas the Δ*5ATs* mutant had lost these activities. By contrast, a strain that had lost only *tagBC* demonstrated only elastase-like activity conferred by *vat, tsh*, and *sha* (Figure 5.4). In addition, pre-incubation of these supernatants with PMSF eliminated or sharply inhibited oligo-peptide cleavage indicating the activity demonstrated was due to the SPATE proteins produced by the strains (Supplemental Figure S3)

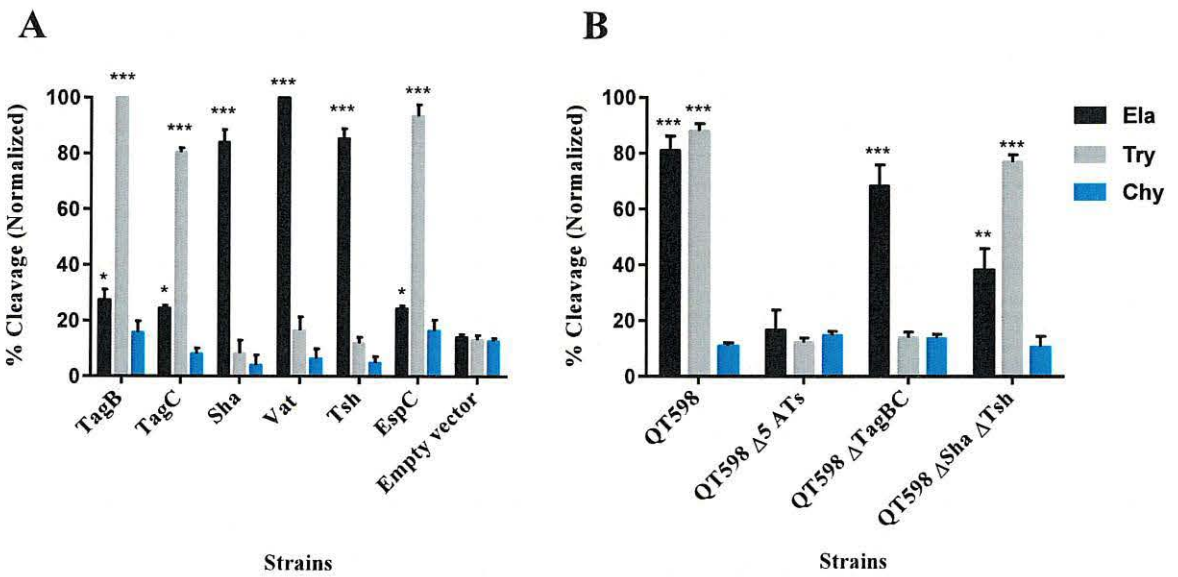

Figure 5.4 Oligopeptide cleavage profiles of SPATEs

A. Enzymatic activity of cloned SPATEs. Five µg of each SPATE-containing supernatant was incubated at 37°C for 3 h with 1mM of synthetic oligopeptide specifically recognized by the following enzymatic activities: Elastase (Ela)-(N-Suc-Ala-Ala-Ala-pNA); Trypsin (Try)-(N-Ben-L-arginine-pNA); or Chymotrypsin (Chy)-(N-Suc-Ala-Ala-Pro-Phe-pNA). Absorbance at 410nm was normalized to the maximum absorbance value. B. Enzymatic activity of supernatants from strain QT598 and SPATE gene mutant derivatives. Samples were tested as described above. Data are the means of three independent experiments, and error bars represent the standard errors of the means (*p < 0.05, **p < 0.01, ***p < 0.001 one-way ANOVA with multiple comparisons vs pBCsk+ (A) or QT598Δ*5ATs* (B)).

Multiple alignment of the new autotransporters with other SPATEs places TagC within the class 1, cytotoxic and enterotoxic SPATEs, along with the EspC SPATE from Enteropathogenic *E. coli* (EPEC) (Figure 5.2). EspC was previously shown to cleave spectrin, Factor V, pepsin and hemoglobin [42,62] and as with TagC and TagB, similarly demonstrated trypsin-like protease activity (Figure 5.4). The SPATE sharing closest identity to TagB is the class 2 SPATE EaaA, identified from commensal *E. coli* ECOR-9 [59] (Figure 5.2). Sha shares more identity to class 2

SPATEs Tsh/Hbp (66% identity) [36,63], TleA (60% identity) [64] and Vat (56% identity) [45]. As such, Sha is likely to share other properties more similar to Tsh (adhesin, hemagglutinin) and Vat (cytotoxin), and the elastase-like substrate specificity of Sha, also shown for Tsh and Vat, is in line with this.

To predict the 3D structure of the passenger domain of new SPATEs, we used the I-Tasser program to generate a 3D structure model and UCSF chimera to compare structures [65,66]. We found that the Sha protein is also predicted to contain the small domain 2 that was identified in Tsh/Hbp and was considered to be characteristic of class 2 SPATEs [32] (Figure 5.5). This domain was however absent in predicted models of TagB and TagC (Supplemental Figure S4).

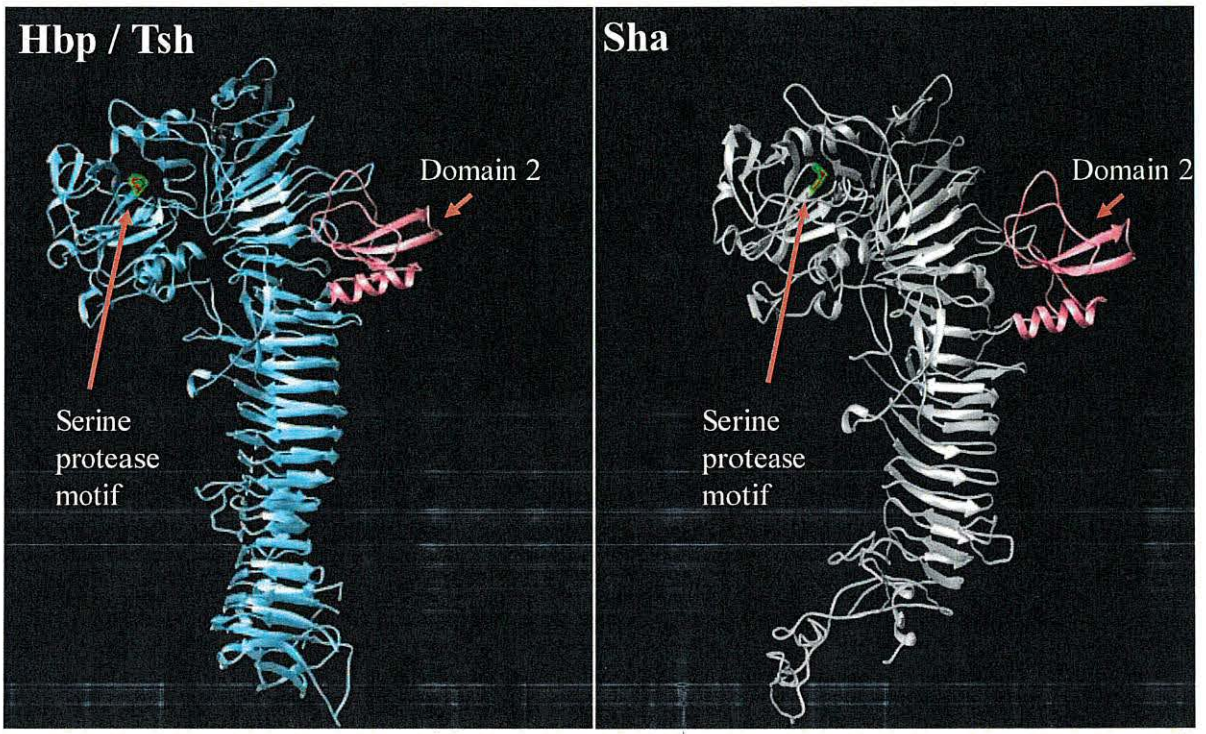

Figure 5.5 Predicted three-dimensional structure of the Sha SPATE passenger domain

Crystal structure of the Heme-binding protein (Hbp) (PDB 1WXR), which is near identical to Tsh, was used to model a homologous structure based on alignment with the Sha protein sequence. The model was generated using the I-TASSER server with 100.0% confidence by the single highest scoring template. Sha is shown to harbor a conserved domain, domain 2 (shown in pink), which is characteristic of class 2 SPATEs.

5.3.5 Increased adherence to epithelial cells is mediated by SPATEs

Some AT proteins can promote adherence to host cells [31,67]. To investigate this with TagB, TagC, and Sha, the different SPATE encoding genes were cloned in the *fim*-negative *E. coli* K-

12 strain ORN172 and tested for increased adherence to avian fibroblasts (CEC-32), human kidney (HEK-293) and bladder (5637) epithelial cells (Figure 5.6). Clones expressing either TagB, TagC, Sha, or Vat adhered significantly to kidney cells, whereas Tsh and EspC did not significantly increase adherence (Figure 5.6 A). For the bladder cells, all SPATEs tested except for Vat and EspC significantly increased adherence (Figure 5.6 B). By contrast, for avian fibroblasts, only TagB and TagC increased adherence (Figure 5.6 C). These cell culture-based results suggest that TagB, TagC, and Sha, as well as Vat and Tsh, may contribute to host cell interactions in the urinary tract, and that TagBC may also contribute to adherence to tissues in poultry. Although some individual SPATEs were shown to increase adherence to host cells, loss of all 5 SPATEs did not reduce adherence of strain QT598 (Supplement Figure S5). This could be due to a great deal of redundancy of function with multiple adhesin outer membrane proteins like type 1 fimbriae, afimbrial adhesins (QT598 Δ5SPATEs didn't lose adherence in presence of mannose) etc.

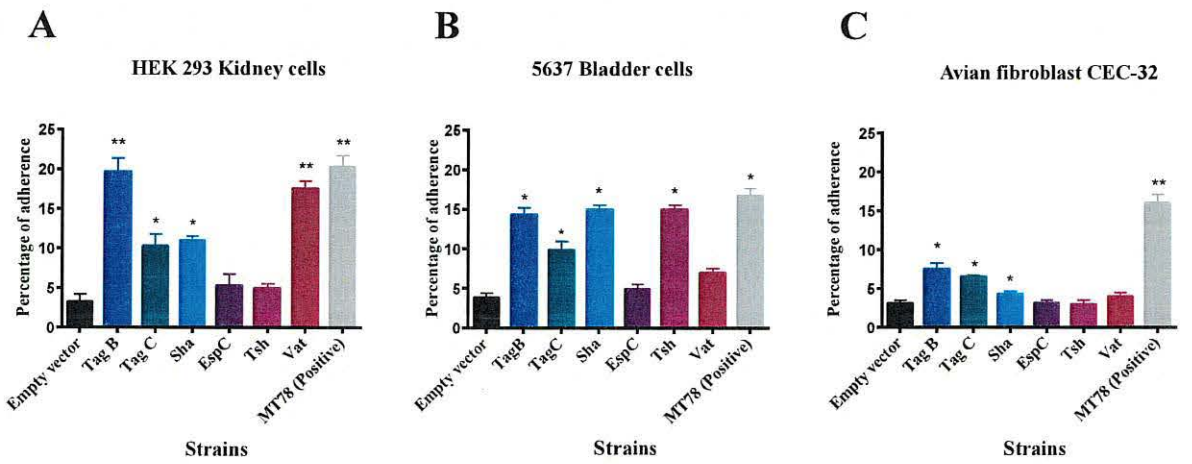

Figure 5.6 TagB, TagC, and Sha SPATEs promote adherence to the human kidney (HEK-293) and bladder (5637) epithelial, and avian fibroblast (CEC-32) cell lines.

Cell monolayers were infected with *E. coli fim*-negative ORN172 expressing SPATE proteins at a multiplicity of infection (MOI) of 10 and incubated at 37°C at 5% CO_2 for 2 h. Adherent bacteria were enumerated by plating on LB agar. Empty vector (pBCsk+) was used as a negative-control and APEC MT78 [80] as a positive control for adherence to cell lines. Data are the averages of three independent experiments. Error bars represent standard errors of the means. (*p < 0.05, **p < 0.01, ***p < 0.001 vs empty vector by one-way ANOVA).

5.3.6 Sha, TagB, Vat, and Tsh are hemagglutinins

Tsh has been previously shown to hemagglutinate chicken and sheep erythrocytes [22,49,68]. To assess whether other SPATEs also show hemagglutinin activity, we verified hemagglutination by the different SPATEs with erythrocytes from a variety of species. Interestingly, Sha, Tsh, and Vat

all demonstrated hemagglutinin activities against sheep, bovine, pig, dog, chicken, turkey, rabbit, horse, and human blood (type O and A groups). In addition, TagB and TagC hemagglutinated sheep, bovine and pig erythrocytes, but not human, turkey, rabbit, dog, chicken, or horse erythrocytes (Table 5.1). However, the titer for TagC was very low for any erythrocytes tested and EspC demonstrated no hemagglutination.

Table 5.1 Hemagglutination activities of different SPATEs

	Erythrocytes – species (titer dilution) [a]								
SPATEs	**Sheep**	**Bovine**	**Pig**	**Chicken**	**Turkey**	**Rabbit**	**Horse**	**Dog**	**Human**
Vat	6	5	4	3	3	7	4	7	7
Tsh	8	7	6	7	4	7	7	7	7
Sha	6	3	5	6	4	3	3	5	5
TagB	6	3	3-4	-	-	-	-	-	-
TagC	+/-	1	+/-	-	+/-	-	-	-	-
EspC	-	-	-	-	-	-	-	-	-
pBCsk+ Vector only	-	-	-	-	-	-	-	-	-

a- Clones expressing SPATEs in *E. coli* ORN172 were adjusted to an O.D.$_{600nm}$ of 0.6 and then concentrated 100-fold. Samples were then diluted two-fold in microwell plates containing final suspensions of 3% erythrocytes from different species. Titers are the average maximal dilution showing agglutination. Both human A and O blood gave similar titers. 0–1: little or no detectable agglutination. See Methods section for details.

5.3.7 TagB, TagC, and Sha mediate autoaggregation, but only Sha increases biofilm formation

Some AT proteins such as AIDA-1 and Ag43 mediate cell-cell interactions and autoaggregation, which can contribute to virulence and facilitate host cell adherence [69–71]. We observed that the absorbance of clones expressing Sha, TagB, and TagC dropped rapidly like the positive control AIDA-1(Figure 5.7). An aggregative adherence pattern was also observed on interaction with

bladder epithelial cell culture (Figure 5.7). As these SPATEs demonstrated autoaggregation, we were interested to know if these plasmids could also confer autoaggregation to ExPEC QT598. However, the introduction of these plasmids did not lead to an autoaggregation phenotype in QT598 (Figure 5.7). In the wild type QT598 background, absence of autoaggregation phenotype could be due to the masking of potential cell interactions by other bacterial surface structures like capsule, fimbriae, flagella etc.

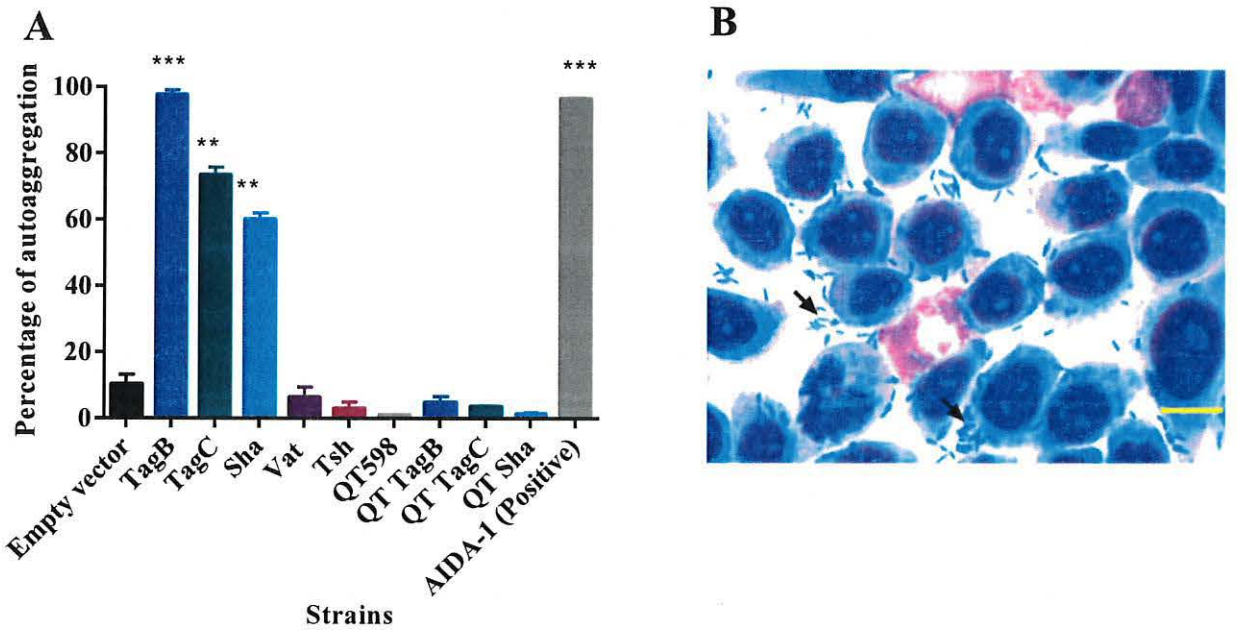

Figure 5.7 TagB, TagC, and Sha are autoaggregating proteins

A. Clones of *E. coli fim*-negative strain ORN172 expressing SPATE proteins were grown 18 h and adjusted to OD_{600} of 1.5 and left to rest at 4°C. Samples were taken at 1 cm from the top surface of the cultures after 3 h to determine the change in OD_{600}. Assays were performed in triplicate, and the rate of autoaggregation was determined by the mean decrease in OD after 3 h. The autoaggregation phenotype was absent when plasmids expressing *tagB*, *tagC*, or *sha* were introduced into APEC strain QT598 (QT TagB, QT TagC, QT Sha respectively). Empty vector (pBCsk+) was used as a negative control and the AIDA-1 AT as a positive control for autoaggregation. Error bars represent standard errors of the means (*p < 0.05, **p < 0.01, ***p < 0.001 compared to empty vector using one-way ANOVA). B. Giemsa stain of the 5637 bladder cell line infected with a *tagB* expressing clone after 2 h demonstrates an aggregative adherence pattern to bladder cells (arrowhead). A similar pattern was found for *tagC* and *sha* expressing clones (not shown here). Bar represents 50 µm.

Proteins involved in autoaggregation can also increase biofilm formation [69]. We, therefore, checked the biofilm-forming capacity of these new SPATE clones at different temperatures (25°C, 30°C, 37°C, and 42°C). TagB and TagC did not increase biofilm formation. However, Sha, Vat, and Tsh significantly increased biofilm production at lower temperatures (25°C and 30°C), but no significant differences in biofilm production were observed at higher temperatures of 37°C and 42°C (Figure 5.8). Thus, the presence of autoaggregation and biofilm phenotypes of SPATEs in

K-12 background is not surprising because of lack of additional molecules decorating its cell surface, whose presence in wild type perhaps potentially interferes with cell interactions.

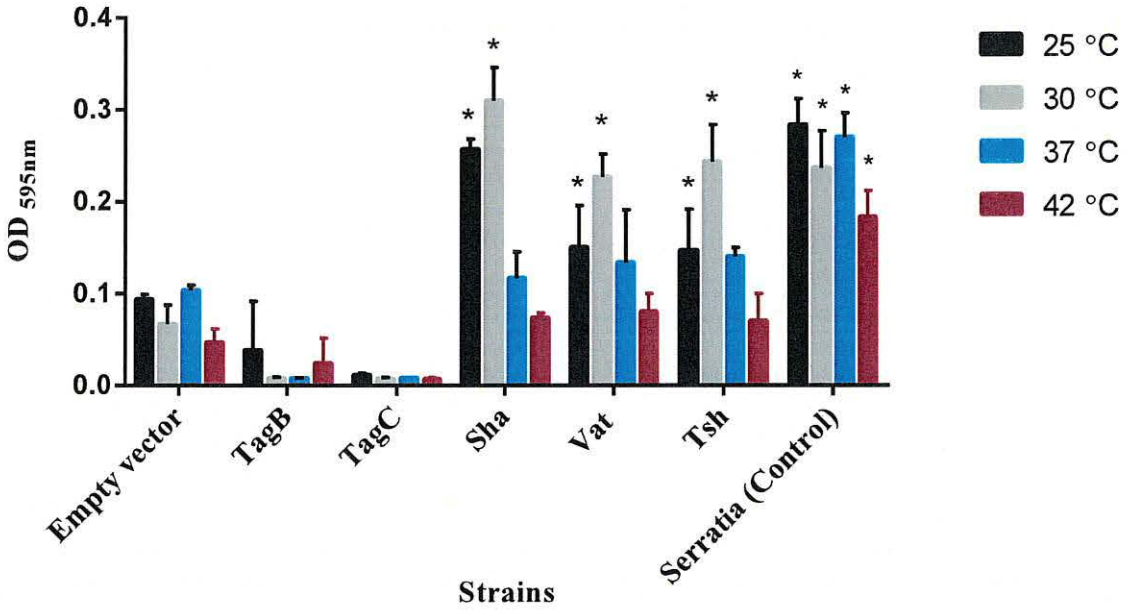

Figure 5.8 Sha, Vat, and Tsh promote biofilm formation

Clones of *E. coli fim*-negative strain ORN172 expressing SPATE proteins were grown at different temperatures (25°C, 30°C, 37°C, and 42°C) in polystyrene plate wells for 48 h and then stained with crystal violet. Remaining crystal violet after washing with acetone was measured as absorbance at 595 nm. Data are the means of three independent experiments, and error bars represent standard errors of the means. Empty vector (pBCsk+) was used as a negative control, and a strong biofilm producing *Serratia* strain [100] served as a positive control for biofilm formation (*p < 0.05, **p < 0.01, ***p < 0.001 compared to empty vector using one-way ANOVA).

5.3.8 Assessment of the cytopathic effect of 5 different SPATEs on bladder cells

Since some SPATEs produce cytopathic activity on host cells, we assessed the cytopathic effect of extracts of supernatants of the different SPATEs as well as the supernatant of wild-type strain QT598 and SPATE-free Δ*5ATs* mutant, on the human bladder 5637 cell line. Incubation of SPATEs from concentrated filtered supernatant (Figure 5.3) of strain QT598 with bladder cells triggered a cytopathic effect, characterized by the dissolution of cytoplasm and enlargement of the nucleus (Figure 5.9), after 5 h of incubation. After 12 h, most of the cells were affected and showed similar morphological changes. These phenotypes were absent upon the treatment with the supernatant of the Δ*5AT* SPATE-free mutant or with culture media alone.

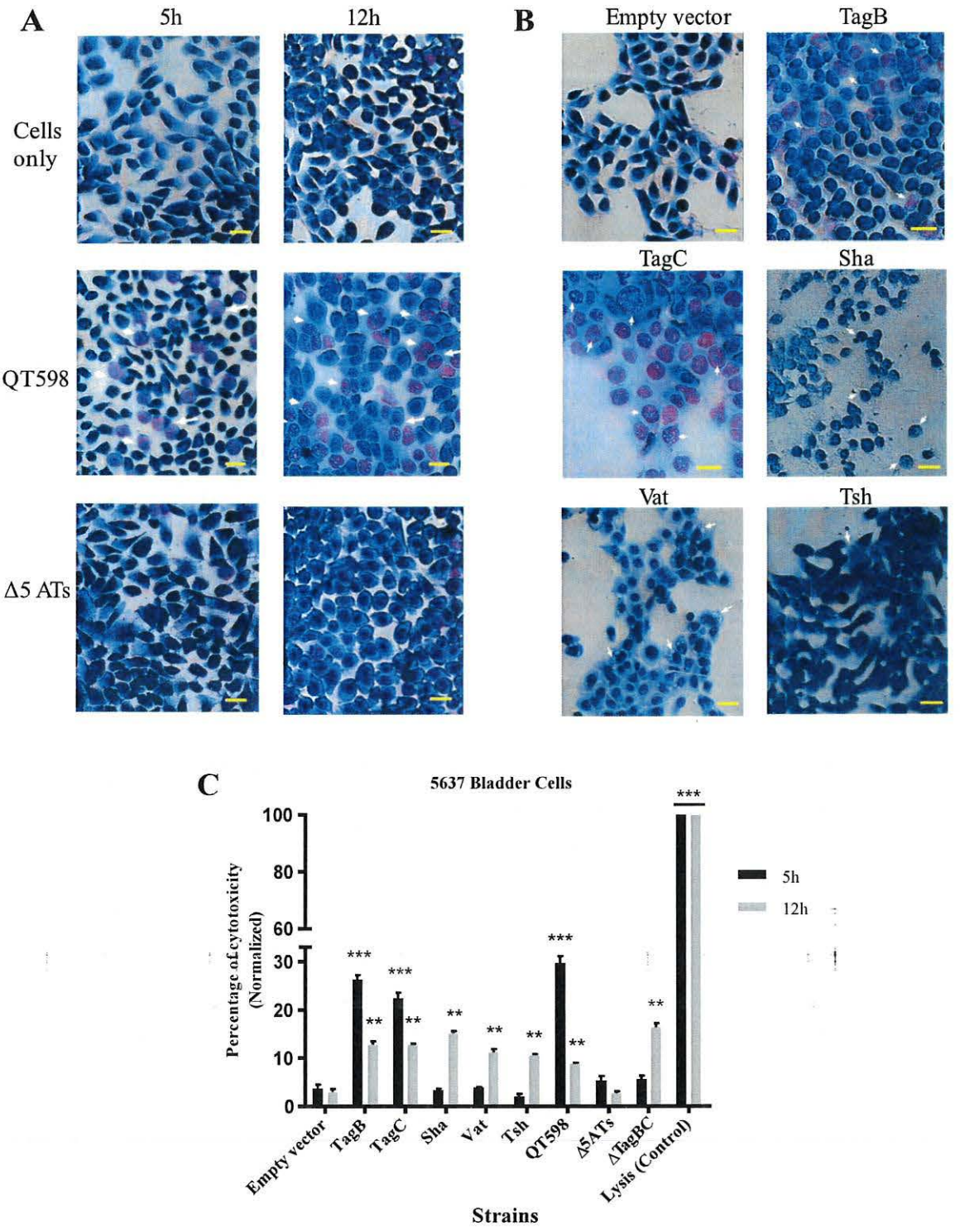

Figure 5.9 All five different SPATEs from strain QT598 induce cytopathic effects

A. Concentrated supernatants (30 µg of protein per well) from wild type QT598 as well SPATE free Δ5*AT*s were incubated with human bladder cell line 5637 for 5 h and 12 h. Cytopathic cells (arrowheads) were found in the

cells treated with QT598 supernatant while there were no morphological changes in the cells treated with supernatant of Δ5*AT*s. B. Concentrated supernatants of *E. coli* BL21 pBCsk+ (30 µg of protein per well) clones overexpressing different SPATEs were incubated with monolayers of 5637 bladder cell lines for 12 h at 37°C. TagB, TagC, Sha, and Vat showed more cytopathic effect (arrowheads) compared to Tsh and empty vector. C. LDH release by 5637 cells after incubation with culture filtrates of different clones (30 µg of protein per well) expressing SPATEs or from supernatants from wild-type *E. coli* strain QT598 and Δ5*AT*s mutant derivatives with 5637 human bladder cells at 37°C for 5 h and 12 h. Empty vector (pBCsk+) was used as a negative control. Lysis solution was added as a positive control for maximum LDH release. Data are the means of three independent experiments, and error bars represent the standard errors of the means (*p < 0.05, **p < 0.01, ***p < 0.001 vs empty vector using one-way ANOVA). Bar represents 50 µm.

Further, we assessed the cytopathic effect of individual SPATEs that were from recombinant clones. Following 12 h of interaction, cells incubated with TagB or TagC proteins elicited distinct cytopathic changes including dissolution of cytoplasm, nuclear enlargement, and vacuolation in the nucleus, cells treated with Sha were rounded, and Vat-treated cells showed numerous vacuoles within the cytoplasm (Figure 5.9). By contrast, cells exposed to Tsh did not show distinct morphological changes. These results suggest that TagB, TagC, Sha and Vat proteases demonstrate cytopathic effects that alter bladder cell morphology, whereas Tsh was less cytopathic to this cell line. We further investigated the cytopathic effect of these SPATEs by measuring the release of lactate dehydrogenase (LDH) after 5 h and 12 h following exposure to supernatant extracts. The release of LDH after 5 h was demonstrated only following exposure to either TagB or TagC (Figure 5.9). Interestingly, although LDH was not detected from samples exposed to Vat, Tsh and Sha after 5 h (Figure 5.9), some LDH release was observed after 12 h of exposure, suggesting these SPATEs may demonstrate a delayed cytotoxic effect. Hence, all 5 SPATEs elicited some cytotoxicity that corresponded with cytotoxic effects that were observed in cells following Giemsa staining. Of further interest, the concentrated supernatant filtrates from ExPEC strain QT598 showed early toxicity comparable to the concentrated supernatant filtrates from *tagB* or *tagC* expressing clones. However, loss of *tagB* and *tagC* resulted in only a late-onset cytotoxic effect at 12 h, and loss of all 5 SPATEs abrogated LDH release at either early or late time points (Figure 5.9). Taken together, these results indicate TagB and TagC can mediate an early (5 h) cytotoxicity, whereas Vat, Tsh, and Sha mediate late-onset (12 h) cytotoxicity, and that these 5 SPATES collectively mediate the overall cytotoxic effects of ExPEC QT598 on bladder epithelial cells.

5.3.9 Cumulative role of SPATEs for colonization during urinary infection in mice

In order to determine the potential role of SPATEs during UTI, we tested isogenic mutants with deletions of the *tagB, tagC*, and *sha* genes in a murine transurethral infection model. We observed no significant differences in colonization of the wild type compared to *tagB,*

tagC or *sha* knockout mutants could be due to functional redundancy of remaining SPATEs (Figure 5.10). To determine the collective role of the SPATEs in UTI for QT598, we deleted all five SPATE encoding genes and did transurethral infections. We again observed no significant difference in the colonization of kidneys or bladder following single-strain infections. By contrast, when a co-infection model was used (1 mouse died after 24 h), the Δ5SPATEs mutant was significantly outcompeted by the wild-type by more than 10-fold in kidneys ($p = 0.0037$) (Figure 5.10).

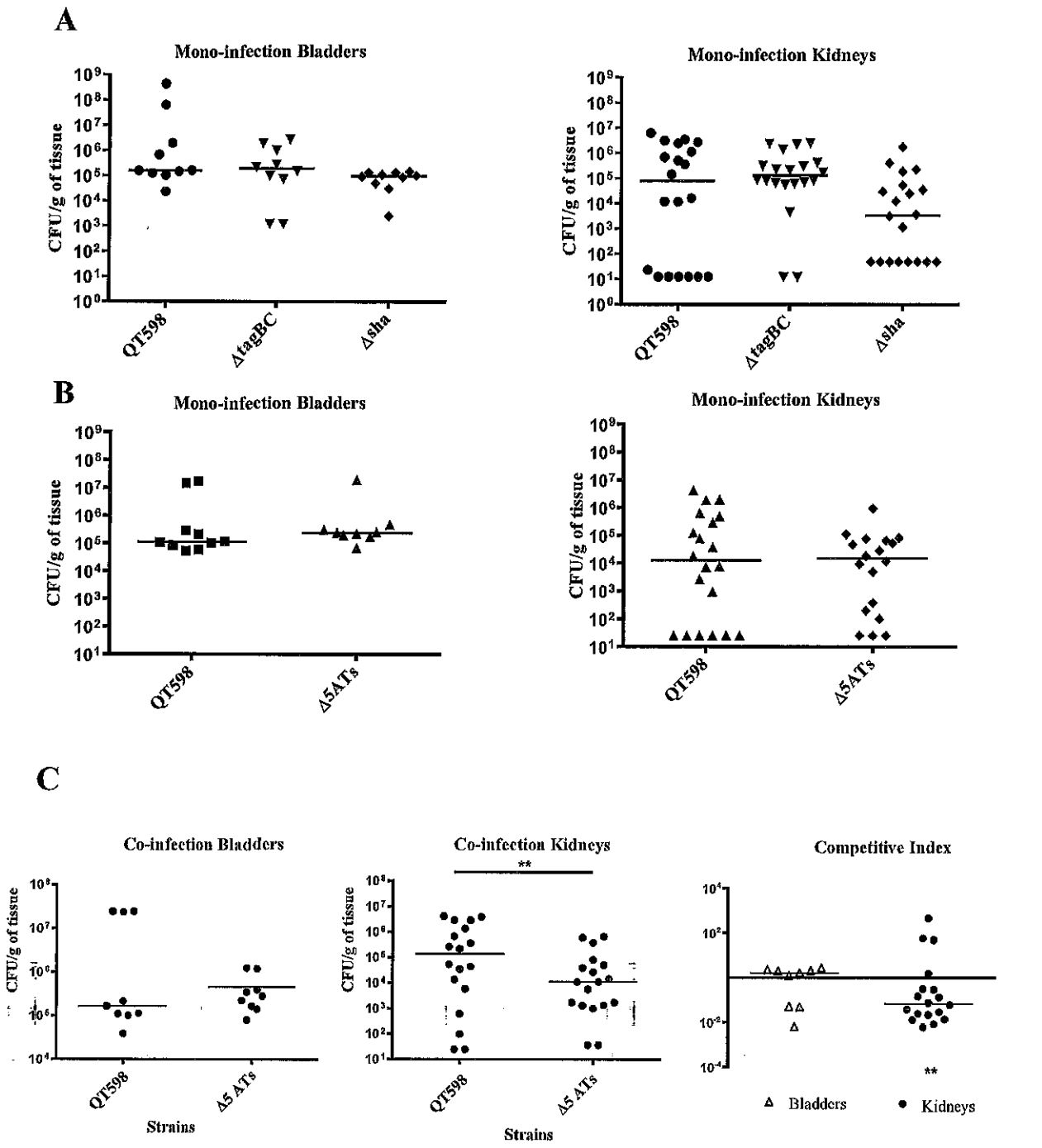

Figure 5.10 Role of SPATEs for *E. coli* QT598 in the murine model of ascending UTI

CBA/J mice were challenged transurethrally with QT598 and isogenic strains Δ*tagBC*, Δ*sha*, or Δ*5ATs* (wherein all 5 SPATE genes are inactivated). Mice were euthanized after 48 h, and bladder and kidneys were harvested for colony counts. A. Single-strain infections to compare wild-type strain QT598 to Δ*tagBC*, Δ*sha* mutants. There were no significant differences in bacterial numbers in either the bladders or kidneys. B. Single-strain infections to compare wild-type strain QT598 to the Δ*5ATs* mutant. Similarly, there were no significant differences in colonization observed. C. Co-infection experiments between the QT598Δ*lac* and the Δ*5ATs* mutant. The Δ*5ATs* mutant colonized the bladder at similar levels to the wild-type (Δ*lac*) strain;

however, the Δ*5ATs* strain was outcompeted in the kidneys by over 10-fold (Data are means ± standard errors of the means of 10 mice (* $p < 0.05$, ** $p < 0.01$, Mann–Whitney Test).

5.3.10 *Sha* gene expression is upregulated during infection in the mouse bladder

The level of expression of SPATE encoding genes from samples grown in different culture conditions as well as from infected mouse bladders was determined. All 5 SPATE genes were expressed in LB medium as well as in minimal M63-glycerol medium. Interestingly, the *vat* gene was upregulated by 10-fold in the minimal medium compared to LB. In bladder samples from infected mice, all the SPATE genes were detected and expressed during infection. Interestingly, the *sha* gene was upregulated 6-fold in the bladder (Figure 5.11). However, expression levels of the four other SPATE genes were not significantly different in bladders when compared to expression during culture in LB.

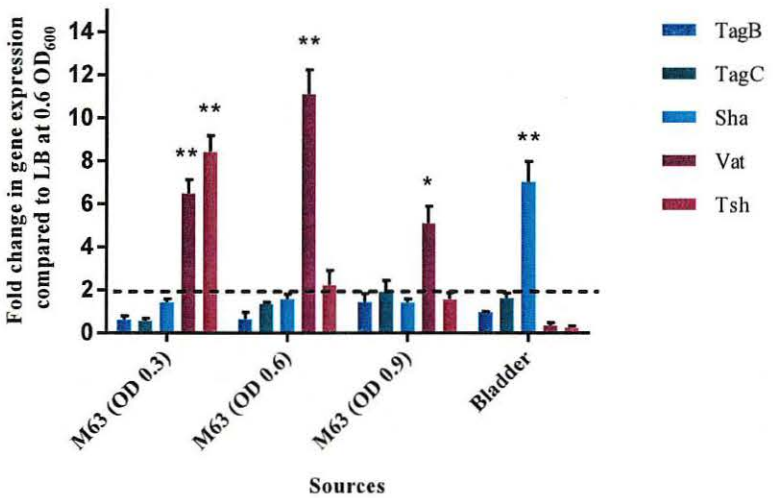

Figure 5.11 Differential expression of some SPATE genes occurs *in vitro* and in mouse bladder

qRT-PCR analysis of SPATE gene transcription from QT598 strain grown in different conditions. Growth in rich medium (LB) to OD_{600} of 0.6 was used as a standard and compared to growth in M63 minimal medium (with glycerol as carbon) at different growth phases (OD_{600} of 0.3, 0.6. and 0.9). RNAs were also extracted from infected mouse bladder. Transcription of *tsh* and *vat* genes were significantly increased in minimal medium. Further, the *sha* gene was shown to be significantly upregulated in the mouse bladder. (*$p < 0.05$, **$p < 0.01$, error bars indicate standard deviations, Student *t*-test). Expression of other SPATE genes was tested under similar conditions. See methods section for details concerning the calculation of gene expression levels. Expressions of other SPATE genes were similar under all conditions tested. The dashed line corresponds to the cutoff for a significant difference in expression.

5.4 Discussion

Some pathogenic *E. coli* produce multiple SPATEs, and this may provide a greater capacity to infect different host species or tissues. Having a combination of SPATEs may also allow a reserve of functions that may include both specific and redundant functions which may importantly be differentially regulated during infection or colonization. UPEC strain CFT073 has 10 autotransporter proteins including 3 SPATEs: Sat, Vat and PicU [41]. *Shigella flexneri* also contains 3 SPATEs: SepA, Pic and SigA [37,72,73]. Similarly, *Citrobacter rodentium*, a model for A/E lesions of EPEC and Enterohemorrhagic *E. coli* (EHEC) also produces 3 SPATEs [74]. The ExPEC strain QT598 we investigated in this report produces a total of 5 SPATEs including three previously uncharacterized members: Sha, TagB, and TagC. Each of the 5 SPATEs demonstrated individual as well as shared properties or functions. Sha, located on a ColV-type plasmid (pEC598), is a class 2 SPATE, and it is closely related to Tsh and Vat proteins. We found this new AT has a modified cleavage site lacking twin asparagine (NN) sites between the passenger domain and the β-barrel. This absence of a typical cleavage site was also seen in *rpeA* (*R*abbit-specific enteropathogenic *Escherichia coli* (REPEC) *p*lasmid-*e*ncoded *a*utotransporter) [75], indicating that the passenger domain is not cleaved from the outer membrane. However, in the case of Sha when cloned in BL21, a band was detected in polyacrylamide gel indicating that the modified cleavage site contributes to the separation of the passenger domain from the β-barrel.

TagB and TagC were found on a genomic island between the conserved *E. coli* genes *yjdI* and *yjdK*. Prevalence of the SPATE sequences among UPEC and APEC demonstrated that *tagB* and *tagC* sequences were present in at least 10% of the UPEC strains and that these genes were largely associated with strains belonging to phylogenetic group B2. Interestingly, genomic islands harboring *tagB* and *tagC* are also present in the genomes of numerous multi-resistant clinical isolates including members of the *E. coli* ST131 pandemic clone such as *E. coli* JJ1877 [76] and many other CTX-producing clinical isolates from urinary tract infections or sepsis (Supplemental Table 2). Further investigation into the potential role of these newly identified SPATE toxins for the virulence of such human ExPEC is therefore warranted.

Although *tagB* and *tagC* were less prevalent in APEC, the strains carrying those genes were mostly O1 strains belonging to phylogenetic group B2 and were all isolated from diseased turkeys. Although *sha* was only present in 1% of UPEC, it was present in 20% of APEC strains. As with Tsh, Sha is plasmid-encoded and these ColV-type plasmids are present in nearly all APEC but are less common in UPEC [77]. Similar phenotypes were observed for the Tsh, Vat, and Sha

autotransporters, including hemagglutination, adherence, protease activity, biofilm formation, and cytopathic effects. As such, the role of these three SPATEs may also be cumulative for some APEC strains.

We assessed the cumulative role of SPATEs in APEC strain QT598 with cell cytotoxicity assays and infection experiments in the murine UTI model. It has been shown that certain APEC strains are highly similar to human ExPEC and can belong to the same clonal groups and contain similar virulence gene profiles [2,6,9,11,12,14,24,25]. Previous reports have also tested APEC strains in the mouse UTI model [78–81]. QT598 is a serogroup O1 strain, which is a common serogroup of both APEC and human ExPEC strains and is clonally related to some human ExPEC, further supporting verification of the role of SPATEs for this strain in a UTI model. QT598 was initially isolated from a young turkey poult and was virulent by subcutaneous infection of 1-day-old chicks. We initially tested QT598 strain in a 3-week-old chicken air sac inoculation model. However, the strain only caused very limited disease and was rapidly cleared in this model. It is possible that the strain is only able to infect very young chicks having immature immunological and physiological systems, or it may be more host specific for infection of turkeys than chickens or our model lacked predisposing conditions like primary viral or mycoplasma infections that could be present in the natural setting. It will be of interest to investigate this in the future.

By cloning each of the SPATE encoding genes in *E. coli* K-12, specific activities of individual SPATEs could be determined. Protease cleavage using oligopeptides demonstrated that Sha, as well as Tsh and Vat, demonstrated elastase-like activity, whereas TagB and TagC demonstrated trypsin-like activity, similar to the EspC autotransporter (Figure 5.4). Oligopeptide degradation was also observed in strain QT598 with TagB and TagC being required for trypsin-like activity, whereas the Class 2 SPATEs contributed to elastase-like activity. As such, the combination of these SPATEs provides an expanded spectrum of protease activity. However, adding a serine protease inhibitor (PMSF) to the supernatant of the SPATEs neutralized their effect on the cleavage of these oligopeptides. Further, when the catalytic site of the ATs was mutated (serine was replaced by alanine) proteolytic activity was absent, indicating that the serine protease motif is important for the activity of these SPATEs (Supplemental Figure S3). Previously, Tsh was shown to be proteolytic to substrates including mucin and factor V, whereas EspC could cleave other proteins such as pepsin and spectrin [62]. This suggests that the combination of SPATEs produced by QT598 can target multiple substrates. It will be of interest to more specifically investigate cleavage of different host substrates by the newly characterized SPATEs Sha, TagB, and TagC to try to identify their mechanisms of interaction with host cells. Adherence to host cell

lines was also increased by the production of SPATEs. In particular, TagB, TagC, and Sha increased adherence to both human and avian epithelial cells, whereas Tsh only increased adherence to bladder cells, and Vat only increased adherence to kidney cells (Figure 5.6). Interestingly, in addition to promoting general adherence to host cells, TagB, TagC, and Sha also mediated bacterial aggregation, suggesting a self-associating phenotype similar to the AIDA-1 autotransporter (Figure 5.7). Although Tsh and Vat were less effective at general adherence to different epithelial cells, these SPATEs as well as Sha were effective hemagglutinins for erythrocytes of a variety of animal species and also demonstrated increased biofilm formation, whereas production of TagB and TagC only conferred limited hemagglutination activity (Table 5.1) and no increase in biofilm formation (Figure 5.8). It is interesting to note that some class 2 SPATEs have been shown to recognize a variety of glycans on leukocyte surfaces [82]. As similar carbohydrates may be present on erythrocyte surfaces, it is not surprising that Sha as well as Tsh and Vat autotransporters demonstrated extensive hemagglutination activity for a variety of erythrocytes. It will be of interest to further determine if these SPATEs can also recognize glycosylated surface receptors on either human or avian leukocytes that may alter host immune function.

Notably, some phenotypes such as autoaggregation, hemagglutination, and biofilm formation were only present when the genes were expressed in high-copy vectors but were absent in the clinical strain. Cloning in a higher copy vector provides a means to constitutively express proteins *in vitro*, whereas these proteins or systems may not always be expressed when in a single copy or on a native plasmid in the clinical strain under *in vitro* growth conditions. Also, in the wild-type clinical strain, there can be a great deal of redundancy of function with multiple proteins (both the autotransporters and other outer membrane proteins and fimbrial adhesins that may similarly mediate hemagglutination to different erythrocytes or adherence to host cells).

Interestingly all the SPATEs demonstrated cytopathic effects on epithelial cells. However, the class 2 SPATEs, Vat, Tsh, and Sha, only caused delayed cell death after 12 h exposure, compared to the TagB and TagC SPATEs that demonstrated cytotoxicity within 5 h of interaction (Figure 5.9). Importantly, loss of all 5 of the SPATE encoding genes from QT598 was required to abrogate the cytopathic effect (Figure 5.9). However, the "slow-acting" cytopathic effect may be due to a less directed or non-specific internalization such as pinocytosis for some of the SPATEs and since this effect only occurs after long-term 12-h exposure it may indicate that the cytotoxic capacity of these SPATEs may be limited and that the roles of such SPATEs may be more specifically linked to other protease functions such as mucinase activity or immunomodulatory

roles as has been proposed as the main function of some of the Class-2 SPATEs. Similarly, a slow effect was seen in the case of EspC, when it was internalized slowly into the cells by pinocytosis, and no receptor was required for this process [83]. Further experiments are in progress to elucidate the cytopathic effects of Sha, TagB, and TagC.

Of further note, loss of all 5 SPATEs resulted in decreased fitness in the kidneys of infected mice (Figure 5.10), whereas loss of individual SPATEs did not have any reduction in virulence or fitness. This suggests that collectively these SPATEs can provide a selective advantage during kidney infection for QT598 in the murine UTI model. The levels of expression of the 5 SPATEs were different depending on the growth conditions – all 5 SPATEs were expressed in LB broth, mass spectrometry results have confirmed that Tsh (48% of coverage) and Vat (22% of coverage) proteins were highly expressed compared to the other SPATE proteins. In minimal M63-glycerol medium, the *vat* gene was upregulated by 10-fold compared to LB, and the *sha* gene was upregulated six-fold in infected bladder compared to culture in LB. These results indicate that SPATE-encoding genes can be subjected to environmental changes that influence their regulation. However, other than the *vat* gene [58], there is very limited information concerning identification of factors that regulate the expression of different SPATEs.

In conclusion, we investigated the role of three new SPATEs in an APEC strain, TagB, TagC, and Sha, which were present in some APEC and UPEC strains. These SPATEs may confer fitness and capabilities to infect multiple hosts. Our findings highlight the potential role of these proteins in virulence and show they significantly contribute to autoaggregation, hemagglutination, adherence to epithelial cell lines and exhibit cytopathic effects. Furthermore, we have shown, in combination, all five ATs contribute to fitness and colonization of QT598 during urinary tract infection in the mouse model. In future studies, it will be of interest to determine mechanisms of action of the TagB, TagC, and Sha autotransporters, identify specific targets and determine the effects of these SPATEs on host immune responses.

5.5 Materials and methods

Strains, media, and PCR screening

Strains and plasmids are listed in Table 5.2. The 697 *E. coli* strains isolated from urinary tract infections were clinical isolates from Guadeloupe. Strains were collected by laboratories or hospitals over a period of 17 months and included community or nosocomial urinary tract infection isolates [61]. The 299 APEC strains were previously described elsewhere [22]. MT156 (QT598) is an APEC serogroup O1 strain that was isolated from the liver of a young turkey poult [53]. *E.*

coli DH5α, ORN172, and BL21 were used for gene cloning and phenotypic tests. Bacteria were grown at 37°C on solid or liquid Luria-Bertani medium (Alpha Bioscience, Baltimore, MD, USA) supplemented with the appropriate antibiotics when required at concentrations of 100μg/ml ampicillin, 30 μg/ml chloramphenicol, or 50 μg/ml of kanamycin. For mice infection studies, QT598 and mutant derivatives were grown in brain heart infusion broth (Alpha Bioscience). M63-glycerol minimal medium contained the following per liter: 5.3 g KH_2PO_4, 13.9 g $K_2HPO_4 \cdot 3H_2O$, and 2.0 g $(NH_4)_2SO_4$. The pH was adjusted to 7.5 with KOH, and the medium was supplemented with 1 mM $MgSO_4$, 1 mM $CaCl_2$, 1 mM thiamine, and 0.6% (wt/vol) glycerol.

Table 5.2 Strains and plasmids used in this study

Strains	Characteristic(s)	References
ORN172	*thr-1 leuB thi-1Δ(argF-lac)U169 xyl-7 ara-13 mtl-2 gal-6 rpsL tonA2 supE44Δ(fimBEACDFGH)::Km pilG1*	[103]
BL21	*fhuA2 [lon] ompT gal [dcm] ΔhsdS*	New England Biolabs
QT1603	HB101 with AIDA-1 operon	[94]
QT598	APEC O1: K, serum resistant	[38]
MT78	APEC O2:K1	[81]
QT4567	QT598 Δ*lacZYA*	This study
QT4726	QT598 Δ*tagBC::kan,* Km^R	This study
QT5187	QT598Δ*tagBC*::FRT	This study
QT5188	QT598Δ*tagBC*Δ*vat::cat,* Cm^R	This study
QT5189	QT598Δ*tagBC*Δ*vat::cat* Δ*sha::kan,* Cm^R Km^R	This study
QT5182	QT598Δ*tagBC*Δ*vat::cat* Δ*sha::kan* Δ*tsh ::tetAR*(B) Cm^R Km^R Tc^R	This study

QT5190	QT598Δ*sha::kan* Δ*tsh::tetAR*(B) Km^R Tc^R	This study
QT5191	QT598Δ*tagBC* Δ*vat::cat* Δ*tsh::tetAR*(B) Cm^R Km^R Tc^R	This study
QT5192	QT598Δ*sha::kan* Km^R	This study
QT5193	QT598Δ*tsh::tetAR*(B) Tc^R	This study
QT12	ORN172/ pBCsk+	This study
QT4750	ORN172 / pIJ551 (Expressing *vat*)	This study
QT4751	ORN172 / pIJ552 (Expressing *tsh*)	This study
QT4767	ORN172 / pIJ553 (Expressing *sha*)	This study
QT5194	BL21 / pIJ548 (Expressing *tagB*)	This study
QT5195	BL21 / pIJ549 (Expressing *tagC*)	This study
QT5197	BL21 / pIJ550 (Expressing *espC*)	This study
QT5198	ORN172 / pIJ548 (Expressing *tagB*)	This study
QT5199	ORN172 / pIJ549 (Expressing *tagC*)	This study
QT5201	ORN172 / pIJ550 (Expressing *espC*)	This study
QT5431	BL21 / pIJ551 (Expressing *vat*)	This study
QT5432	BL21 / pIJ552 (Expressing *tsh*)	This study
QT5433	BL21 / pIJ553 (Expressing *sha*)	This study
Plasmids		
pKD3	Plasmid used for amplification of *cat* cassette	[91]

pKD4	Plasmid used for amplification of *kan* cassette	[91]
pKD13	Plasmid used for amplification of *kan* cassette	[91]
pKD46	λ Red plasmid; Amp^r	[91]
pCP20	FLP recombinase, Amp^r	[91]
pBCsk+	Cloning vector; Cm^r	SnapGene
pIJ548	pBCsk+::*tagB*	This study
pIJ549	pBCsk+::*tagC*	This study
pIJ550	pBCsk+::*espC*	This study
pIJ551	pBCsk+::*vat*	This study
pIJ552	pBCsk+::*tsh*	This study
pIJ553	pBCsk+::*sha*	This study

Multiplex PCR was performed to determine the prevalence of different ATs within clinical isolates using primers listed in Supplemental Table 3. PCR amplification was done in a 25 µl reaction mixture containing 10 mM of primers, 1X of Taq FroggaMix (FroggaBio, Toronto, ON, Canada), DNA templates and deionized water when necessary. To detect *sat, tsh, tagB* and *tagC* genes, the reaction mixture was placed in a thermocycler (Eppendorf, Mississauga, ON, Canada) and set for initial denaturation at 95°C for 2 min followed by 30 cycle of denaturation at 95°C for 30 sec, annealing at 58°C for 40 sec and extension at 72°C for 30 sec. A final extension step was added at 72°C for 5 min. In order to detect *sha* gene, PCR was set for initial denaturation at 95°C for 2 min, 35 cycle of denaturation (95°C, 30 sec), annealing (56°C, 40 sec) and extension (72°C, 1 min), and a final extension step at 72°C for 5 min. To detect *vat* gene, PCR was set for initial denaturation at 95°C for 2 min, 30 cycle of denaturation (95°C, 30 sec), annealing (60°C, 40 sec) and extension (72°C, 30 sec), and a final extension step at 72°C for 5 min. The phylogenetic group of strains was determined by multiplexed PCR as described [84]. Amplified samples were separated by electrophoresis on 0.8% agarose gel stained with gel stain (Civic Bioscience,

Beloeil, QC, Canada) and DNA was visualized using Gel Doc (Syngene Chemi Genius, Frederick, MD, USA) at 400 nm.

DNA and genetic manipulations

Plasmid DNA was extracted using the EZ DNA Miniprep kit (Bio Basic, Markham, ON, Canada). PCR products and DNA were purified using the EZ-10 Spin Column PCR Product Purification Kit (Bio Basic). DNA for SPATE-encoding genes was amplified using Q5 High Fidelity-DNA polymerase (New England Biolabs, Whitby, ON, Canada).

Bioinformatic analysis

Presence of AT sequences *in silico* was determined in *E. coli* genomes available from the NCBI database by Blast analyses using the *tagB, tagC* and *sha* sequences from the QT598 genome. Phylogenetic analyses of the predicted full-length passenger domain sequence of each SPATE were performed by Clustal W, and the phylogenetic tree was constructed using PhyML/bootstrapping in MEGA6 [85]. The Conserved Domain Database (CDD) and SignalP were used to predict the three domains of the AT proteins [86,87]. The I-TASSER server and chimera were used for three-dimensional (3D) structure [65,66] visualization of the predicted Sha AT protein, and the Protein Data Bank (PDB) server was used to obtain the predicted 3-D structure of the Sha protein for comparison to Hbp [88]. Amino acid sequence comparisons were performed using Clone Manager Suite 7 (SciED, Denver, CO, USA) and online BLAST programs available from the National Center for Biotechnology Information (NCBI).

Construction of plasmids

AT-encoding genes with their own native promoters were amplified by PCR using specific primers (listed in Supplemental Table 3). The *tagB, tagC, sha, vat*, and *tsh* genes were amplified from QT598. The *espC* gene was amplified from EPEC strain E2348/69 (Accession number AF297061) [60]. To clone *tagB, tagC, espC, sha, tsh*, and *vat*, PCR products contained 15 bp extensions homologous to the pBCsk+ multi-cloning site. Linearized pBCsk+ digested with *Xho*I and *BamHI* was used to clone inserts by fusion reaction with the Quick-fusion cloning kit (Biotool, Houston, TX, USA). All the recombinant plasmids (pIJ548, pIJ549, pIJ550, pIJ551, pIJ552, pIJ553) were first transformed into *E. coli* DH5α then the plasmids were extracted using a Miniprep kit according to the manufacturer's recommendations (Bio Basic) and transformed into *E. coli* BL21 for protein expression into culture supernatants and into the *fim*-negative *E. coli* strain ORN172 for other phenotypic assays.

Mutagenesis of SPATE-encoding genes

Mutants were generated using the lambda red recombinase method [89]. The *tagBC* genes were first replaced with a kanamycin resistance cassette, from plasmid pKD13 with knock out primers: CMD 2094 and CMD 2095 (Supplemental Table 3). PCR products were electroporated into QT598 containing the lambda red recombinase-expressing plasmid pKD46. Deletion of the *tagB* and *tagC* was confirmed by PCR with screening primers (Supplemental Table 3). The kanamycin resistance cassette, flanked by FLP recombination target (FRT) sequences, was removed by the introduction of plasmid pCP20 expressing the FLP recombinase [90]. Then, the *vat* gene was replaced by a chloramphenicol resistance cassette amplified from pKD4 in the background QT598Δ*tagBC*::FRT (QT5187) using the same approach. Similarly, kanamycin resistance cassette amplified from plasmid pKD3 was used to replace the *sha* gene in QT598 Δ*tagBC* Δ*vat::cat* (QT5188). Finally, the *tsh* gene was replaced with a tetracycline-resistance cassette by allelic exchange as detailed elsewhere [22] in QT598 Δ*tagBC* Δ*vat::cat* Δ*sha::kan* (QT5189) generating the five SPATE genes mutant, Δ5*ATs* mutant (QT598 Δ*tagBC* Δ*vat::cat* Δ*sha::kan* Δ*tsh::tetAR*(B)) (QT5182).

Protein preparation and analysis

Culture supernatants, from LB broth cultures of *E. coli* BL21 expressing AT proteins were centrifuged at 7500 × g for 15 min at 4°C. Supernatants were filtered through 0.22 µm filters and concentrated through 50 kDa Amicon filters (Millipore Sigma, St. Louis, MO, USA). Protein concentrations were determined using the Pierce Coomassie Plus Assay Reagent kit (Thermo Fisher Scientific, St. Laurent, QC, Canada) and proteins were visualized on SDS-PAGE by Coomassie blue as well as silver staining and identified based on the protein markers (10–200 kDa) (Bio Basic). To identify the proteins, bands were excised from denatured gels. Protein digestion by the trypsin, peptide labeling, and mass spectrometry analyses was performed by the proteomics platform of the Institut de Recherche en Immunologie et en Cancérologie (IRIC) of the Université de Montréal (Montréal, QC, Canada). The data were visualized and analyzed using Scaffold 4 Proteomics software.

Oligopeptide cleavage assays

Synthetic peptide cleavage was performed as previously described in [91] with slight modifications. Briefly, 5 µg/ml of each SPATES was added to 200 µl of three different pNA-conjugated oligopeptides: N-Succinyl-Ala-Ala-Ala-p-nitroanilide, N-Benzoyl-L-arginine 4-nitroanilide and N-succinyl-ala-ala-pro-phe-p-nitroanilide (Millipore Sigma) at 1 mM concentration

in a buffer containing 0.2 M NaCl, 0.01 mM$ZnSO_4$, 0.1 M MOPS (3-(N-morpholino) propane sulfonic acid), pH 7.3 were incubated at 37°C for 3 h and absorbance readings were determined at 410 nm. Readings were normalized to the maximum absorbance of positive control. All reactions were performed in triplicate.

Autoaggregation

The autoaggregation test was carried out as described before [92]. Briefly, overnight cultures were adjusted to an OD_{600} of 1.5. A volume of 10 ml of each culture was placed in sterile 20 ml glass tubes. Tubes were then vortexed for 5 s then left at 4°C for 3 h. Samples 1 cm from the top were taken, and the percentage of change in OD_{600} was used as the value for autoaggregation.

Hemagglutination tests

Hemagglutination in microtiter plates was performed as described by [93] with some modifications. Human, chicken, turkey, pig, bovine, canine, rabbit, horse and sheep red blood cells (RBCs) were washed and resuspended in PBS at a final concentration of 3%. The *E. coli fim*-negative K-12 strain ORN172 expressing different SPATEs was grown overnight at 37°C in LB medium, harvested and adjusted to an optical density ($O.D._{600}$) of 60. Suspensions were serially diluted in 96-well round bottom plates containing 20 µl of PBS mixed with 20 µl of 3% red blood cells and incubated for 30 min at 4°C.

Biofilm assay

Biofilm formation on polystyrene surfaces was assessed in 96-well plates as previously described [67]. Strains were grown at various temperatures (25°C, 30°C, 37°C, and 42°C) for 48 h under static conditions in LB medium. Wells were washed and stained with 0.1% crystal violet (Millipore Sigma) for 15 min, then 200 µl of ethanol-acetone (80:20) solution was added, followed by measuring at an optical density at OD_{595}.

Adherence assays

The 5637 human bladder cells (ATCC HTB-9), human embryonic kidney cells HEK-293 (ATCC® CRL-1573™), and the avian fibroblast cell line (CEC-32) were used to determine adherence of *E. coli* ORN172 expressing different SPATEs as described before [94]. The 5637 cells were maintained in RPMI 1640 (Thermo Fisher Scientific) supplemented with 10% heat-inactivated fetal bovine serum (FBS) at 37°C in 5% CO_2, and 2×10^5 cells/well were seeded into 24-well cell culture plates. Cell lines were washed twice with phosphate-buffered saline (pH 7.2) and then incubated at a multiplicity of infection (MOI) of 10 at 37°C for 2 h in RPMI 1640 medium with 10%

FBS. Non-adherent bacteria were removed by washing with PBS three times. Cells were then exposed to 1% Triton X-100 for 5 min, and serial dilutions were plated on LB agar plus an antibiotic. For HEK-293 cells, Eagle's Minimum Essential Medium supplemented with 10% of FBS was used. For CEC-32 cells Dulbecco's Modified Eagle's medium supplemented with 10% of FBS was used. The adherence assays were done in triplicate for each sample.

Determination of cytopathic effects

The 5637 cells were maintained in RPMI 1640 medium (Thermo Fisher Scientific) supplemented with 10% heat-inactivated FBS at 37°C in 5% CO_2, and 2×10^5 cells/well were seeded into eight-well chamber slides (Thermo Fisher Scientific) and allowed to grow to 75% confluence. Thirty µg/ml of each SPATE (final concentration) was added directly to monolayers and incubated for 5 h or 12 h at 37°C with 5% CO_2. Cells were then washed twice with PBS (phosphate-buffered saline), fixed with 70% methanol, and stained with Giemsa stain.

Lactate dehydrogenase (LDH) release assay

Culture supernatants were incubated with monolayers of 5637 cells in RPMI 1640 supplemented with 10% heat inactivated FBS at 37°C in 5% CO_2 for up to 12 h. Release of LDH was quantified by CytoTox 96® Non-Radioactive Cytotoxicity Assay kit (Promega, Madison, WI, USA) at 5 h and 12 h. A lysis solution (provided in the kit) was added to the non-infected cells to generate the maximum LDH release control from lysed cells.

Ascending urinary tract infection in mice

For single strain infections with the wild-type parent QT598 and isogenic SPATE mutants QT598Δ*tagBC* and QT598Δ*sha*, 25 µl (10^9 CFU/ml) were tested in an ascending UTI model adapted from [95] with 10 mice in each group. Similarly, a murine ascending UTI model with 10 mice in each group was used for co-infection, in which a virulent Δ*lacZYA* derivative of QT598 was co-infected with the Δ*5ATs* strain, a QT598-derivative lacking all 5 SPATE-encoding genes. Twenty-five µl (10^9 CFU) of a mixed culture containing equal amounts of each strain were inoculated through a catheter in six-week-old CBA/J female mice. Mice were euthanized after 48 h, and bladders and kidneys were harvested aseptically, homogenized, diluted and plated on MacConkey agar plates. Bladder samples were frozen at −80°C in TRIzol® reagent (Thermo Fisher Scientific) for RNA extraction.

qRT-PCR analysis of SPATE gene expression *in vivo* and *in vitro*

Expression of the 5 SPATE-encoding genes was determined after growth in LB medium, minimal M63 medium, and from infected mouse bladders. Total RNAs from bacterial samples were extracted in the EZ-10 Spin Column Total RNA Miniprep Kit (Bio Basic) as described elsewhere [96]. Briefly, to extract RNA from infected bladder, samples were homogenized with TRIzol® reagent (Thermo Fisher Scientific), centrifuged for 30 sec at 12,000 × g, the supernatant was incubated with ethanol (95–100%) and transferred into Zymo-Spin™ IICR Column to extract RNA using Direct-zol RNA Miniprep kit (Zymo Research, Irvine, CA, USA) according to the manufacturer's recommendations. All RNA samples were treated with TURBO DNase (Thermo Fisher Scientific). PCR (35 cycles) was used to verify DNA contamination. cDNAs were synthesized by using the Iscript™ Reverse transcription supermix according to the manufacturer's protocol (Bio-Rad Life Science, Mississauga, ON, Canada). The RNA polymerase sigma factor *rpoD* gene was used as a housekeeping control. Primers designed to amplify *rpoD, tagB, tagC, vat, tsh,* and *sha* (Supplemental Table 3) were used. For each sample, 50 ng of cDNA and 100 nM concentrations of each primer set were mixed with 10 µl of SsoFast Evagreen supermix (Bio-Rad Life Science) per well. Assays were performed in triplicate on a Corbett Rotorgene (Thermo Fisher Scientific) instrument. All data were normalized to *rpoD* expression levels. Melting-curve analysis was verified to differentiate accumulation of Evagreen-bound DNA and determine that signal was gene-amplification specific and not due to the primer-dimer formation. The data were analyzed by the $2^{-\Delta\Delta CT}$ method [97].

Statistical analyses

Experimental data were expressed as a mean ± standard error of the mean (SEM) in each group. The means of groups were combined and analyzed by Student *t*-test for pairwise comparisons and analysis of variance (ANOVA) to compare means of more than two populations. For mouse infection experiments, the Mann–Whitney test was used to compare the samples by pairs, and the Kruskal–Wallis test was used to compare groups. A P value of <0.05 was considered statistically significant. All data were analyzed with the Graph Pad Prism 7 software (GraphPad Software, San Diego, CA, USA).

Ethics statement

The protocol for mice urinary tract infection was approved by the animal ethics evaluation committee – *Comité Institutionel de Protection des Animaux* (CIPA No 1608–02) of the INRS-Institut Armand-Frappier.

Nucleotide accession numbers

Sections of the genome of *E. coli* strain QT598 containing the five different SPATE-encoding genes were submitted to NCBI Genbank from the analysis of whole-genome survey sequence. The corresponding accession numbers are *tsh* (MH899683), *sha* (MH899684), *vat* (MH899682), and *tagB* and *tagC* (MH899681) genetic regions.

Acknowledgments

We thank E. Bonneil, manager at the proteomics platform of Université de Montréal for assistance with mass spectrometry and peptide analysis and Y. Lopez de Los Santos for assistance for 3-D model prediction comparison of autotransporters. Funding for this work was supported by NSERC Canada Discovery Grants 2014-06622 and 2019-06642 (C.M.D.) and a collaborative ACIP grant from the Institut Pasteur International Network (to A.T., S.G.-R., and C.M.D).

5.6 References

1. Croxen MA, Finlay BB. Molecular mechanisms of *Escherichia coli* pathogenicity. Nat Rev Microbiol. 2010;8(1):26–38.
2. Kaper JB, Nataro JP, Mobley HL. Pathogenic *Escherichia coli.* Nature Rev Microbiol. 2004;2(2):123.
3. Bauchart P, Germon P, Bree A, et al. Pathogenomic comparison of human extraintestinal and avian pathogenic *Escherichia coli*–search for factors involved in host specificity or zoonotic potential. Microb Pathog. 2010;49(3):105–115.
4. Bélanger L, Garenaux A, Harel J, et al. *Escherichia coli* from animal reservoirs as a potential source of human extraintestinal pathogenic *E. coli.* FEMS Immunol Med Microbiol. 2011;62(1):1–10.
5. Clermont O, Olier M, Hoede C, et al. Animal and human pathogenic *Escherichia coli* strains share common genetic backgrounds. Infect Genet Evol. 2011;11(3):654–662.
6. Ewers C, Li G, Wilking H, et al. Avian pathogenic, uropathogenic, and newborn meningitis-causing *Escherichia coli*: how closely related are they?. Int J Med Microbiol. 2007;297(3):163–176.
7. Moulin-Schouleur M, Schouler C, Tailliez P, et al. Common virulence factors and genetic relationships between O18: K1:H7 *Escherichia coli* isolates of human and avian origin. J Clin Microbiol. 2006;44(10):3484–3492.
8. Nandanwar N, Janssen T, Kuhl M, et al. Extraintestinal pathogenic *Escherichia coli* (ExPEC) of human and avian origin belonging to sequence type complex 95 (STC95) portray indistinguishable virulence features. Int J Med Microbiol. 2014;304(7):835–842.
9. Johnson JR, Russo TA. Extraintestinal pathogenic *Escherichia coli*:"the other bad *E.coli*". J Lab Clin Med. 2002;139(3):155–162.
10. Guabiraba R, Schouler C. Avian colibacillosis: still many black holes. FEMS Microbiol Lett. 2015;362(15):fnv118.
11. Dho-Moulin M, Fairbrother JM. Avian pathogenic *Escherichia coli* (APEC). Vet Res. 1999;30(2–3):299–316.
12. Dziva F, Stevens MP. Colibacillosis in poultry: unravelling the molecular basis of virulence of avian pathogenic *Escherichia coli* in their natural hosts. Avian Pathol. 2008;37(4):355–366.
13. Dziva F, Hauser H, Connor TR, et al. Sequencing and functional annotation of avian pathogenic *Escherichia coli* serogroup O78 strains reveal the evolution of *E.coli* lineages pathogenic for poultry via distinct mechanisms. Infect Immun. 2013;81(3):838–849.
14. Johnson TJ, Kariyawasam S, Wannemuehler Y, et al. The genome sequence of avian pathogenic *Escherichia coli* strain O1: K1: H7 shares strong similarities with human extraintestinal pathogenic *E.coli* genomes. J Bacteriol. 2007;189(8):3228–3236.
15. Johnson TJ, Nolan LK. Pathogenomics of the virulence plasmids of *Escherichia coli.* Microbiol Mol Biol Rev. 2009;73(4):750–774.
16. Johnson TJ, Wannemuehler YM, Johnson SJ, et al. Plasmid replicon typing of commensal and pathogenic *Escherichia coli* isolates. Appl Environ Microbiol. 2007;73(6):1976–1983.
17. Mellata M, Touchman JW, Curtiss R. Full sequence and comparative analysis of the plasmid pAPEC-1 of avian pathogenic *E.coli* chi7122 (O78: K80:H9). PLoS One. 2009;4(1):e4232.
18. Peigne C, Bidet P, Mahjoub-Messai F, et al. The plasmid of *Escherichia coli* strain S88 (O45: K1:H7) that causes neonatal meningitis is closely related to avian pathogenic *E.coli* plasmids and is associated with high-level bacteremia in a neonatal rat meningitis model. Infect Immun. 2009;77(6):2272–2284.
19. Cordoni G, Woodward MJ, Wu H, et al. Comparative genomics of European avian pathogenic *E.coli* (APEC). BMC Genomics. 2016;17(1):960.
20. Leimbach A, Hacker J, Dobrindt U. *E.coli* as an all-rounder: the thin line between commensalism and pathogenicity. Curr Top Microbiol Immunol. 2013;358:3–32.

21. Mokady D, Gophna U, Ron EZ. Extensive gene diversity in septicemic *Escherichia coli*strains. J Clin Microbiol. 2005;43(1):66–73.
22. Dozois CM, Dho-Moulin M, Bree A, et al. Relationship between the Tsh autotransporter and pathogenicity of avian *Escherichia coli* and localization and analysis of the Tsh genetic region. Infect Immun. 2000;68(7):4145–4154.
23. Dozois CM, Daigle F, Curtiss R 3rd. Identification of pathogen-specific and conserved genes expressed in vivo by an avian pathogenic *Escherichia coli* strain. Proc Natl Acad Sci U S A. 2003;100(1):247–252.
24. Johnson TJ, Johnson SJ, Nolan LK. Complete DNA sequence of a ColBM plasmid from avian pathogenic *Escherichia coli* suggests that it evolved from closely related ColV virulence plasmids. J Bacteriol. 2006;188(16):5975–5983.
25. Krishnan S, Chang AC, Hodges J, et al. Serotype O18 avian pathogenic and neonatal meningitis *Escherichia coli* strains employ similar pathogenic strategies for the onset of meningitis. Virulence. 2015;6(8):777–786.
26. Johnson TJ, Wannemuehler Y, Johnson SJ, et al. Comparison of extraintestinal pathogenic *Escherichia coli* strains from human and avian sources reveals a mixed subset representing potential zoonotic pathogens. Appl Environ Microbiol. 2008;74(22):7043–7050.
27. Mellata M. Human and avian extraintestinal pathogenic *Escherichia coli*: infections, zoonotic risks, and antibiotic resistance trends. Foodborne Pathog Dis. 2013;10(11):916–932.
28. Rodriguez-Siek KE, Giddings CW, Doetkott C, et al. Comparison of *Escherichia coli* isolates implicated in human urinary tract infection and avian colibacillosis. Microbiology. 2005;151(Pt 6):2097–2110.
29. Henderson IR, Navarro-Garcia F, Nataro JP. The great escape: structure and function of the autotransporter proteins. Trends Microbiol. 1998;6(9):370–378.
30. Klemm P, Vejborg RM, Sherlock O. Self-associating autotransporters, SAATs: functional and structural similarities. Int J Med Microbiol. 2006;296(4–5):187–195.
31. Wells TJ, Totsika M, Schembri MA. Autotransporters of *Escherichia coli*: a sequence-based characterization. Microbiology. 2010;156(8):2459–2469.
32. Ruiz-Perez F, Nataro JP. Bacterial serine proteases secreted by the autotransporter pathway: classification, specificity, and role in virulence. Cell Mol Life Sci. 2014;71(5):745–770.
33. Albenne C, Ieva R. Job contenders: roles of the beta-barrel assembly machinery and the translocation and assembly module in autotransporter secretion. Mol Microbiol. 2017;106(4):505–517.
34. Bernstein HD. Looks can be deceiving: recent insights into the mechanism of protein secretion by the autotransporter pathway. Mol Microbiol. 2015;97(2):205–215.
35. Henderson IR, Navarro-Garcia F, Desvaux M, et al. Type V protein secretion pathway: the autotransporter story. Microbiol Mol Biol Rev. 2004;68(4):692–744.
36. Otto BR, Van Dooren SJ, Nuijens JH, et al. Characterization of a hemoglobin protease secreted by the pathogenic *Escherichia coli* strain EB1. J Exp Med. 1998;188(6):1091–1103.
37. Henderson IR, Czeczulin J, Eslava C, et al. Characterization of Pic, a Secreted Protease of *Shigella flexneri* and Enteroaggregative *Escherichia coli*. Infect Immun. 1999;67(11):5587–5596.
38. Brunder W, Schmidt H, Karch H. EspP, a novel extracellular serine protease of enterohaemorrhagic *Escherichia coli* O157: H7 cleaves human coagulation factor V. Mol Microbiol. 1997;24(4):767–778.
39. Eslava C, Navarro-García F, Czeczulin JR, et al. Pet, an autotransporter enterotoxin from enteroaggregative *Escherichia coli*. Infect Immun. 1998;66(7):3155–3163.
40. Guyer DM, Henderson IR, Nataro JP, et al. Identification of sat, an autotransporter toxin produced by uropathogenic *Escherichia coli*. Mol Microbiol. 2000;38(1):53–66.
41. Parham NJ, Srinivasan U, Desvaux M, et al. PicU, a second serine protease autotransporter of uropathogenic *Escherichia coli*. FEMS Microbiol Lett. 2004;230(1):73–83.

42. Stein M, Kenny B, Stein MA, et al. Characterization of EspC, a 110-kilodalton protein secreted by enteropathogenic *Escherichia coli* which is homologous to members of the immunoglobulin A protease-like family of secreted proteins. J Bacteriol. 1996;178(22):6546–6554.
43. Subashchandrabose S, Smith SN, Spurbeck RR, et al. Genome-wide detection of fitness genes in uropathogenic *Escherichia coli* during systemic infection. PLoS Pathog. 2013;9(12):e1003788.
44. Guyer DM, Radulovic S, Jones F-E, et al. Sat, the secreted autotransporter toxin of uropathogenic *Escherichia coli*, is a vacuolating cytotoxin for bladder and kidney epithelial cells. Infect Immun. 2002;70(8):4539–4546.
45. Parreira VR, Gyles CL. A novel pathogenicity island integrated adjacent to the *thrW* tRNA gene of avian pathogenic *Escherichia coli* encodes a vacuolating autotransporter toxin. Infect Immun. 2003;71(9):5087–5096.
46. Parham NJ, Pollard SJ, Desvaux M, et al. Distribution of the serine protease autotransporters of the Enterobacteriaceae among extraintestinal clinical isolates of *Escherichia coli*. J Clin Microbiol. 2005;43(8):4076–4082.
47. Restieri C, Garriss G, Locas MC, et al. Autotransporter-encoding sequences are phylogenetically distributed among *Escherichia coli* clinical isolates and reference strains. Appl Environ Microbiol. 2007;73(5):1553–1562.
48. Spurbeck RR, Dinh PC Jr., Walk ST, et al. *Escherichia coli* isolates that carry *vat*, *fyuA*, *chuA*, and *yfcV* efficiently colonize the urinary tract. Infect Immun. 2012;80(12):4115–4122.
49. Provence DL, Curtiss R. Isolation and characterization of a gene involved in hemagglutination by an avian pathogenic *Escherichia coli* strain. Infect Immun. 1994;62(4):1369–1380.
50. Cyoia PS, Rodrigues GR, Nishio EK, et al. Presence of virulence genes and pathogenicity islands in extraintestinal pathogenic *Escherichia coli* isolates from Brazil. J Infect Dev Ctries. 2015;9(10):1068–1075.
51. Maluta RP, Logue CM, Casas MR, et al. Overlapped sequence types (STs) and serogroups of avian pathogenic (APEC) and human extra-intestinal pathogenic (ExPEC) *Escherichia coli* isolated in Brazil. PLoS One. 2014;9(8):e105016.
52. Otto BR, van Dooren SJ, Dozois CM, et al. *Escherichia coli* hemoglobin protease autotransporter contributes to synergistic abscess formation and heme-dependent growth of *Bacteroides fragilis*. Infect Immun. 2002;70(1):5–10.
53. Marc D, Dho-Moulin M. Analysis of the *fim* cluster of an avian O2 strain of *Escherichia coli*: serogroup-specific sites within *fimA* and nucleotide sequence of *fimI*. J Med Microbiol. 1996;44(6):444–452.
54. Dozois CM, Fairbrother JM, Harel J, et al. *pap*-and *pil*-related DNA sequences and other virulence determinants associated with *Escherichia coli* isolated from septicemic chickens and turkeys. Infect Immun. 1992;60(7):2648–2656.
55. Dobrindt U, Agerer F, Michaelis K, et al. Analysis of genome plasticity in pathogenic and commensal *Escherichia coli* isolates by use of DNA arrays. J Bacteriol. 2003;185(6):1831–1840.
56. Wang X, Wei L, Wang B, et al. Complete genome sequence and characterization of avian pathogenic *Escherichia coli* field isolate ACN001. Stand Genomic Sci. 2016;11:13.
57. Kostakioti M, Stathopoulos C. Role of the alpha-helical linker of the C-terminal translocator in the biogenesis of the serine protease subfamily of autotransporters. Infect Immun. 2006;74(9):4961–4969.
58. Nichols KB, Totsika M, Moriel DG, et al. Molecular characterization of the vacuolating autotransporter Toxin in Uropathogenic *Escherichia coli*. J Bacteriol. 2016;198(10):1487–1498.
59. Sandt CH, Hill CW. Four Different Genes Responsible for Nonimmune Immunoglobulin-Binding Activities within a Single Strain of *Escherichia coli*. Infect Immun. 2000;68(4):2205–2214.

60. Mellies JL, Navarro-Garcia F, Okeke I, et al. espC pathogenicity island of enteropathogenic *Escherichia coli* encodes an enterotoxin. Infect Immun. 2001;69(1):315–324.
61. Guyomard-Rabenirina S, Malespine J, Ducat C, et al. Temporal trends and risks factors for antimicrobial resistant Enterobacteriaceae urinary isolates from outpatients in Guadeloupe. BMC Microbiol. 2016;16(1):121.
62. Dutta PR, Cappello R, Navarro-García F, et al. Functional comparison of serine protease autotransporters of Enterobacteriaceae. Infect Immun. 2002;70(12):7105–7113.
63. Stathopoulos C, Provence DL, Curtiss R. Characterization of the Avian Pathogenic *Escherichia coli*Hemagglutinin Tsh, a Member of the Immunoglobulin A Protease-Type Family of Autotransporters. Infect Immun. 1999;67(2):772–781.
64. Gutierrez D, Pardo M, Montero D, et al. TleA, a Tsh-like autotransporter identified in a human enterotoxigenic *Escherichia coli* strain. Infect Immun. 2015;83(5):1893–1903.
65. Yang J, Yan R, Roy A, et al. The I-TASSER Suite: protein structure and function prediction. Nat Methods. 2015;12(1):7.
66. Pettersen EF, Goddard TD, Huang CC, et al. UCSF Chimera—a visualization system for exploratory research and analysis. J Comput Chem. 2004;25(13):1605–1612.
67. Genevaux P, Muller S, Bauda P. A rapid screening procedure to identify mini-Tn10 insertion mutants of *Escherichia coli* K-12 with altered adhesion properties. FEMS Microbiol Lett. 1996;142(1):27–30.
68. Kostakioti M, Stathopoulos C. Functional analysis of the Tsh autotransporter from an avian pathogenic *Escherichia coli* strain. Infect Immun. 2004;72(10):5548–5554.
69. Sherlock O, Vejborg RM, Klemm P. The TibA adhesin/invasin from enterotoxigenic *Escherichia coli* is self recognizing and induces bacterial aggregation and biofilm formation. Infect Immun. 2005;73(4):1954–1963.
70. Hasman H, Chakraborty T, Klemm P. Antigen-43-mediated autoaggregation of *Escherichia coli* is blocked by fimbriation. J Bacteriol. 1999;181(16):4834–4841.
71. Benz I, Schmidt MA. Cloning and expression of an adhesin (AIDA-I) involved in diffuse adherence of enteropathogenic *Escherichia coli*. Infect Immun. 1989;57(5):1506–1511.
72. Al-Hasani K, Henderson IR, Sakellaris H, et al. The *sigA* gene which is borne on the *she* pathogenicity island of *Shigella flexneri* 2a encodes an exported cytopathic protease involved in intestinal fluid accumulation. Infect Immun. 2000;68(5):2457–2463.
73. Benjelloun-Touimi Z, Sansonetti PJ, Parsot C. SepA, the major extracellular protein of *Shigella flexneri*: autonomous secretion and involvement in tissue invasion. Mol Microbiol. 1995;17(1):123–135.
74. Vijayakumar V, Santiago A, Smith R, et al. Role of class 1 serine protease autotransporter in the pathogenesis of *Citrobacter rodentium* colitis. Infect Immun. 2014;82(6):2626–2636.
75. Leyton DL, Adams LM, Kelly M, et al. Contribution of a novel gene, *rpeA*, encoding a putative autotransporter adhesin to intestinal colonization by rabbit-specific enteropathogenic *Escherichia coli*. Infect Immun. 2007;75(9):4664–4669.
76. Johnson TJ, Aziz M, Liu CM, et al. Complete genome sequence of a CTX-M-15-producing *Escherichia coli* strain from the H30Rx subclone of sequence type 131 from a patient with recurrent urinary tract infections, closely related to a lethal urosepsis isolate from the patient's sister. Genome Announc. 2016;4(3):e00334–16.
77. Johnson TJ, Siek KE, Johnson SJ, et al. DNA sequence of a ColV plasmid and prevalence of selected plasmid-encoded virulence genes among avian *Escherichia coli* strains. J Bacteriol. 2006;188(2):745–758.
78. Jakobsen L, Hammerum AM, Frimodt-Møller N. Virulence of *Escherichia coli* B2 isolates from meat and animals in a murine model of ascending urinary tract infection (UTI): evidence that UTI is a zoonosis. J Clin Microbiol. 2010;48(8):2978–2980.

79. Mellata M, Johnson J, Curtiss III R. *Escherichia coli*isolates from commercial chicken meat and eggs cause sepsis, meningitis and urinary tract infection in rodent models of human infections. Zoonoses Public Health. 2018;65(1):103–113.
80. Pavanelo DB, Houle S, Matter LB, et al. The periplasmic trehalase affects type 1 fimbriae production and virulence of the extraintestinal pathogenic *E.coli* strain MT78. Infect Immun. 2018;IAI:00241.
81. Skyberg JA, Johnson TJ, Johnson JR, et al. Acquisition of avian pathogenic *Escherichia coli* plasmids by a commensal *E.coli* isolate enhances its abilities to kill chicken embryos, grow in human urine, and colonize the murine kidney. Infect Immun. 2006;74(11):6287–6292.
82. Ruiz-Perez F, Wahid R, Faherty CS, et al. Serine protease autotransporters from *Shigella flexneri* and pathogenic *Escherichia coli* target a broad range of leukocyte glycoproteins. Proc Nat Acad Sci. 2011;108(31):12881–12886.
83. Vidal JE, Navarro-García F. Efficient translocation of EspC into epithelial cells depends on enteropathogenic *Escherichia coli* and host cell contact. Infect Immun. 2006;74(4):2293–2303.
84. Clermont O, Christenson JK, Denamur E, et al. The Clermont *Escherichia coli* phylo-typing method revisited: improvement of specificity and detection of new phylo-groups. Environ Microbiol Rep. 2013;5(1):58–65.
85. Tamura K, Stecher G, Peterson D, et al. MEGA6: molecular evolutionary genetics analysis version 6.0. Mol Biol Evol. 2013;30(12):2725–2729.
86. Bendtsen JD, Nielsen H, von Heijne G, et al. Improved prediction of signal peptides: signalP 3.0. J Mol Biol. 2004;340(4):783–795.
87. Marchler-Bauer A, Lu S, Anderson JB, et al. CDD: a Conserved Domain Database for the functional annotation of proteins. Nucleic Acids Res. 2010;39(suppl_1):D225–D9.
88. Kouranov A, Xie L, de la Cruz J, et al. The RCSB PDB information portal for structural genomics. Nucleic Acids Res. 2006;34(suppl_1):D302–D5.
89. Datsenko KA, Wanner BL. One-step inactivation of chromosomal genes in *Escherichia coli* K-12 using PCR products. Proc Nat Acad Sci. 2000;97(12):6640–6645.
90. Cherepanov PP, Wackernagel W. Gene disruption in *Escherichia coli*: Tc R and Km R cassettes with the option of Flp-catalyzed excision of the antibiotic-resistance determinant. Gene. 1995;158(1):9–14.
91. Benjelloun-Touimi Z, Tahar MS, Montecucco C, et al. SepA, the 110 kDa protein secreted by *Shigella flexneri*: two-domain structure and proteolytic activity. Microbiology. 1998;144(7):1815–1822.
92. Charbonneau M-È, Berthiaume F, Mourez M. Proteolytic processing is not essential for multiple functions of the *Escherichia coli* autotransporter adhesin involved in diffuse adherence (AIDA-I). J Bacteriol. 2006;188(24):8504–8512.
93. Provence D, Curtiss R. Role of *crl* in avian pathogenic *Escherichia coli*: a knockout mutation of *crl* does not affect hemagglutination activity, fibronectin binding, or curli production. Infect Immun. 1992;60(11):4460–4467.
94. Matter LB, Barbieri NL, Nordhoff M, et al. Avian pathogenic *Escherichia coli* MT78 invades chicken fibroblasts. Vet Microbiol. 2011;148(1):51–59.
95. Hagberg L, Engberg I, Freter R, et al. Ascending, unobstructed urinary tract infection in mice caused by pyelonephritogenic *Escherichia coli* of human origin. Infect Immun. 1983;40(1):273–283.
96. Porcheron G, Habib R, Houle S, et al. The small RNA RyhB contributes to siderophore production and virulence of uropathogenic *Escherichia coli*. Infect Immun. 2014;82(12):5056–5068.
97. Livak KJ, Schmittgen TD. Analysis of relative gene expression data using real-time quantitative PCR and the 2− ΔΔCT method. Methods. 2001;25(4):402–408.
98. Saitou N, Nei M. The neighbor-joining method: a new method for reconstructing phylogenetic trees. Mol Biol Evol. 1987;4(4):406–425.

99. Jones DT, Taylor WR, Thornton JM. The rapid generation of mutation data matrices from protein sequences. Bioinformatics. 1992;8(3):275–282.
100. Labbate M, Queck SY, Koh KS, et al. Quorum sensing-controlled biofilm development in *Serratia liquefaciens* MG1. J Bacteriol. 2004;186(3):692–698.
101. Woodall LD, Russell PW, Harris SL, et al. Rapid, synchronous, and stable induction of type 1 piliation in *Escherichia coli* by using a chromosomal *lacUV5* promoter. J Bacteriol. 1993;175(9):2770–2778.

5.7 Supplement Figures of Article 1

Figure S1

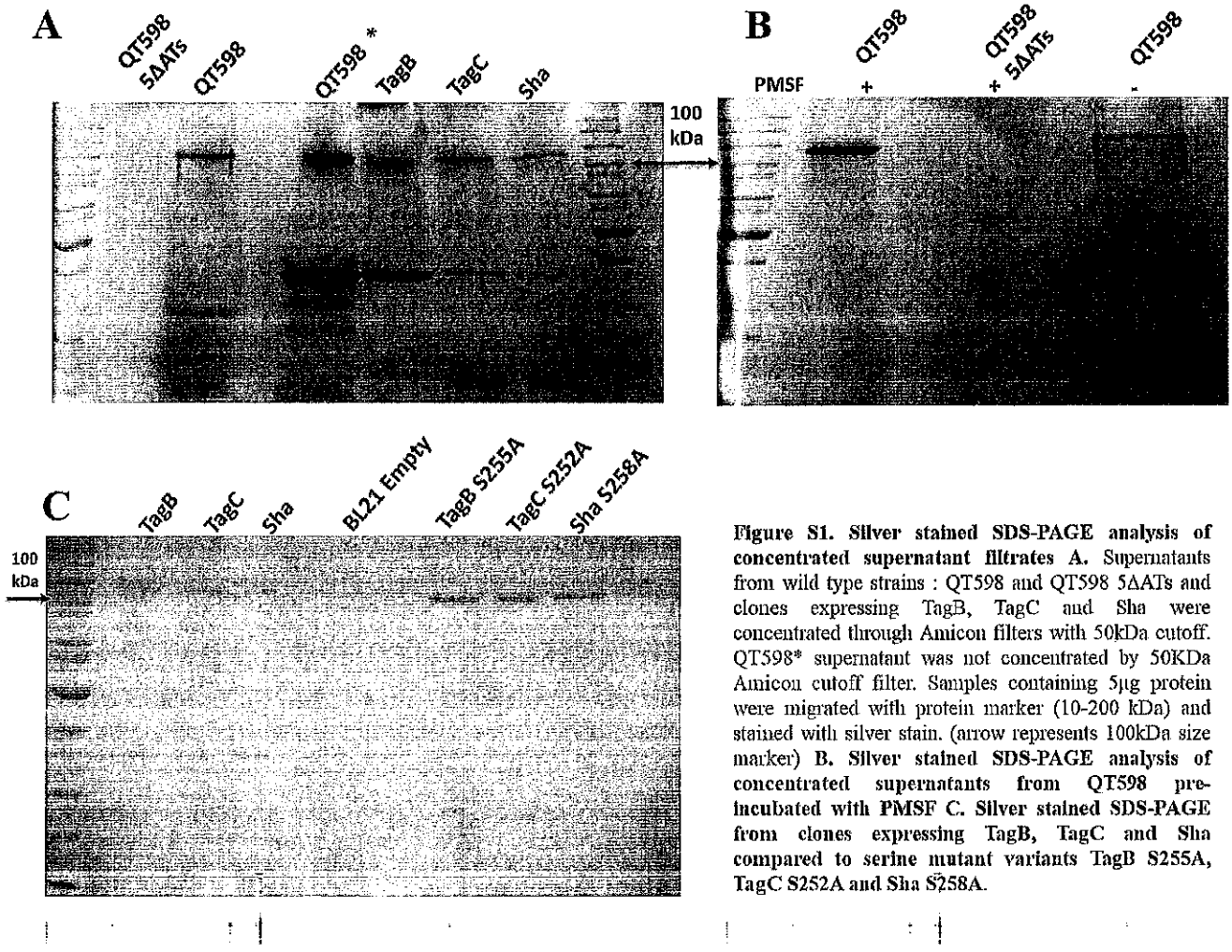

Figure S1. Silver stained SDS-PAGE analysis of concentrated supernatant filtrates A. Supernatants from wild type strains : QT598 and QT598 5ΔATs and clones expressing TagB, TagC and Sha were concentrated through Amicon filters with 50kDa cutoff. QT598* supernatant was not concentrated by 50KDa Amicon cutoff filter. Samples containing 5µg protein were migrated with protein marker (10-200 kDa) and stained with silver stain. (arrow represents 100kDa size marker) **B. Silver stained SDS-PAGE analysis of concentrated supernatants from QT598 pre-incubated with PMSF C. Silver stained SDS-PAGE from clones expressing TagB, TagC and Sha compared to serine mutant variants TagB S255A, TagC S252A and Sha S258A.**

Figure S2

S2A

TagB

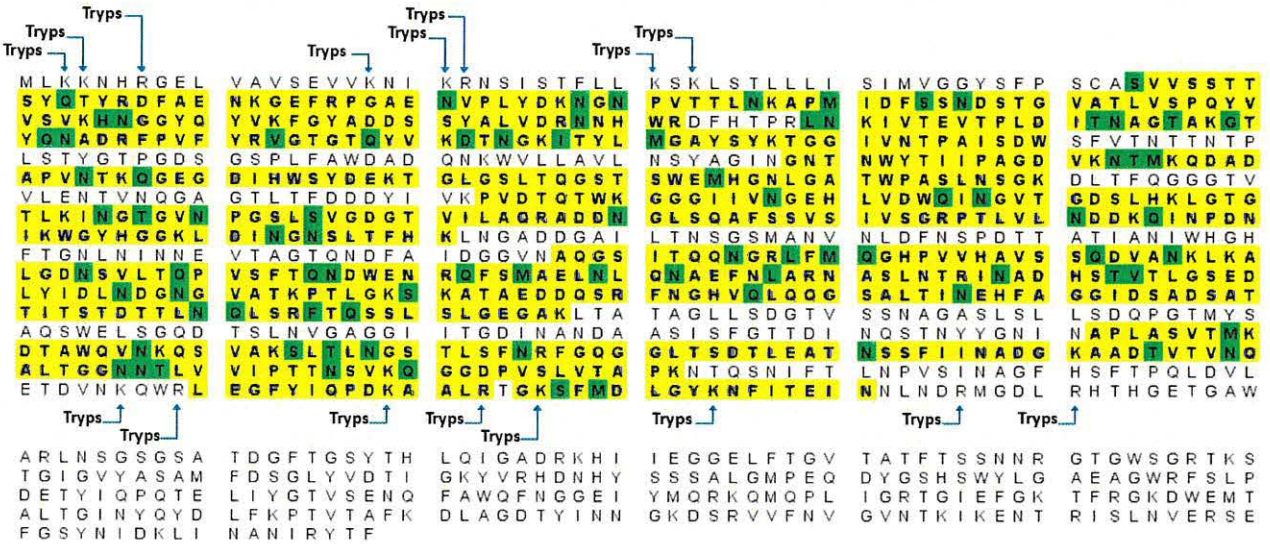

S2B

TagC

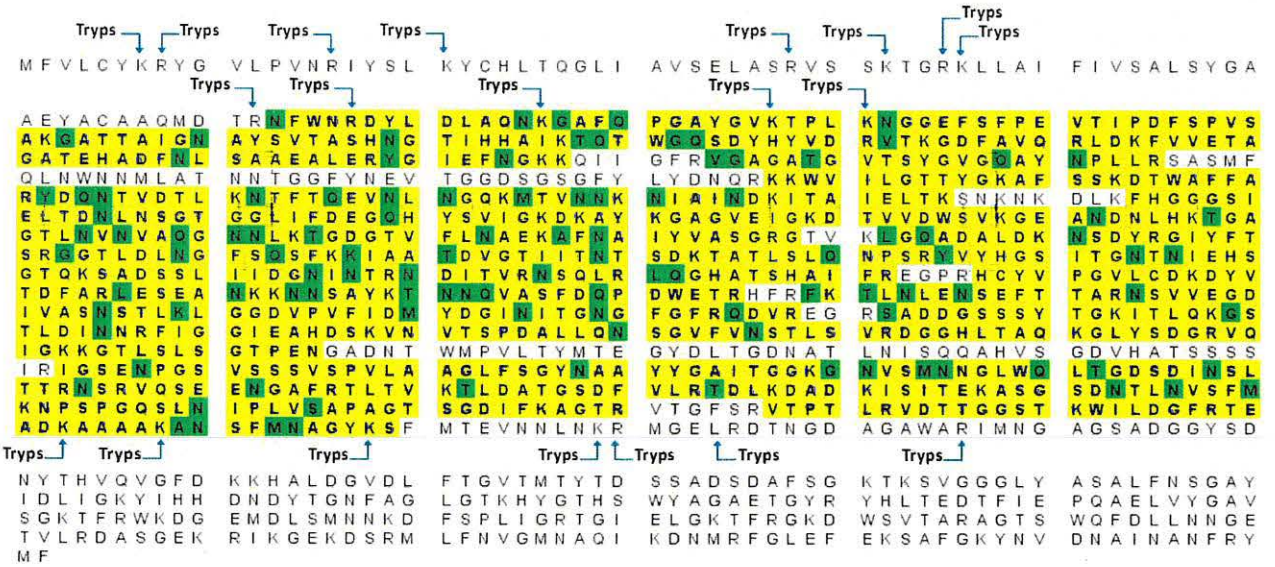

S2C

Sha

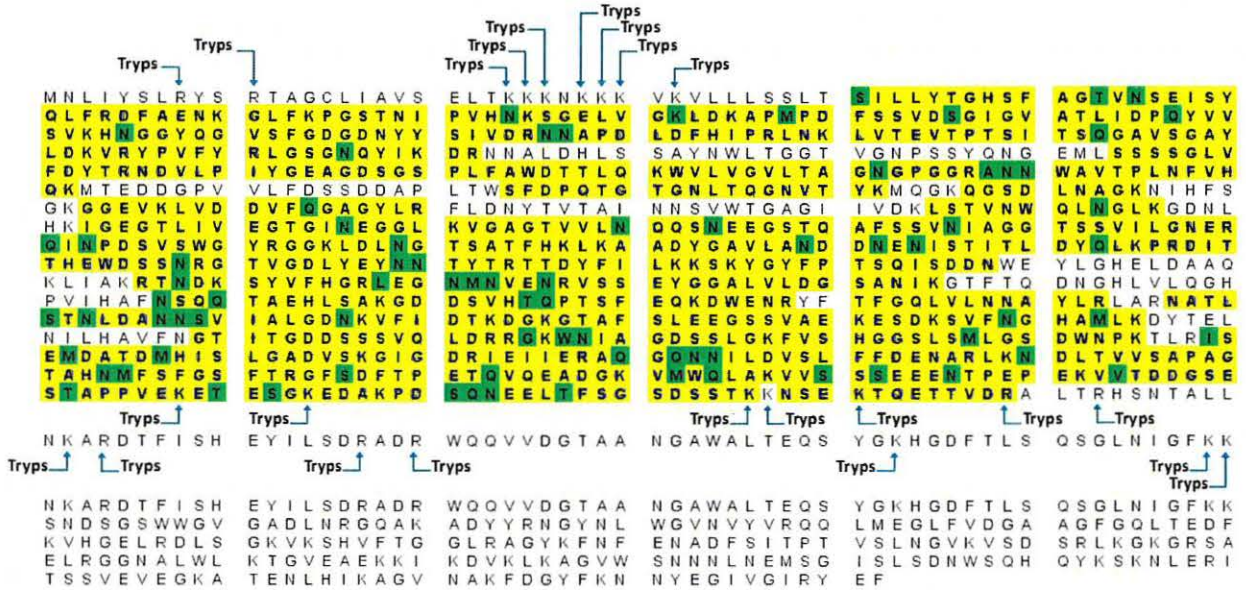

S2D

Vat

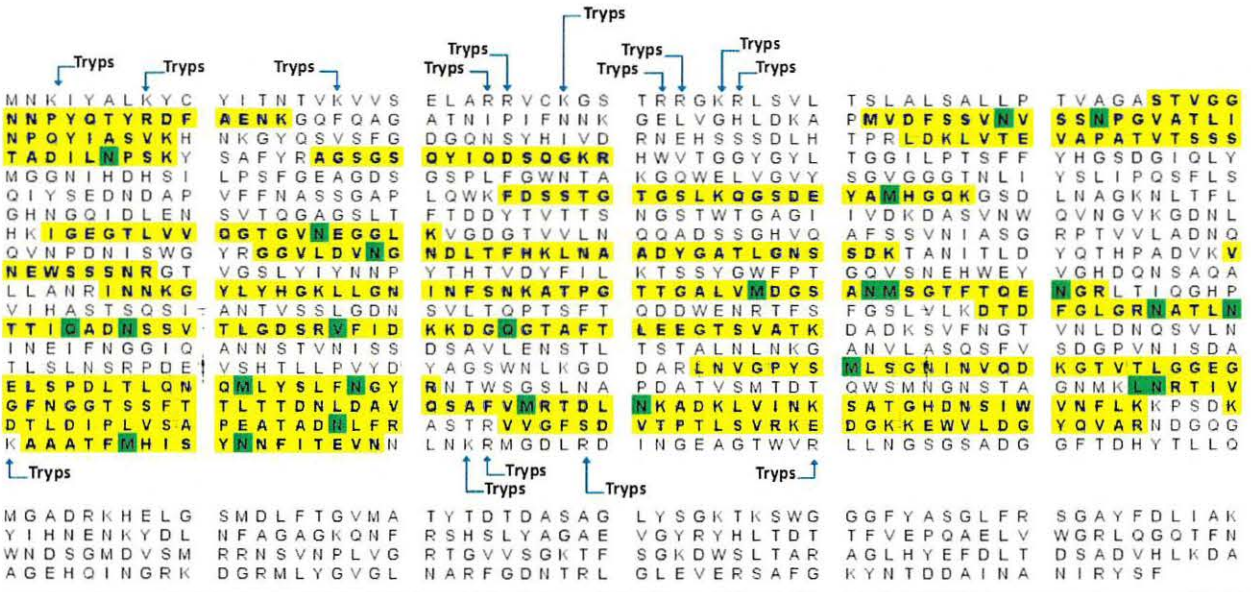

S2E

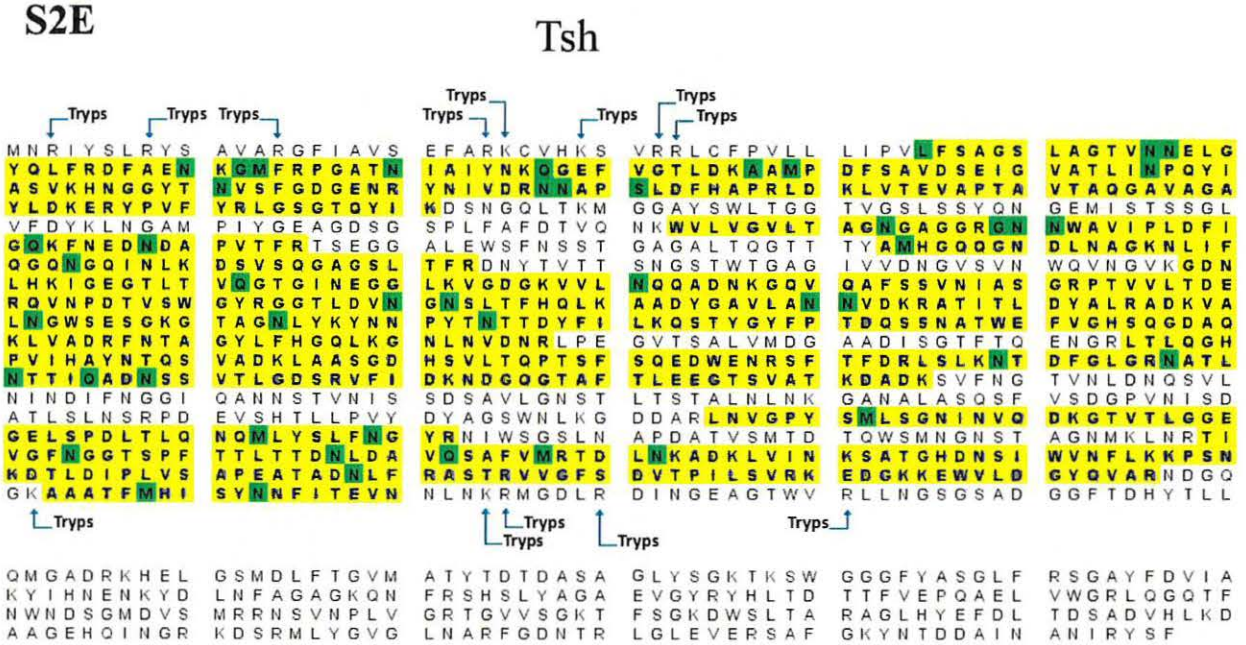

Figure S2. Sequence coverage of autotransporters. LC-MS analysis of each sample. The peptides sequence that have been identified are highlighted in yellow and modifications are highlighted in green **A. TagB**. A total of 676 of 1278 amino acids was detected (53% of coverage) **B. TagC**. A total of 864 of 1322 amino acids was detected (64% of coverage)., **C. Sha**. A total of 816 of 1302 amino acids was detected (63% of coverage). **D. Vat**. A total of 450 of 1376 amino acids was detected (33% of coverage) from QT598 WT. **E. Tsh**. A total of 746 of 1377 amino acids was detected (54% of coverage) from QT598 WT. Blue arrows are the predicted Trypsin sites in both N-terminal and C-terminal of each proteins.

Figure S3

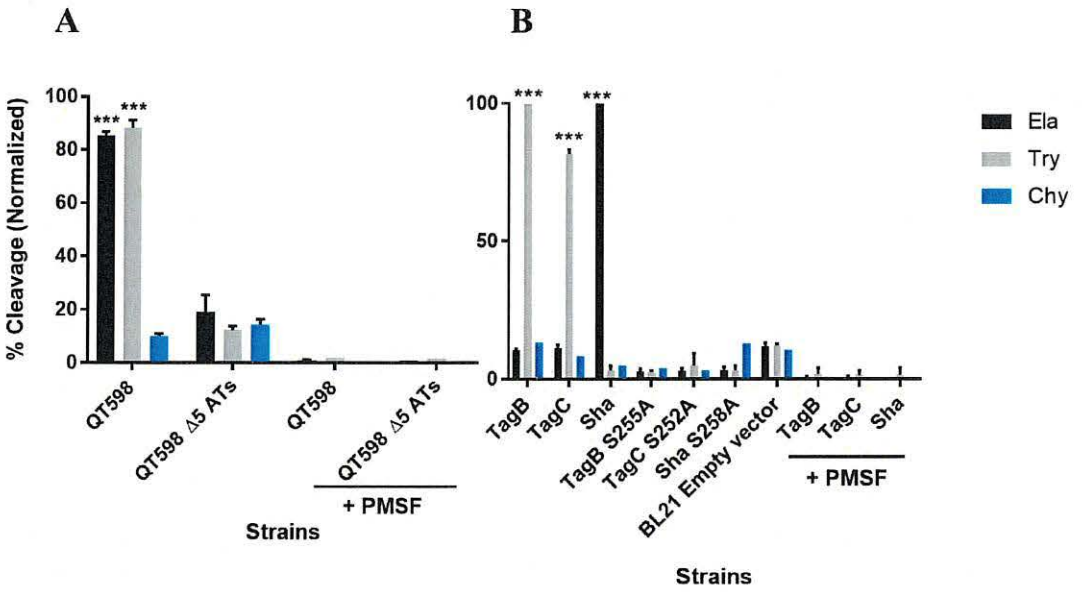

Figure S3. Oligopeptide cleavage profiles of SPATEs from wild-type (A) and clonal backgrounds (B). 5 µg of each SPATE-containing supernatant filtrate from clones in BL21 / supernatant from QT598 and its SPATE-free *Δ5AT* mutant was incubated at 37°C for 3 h with 1mM of synthetic oligopeptide specifically recognized by the following enzymatic activities: **Elastase (Ela)**-(N-Suc-Ala-Ala-Ala-pNA) ; **Trypsin (Try)**-(N-Ben-L-arginine-pNA); or **Chymotrypsin (Chy)**-(N-Suc-Ala-Ala-Pro-Phe-pNA). Absorbance at 410 nm was normalized to the maximum absorbance value. Data are the means of three independent experiments and error bars represent the standard errors of the means. (* $p<0.05$, ** $p<0.01$, *** $p<0.001$ one - way ANOVA with multiple comparisons vs QT598*Δ5AT* (A) or BL21 empty vector (B)

Figure S4

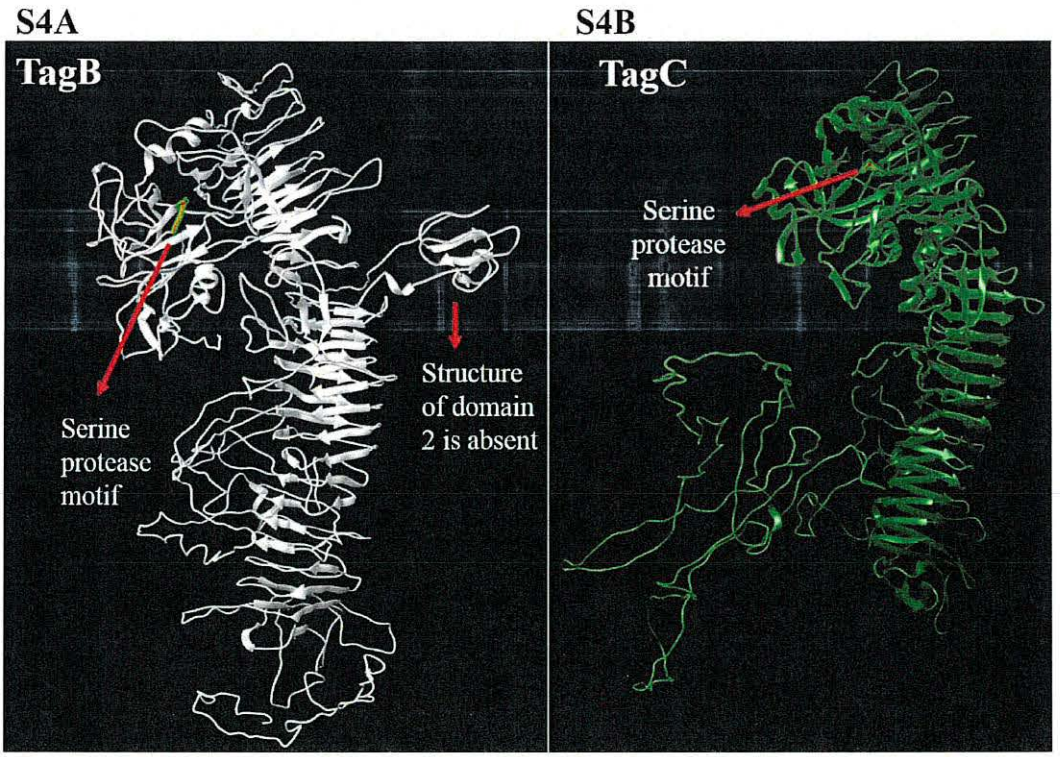

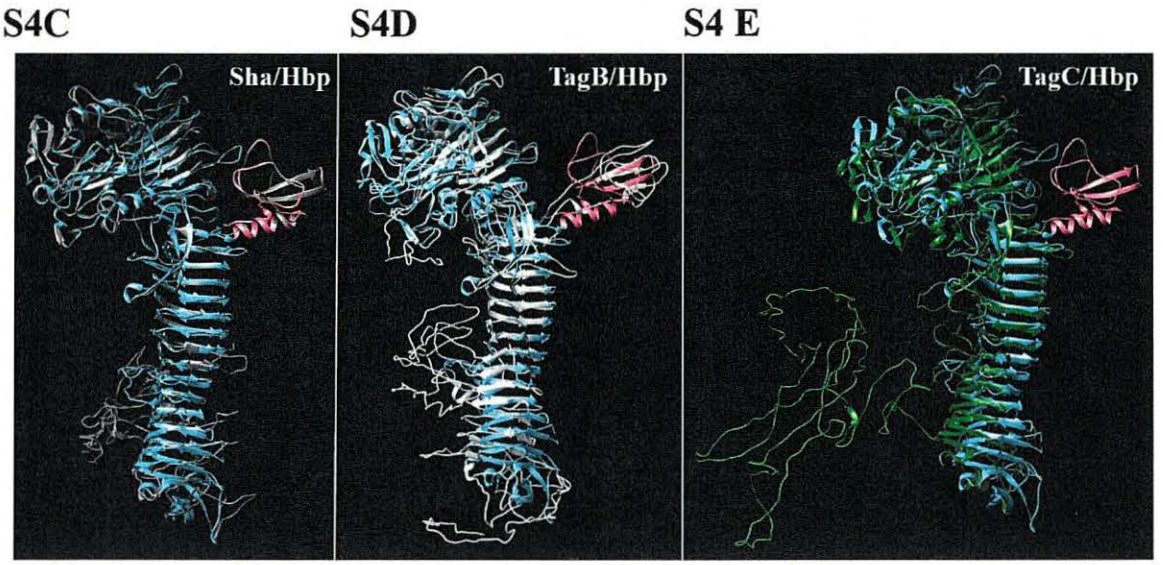

Figure S4. Stereo ribbon diagram showing the predicted 3-dimensional structures of TagB and TagC passenger domains derived from the Hbp/Tsh and EspP crystal structures. **A**. Predictedl structure of TagB. The model was generated using the I-TASSER server with Hbp (PDB 1WXR) template. The structure of domain 2 is absent in TagB. **B**.Predicted structure of TagC. The model was generated using the the I-TASSER server with EspP (extracellular serine protease plasmid-encoded, PDB 3SZE) template. **C.** Overlap of Hbp (blue) with Sha (grey) . The structure of the domain 2 is present in Sha.. **D.** Overlap of Hbp (blue) with TagB (white). The domain 2 structure is not conserved in TagB **E.** Overlap of Hbp (blue) with TagC (green) The domain 2 (pink) is absent in TagC.

Figure S5

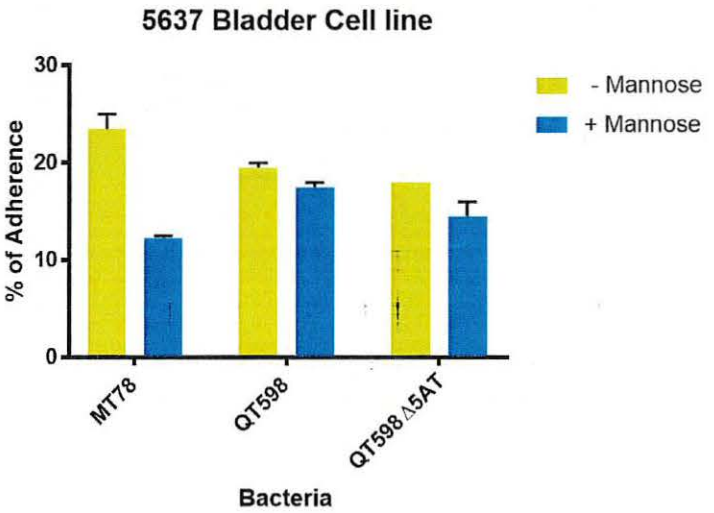

Figure S5. No difference in percentage of adherence to human bladder (5637) epithelial cell line by QT598 and its SPATEs free mutant. Cell monolayers were infected with QT598 and QT598 5ΔATs at a multiplicity of infection (MOI) of 10 and incubated at 37°C at 5% CO_2 for 2 hours. Adherent bacteria were enumerated by plating on LB agar. Empty vector (pBCsk+) was used as a negative-control and APEC MT78 as a positive control for adherence to cell lines. Data are the averages of three independent experiments. Error bars represent standard errors of the means.

Supplement Tables

Supplement Table 1 List of *E. coli* strains and accession numbers for Vat proteins identical to Vat_{QT598}

Strain/isolate	Accession number	Information or source
KTE28	ELC53090.1	UTI
UMEA 4076-1	ERA51660.1	UTI
004PP2015	OCS73020.1	Turkey colibacillosis
FEX675	PPE49807.1	Retail chicken meat potential ExPEC
VRES0524	SQW13100.1	Turkey feces
VRES0524	SQV09766.1	Turkey feces
VRES0540	SQX23694.1	Turkey feces
VRES0561	SQW81848.1	Turkey feces
VRES0558	SQW95192.1	Turkey feces
VRES0563	SQX99582.1	Turkey feces
VRES0557	SQZ03425.1	Turkey feces
VRES0564	SRZ55961.1	Turkey feces
VRES0569	SQX13605.1	Turkey feces
VRES0574	SQX78012.1	Turkey feces
VRES0567	SQX85253.1	Turkey feces
VRES0560	SRB39602.1	Turkey feces
VRES0571	SQX68131.1	Turkey feces
VRES0528	SRB74388.1	Turkey feces
VRES0550	SRA14460.1	Turkey feces
VRES0527	SQV24988.1	Turkey feces
VRES0541	SQV90344.1	Turkey feces
VRES0531	SRZ02671.1	Turkey feces
VRES0529	SQW37114.1	Turkey feces
VRES0584	SQX38949.1	Turkey feces
VRES0585	SQY07345.1	Turkey feces
VRES0533	SRY84987.1	Turkey feces
VRES0536	SQW01088.1	Turkey feces
VRES0580	SQW89426.1	Turkey feces
VRES0535	SQW64783.1	Turkey feces
VRES0668	SQZ94674.1	Turkey feces
VRES0568	SQX57971.1	Turkey feces
VRES0552	SRA59934.1	Turkey feces
VRES0570	SQX27250.1	Turkey feces
VRES0573	SQY17530.1	Turkey feces
VRES0581	SQV73047.1	Turkey feces
VRES0559	SQY77711.1	Turkey feces
VRES0572	SQY89347.1	Turkey feces
VRES0532	SQW23350.1	Turkey feces
SC371	RDQ09216.1	Surface water lake Superior
VRES0562	SVF57037.1	Turkey feces
VRES0586	SVF61232.1	Turkey feces

Supplement Table 2 List of *E. coli* strains that contain Tag genomic islands - (*tagB* and *tagC* genes)

Strain/isolate	Accession number	Information or source
DA33135	CP029576.1	Clinical source, Sweden
Ecol_448	CP015076.1	Clinical source, Argentina
Ecol_743	CP015069.1	Human isolate, Dubai
SE15	AP009378.1	Human commensal, B2 group [1]
Ecol_745	CP015074.2	Human isolate, Morocco
Eco 889	CP015159.1	NIH, human urine
MVAST0167	CP014492.1	ST131, Minnesota
55989	CP028304.1	UTI, Pakistan
AR_451	CP030337.1	Antimicrobial resistant strain
E41-1	CP028483.1	Human sputum, Shanghai
AR_0081	CP027534.1	Antimicrobial resistant
NQ3	CP024720.1	Domestic yak
LS4	CP024717.1	Domestic yak
AR_0055	CP021935.1	Antimicrobial resistant
H105	CP021454.1	ST131, vaginal swab Germany
AR_0058	CP021689.1	Antimicrobial resistant
81009	CP021179.1	O25b: H4 urine isolate United Arab Emirates
AR_0104	CP020116.1	Antimicrobial-resistant
Ecol_AZ162	CP019015.1	Antimicrobial-resistant, human, Boston
Ecol_867	CP019000.1	Antimicrobial-resistant, Toronto, Canada
Ecol_656	CP018979.1	Human Beijing, China
Ecol_542	CP018970.1	Vietnam
Ecol_276	CP018953.1	Human Antimicrobial-resistant, U.S.A.
NCTC 13441	LT632320.1	O25b:H4 ST131 uropathogenic strain, CTX-M-15
O25b:H4	CP015085.1	Urinary tract pathogenic, Saudi Arabia
Ecol 732	CP015138.1	Human AR strain, Bangkok
JJ1887	CP014316.1	UTI, ST131 strain [2]
ZH193	CP014497.1	Human ST131, New York
JJ2434	CP013835.1	Human Minneapolis
CD306	CP013831.1	ST131 from a Cat, New York
P46212	CP013658.1	Oxford, U.K. human urine [3]
EC958	HG941718.1	UTI, blood, England [4]
JJ1886	CP006784.1	USA, fatal sepsis [5]
Z247	CP021207.1	Human blood, China [6]
Ecol 244	CP019020.1	Argentina, human clinical
G749	CP014488.1	Human clinical, Seattle Washington
MNCRE44	CP010876.1	Human ST131 sputum [7]
ZH063	CP014522.1	Human ST131, Winnipeg, Canada
Ecol AZ159	CP019008.1	Human Bogota, Columbia Human ST131, Minneapolis

SaT040	CP014495.1	Human ST131, Burlingtonm, VT
JJ1897	CP013837.1	Human ST131, Minneapolis
PCN033	CP014488.1	O11 group D, PorcineExPEC [8]
FHI40	LM996283.1	Non-O157 STEC human Norway
RM9387	CP009104.1	O104 STEC, cattle feces [9]
M18	CP010219.1	Mouse feces, China
CI5	CP011018.1	Uropathogenic strain, pyelonephritis [10]
M3	CP010183.1	Mouse feces, China
M1	CP010180.1	Mouse feces, China
M8	CP010191.1	Mouse feces, China

References

1. Toh, H., et al., Complete genome sequence of the wild-type commensal *Escherichia coli* strain SE15, belonging to phylogenetic group B2. Journal of bacteriology, 2010. **192**(4): p. 1165-1166.

2. Johnson, T.J., et al., Complete genome sequence of a CTX-M-15-producing *Escherichia coli* strain from the H30Rx subclone of sequence type 131 from a patient with recurrent urinary tract infections, closely related to a lethal urosepsis isolate from the patient's sister. Genome announcements, 2016. **4**(3): p. e00334-16.

3. Stoesser, N., et al., Evolutionary history of the global emergence of the *Escherichia coli* epidemic clone ST131. MBio, 2016. **7**(2): p. e02162-15.

4. Forde, B.M., et al., The complete genome sequence of *Escherichia coli* EC958: a high quality reference sequence for the globally disseminated multidrug resistant E. coli O25b: H4-ST131 clone. PLoS One, 2014. **9**(8): p. e104400.

5. Andersen, P.S., et al., Complete genome sequence of the epidemic and highly virulent CTX-M-15-producing H30-Rx subclone of *Escherichia coli* ST131. Genome announcements, 2013. **1**(6): p. e00988-13.

6. Zheng, B., et al., Coexistence of MCR-1 and NDM-1 in clinical *Escherichia coli* isolates. Clinical Infectious Diseases, 2016. **63**(10): p. 1393-1395.

7. Johnson, T.J., et al., Complete genome sequence of a carbapenem-resistant extraintestinal pathogenic *Escherichia coli* strain belonging to the sequence type 131 H30R subclade. Genome announcements, 2015. **3**(2): p. e00272-15.

8. Liu, C., et al., Genome analysis and in vivo virulence of porcine extraintestinal pathogenic *Escherichia coli* strain PCN033. BMC genomics, 2015. **16**(1): p. 717.

9. Yan, X., et al., Genome sequencing and comparative genomics provides insights on the evolutionary dynamics and pathogenic potential of different H-serotypes of Shiga toxin-producing *Escherichia coli* O104. BMC microbiology, 2015. **15**(1): p. 83.

10. Mehershahi, K.S., S.N. Abraham, and S.L. Chen, Complete genome sequence of uropathogenic *Escherichia coli* strain CI5. Genome announcements, 2015. **3**(3): p. e00558-15.

Supplement Table 3 Primers used in this study

Primers	Characteristics	Sequence
CMD 96	Vat_screening F	AACGGTTGGTGGCAACAATCC
CMD 97	Vat_screening R	AGCCCTGTAGAATGGCGAGTA
CMD 100	Tsh_screening F	AGTCAGGGGGATGCACAGAAA
CMD 101	Tsh_screening R	GCGGTTCTCCCAGTCCTCC
CMD 1782	Sha_cloning_F	GTGTGAATTCACCATGAACTTAATATATTCTCTTCGTTA CAGCAG
CMD 1784	Sha_ cloning _R	CAGACCCGGGGGATGGCAAGGCGCAGAAT
CMD 1785	Sha_screening_F	GCCTGAACATCGGCTTCAAGA
CMD 1786	Sha_screening_R	TCAGAACTCATATCGAATACCGAC
CMD 1853	Sha_prom_F	ACATGGATCCACGAAGACGAGCGCATACAGAAAATCA
CMD 1854	Sha_KO_F	CCTTATATTTTTGTCTATCTATTGAACTATAAGTGTGTTA ATGAATCATGTGTAGGCTGGAGCTGCTTCG
CMD 1855	Sha_KO_R	AAACAA ATC AAT CCC GAA TAT AAG TAT AAT CAGAAC TCA TAT CGA ATA CCA TTC CGG GGA TCCGTC GAC C
CMD 1949	Tsh_cloning F	CACGTCTATCGATTCAGCCCGTCCACATTCAG
CMD 1950	Tsh_cloning R	TACATGGATCCCTCGCAGCAAAGGGACAAAGC
CMD 1951	Vat_cloning F	TATTGGATCCTCCGCTCTGAACCGCCACGC
CMD 1952	Vat_cloning R	CGCCAAGCTTCGTAATCAGATAATCGCAGC
CMD 2094	TagB KO_F	TATGTTTTTATTTTTGTTTTGTTTTATTTATCAGATTTTGT TGTTTTTTAATTCCGGGGATCCGTCGACC
CMD 2095	TagB KO_R	CAGGTTTTCTTTTTTATCTACTCTCCTGCTCAGAATGTA TAACGAATATTTGTAGGCTGGAGCTGCTTCG
CMD 2096	TagBKO_screening F	GCTGCCATAGCTGAACCTGCG
CMD 2097	TagBKO_screening R	CAGAGGCACGGCCACTGAAC
CMD 2098	TagC KO_F	AGTTATATTTGTTTGTATTATGTTATAAACGTTATGGAGT CTTACCCGTGATTCCGGGGATCCGTCGACC
CMD 2099	TagC KO_R	CCTTGTCAGAACATATACCGGAAATTCGCGTTTATTGC GTTATCCACGTTTGTAGGCTGGAGCTGCTTCG
CMD 2100	TagC_screening F	TGCAATGTGGGTATGGAGTCG
CMD 2101	TagCKO_sceening R	GTGGCCTTCGCGTATTTCC
CMD 2104	Vat KO_F	ATGGTTATTAATGTAACTTTGGAATATACGTTCCGGAAT CATTTACTATGGTGTAGGCTGGAGCTGCTTC
CMD 2105	Vat KO_R	CAGATAATCGCA GCA AAG GGA CAA AGC AAT AGTCCCTTTGCT GCA CAG CAA TGG GAA TTA GCCATGGTCC
CMD 2154	TagB_ cloning F	GGTACCGGGCCCCCCCTCGAGGCGTTAGCTTGGTTGT TGGTGCG
CMD 2155	TagB_ cloning R	CGCTCTAGAACTAGTGGATCCCAGAGGCACGGCCACT GAACT
CMD 2156	TagC_ cloning F	GGTACCGGGCCCCCCCTCGAG ACCTTTGGCGGCGCAATACA
CMD 2157	TagC_ cloning R	CGCTCTAGAACTAGTGGATCCATATTGAACGCTCTGGG GACG
CMD 2158	EspC_ cloning F	GGTACCGGGCCCCCCCTCGAGACCGGCTCTTTTGGAC TCTCCG

CMD 2159	EspC_ cloning R	CGCTCTAGAACTAGTGGATCCAGGTTATCCAGCCGGG TAAG
CMD 2166	EspC_screening F	GGTTTCAGGGTTGGGGCTGGG
CMD 2167	EspC_screening R	CCTCCCCCCACGGATTTGGTT
CMD 2188	qPCR Sha _F	GATAGTGGTTCTCCGCTCTTTG
CMD 2189	qPCR Sha _R	AGCCCAGTTGTTTGCTCTAC
CMD 2328	qPCR TagB_F	GGGAGACGGAACCGTATATTG
CMD 2329	qPCR TagB_R	CGTCGTTTAGCACCAGAGTAG
CMD 2330	qPCR TagC_F	GCCGGGTTCAGATTGGAAAG
CMD 2331	qPCR TagC_R	GTACGGGCATCCAGGTATTATC
CMD 2332	qPCR Vat_F	AGCACGAACTGGGAAGTATG
CMD 2333	qPCR Vat_R	ACAGACCACTGGCATAGAAAC
CMD 2334	qPCR Tsh_F	ACTCCACGGCAGGAAATATG
CMD 2335	qPCRTsh_R	TGAACCGCGTCCAGATTATC

6 ARTICLE 2: SPATES INTERNALIZATION IN EPITHELIAL CELLS

The Serine Protease Autotransporters TagB, TagC, and Sha from Extraintestinal pathogenic *Escherichia coli* are internalized by human bladder epithelial cells and cause actin cytoskeletal disruption

Authors: Pravil Pokharel[1,2], Juan Manuel Díaz[2,3], Hicham Bessaiah[1,2], Sébastien Houle[1,2], Alma Lilián Guerrero-Barrera[3], and Charles M. Dozois[1,2,4]

[1] Institut national de recherche scientifique (INRS) - Centre Armand-Frappier Santé Biotechnologie, Laval, Quebec, Canada
[2] Centre de recherche en infectiologie porcine et avicole (CRIPA), Saint-Hyacinthe, Quebec, Canada
[3] Laboratorio de Biología Celular y Tisular, Departamento de Morfología, Universidad Autónoma de Aguascalientes (UAA), Aguascalientes, Mexico.
[4] Institut Pasteur International Network, Laval, Quebec H7V 1B7, Canada

Title of Journal: International Journal of Molecular Sciences (IJMS)

Received: 1 March 2020 / **Revised:** 10 April 2020 / **Accepted:** 23 April 2020 / **Published:** 26 April 2020

https://doi.org/10.3390/ijms21093047

Contribution of authors:

P.P. conceived, planned and carried out all the experiments and analysed the results **P.P., J.M.D. and H.B.** contributed to the interpretation of the results. **P.P.** took the lead in writing the manuscript. **J.M.D. and A.L.G.B.** prepared antibodies. **J.M.D., H.B., S.H. and CMD.** provided critical feedback and helped shape the research, analysis and review and editing of manuscript. **C.M.D.** supervised the project and acquired grant.

6.1 Abstract

TagB, TagC (*t*andem *a*utotransporter *g*enes *B* and *C*) and Sha (*S*erine-protease *h*emagglutinin *a*utotransporter) are recently described members of the SPATE (serine protease autotransporters of *Enterobacteriaceae*) family. These SPATEs can cause cytopathic effects on bladder cells individually, but cumulative role of SPATEs was necessary for urinary tract infection in a mouse model. Bladder epithelial cells form an important barrier in the urinary tract. Some SPATEs produced by pathogenic *E. coli* are known to breach the bladder epithelium. The capacity of these newly described SPATEs to alter bladder epithelial cells and the role of the serine protease active site were investigated. All three SPATE proteins were internalized by bladder epithelial cells and altered the distribution of actin cytoskeleton. Sha and TagC were also shown to degrade mucin and gelatin respectively. Inactivation of the serine catalytic site in each of these SPATEs did not affect secretion of the SPATEs from bacterial cells, but abrogated entry into epithelial cells, cytotoxicity and proteolytic activity. Thus, our results show that the serine catalytic triad of these proteins is required for internalization in host cells, actin disruption, and degradation of host substrates such as mucin and gelatin.

6.2 Introduction

Urinary tract infections (UTIs) present a broad range of symptoms and include urosepsis, pyelonephritis (or upper UTI, with infection in the kidney) and cystitis (or lower UTI, with bacteria infecting the bladder) [1, 2]. Uropathogenic *Escherichia coli* (UPEC) is the main cause of community-acquired UTIs (about 80–90%) [3], and the ability of UPEC to establish a UTI is due to the expression of a variety of virulence factors. These factors include type 1 and P fimbriae (pili), flagella, capsular polysaccharides, iron acquisition systems, and toxins including hemolysin, cytotoxic necrotizing factor (CNF), and serine protease autotransporters of *Enterobacteriaceae* (SPATEs) [4].

The bladder urothelium constitutes a physical barrier to ascending urinary tract infections [5]. UPEC can produce toxins that damage bladder tissue that can lead to release of host nutrients and counter host defenses and innate immunity. A pore-forming toxin HlyA which can lyse erythrocytes and nucleated host cells [6] can induce apoptosis [7], promote exfoliation of bladder epithelial cells and extensive uroepithelial damage [8-11]. Another UPEC toxin, cytotoxic necrotizing factor 1 (CNF1) has been reported to mediate bacterial entry into host epithelial cells [12], induce apoptotic death of bladder epithelial cells [13], and potentially bladder cell exfoliation [13]. SPATEs such as Sat, Pic, and Vat were also shown to effect bladder or kidney epithelial cells [14-16].

An important step to understand the role of SPATEs in UPEC pathogenesis is to elucidate molecular mechanisms underlying their effect on the bladder epithelium and during urinary tract colonization. The proteolytic activity of SPATEs is mediated by a serine protease catalytic triad of aspartic acid (D), serine (S), and histidine (H) where serine is the nucleophile, and aspartic acid interacts with histidine [17]. Mutations within the catalytic triad have been shown to abolish proteolytic activity in a number of SPATEs [15, 17-19].

Recently, members of our group identified three new SPATEs: TagB, TagC (*t*andem *a*utotransporter *g*enes *B* and *C*) and Sha (*S*erine-protease *h*emagglutinin *a*utotransporter) in some strains of extra-intestinal pathogenic *E. coli* (ExPEC). In ExPEC strain QT598, *tagB* and *tagC* are tandemly encoded on a genomic island, and were present in 10% of UTI isolates and 4.7% of avian pathogenic *E. coli* (APEC) that we screened [20]. Further, Sha, which is encoded on a virulence plasmid in ST598 was present in 1% of UTI isolates and 20% of avian pathogenic *E. coli* [20]. *tagBC* genes are also present in the genomes of sequenced UPEC strains such as multidrug-resistant CTX-M-15-producing ST131 isolate *E. coli* JJ1886 (Accession number CP006784), *E. coli* CI5 (Accession number CP011018), and multidrug-resistant uropathogenic *E.*

coli strain NA114 (Accession number CP002797.2). When cloned into *E. coli* K-12, TagB, TagC and Sha mediated autoaggregation, biofilm formation (only Sha), hemagglutination and adherence to human HEK 293 renal and 5637 bladder cell lines [20]. Further, TagB and TagC exhibited cytopathic effects on the bladder epithelial cell line [20]. Following transurethral infection of CBA/J mice with a *tagBC* mutant or *sha* mutant, no significant difference in colonization was observed. However, the competitive fitness of a mutant derivative lacking all of the SPATEs present in QT598 was significantly lower in the kidney [20].

The purpose of this report was to more fully investigate the effects of the TagB, TagC and Sha SPATEs on 5637 bladder epithelial cell line focusing on the actin cytoskeleton. We also investigated potential entry of SPATE proteins within these bladder epithelial cells and whether they demonstrate mucinase or gelatinase activity.

6.3 Results

6.3.1 Processing and secretion of TagB, TagC, and Sha is independent of the serine protease motif

To evaluate the importance of the serine protease motif for processing and secretion of three novel SPATEs, we generated variant proteins of TagB, TagC, and Sha lacking the serine catalytic site. Plasmids expressing *tagB*, *tagC* or *sha* [20] were used as the templates for construction of site-directed mutant clones wherein the serine site was substituted for an alanine at residue S255, S252, and S258 respectively (Supplemental Figures S1 and S2). Each of these three plasmids expressing mutant SPATEs, produced a high-molecular-weight protein (>100 kDa) in culture supernatants that corresponded to the expected size of the native protein, and also lacked breakdown products that are present in samples containing native SPATEs that exhibit some autoproteolytic activity (Figure 6.1 A, asterisks). This demonstrated that the serine protease motif is not necessary for SPATE secretion and release from bacterial cells.

To further localize each of the SPATEs expressed from plasmids in *E. coli* BL21 on the bacterial cell surface, we used immunogold labeling and transmission electron microscopy. Polyclonal antibodies against the entire secreted Vat SPATE [20] were used as they were shown to strongly cross-react and recognize conserved epitopes of the other SPATEs. Thus, we used these polyclonal "SPATE antibodies" for the detection of other SPATEs in our experiments.

E. coli BL21 pBCsk+ expressing TagB, TagC and Sha were immunogold-labeled (Figure 6.1 B-D); demonstrating localization of these SPATEs on the bacterial surface, as well as release into

culture supernatant. The inset depicts the heavily concentrated proteins on the bacterial surface that appears to cluster around each other and produce fiber like aggregates on the cell surface (white chevron, Figure 6.1 B-D). *E. coli* BL21 bacteria containing only the empty plasmid vector were not labeled after immunogold labeling with anti-SPATE antibodies and secondary anti-rabbit immunoglobulin conjugated to 10-nm gold particles (Figure 6.1 E).

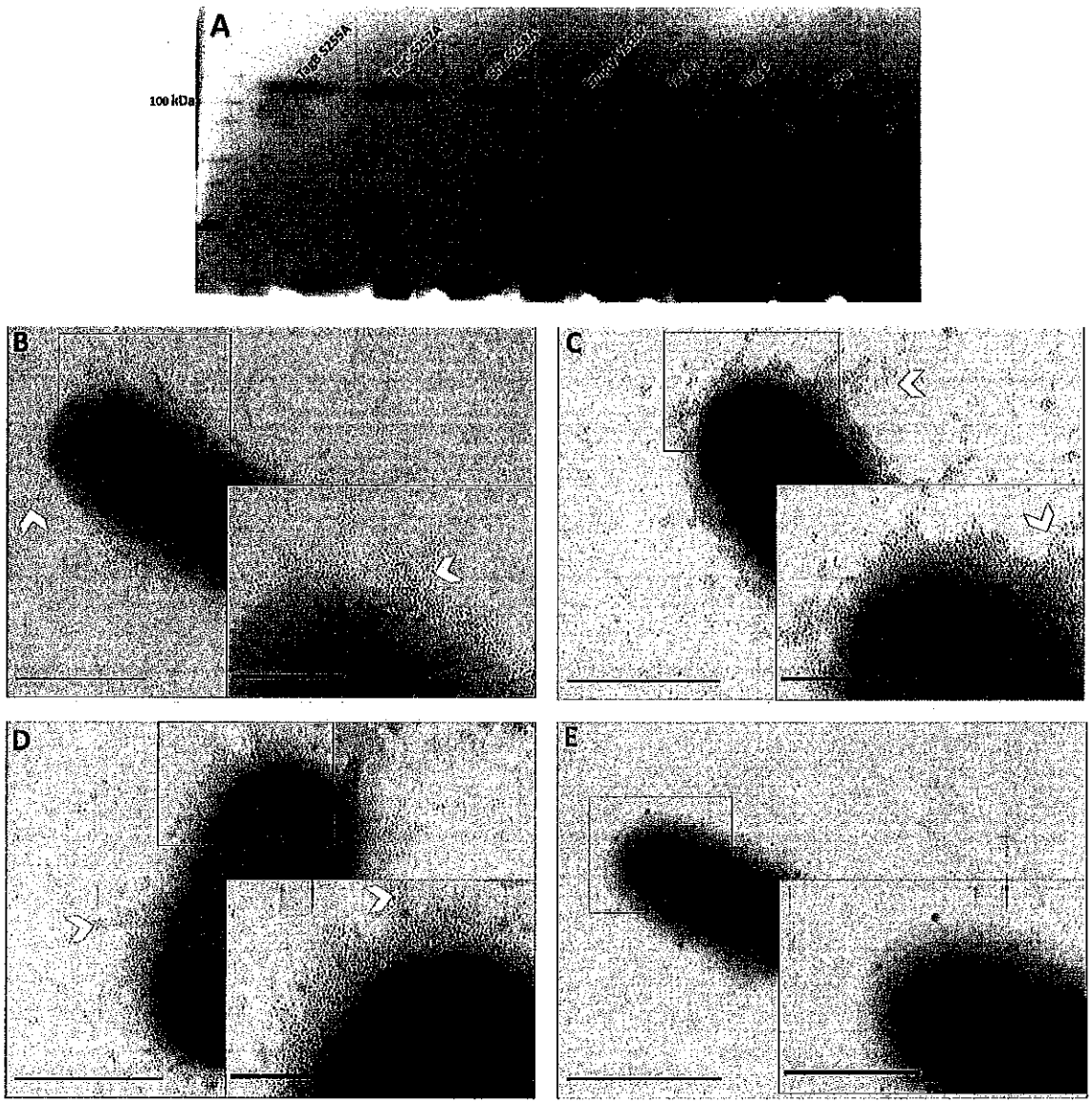

Figure 6.1 Detection of SPATEs

A. Silver stained SDS-PAGE analysis of concentrated supernatants of *E. coli* BL21 expressing SPATE proteins. Filtered supernatants from clones expressing TagB, TagC and Sha or the variant TagB S255A, TagC S252A and Sha S258A proteins were concentrated through Amicon filters with a 50 kDa cutoff. Samples containing 5µg of protein were migrated and stained with silver stain. B - E. Immunogold Electron Microscopy (EM) of SPATEs localized to the outer membrane and extracellular medium. Immunogold-TEM micrographs of SPATEs using SPATE-specific antiserum. Bacteria were cultured to 0.6 OD_{600nm} in Luria-Bertani medium. *E. coli* BL21

pBCsk+ expressing TagB (B), TagC (C), and Sha (D) labelled with immunogold particles. (E) *E. coli* BL21 pBcsk+ (vector only control) shows no immunogold staining. Insets represents boxed areas of higher magnification showing clustering of SPATE proteins. All images were acquired at ×17,000 magnification; scale bars represent 1 µm, and 0.5 µm (Insets).

6.3.2 The Serine catalytic motif of SPATEs is not required for autoaggregation or hemagglutination activity

To determine if the serine catalytic site of each of the three SPATEs is involved in autoaggregation or hemagglutination activity, we tested these phenotypes with our mutant SPATEs as described in [20]. Macroscopic analysis of autoaggregation of *E. coli* BL21 expressing TagB S255A, TagC S252A, or Sha S258A showed that bacterial cells settled at the bottom of the tube under static incubation similar to their respective native protein-expressing clones. The percentage of reduction in turbidity is given as a percentage of the initial OD_{600} value and was similar for both mutant and native proteins (Figure 6.2). The reduction in turbidity of the negative control *E. coli* BL21 pBCsk+ was significantly lower compared to clones expressing TagB, TagC, Sha, or AIDA-1 (positive control) (Figure 6.2). AIDA-1 (Adhesin Involved in Diffuse Adherence) of *E. coli* is a characterized self-associating autotransporter protein which mediates bacterial cell-cell interactions and autoaggregation [21].

These results show that inactivation of the serine catalytic site in each SPATE does not affect autoaggregation. It is therefore likely that other motifs or residues present in these proteins contribute to autoaggregation of bacterial cells.

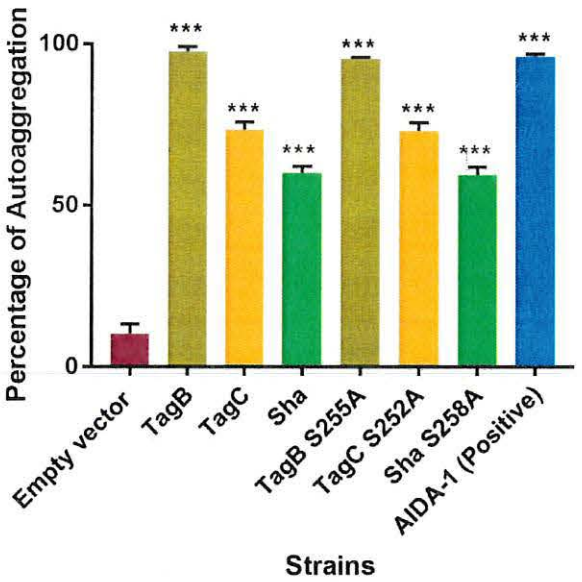

Figure 6.2 Autoaggregation phenotype is independent of the serine protease motif

Clones of *E. coli* BL21 expressing TagB, TagC, Sha or their respective serine-site mutants were grown 18 h and adjusted to an OD_{600} of 1.5 and left to rest at 4°C. Samples were taken at 1 cm from the top surface of the cultures after 3 h to determine the change in OD_{600}. Assays were performed in triplicate, and the rate of autoaggregation was determined by the mean decrease in OD_{600nm} after 3 h. *E. coli* BL21 pBCsk+ vector without insert (empty vector) was used as a negative control and the AIDA-1 autotransporter was the positive control for autoaggregation. Error bars represent standard errors of the means (* $p < 0.05$, ** $p < 0.01$, *** $p < 0.001$ compared to empty vector using one-way ANOVA).

Likewise, Sha S258A showed similar hemagglutination of human blood as reported previously for the Sha native protein [20]. When cloned in the hemagglutination negative *E. coli* strain ORN172 there was no hemagglutination activity for either the native or mutant TagB or TagC proteins. In addition to autoaggregation and hemagglutination activity the adherence capability of the serine catalytic site mutants of the SPATEs to 5637 human bladder epithelial cells was not affected (Supplement Figure S3). Hence, loss of the serine catalytic site did not affect autoaggregation, adherence or hemagglutination phenotypes associated with each of the SPATEs compared to the native proteins.

6.3.3 Cytopathic effect of TagB and TagC requires the serine protease motif

To assess the role of the serine protease motif for the cytopathic effect of SPATEs, extracts of supernatants of the different SPATEs (30 µg of protein per well) were incubated with human bladder epithelial cell line 5637 for 5h. Then the cells were fixed, stained with Giemsa stain and observed by light microscopy. Cytopathic changes (dissolution in cytoplasm, enlargement of the nucleus with vacuoles) observed under the microscope for TagB and TagC (Figure 6.3 A) were absent from cells treated with either TagB or TagC proteins lacking the serine protease active site. In addition, no significant morphological changes were observed with cells treated with either Sha or the mutant, Sha S258A, protein. No cytopathic effect was observed after treatment of cells with concentrated filtered supernatant from *E. coli* BL21 pBCsk+ (empty vector) or media alone (Figure 6.3 A). To examine this cytopathic effect quantitatively, we measured lactate dehydogenase (LDH) release from epithelial cells incubated with each of SPATEs or their respective catalytic site mutant proteins. There was release of LDH after 5 h upon exposure of cells to TagB or TagC. However, the catalytic site mutant proteins did not release LDH from cells (Figure 6.3 B). Further, no LDH release was detected from cells treated with either Sha or its catalytic site mutant variant (Figure 6.3 B), indicating that cytotoxicity to human bladder epithelial cells by TagB and TagC was dependent on the serine protease catalytic site.

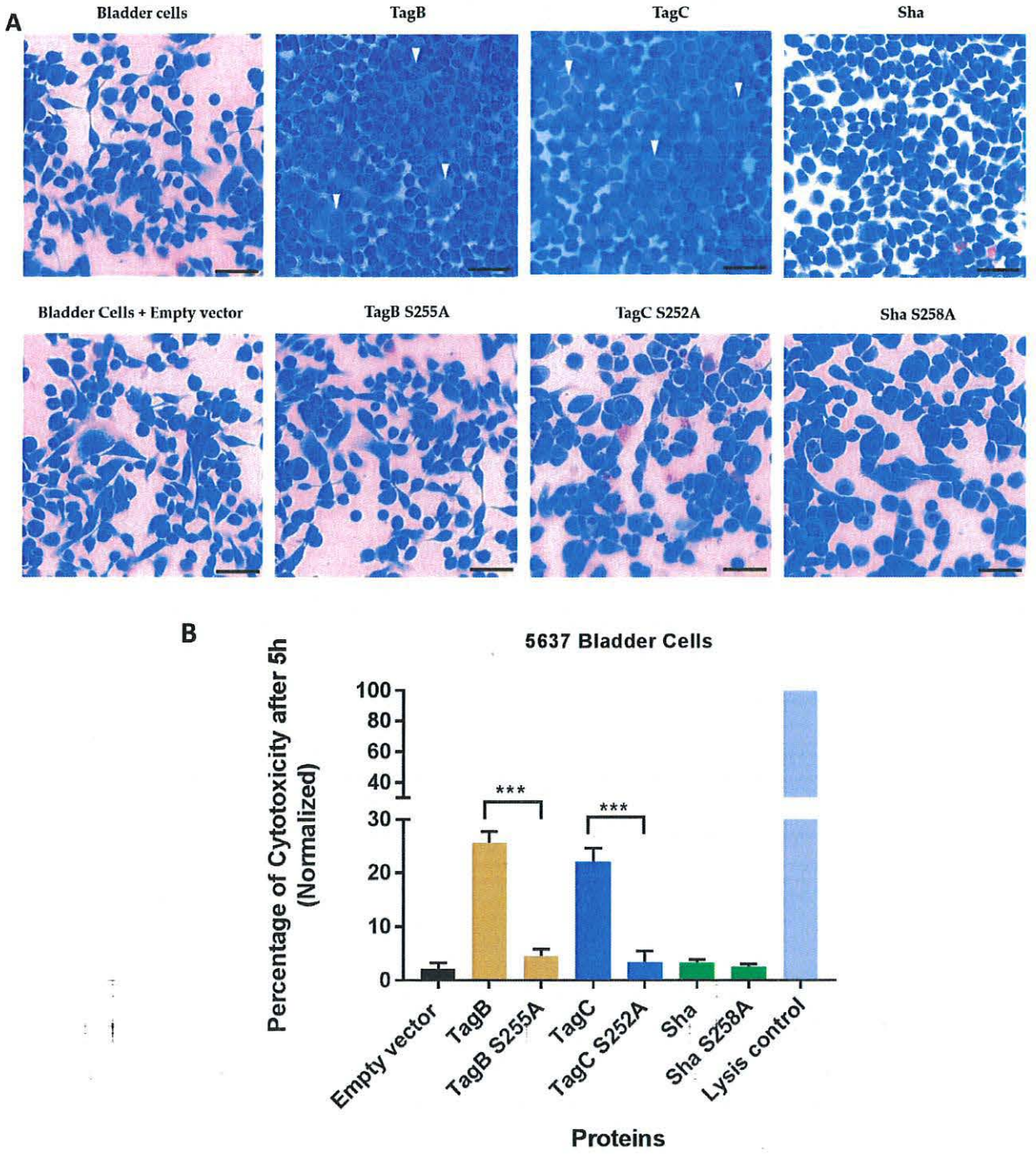

Figure 6.3 The serine catalytic site is necessary for cytopathic effect of TagB and TagC

A. Concentrated supernatants containing 30 µg of protein per well of *E. coli* BL21 clones expressing TagB, TagC, Sha or their respective serine mutant variant proteins were incubated with monolayers of the 5637 human bladder epithelial cell line for 5 h at 37°C. Cytopathic effects (white triangle) were absent in cells treated with the serine catalytic site mutant variants of TagB or TagC. The Empty vector (pBCsk+) without insert was used as a negative control. The scale bar represents 20 µm. B. Cytotoxicity measured by LDH release from 5637 human bladder cells after incubation with supernatant filtrates of different clones (30 µg of protein per well) at 37°C for 5 h. Empty vector (pBCsk+) was used as a negative control and maximum LDH release (positive control) was determined by treatment with lysis solution. Data are the means of three independent

experiments, and error bars represent the standard errors of the means. Significant differences between lysis caused by native and mutant SPATEs were determined using Student's t-test with ***p < 0.001).

6.3.4 Exposure to TagB, TagC, or Sha altered actin distribution in bladder epithelial cells

Based on the cellular changes seen with bladder epithelial cells after exposure to TagB and TagC, we hypothesized that TagB and TagC could alter the distribution of cytoskeletal components such as actin, with actin being one of the most abundant intracellular proteins in the eukaryotic cell. So, to examine the effect on F-actin cytoskeleton organization, 5637 bladder cells were incubated with native and mutant TagB, TagC or Sha (30 μg of protein per well) for 5 h at 37°C, stained with fluorescently labeled phalloidin, and then observed under confocal microscopy. Cells treated with the supernatant extract from the empty vector containing clone were uniform, smooth-edged, and contained clearly visible actin stress fibers (yellow triangle) and strong actin staining around the cell (Figure 6.4 A). By contrast, bladder cells treated with TagB showed reduced actin stress fibers and less actin staining (Figure 6.4 A). Bladder cells treated with TagC, also had a pronounced effect on the cytoskeleton as demonstrated by the absence of actin stress fibers and reduced levels of actin staining. Sha treated cells showed a loss of actin stress fibers and the presence of punctate patterns of actin within the cytoplasm of the cells (yellow arrowheads, Figure 6.4 A). By contrast, the TagB, TagC, and Sha mutants lacking the serine protease catalytic sites demonstrated no changes in the actin cytoskeleton and had actin stress fibers like negative control cells, indicating that the serine protease activity of these SPATEs mediates the changes in actin distribution within bladder cells. To quantify the level of phalloidin binding, we measured the staining intensity and distribution of fluorescence of phalloidin around each cell using ImageJ software [22]. Fluorescence intensity for cells was calculated using the channel for actin staining. In comparison with the negative control (empty vector), the density of F-actin staining was significantly lower in cells treated with TagB, TagC or Sha. Cells treated with the serine catalytic site mutant proteins, demonstrated F-actin staining that was greater when compared to cells treated with the native SPATE proteins (Figure 6.4 B). Overall, these results demonstrate that these SPATEs alter the cytoskeleton and reduce the distribution of actin in bladder epithelial cells.

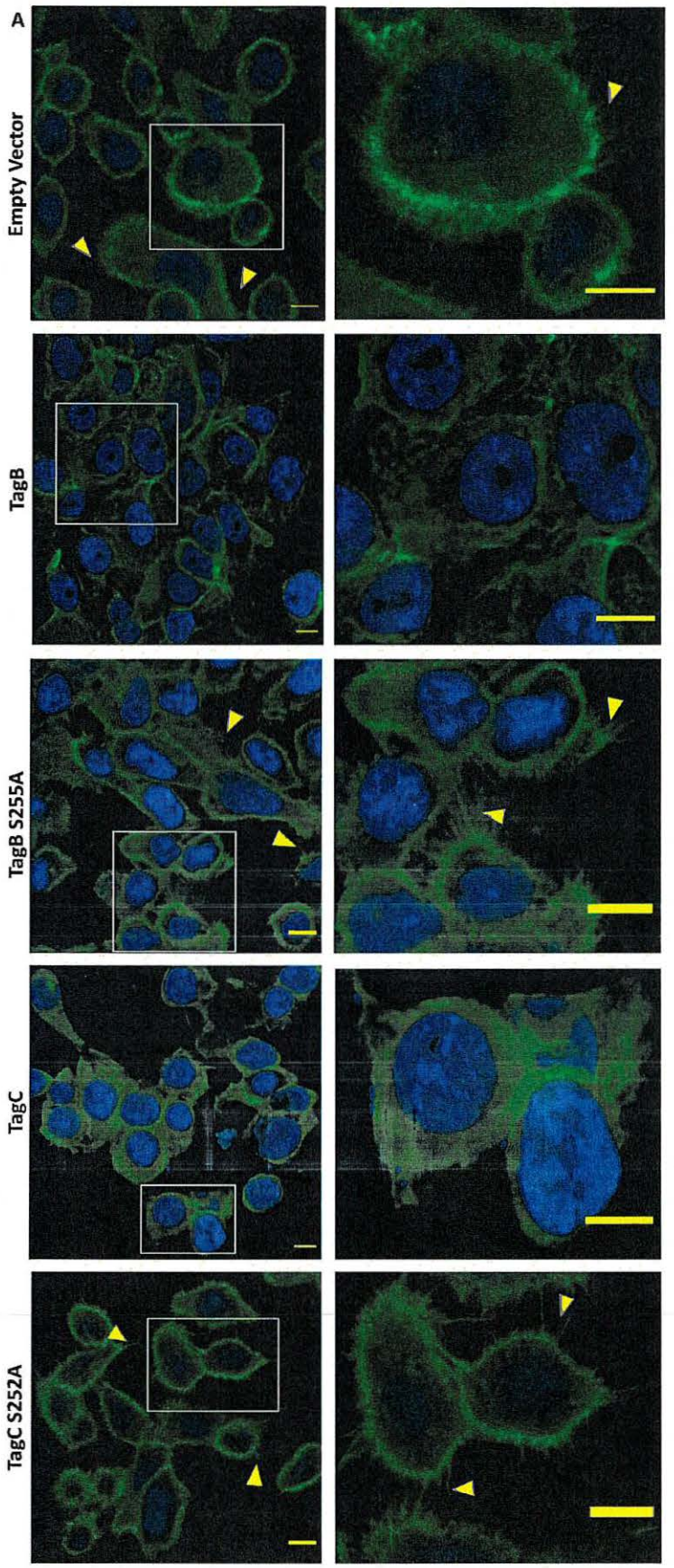
A
Empty Vector
TagB
TagB S255A
TagC
TagC S252A

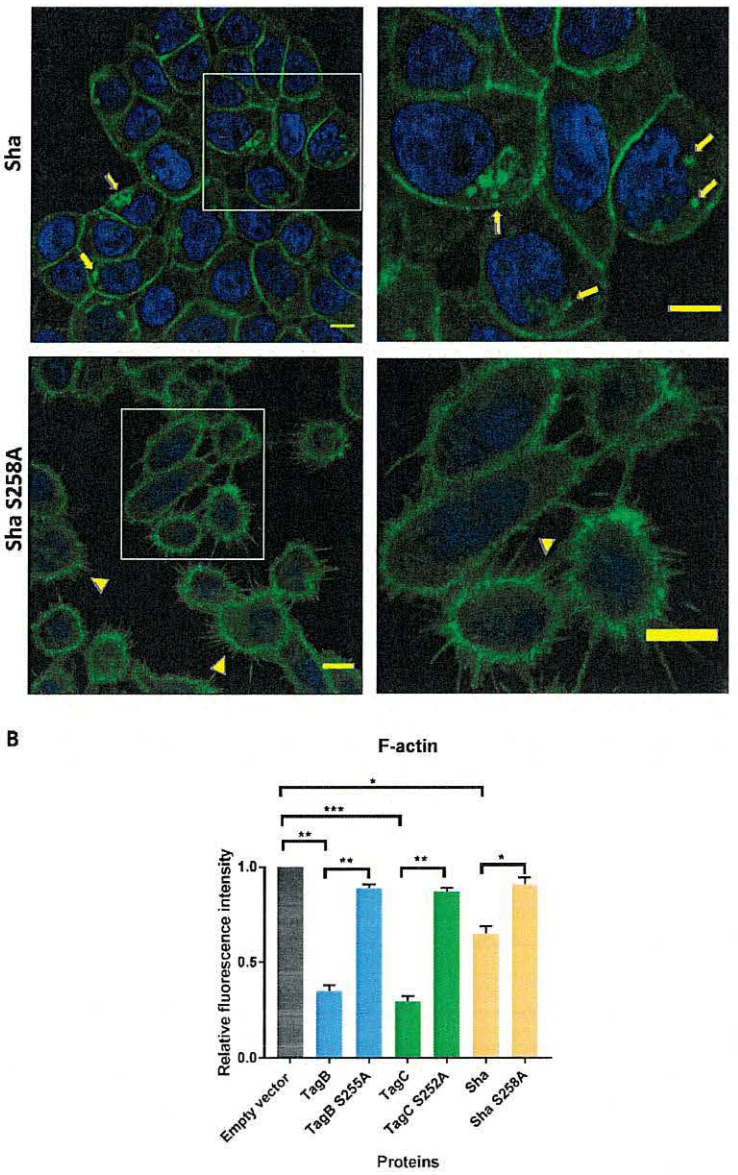

Figure 6.4 Effects of TagB, TagC, and Sha on the actin cytoskeleton of bladder epithelial cells is serine-protease-motif dependent.

A. Concentrated supernatant extracts (30 µg of protein per well) from *E. coli* BL21 clones expressing TagB, TagC or Sha and their respective serine catalytic site mutants were incubated with monolayers of human bladder (5637) epithelial cells for 5 h at 37°C. After incubation, cells were fixed and permeabilized. Actin was stained with fluorescently labeled phalloidin (green) and the nucleus was stained by DAPI (blue). Cells treated with the filtered supernatant of *E. coli* BL21 pBCsk+ without insert (empty vector) were used as a negative control. Slides were observed by confocal microscopy. Inset images from the left panels are magnified in the panels to the right. Bars represent 10 µm. B. Quantitative analysis of fluorescence intensity of F-actin. Analysis of fluorescent intensity was done at the original magnification by measuring the mean gray value with ImageJ software [22] with an n value of at least 10 cells. Data values represent the mean ± SEM of at least three independent experiments. (* $p < 0.05$, ** $p < 0.01$, *** $p < 0.001$ one-way ANOVA with multiple comparisons)

6.3.5 SPATE entry into bladder epithelial cells is dependent on the serine protease active site

We previously showed that TagB and TagC demonstrated cytotoxicity as measured by lactate dehydrogenase (LDH) release from epithelial cells within 5 h [20]. This toxicity could be due to the interaction of the SPATEs with targets inside host cells. So, to gain insight into the potential internalization of these SPATEs, we employed immunofluorescence labeling of proteins followed by visualization using confocal or immunogold electron microscopy. Firstly, confocal Z-sections (optical slices) of 5637 bladder cells treated with SPATEs were examined to determine if SPATEs were translocated within cells. After 5 hours of incubation, TagB, TagC and Sha (red color) were found within cells as evidenced by cell sectioning analysis (Figure 6.5 A). By contrast, the serine active-site mutant variants were unable to enter epithelial cells and were not detected (absence of red staining) (Figure 6.5 A), suggesting that serine protease activity is needed for the entry of SPATEs within cells. Interestingly, TagB within cells also co-localized with actin (green color) in the outer border of the cell (Figure 6.5 A). Further, cells incubated with serine mutant variants of SPATEs did not enter cells, and these cells also produced actin stress fibers (Figure 6.5).

A

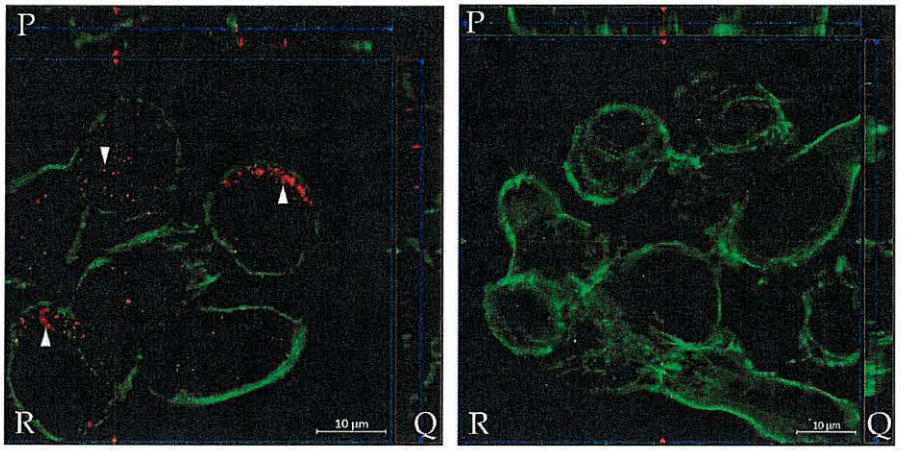

TagB TagB S255A

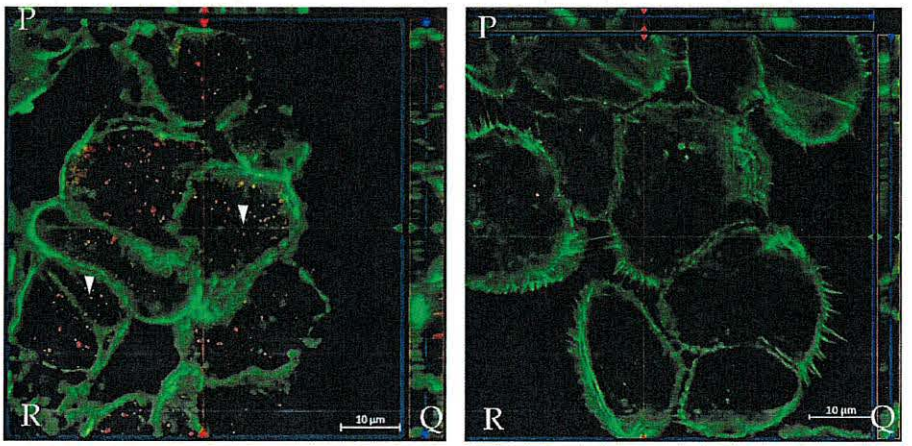

TagC TagC S252A

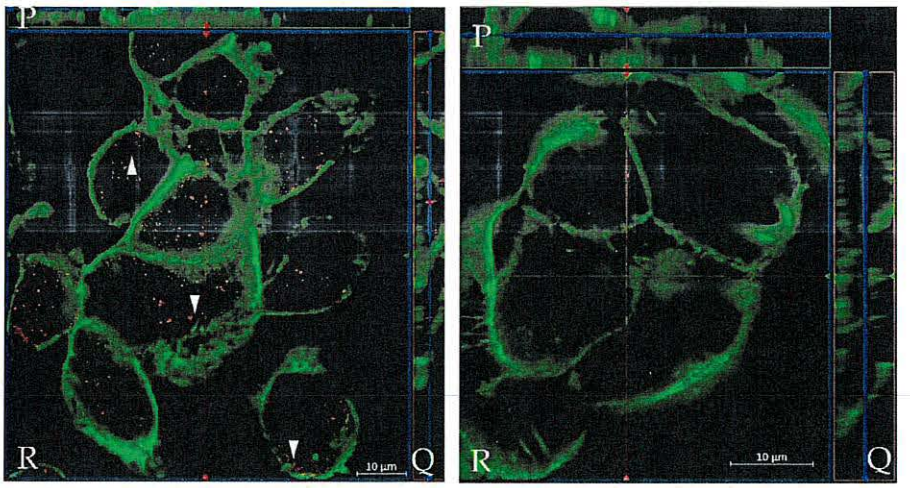

Sha Sha S258A

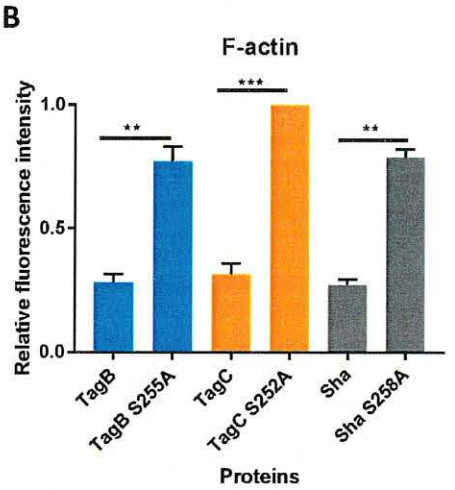

Figure 6.5 Intracellular localization of TagB, TagC, and Sha determined by confocal microscopy

A. Z-stack imaging showing the localization of TagB, TagC, and Sha and their respective serine active site mutant variants during interaction with 5637 bladder epithelial cells after 5 h of incubation. SPATEs were detected by Alexa Fluor 594 (white arrowheads, red fluorescence) using anti-mouse secondary antibody and actin was stained by Alexa Fluor 488- phalloidin (green fluorescence). Images are displayed in a 3D section view with large Z-sections in the X-Y direction (R), Z-projection in the X–Z direction (P), and Z-projection in the Y–Z direction (Q). The green and red lines in R indicate the orthogonal planes of the X–Z and Y–Z projection. For each selected section, the signal was gathered from a span of 5 µm. Scale bar: 10µm B. Quantitative analysis of fluorescence intensity of F-actin in the cells treated with native or mutant SPATEs. Analysis of fluorescent intensity was done in green channel by measuring the mean gray value on ImageJ. Data represent the mean ± SEM of at least three independent experiments. Significant differences between lysis caused by native and mutant SPATEs were determined using Student's t-test with $^{**}p < 0.01$, $^{***}p < 0.001$).

Analysis of thin-sections of SPATE-treated cells using immunogold staining and transmission electron microscopy (TEM) also confirmed the intracellular localization of all three SPATEs within cells. TagB and Sha were found in the cytoplasm, whereas TagC was present in the nucleus (Figure 6.6). However, in multiple independent experiments, we failed to detect the presence of serine mutant variants of TagB, TagC, or Sha within cells. The serine catalytic-site mutant proteins when visualized were almost exclusively observed on the extracellular surface of cells as seen in cells treated with TagB S255A (Figure 6.6 D).

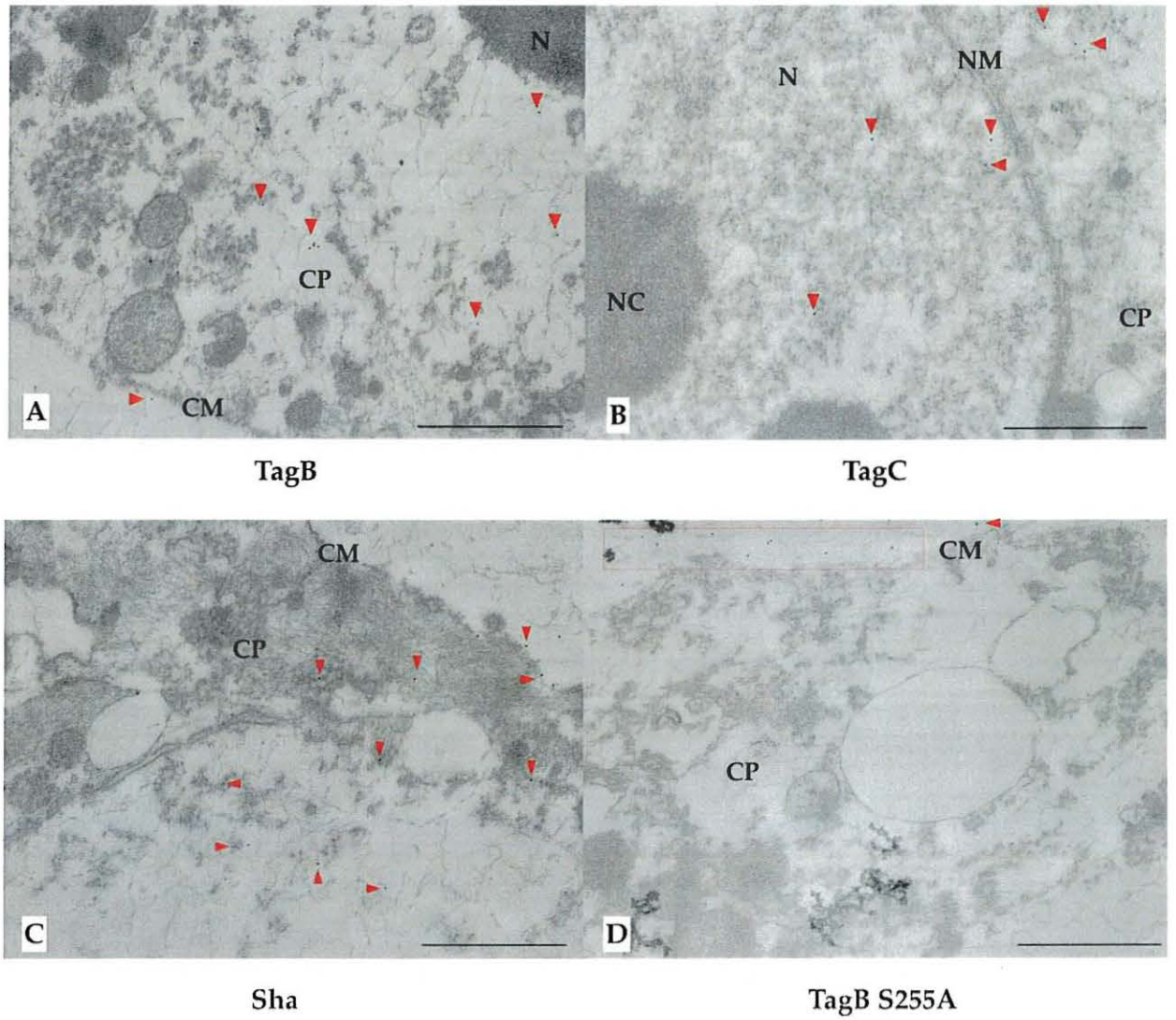

Figure 6.6 Transmission electron micrographs of 5637 bladder cells showing internalized SPATEs, immunolabelled with 10-nm-diameter gold particles after 5 hours incubation of proteins with 5637 bladder cells.

Gold particles are highlighted with red triangles. (A) TagB is principally located in the cytoplasm (CP). (B) For Tag C, gold particles were associated with the nucleus (N) and cytoplasm (CP). (C) Sha was located mainly in the cytoplasm (CP). (D) For the serine mutant variants of TagB, TagC and Sha, gold particles were only localized on the extracellular surface of cells (red box). Only the TagB S255A mutant protein localization is shown. Cell membrane (CM), Cytoplasm (CP), Nuclear Membrane (NM), Nucleus (N), Nucleolus (NC) Bars, 1µm

6.3.6 Sha exhibits serine protease-dependent mucinase activity

Epithelial cell damage caused by SPATEs was shown to require protease activity, and some other SPATEs were previously shown to demonstrate activity against host proteins such as mucin or gelatin [18, 23]. Further, we also tested for mucinase activity, since two of the novel SPATEs identified in APEC QT598, Sha and TagB [20], belong to the class 2 SPATE family whose

members have been shown to demonstrate mucinolytic activity. Clones of *E. coli* BL21 expressing each of the SPATEs were grown on agar plates containing 0.5% porcine gastric mucin for 24 h at 37°C, followed by amido black staining. Plates containing clones growing on discs expressing Sha revealed clear zones of mucin lysis (Figure 6.7 A) and the lysis zone produced by Sha was intermediate when compared to clones expressing either Tsh (positive control) or Vat. Mucin containing plates had a clearing zone with a diameter of 3.9 ± 0.1 cm after exposure to Sha expressing bacteria which was less than following exposure to Tsh expressing cells (4.2 ± 0.1 cm), but more than following exposure to Vat expressing cells (3.7 ± 0.2 cm). By contrast, TagB and TagC were mucinase-negative as evidenced by the absence of any clearing zones (Figure 6.7 B). Further, the critical role of the serine catalytic site of Sha for mucinase activity was demonstrated with the clone expressing Sha S258A which did not produce a zone of mucin lysis (Figure 6.7 B). The clone containing only the empty vector (negative control) did not grow well in the presence of mucin and demonstrated no clearing zone. When mucin was treated with culture filtrates of SPATE proteins (Figure 6.7 C), it was not degraded by either TagB, TagC or in the negative control (empty vector). Sha as well as Tsh and Vat degraded mucin, whereas the serine protease mutant of Sha, Sha S258A, did not. Hence, the serine catalytic site of Sha is required for mucinase activity.

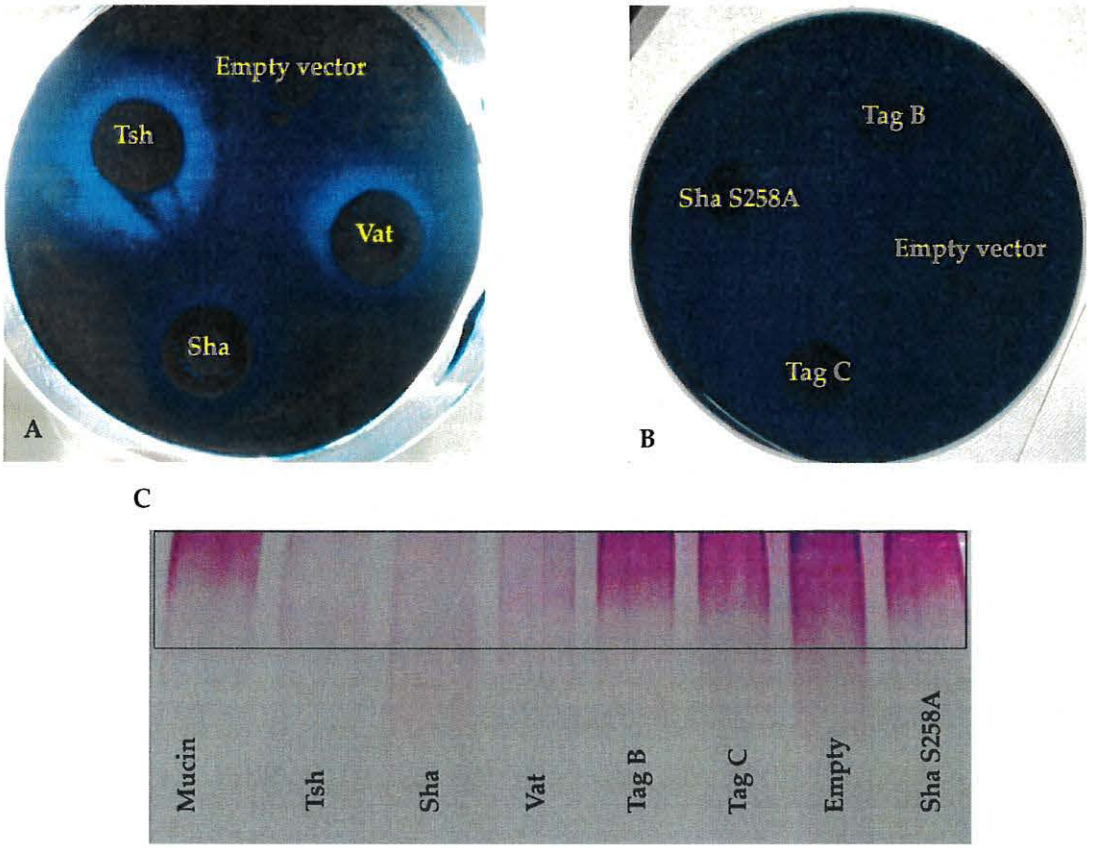

Figure 6.7 Mucinolytic activity of Sha, but not the TagB and TagC SPATEs

Mucinase activity was tested in a medium containing 1.5% agarose and 0.5% porcine gastric mucin. Filter discs inoculated with clones containing the empty vector, expressing Sha, Vat, Tsh, (A) TagB, TagC or Sha S258A (B) were placed on the agar surface and incubated overnight at 37°C. Mucin lysis zones were visualized by staining with 0.1% amido-black in 3.5 M acetic acid for 15 min, followed by destaining with 5% acetic acid and 0.5% glycerol for 6 h to overnight. (C) Zones of 0.5% porcine gastric mucin hydrolysis are visible in the stacking region of the SDS-PAGE gel (boxed area), concentrated supernatant extracts of SPATEs (5 µg of protein per well) were incubated at 37 °C for 48 h with mucin prior to migration. The gel was stained with a PAS glycoprotein staining kit.

6.3.7 TagC exhibits serine protease-dependent gelatinase activity

Some SPATEs were previously reported to degrade extracellular matrix proteins such as collagen and gelatin [23]. We previously demonstrated that TagB, TagC and Sha could mediate increased adherence to chicken fibroblasts [20], which are cells that are associated with connective tissues and produce extracellular matrix proteins such as collagen. The hydrolyzed form of collagen – gelatin was used as a substrate to test for potential gelatinase activity from supernatant extracts containing SPATEs. Culture supernatant filtrate from *Pseudomonas aeruginosa* was used as a positive control, since it is known to demonstrate gelatinase activity [24]). Samples were incubated with 1% bovine gelatin for 48 h at 37°C. Culture filtrates containing TagC as well as other SPATEs EspC, Tsh and Vat demonstrated gelatinase activity (Figure 6.8 A). By contrast, neither TagB nor

Sha demonstrated gelatinase activity, since high-molecular-weight bands, indicating intact gelatin, remained after exposure to these SPATEs. Further, gelatinase activity from TagC was shown to be dependent on the serine protease motif, since the *E. coli* clone expressing a serine active site mutant protein, TagC S252A, did not generate a hydrolysis zone on medium containing 1% gelatin, whereas the TagC expressing clone did exhibit a hydrolysis zone (Figure 6.8 B).

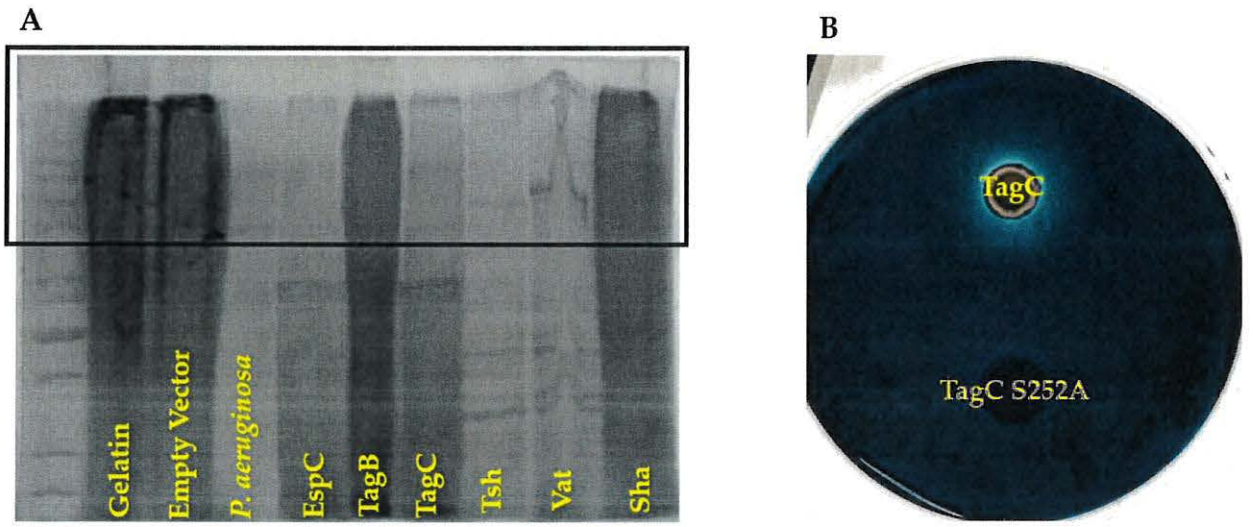

Figure 6.8 TagC demonstrates serine-protease dependent gelatinase activity

A. Zones of 1% bovine skin gelatin hydrolysis are visible in the stacking region of the SDS-PAGE gel (boxed area), concentrated supernatant extracts of SPATEs (5 µg of protein per well) were incubated at 37 °C for 48 h prior to migration. B. Gelatinase activity of TagC was tested in a medium containing 1.5% agarose and 1% bovine skin gelatin. The disc inoculated with a clone expressing TagC or its serine catalytic site mutant variant, TagC S252A, were inoculated on the agar surface and were incubated for 48 h at 37°C. Zones of gelatin lysis were visualized by staining with 0.1% amido-black in 3.5 M acetic acid for 15 min, followed by destaining with 5% acetic acid and 0.5% glycerol for 6 h.

6.4 Discussion

Colonization of the bladder is vital for UTI pathogenesis and UPEC deploys an array of virulence factors to infect and colonize the bladder, including secreted toxins [25]. Hemolysin A [8, 9], UpxA (TosA) [26], cytotoxic necrotizing factor-1 (CNF-1) [27, 28], and a variety of SPATEs (serine-protease autotransporters of *Enterobacteriaceae*) [29] are known toxins of host cells that are produced by some UPEC strains. The recent identification of new members of the SPATEs family present in some pathogenic *E. coli* and their cytotoxic activity on bladder cell lines [20], led us to further investigate mechanisms underlying the cytotoxic and proteolytic activity of the TagB, TagC and Sha SPATEs on an established human urinary bladder cell line [30, 31] and other properties of these virulence-associated proteins.

TagB, TagC and Sha proteins demonstrated autoaggregating activity, and also promoted adherence of *E. coli* strain BL21 to the human HEK 293 renal and 5637 bladder human cell lines. Further, Sha also contributed to increased biofilm production [20]. SPATEs present on the bacterial surface are likely to contribute to the autoaggregation phenomenon (Figure 6.1 A). TagB and TagC also exhibited cytopathic effects on the bladder epithelial cell line. Further, we also previously determined that proteolytic activity of these SPATEs was strongly inhibited upon addition of serine protease inhibitor (PMSF), providing evidence for the importance of the serine protease motif in the activity of these SPATEs [20]. To further investigate the role of the serine protease activity, we generated catalytic site mutants of these three SPATEs. It is of note that the serine protease consensus motif (GDSGS) is conserved among different members of SPATEs [20, 32-35]. Importantly, loss of the serine active site did not affect the processing or secretion of the SPATE proteins into the extracellular milieu (Figure 6.1 A). Further, loss of the serine active site also eliminated any autoproteolytic activity (Figure 6.1 A). Similarly, autoproteolytic activity has also been reported for other SPATEs including EspP, Sat, Pic [36], and for AspA autotransporter from *Neisseria meningitidis* [37]. Thus, from our results, it is clear that the processing of the passenger domain across the bacterial surface and autocatalytic activities of the TagB, TagC, and Sha is independent of the proteolytic serine site.

We investigated the role of the serine catalytic site of TagB, TagC and Sha in autoaggregation or hemagglutination, as either SPATE protease activity on the bacterial or host cell surfaces could have possibly mediated these phenotypes. For instance, cleavage could have led to certain domains within the protein leading to exposure of hydrophobic sites which could promote aggregation [38]. However, the serine protease site was not required for TagB, TagC or Sha-mediated aggregation (Figure 6.2). These results indicate that other specific SPATE structural domains are likely to be responsible for aggregation. However, importantly, the autoaggregation phenotype is not a generalized phenotype of SPATEs, since in previous experiments, both the Tsh and Vat SPATEs did not demonstrate any autoaggregation phenotype [20]. Currently, the molecular mechanism of autoaggregation of TagB, TagC and Sha is unknown. Unlike the three SPATEs described herein, loss of the active site serine of the Hap adhesin, a *Haemophilus influenzae* serine protease autotransporter, abrogated autoproteolytic processing leading to retention of this AT protein on the bacterial cell surface [39]. In fact, the increase in Hap present on the bacterial surface also increased aggregation, formation of microcolonies, and adherence of *H. influenzae* to host cells [40]. With regards to hemagglutination activity of the Sha protein, the serine active site was also dispensable. We found that Sha S258A hemagglutinated human blood with a similar titer to the native Sha protein. Similarly, a Tsh S259A variant protein was also

able to bind to avian erythrocytes, turkey hemoglobin, collagen IV, fibronectin, and laminin [41]. Considering that the TagB S255A, TagC S252A and Sha S258A variant SPATEs all retained the respective phenotypes present in the native SPATE proteins, this suggests that, despite lacking catalytic activity, that these variants are likely to have maintained a properly folded conformation.

In contrast to adherence or aggregation phenotypes, the presence of a serine protease motif was clearly required for cytotoxicity and entry of the SPATE proteins into bladder epithelial cells. In this study, the TagB S255A and TagC S252A mutant proteins were no longer cytopathic. Our results are similar to those described for other SPATEs [15, 41, 42] which have demonstrated a key role for the serine active site with regards to any native proteolytic or cytopathic activity of SPATEs on protein substrates or host cells.

Since TagC shares 60% identity/74% similarity with another SPATE , EspC, a non-LEE-encoded enterotoxin of enteropathogenic *E. coli* (EPEC) which causes cytotoxic effects and cleavage of cytoskeletal actin-associated protein [43]; we explored potential cellular targets in relation to the cytopathic effect observed in bladder epithelial cells. Following treatment with either TagB, TagC or Sha, reorganization of the cytoskeleton and loss of actin stress fibers were seen in bladder epithelial cells (Figure 6.4). The effect of TagC was severe with faint staining remaining for actin compared to TagB interaction with cells. Exposure to Sha caused punctate localization of actin within the cytoplasm. Diminished actin staining and the formation of punctate actin accumulation suggests that each of these SPATEs are targeting the actin cytoskeleton or other cellular targets that lead to modifications in actin fiber formation or distribution within bladder cells. As expected, alterations in actin distribution were absent from bladder cells exposed to the serine catalytic site mutant variant proteins TagB S255A, TagC S252A, or Sha S258A, confirming the critical cytopathic role of serine protease activity.

Many pathogens exploit host actin for various stages of infection including cellular invasion, intracellular replication, and dissemination by different mechanisms [44, 45]. Specifically, during UTIs, UPEC utilizes the Rho family GTPase member Rac1 to mediate actin polymerization for *E. coli* bladder epithelial cell invasion [46]. It has been well documented that there is a relation between intracellular growth of UPEC in the bladder epithelium and the host F-actin cytoskeleton [47]. Based on the observation of actin rearrangement observed in bladder cells, it is also possible that the TagB, TagC and Sha SPATEs might also contribute to UPEC invasion of the bladder epithelium, as these proteases may promote adhesion and loss of integrity of the protective epithelial barrier which could increase bacterial entry into epithelial cells as well as increase entry and systemic spread of the bacteria to other tissue sites during infection.

Before reaching the epithelial cell surface in the urinary tract, bacteria must cross the protective mucus layer that is coated with mucin [48]. Mucin serves as a primary antibacterial defense in the bladder and contributes to host innate defense by providing a barrier and by trapping bacteria [49]. Many pathogens can invade or reduce the viscosity of mucin by cleaving it [50-52]. Certain SPATEs, belonging to the Class 2 family including Pic [18] [53], PicC of *Citrobacter rodentium* [54], and Tsh demonstrate mucinase activity [55]. We, therefore, tested whether any of the three novel SPATEs were mucinolytic, and only Sha was identified as a mucinase (Figure 6.7). The zone of mucinolytic activity of Sha was intermediate when compared to Vat and Tsh and, as has been shown for Pic [18], the serine catalytic site of Sha was required for mucinase activity. From this standpoint, it is interesting to note that in strain QT598, 3 of the 5 SPATEs (Tsh, Vat and Sha) demonstrate mucinase activity [20] which might facilitate bacterial colonization by degrading mucus to overcome the mucous barrier at the interface of epithelial surfaces. This common phenotype of mucinase shown by three members of Class 2 SPATEs of QT598 might be due to presence of domain 2, a conserved domain among class 2 family of SPATEs thought to be involved in substrate recognition [20]. TagC was also shown to degrade gelatin, which is the hydrolyzed form of collagen, although this activity was absent from Sha and TagB. Collagen is an abundant and ubiquitous extracellular matrix protein that forms an essential component of connective tissues [56]. From this standpoint, the TagC protease may contribute to tissue invasion and systemic spread of ExPEC by degradation of extracellular matrix proteins. As expected, the activity of TagC on gelatin was also dependent on the active serine catalytic site. Similarly, Pic [23] also demonstrated gelatinase activity that required an active serine catalytic site.

Previous reports have described different mechanisms of internalization of SPATEs and types of cytoskeletal damage in various epithelial cells *in vitro*. The Pet SPATE from enteroaggregative *E. coli* (EAEC) is internalized by a retrograde trafficking pathway [57] through the Pet host cell receptor, cytokeratin 8 [58]. Once internalized, Pet causes loss of actin stress fibers due to the breakdown of spectrin [59, 60]. Internalization of EspC by EPEC requires the type 3 secretion system [61] and leads to cleavage of cytoskeletal proteins [43]. Sat is secreted by UPEC ,enters the cell by an unknown mechanism and localizes to the cytoskeletal fraction of fodrin/spectrin and integrin present within bladder and kidney epithelial cells [15]. In the present report, we have demonstrated that TagB, TagC, and Sha are also internalized in bladder epithelial cells by a mechanism that requires an active serine catalytic domain. We used confocal Z-sections to verify the intracellular localization of the SPATEs within human bladder epithelial cells. Of note, we observed the internalization of TagB, TagC and Sha within bladder cells after 5 hours and this was concomitant with diminished fluorescence staining of actin in the vicinity of the localized

SPATEs. This observation was pronounced following exposure to TagB, and TagB was shown to be closely associated with actin. Furthermore, to confirm the internalization of SPATEs within bladder epithelial cells, we carried out immunogold TEM of cross-sections of cells to demonstrate SPATE proteins within epithelial cells. TEM demonstrated localization of TagB and Sha in the cytoplasm, whereas TagC targeted the nucleus. We speculate that, since TagC has previously been shown to promote nuclear enlargement [20], TagC may alter nuclear targets and elicit a significant increase in nuclear size. The entry of these SPATEs into host bladder cells does not require a type 3 secretion mechanism since it is absent from *E. coli* QT598 and *E. coli* BL21, and SPATE proteins from bacterial supernatants entered bladder epithelial cells directly. Future studies will elucidate the cytoplasmic or nucleo-cytoplasmic shuttling pathways that mediate the entry and trafficking of these three SPATEs. Importantly, the serine catalytic site was required for cell entry and cytotoxicity of all three SPATEs, since serine protease active site mutants were unable to enter cells or cause any cytopathic effects, further demonstrating a critical role for the serine catalytic site of these SPATEs.

Taken together, the TagB, TagC, and Sha SPATE proteins mediate multiple activities. These include adhesion, aggregation, cytopathic effects, mucinase and gelatinase activities that may collectively contribute to different stages of bacterial infection including initial colonization, invasion of host epithelia, and an increased potential for systemic infection.

6.5 Materials and Methods

Ethics statement

This study was performed in accordance with the ethical standards of the University of Quebec, INRS. A protocol for obtaining biological samples from human blood donors was reviewed and approved by the ethics committee - *Comité d'éthique en recherche* (CER 19-507) of INRS.

Bacterial strains, plasmids and growth conditions

E. coli clones expressing TagB, TagC or Sha were described previously [20]. All DNA constructs were transformed into *E. coli* strain BL21 or the type 1 fimbriae *fim*-negative *E. coli* strain ORN172. Strains were grown at 37°C on solid or liquid Luria-Bertani medium (Alpha Bioscience, Baltimore, MD, USA) supplemented with the appropriate antibiotics when required at concentrations of 100µg/ml ampicillin, 30 µg/ml chloramphenicol, or 50 µg/ml of kanamycin. Strains, plasmids and primers are listed in Table 6.1 .

Table 6.1 Strains and plasmids used in this study

Strains	Characteristic(s)	References
QT598	APEC O1: K1, serum resistant	[24]
ORN172	*thr-1 leuB thi-1Δ (argF-lac)U169 xyl-7 ara-13 mtl-2 gal-6 rpsL tonA2 supE44Δ (fimBEACDFGH)::Km pilG1*	[66]
BL21	*fhuA2 [lon] ompT gal [dcm] ΔhsdS*	New England Biolabs
QT1603	HB101 with AIDA-1 operon	[67]
QT4767	ORN172/pIJ553 (Expressing *sha*)	[23]
QT5194	BL21/pIJ548 (Expressing *tagB*)	
QT5195	BL21/pIJ549 (Expressing *tagC*)	
QT5197	BL21/pIJ550 (Expressing *espC)*	
QT5198	ORN172/pIJ548 (Expressing *tagB*)	
QT5199	ORN172/pIJ549 (Expressing *tagC*)	
QT5431	BL21/pIJ551 (Expressing *vat*)	
QT5432	BL21/pIJ552 (Expressing *tsh*)	
QT5433	BL21/pIJ553 (Expressing *sha*)	
QT5437	BL21 + pIJ554 (Expressing *tagB S255A*)	This study
QT5438	BL21 + pIJ555 (Expressing *tagC S252A)*	This study
QT5439	BL21 + pIJ556 (Expressing *sha S258A)*	This study

QT5598	ORN172 + pIJ554 (Expressing *tagB S255A*)	This study
QT5599	ORN172 + pIJ555 (Expressing *tagC S252A)*	This study
QT5600	ORN172 + pIJ556 (Expressing *sha S258A)*	This study
QT3046	*Pseudomonas aeruginosa* PA14	Eric Déziel, INRS
Plasmids		
pBCsk+	Cloning vector; Cm^r	Stratagene, La Jolla, CA
pIJ548	pBCsk+::*tagB*	[23]
pIJ549	pBCsk+::*tagC*	
pIJ551	pBCsk+::*vat*	
pIJ552	pBCsk+::*tsh*	
pIJ553	pBCsk+::*sha*	
pIJ554	pBCsk+::*tagB S255A*	This study
pIJ555	pBCsk+::*tagC S252A*	This study
pIJ556	pBCsk+::*sha S258A*	This study

Site-directed mutagenesis

Site-directed mutagenesis was performed using the Q5® Site-Directed Mutagenesis Kit as specified by the manufacturer. pIJ548, pIJ544 and pIJ553 were used as a template for the construction of the serine catalytic site mutants TagB S255A (pIJ554), TagC S252A (pIJ555), and Sha S258A (pIJ556) at 25 to 50 ng per reaction with 10 pmol of each of the complementary

primers. Primers used to generate the single point mutation substituting alanine for serine for TagB were 5'-TCCCGGTGACgcCGGCTCTCCT-3'and 5'-GTACCGTAGGTTGAGAGTG-3'; TagC were 5'-AGGAGGAGACgcCGGTTCCGGA-3'and 5'-GTCACTTCATTATAAAATCCACC-3'; and Sha were 5'-GGCTGGTGATgcCGGTTCTCCGC-3' and 5'-TCACCATAGATCGGTAATAC-3'. Following mutagenesis, all constructs were verified by sequencing at the proteomics platform of the Institut de Recherche en Immunologie et en Cancérologie (IRIC) of the Université de Montréal (Montréal, QC, Canada) (Supplement Figure S1).

Recombinant protein and antibody preparation

Expression and purification of SPATE proteins from concentrated filtered culture supernatant fractions were obtained as described previously [20] and the extract was checked by silver staining before each assay. Antibodies against ~ 112 kDa Vat protein were used to generate a Vat-specific rabbit polyclonal antibody, according to a standard protocol [65] (Laboratorio de Biología Celular y Tisular, Departamento de Morfología, Universidad Autónoma de Aguascalientes (UAA), Aguascalientes, Mexico). Since SPATE proteins contain some highly conserved epitopes, anti-Vat antibodies were used to detect and label each of the SPATE proteins. The alignment of the passenger domain of Vat with TagB, TagC, and Sha share identities of 39%, 30%, 56% respectively. Specific epitopes are not established but Vat-antibodies demonstrate multiple conserved residues (Supplement Figure S4) and strong immune cross-reactivity. Cross-reactivity of antibodies raised against other SPATEs have also been reported. Antibodies raised against Pet protein (45% identity with EspC and 60 gaps) cross-reacted with EspC [66]. Likewise in the supernatant of CFT073, anti-Pic (44% identity with Vat and 76 gaps) antibodies were used to detect Vat and PicU SPATEs [53]. Polyclonal antisera adsorption was done by incubating the filtered supernatant of *E. coli* BL21 pBCsk+ without insert with a 1:50 dilution of the Vat polyclonal antiserum for 1 h at room temperature under mild agitation followed by centrifugation at 2000 ×g for 5 min at 4 °C.

Autoaggregation and hemagglutination tests

Autoaggregation of bacterial cells was measured by a settling assay as performed previously [20]. The sedimentation of 10 ml of each culture of *E. coli* BL21 cells expressing native or serine active site mutant SPATEs were adjusted to an OD_{600nm} 1.5 from an overnight culture grown at 37 °C in liquid Luria-Bertani medium. Then, they were monitored for a reduction in turbidity from the top of the tube which was left at 4°C for 3 h. The reduction of turbidity was plotted as a ratio against the initial turbidity.

For hemagglutination assays, human blood cells (RBCs) were washed and resuspended in PBS at a final concentration of 3% using a protocol adapted from [67]. The *E. coli fim*-negative K-12 strain ORN172 expressing either native or serine active site mutant SPATEs was grown overnight at 37°C in Luria-Bertani medium, harvested and adjusted to an optical density ($O.D._{600nm}$) of 60. Suspensions were serially diluted in 96-well round-bottom plates containing 20 µl of PBS mixed with 20 µl of 3% red blood cells and incubated for 30 min at 4°C.

Epithelial cell culture.

The 5637 bladder epithelial cell line was routinely cultured in RPMI 1640 medium (Thermo Fisher Scientific) supplemented with 10% heat-inactivated FBS at 37°C in humidified 5% CO_2, and 2×10^5 cells/well were seeded into eight-well chamber slides (Thermo Fisher Scientific, Waltham, Massachusetts, USA) and allowed to grow to 75% confluence.

To determine cytopathic effects on bladder cells, a final concentration of 30 µg/ml of native SPATEs or the serine catalytic site mutants were added directly to monolayers and incubated for 5 h in RPMI 1640 medium at 37°C with 5% CO_2. Cells were then washed twice with PBS (phosphate-buffered saline), fixed with 70% methanol, and stained with Giemsa stain. Cell morphology was analyzed at a magnification of ×20 with standard bright-field light microscopy. For the lactate dehydrogenase assay, supernatant from cells treated with native or mutant SPATEs were collected and the release of LDH in cell culture supernatants were quantified by using the CytoTox 96® Non-Radioactive Cytotoxicity Assay kit (Promega, Madison, WI, USA). Maximum LDH release (positive control) was determined by adding lysis solution (provided in the kit) to the non-infected cells.

For fluorescence actin-staining and immunostaining assays, cells were fixed with 3.0–4.0% formaldehyde in PBS, washed, permeabilized by addition of 0.1% Triton X-100-PBS, stained with 0.05 µg of Alexa Fluor 488-phalloidin/ml (AAT Bioquest, Sunnyvale, CA, USA) at 37°C for 1h and counterstained with ProLong Gold/DAPI antifade reagent (Invitrogen, Carlsbad, CA, USA). After image acquisition using confocal microscope, the actin staining intensity was quantified by measuring mean gray value (mean pixel intensity) in ImageJ (https://imagej.nih.gov/ij/) [22]. The cells of interest as well as background with no fluorescence were selected manually to analyze the areas integrated intensities and mean gray value. The value was then corrected and total fluorescence (CTF) was calculated as CTF = Integrated Density – (Area of selected cell X Mean fluorescence of background readings). The averaged corrected mean gray value was used to generate relative quantitative comparison of fluorescence intensity.

SPATE protein localization in bladder cells was detected by immunofluorescence. Treated cells were fixed, permeabilized and incubated with blocking solution (PBS with 5% BSA) for 1 h at 37°C. Samples were then incubated with rabbit anti-SPATE polyclonal antibodies (UAA, Mexico) for 2 h at 37°C. This was followed by incubation with secondary antibody Alexa Fluor 594-labeled goat anti-rabbit IgG antibody (Thermo Fisher Scientific, Waltham, Massachusetts, USA). Samples were mounted and imaged with the 60X objective of an LSM780 confocal microscope (Carl Zeiss Microimaging). Images were processed with ZEN 2012 software (Carl Zeiss, Jena, Germany).

Electron microscopy

Immunogold labeling of intact bacterium was carried out by culturing *E. coli* BL21 expressing different SPATEs as well as empty vector without insert in Luria-Bertani medium supplemented with 30 µg/ml chloramphenicol for 5 h. Bacterial suspensions (50 µl) were spotted on nickel-coated TEM grids. After 15 min, the liquid was wicked away with bibulous paper and blocked with drops of PBS containing 1% ovalbumin for 15 min. A blocking solution was exchanged with a drop of SPATE antiserum diluted 1:100 in PBS. After 15 min, excess fluid was wicked away with bibulous paper and exchanged for PBS containing 1% ovalbumin drops for 5 min. The wash was repeated and then incubated in suitable goat anti-rabbit IgG (H+L), Alexa Fluor 488-10 nm colloidal gold secondary antibodies (Thermo Fisher Scientific, Waltham, Massachusetts, USA) diluted 1:250 in incubation solution. After 15 min, grids were washed twice with PBS drops and rinsed twice with distilled water. Grids were dried with bibulous paper and imaged on a Philips CM-100 transmission electron microscope.

For immunogold labeling of epithelial cell thin sections, cells were fixed in 0.1% glutaraldehyde + 4% paraformaldehyde in cocodylate buffer at pH 7.2, and post-fixed in 1.3% osmium tetroxide in collidine buffer. After dehydration by successive passages through 25, 50, 75 and 95% solutions of acetone in water, 15-30 minutes each; samples were immersed for 16-18 hours in SPURR: acetone (1:1). Samples were then embedded in BEEM capsules using SPURR resin with the ELR-4221 kit (Polysciences Inc, Warrington, Pennsylvania, USA) followed by placing the capsules at 60°- 65°C for 20-30 hours to polymerize the resin. After resin polymerization, samples were cut using an ultramicrotome (Ultratome) and were put onto Formvar and carbon covered-copper 200-mesh grids treated with sodium metaperiodate and were blocked with 1% BSA in PBS. Grids were then incubated with primary antibodies, washed, and incubated with goat anti-rabbit IgG (H+L), Alexa Fluor 488-10 nm colloidal gold secondary antibodies (Thermo Fisher Scientific, Waltham, Massachusetts, USA). After washing, samples were contrasted with uranyl

acetate and lead citrate and subsequently visualized using a Philips EM 300 transmission electron microscope.

Cleavage of protein substrates

For mucinase activity, cultures of *E. coli* BL21 expressing SPATEs were incubated for 24 h at 37 °C on a medium containing 1.5% agarose and 0.5% porcine gastric mucin (Sigma-Aldrich, St. Louis, Missouri, USA). Plates were subsequently stained with 0.1% amido-black in 3.5 M acetic acid for 15 min, followed by destaining with 5% acetic acid and 0.5% glycerol for 6 h to overnight. Zones of mucin lysis were visualized as discolored halos around colonies. For the Periodic Acid Schiff (PAS) assay to detect mucin degradation [54], 5 µg of each SPATE protein were incubated with 5 µg of 0.5% porcine gastric mucin (Sigma-Aldrich, St. Louis, Missouri, USA) in 30 µl of MOPS buffer and incubated for 48 h at 37°C. Treated samples were electrophoresed on an 8% SDS-PAGE gel and the gel staining was developed using a colorimetric Pierce™ Glycoprotein Staining Kit (Thermo Fischer Scientific).

For gelatinase activity, 5 µg of each SPATE protein were incubated with 5 µg of bovine skin gelatin (Sigma-Aldrich, St. Louis, Missouri, USA) in 30 µl of MOPS buffer and incubated for 48 h at 37°C. Samples were then boiled with Laemmli sample buffer, were electrophoresed on an 8% SDS-PAGE gel and then resolved by Coomassie blue staining. In addition, gelatinase activity was also tested by growing the clones on agar plates containing 1.5% agarose and 1% bovine skin gelatin for 48 h at 37 °C. Plates were subsequently stained with 0.1% amido-black in 3.5 M acetic acid for 15 min, followed by destaining with 5% acetic acid and 0.5% glycerol for 6 h to overnight. Zones of gelatin lysis consist of discolored halos around colonies.

Statistical analysis

Experimental data were expressed as a mean ± standard error of the mean (SEM) in each group. The means of groups were combined and analyzed by Student *t*-test for pairwise comparisons and analysis of variance (ANOVA) to compare means of more than two populations. A P value of <0.05 was considered statistically significant. All data were analyzed with the Graph Pad Prism 7 software (GraphPad Software, San Diego, CA, USA).

Conclusions

In conclusion, TagB, TagC, and Sha are novel SPATEs that demonstrate different proteolytic activities on different substrates as well as distinct cytopathic effects on bladder epithelial cells. Additional molecular *in vitro* and *in vivo* studies are in progress in an effort to understand the link between protease activity of the TagB, TagC, and Sha SPATEs and how these proteases disrupt

or alter the actin cytoskeleton during ExPEC infections. It will of further interest to also investigate their potential interactions with other host cell or extracellular matrix proteins, and determine how these relatively large proteins (generally greater than 100 kDa) manage to enter host cells through serine protease activity and what specific trafficking pathways may be involved in their localization or association with specific cellular compartments.

Funding

Funding for this work was supported by NSERC Canada Discovery Grants 2014-06622 and 2019-06642 and scholarships from the CRIPA-FRQNT networks to P.P. and J.M.D.

Acknowledgments

We thank Arnaldo Nakamura for assistance in electron microscopy and Jessy Tremblay for assistance in confocal immunofluorescence microscopy imaging.

6.6 References

1. Foxman, Betsy, and Patricia Brown. "Epidemiology of Urinary Tract Infections: Transmission and Risk Factors, Incidence, and Costs." *Infectious disease clinics of North America* 17, no. 2 (2003): 227-41.
2. Foxman, Betsy. "Urinary Tract Infection Syndromes: Occurrence, Recurrence, Bacteriology, Risk Factors, and Disease Burden." *Infectious disease clinics of North America* 28, no. 1 (2014): 1-13.
3. Flores-Mireles, Ana L, Jennifer N Walker, Michael Caparon, and Scott J Hultgren. "Urinary Tract Infections: Epidemiology, Mechanisms of Infection and Treatment Options." *Nature reviews microbiology* 13, no. 5 (2015): 269-84.
4. O'Brien, Valerie P, Thomas J Hannan, Hailyn V Nielsen, and Scott J Hultgren. "Drug and Vaccine Development for the Treatment and Prevention of Urinary Tract Infections." *Microbiology spectrum* 4, no. 1 (2016).
5. Lewis, Simon A. "Everything You Wanted to Know About the Bladder Epithelium but Were Afraid to Ask." *American Journal of Physiology-Renal Physiology* 278, no. 6 (2000): F867-F74.
6. Keane, WILLIAM F, R Welch, G Gekker, and Ph K Peterson. "Mechanism of *Escherichia coli* Alpha-Hemolysin-Induced Injury to Isolated Renal Tubular Cells." *The American journal of pathology* 126, no. 2 (1987): 350.
7. Russo, Thomas A, Bruce A Davidson, Stacy A Genagon, Natalie M Warholic, Ulrike MacDonald, Patrick D Pawlicki, Janet M Beanan, Ruth Olson, Bruce A Holm, and Paul R Knight III. "*E. coli* Virulence Factor Hemolysin Induces Neutrophil Apoptosis and Necrosis/Lysis in Vitro and Necrosis/Lysis and Lung Injury in a Rat Pneumonia Model." *American Journal of Physiology-Lung Cellular and Molecular Physiology* 289, no. 2 (2005): L207-L16.
8. Smith, Yarery C, Susan B Rasmussen, Kerian K Grande, Richard M Conran, and Alison D O'Brien. "Hemolysin of Uropathogenic *Escherichia coli* Evokes Extensive Shedding of the Uroepithelium and Hemorrhage in Bladder Tissue within the First 24 Hours after Intraurethral Inoculation of Mice." *Infection and immunity* 76, no. 7 (2008): 2978-90.
9. Dhakal, Bijaya K, and Matthew A Mulvey. "The Upec Pore-Forming Toxin A-Hemolysin Triggers Proteolysis of Host Proteins to Disrupt Cell Adhesion, Inflammatory, and Survival Pathways." *Cell host & microbe* 11, no. 1 (2012): 58-69.
10. Wiles, Travis J, and Matthew A Mulvey. "The Rtx Pore-Forming Toxin A-Hemolysin of Uropathogenic *Escherichia coli*: Progress and Perspectives." *Future microbiology* 8, no. 1 (2013): 73-84.
11. Ristow, Laura C, and Rodney A Welch. "Hemolysin of Uropathogenic *Escherichia Coli*: A Cloak or a Dagger?" *Biochimica et Biophysica Acta (BBA)-Biomembranes* 1858, no. 3 (2016): 538-45.
12. Visvikis, Orane, Laurent Boyer, Stéphanie Torrino, Anne Doye, Marc Lemonnier, Patrick Lorès, Monica Rolando, Gilles Flatau, Amel Mettouchi, and Daniel Bouvard. *"Escherichia coli* Producing Cnf1 Toxin Hijacks Tollip to Trigger Rac1-Dependent Cell Invasion." *Traffic* 12, no. 5 (2011): 579-90.
13. Mills, Melody, Karen C Meysick, and Alison D O'Brien. "Cytotoxic Necrotizing Factor Type 1 of Uropathogenic *Escherichia coli* Kills Cultured Human Uroepithelial 5637 Cells by an Apoptotic Mechanism." *Infection and immunity* 68, no. 10 (2000): 5869-80.
14. Guyer, Debra M, Suzana Radulovic, Faye-Ellen Jones, and Harry LT Mobley. "Sat, the Secreted Autotransporter Toxin of Uropathogenic *Escherichia coli*, Is a Vacuolating Cytotoxin for Bladder and Kidney Epithelial Cells." *Infection and immunity* 70, no. 8 (2002): 4539-46.

15. Maroncle, Nathalie M, Kelsey E Sivick, Rebecca Brady, Faye-Ellen Stokes, and Harry LT Mobley. "Protease Activity, Secretion, Cell Entry, Cytotoxicity, and Cellular Targets of Secreted Autotransporter Toxin of Uropathogenic *Escherichia coli*." *Infection and immunity* 74, no. 11 (2006): 6124-34.
16. Heimer, Susan R, David A Rasko, C Virginia Lockatell, David E Johnson, and Harry LT Mobley. "Autotransporter Genes Pic and Tsh Are Associated with *Escherichia coli* Strains That Cause Acute Pyelonephritis and Are Expressed During Urinary Tract Infection." *Infection and immunity* 72, no. 1 (2004): 593-97.
17. Carter, Paul, and James A Wells. "Dissecting the Catalytic Triad of a Serine Protease." *Nature* 332, no. 6164 (1988): 564.
18. Gutierrez-Jimenez, Javier, Ivonne Arciniega, and Fernando Navarro-García. "The Serine Protease Motif of Pic Mediates a Dose-Dependent Mucolytic Activity after Binding to Sugar Constituents of the Mucin Substrate." *Microbial pathogenesis* 45, no. 2 (2008): 115-23.
19. Navarro-Garcia, Fernando, Javier Gutierrez-Jimenez, Carlos Garcia-Tovar, Luis A Castro, Hector Salazar-Gonzalez, and Vanessa Cordova. "Pic, an Autotransporter Protein Secreted by Different Pathogens in the *Enterobacteriaceae* Family, Is a Potent Mucus Secretagogue." *Infection and immunity* 78, no. 10 (2010): 4101-09.
20. Habouria, Hajer, Pravil Pokharel, Segolène Maris, Amélie Garénaux, Hicham Bessaiah, Sébastien Houle, Frédéric J Veyrier, Stéphanie Guyomard-Rabenirina, Antoine Talarmin, and Charles M Dozois. "Three New Serine-Protease Autotransporters of *Enterobacteriaceae* (SPATEs) from Extra-Intestinal Pathogenic *Escherichia coli* and Combined Role of Spates for Cytotoxicity and Colonization of the Mouse Kidney." *Virulence* 10, no. 1 (2019): 568-87.
21. Benz, Inga, and M Alexander Schmidt. "Aida-I, the Adhesin Involved in Diffuse Adherence of the Diarrhoeagenic *Escherichia coli* Strain 2787 (O126: H27), Is Synthesized Via a Precursor Molecule." *Molecular microbiology* 6, no. 11 (1992): 1539-46.
22. Abràmoff, Michael D, Paulo J Magalhães, and Sunanda J Ram. "Image Processing with Imagej." *Biophotonics international* 11, no. 7 (2004): 36-42.
23. Henderson, Ian R, John Czeczulin, Carlos Eslava, Fernando Noriega, and James P Nataro. "Characterization of Pic, a Secreted Protease Of *Shigella Flexneri* and Enteroaggregative *Escherichia coli*." *Infection and immunity* 67, no. 11 (1999): 5587-96.
24. Pickett, MJ, JR Greenwood, and SM Harvey. "Tests for Detecting Degradation of Gelatin: Comparison of Five Methods." *Journal of clinical microbiology* 29, no. 10 (1991): 2322-25.
25. Xicohtencatl-Cortes, Juan, Zeus Saldaña, Wanyin Deng, Elsa Castañeda, Enrique Freer, Phil I Tarr, B Brett Finlay, José Luis Puente, and Jorge A Girón. "Bacterial Macroscopic Rope-Like Fibers with Cytopathic and Adhesive Properties." *Journal of Biological Chemistry* 285, no. 42 (2010): 32336-42.
26. Vigil, Patrick D, Travis J Wiles, Michael D Engstrom, Lev Prasov, Matthew A Mulvey, and Harry LT Mobley. "The Repeat-in-Toxin Family Member Tosa Mediates Adherence of Uropathogenic *Escherichia coli* and Survival During Bacteremia." *Infection and immunity* 80, no. 2 (2012): 493-505.
27. Rippere-Lampe, Karen E, Alison D O'Brien, Richard Conran, and Hank A Lockman. "Mutation of the Gene Encoding Cytotoxic Necrotizing Factor Type 1 (Cnf 1) Attenuates the Virulence of Uropathogenic *Escherichia coli*." *Infection and immunity* 69, no. 6 (2001): 3954-64.
28. Davis, Jon M, Susan B Rasmussen, and Alison D O'Brien. "Cytotoxic Necrotizing Factor Type 1 Production by Uropathogenic *Escherichia coli* Modulates Polymorphonuclear Leukocyte Function." *Infection and immunity* 73, no. 9 (2005): 5301-10.
29. Pokharel, Pravil, Hajer Habouria, Hicham Bessaiah, and Charles M Dozois. "Serine Protease Autotransporters of the *Enterobacteriaceae* (SPATEs): Out and About and Chopping It Up." *Microorganisms* 7, no. 12 (2019): 594.

30. Martinez, Juan J, Matthew A Mulvey, Joel D Schilling, Jerome S Pinkner, and Scott J Hultgren. "Type 1 Pilus-Mediated Bacterial Invasion of Bladder Epithelial Cells." *The EMBO journal* 19, no. 12 (2000): 2803-12.
31. Mulvey, Matthew A, Joel D Schilling, and Scott J Hultgren. "Establishment of a Persistent *Escherichia coli* Reservoir During the Acute Phase of a Bladder Infection." *Infection and immunity* 69, no. 7 (2001): 4572-79.
32. Eslava, Carlos, Fernando Navarro-García, John R Czeczulin, Ian R Henderson, Alejandro Cravioto, and James P Nataro. "Pet, an Autotransporter Enterotoxin from Enteroaggregative *Escherichia coli*." *Infection and immunity* 66, no. 7 (1998): 3155-63.
33. Brunder, Werner, Herbert Schmidt, and Helge Karch. "Espp, a Novel Extracellular Serine Protease of Enterohaemorrhagic *Escherichia coli* O157: H7 Cleaves Human Coagulation Factor V." *Molecular microbiology* 24, no. 4 (1997): 767-78.
34. Dozois, Charles M, Maryvonne Dho-Moulin, Annie Brée, John M Fairbrother, Clarisse Desautels, and Roy Curtiss. "Relationship between the Tsh Autotransporter and Pathogenicity of Avian *Escherichia coli* and Localization and Analysis of the Tsh Genetic Region." *Infection and immunity* 68, no. 7 (2000): 4145-54.
35. Stein, Markus, Brendan Kenny, Murry A Stein, and B Brett Finlay. "Characterization of Espc, a 110-Kilodalton Protein Secreted by Enteropathogenic *Escherichia coli* Which Is Homologous to Members of the Immunoglobulin a Protease-Like Family of Secreted Proteins." *Journal of bacteriology* 178, no. 22 (1996): 6546-54.
36. Dutta, Pinaki R, Renato Cappello, Fernando Navarro-García, and James P Nataro. "Functional Comparison of Serine Protease Autotransporters of *Enterobacteriaceae*." *Infection and immunity* 70, no. 12 (2002): 7105-13.
37. Turner, David PJ, Karl G Wooldridge, and Dlawer AA Ala'Aldeen. "Autotransported Serine Protease a of *Neisseria Meningitidis*: An Immunogenic, Surface-Exposed Outer Membrane, and Secreted Protein." *Infection and immunity* 70, no. 8 (2002): 4447-61.
38. Jonsson, Per, and Torkel Wadström. "Cell Surface Hydrophobicity Ofstaphylococcus Aureus Measured by the Salt Aggregation Test (Sat)." *Current Microbiology* 10, no. 4 (1984): 203-09.
39. Hendrixson, David R, Maria L De La Morena, Christos Stathopoulos, and Joseph W St Geme III. "Structural Determinants of Processing and Secretion of the *Haemophilus Influenzae* Hap Protein." *Molecular microbiology* 26, no. 3 (1997): 505-18.
40. Hendrixson, David R, and Joseph W St Geme III. "The Haemophilus Influenzae Hap Serine Protease Promotes Adherence and Microcolony Formation, Potentiated by a Soluble Host Protein." *Molecular cell* 2, no. 6 (1998): 841-50.
41. Kostakioti, Maria, and Christos Stathopoulos. "Functional Analysis of the Tsh Autotransporter from an Avian Pathogenic *Escherichia coli* Strain." *Infection and immunity* 72, no. 10 (2004): 5548-54.
42. Brockmeyer, Jens, Sabrina Spelten, Thorsten Kuczius, Martina Bielaszewska, and Helge Karch. "Structure and Function Relationship of the Autotransport and Proteolytic Activity of Espp from Shiga Toxin-Producing *Escherichia coli*." *PloS one* 4, no. 7 (2009): e6100.
43. Navarro-Garcia, Fernando, Antonio Serapio-Palacios, Jorge E Vidal, M Isabel Salazar, and Gabriela Tapia-Pastrana. "Espc Promotes Epithelial Cell Detachment by Enteropathogenic *Escherichia coli* Via Sequential Cleavages of a Cytoskeletal Protein and Then Focal Adhesion Proteins." *Infection and immunity* 82, no. 6 (2014): 2255-65.
44. Gruenheid, Samantha, and B Brett Finlay. "Microbial Pathogenesis and Cytoskeletal Function." *Nature* 422, no. 6933 (2003): 775.
45. Rottner, Klemens, Theresia EB Stradal, and Juergen Wehland. "Bacteria-Host-Cell Interactions at the Plasma Membrane: Stories on Actin Cytoskeleton Subversion." *Developmental cell* 9, no. 1 (2005): 3-17.

46. Martinez, Juan J, and Scott J Hultgren. "Requirement of Rho-Family Gtpases in the Invasion of Type 1-Piliated Uropathogenic *Escherichia coli*." *Cellular microbiology* 4, no. 1 (2002): 19-28.
47. Eto, Danelle S, Jamie L Sundsbak, and Matthew A Mulvey. "Actin-Gated Intracellular Growth and Resurgence of Uropathogenic *Escherichia coli*." *Cellular microbiology* 8, no. 4 (2006): 704-17.
48. Balish, Marion J, Jean Jensen, and David T Uehling. "Bladder Mucin: A Scanning Electron Microscopy Study in Experimental Cystitis." *The Journal of urology* 128, no. 5 (1982): 1060-63.
49. Parsons, C Lowell, Carol Greenspan, Steven W Moore, and S Grant Mulholland. "Role of Surface Mucin in Primary Antibacterial Defense of Bladder." *Urology* 9, no. 1 (1977): 48-52.
50. Lehker, Michael W, and Daniel Sweeney. "Trichomonad Invasion of the Mucous Layer Requires Adhesins, Mucinases, and Motility." *Sexually Transmitted Infections* 75, no. 4 (1999): 231-38.
51. Mantle, M, and SD Husar. "Binding of Yersinia Enterocolitica to Purified, Native Small Intestinal Mucins from Rabbits and Humans Involves Interactions with the Mucin Carbohydrate Moiety." *Infection and immunity* 62, no. 4 (1994): 1219-27.
52. Finkelstein, Richard A, Mary Boesman-Finkelstein, and Peter Holt. "*Vibrio Cholerae* Hemagglutinin/Lectin/Protease Hydrolyzes Fibronectin and Ovomucin: Fm Burnet Revisited." *Proceedings of the National Academy of Sciences* 80, no. 4 (1983): 1092-95.
53. Parham, Nick J, Usha Srinivasan, Mickaël Desvaux, Betsy Foxman, Carl F Marrs, and Ian R Henderson. "Picu, a Second Serine Protease Autotransporter of Uropathogenic *Escherichia coli*." *FEMS microbiology letters* 230, no. 1 (2004): 73-83.
54. Bhullar, Kirandeep, Maryam Zarepour, Hongbing Yu, Hong Yang, Matthew Croxen, Martin Stahl, B Brett Finlay, Stuart E Turvey, and Bruce A Vallance. "The Serine Protease Autotransporter Pic Modulates *Citrobacter rodentium* Pathogenesis and Its Innate Recognition by the Host." *Infection and immunity* 83, no. 7 (2015): 2636-50.
55. Kobayashi, Renata KT, Luis Carlos J Gaziri, and Marilda C Vidotto. "Functional Activities of the Tsh Protein from Avian Pathogenic *Escherichia coli* (APEC) Strains." *Journal of veterinary science* 11, no. 4 (2010): 315-19.
56. Ricard-Blum, Sylvie. "The Collagen Family." *Cold Spring Harbor perspectives in biology* 3, no. 1 (2011): a004978.
57. Navarro-García, Fernando, Adrián Canizalez-Roman, Kaitlin E Burlingame, Ken Teter, and Jorge E Vidal. "Pet, a Non-Ab Toxin, Is Transported and Translocated into Epithelial Cells by a Retrograde Trafficking Pathway." *Infection and immunity* 75, no. 5 (2007): 2101-09.
58. Nava-Acosta, Raul, and Fernando Navarro-Garcia. "Cytokeratin 8 Is an Epithelial Cell Receptor for Pet, a Cytotoxic Serine Protease Autotransporter of *Enterobacteriaceae*." *MBio* 4, no. 6 (2013): e00838-13.
59. Navarro-García, Fernando, Cynthia Sears, Carlos Eslava, Alejandro Cravioto, and James P Nataro. "Cytoskeletal Effects Induced by Pet, the Serine Protease Enterotoxin of Enteroaggregative *Escherichia coli*." *Infection and immunity* 67, no. 5 (1999): 2184-92.
60. Dutta, Pinaki R, Bao Quan Sui, and James P Nataro. "Structure-Function Analysis of the Enteroaggregative *Escherichia coli* Plasmid-Encoded Toxin Autotransporter Using Scanning Linker Mutagenesis." *Journal of Biological Chemistry* 278, no. 41 (2003): 39912-20.
61. Vidal, Jorge E, and Fernando Navarro-García. "Espc Translocation into Epithelial Cells by Enteropathogenic *Escherichia coli* Requires a Concerted Participation of Type V and Iii Secretion Systems." *Cellular microbiology* 10, no. 10 (2008): 1975-86.

62. Marc, D, and Maryvonne Dho-Moulin. "Analysis of the Fim Cluster of an Avian O2 Strain of *Escherichia coli*: Serogroup-Specific Sites within Fima and Nucleotide Sequence of Fimi." *Journal of medical microbiology* 44, no. 6 (1996): 444-52.
63. Woodall, LAURA D, PERRY W Russell, SANDRA L Harris, and PAUL E Orndorff. "Rapid, Synchronous, and Stable Induction of Type 1 Piliation in *Escherichia coli* by Using a Chromosomal Lacuv5 Promoter." *Journal of bacteriology* 175, no. 9 (1993): 2770-78.
64. Charbonneau, Marie-Ève, Frédéric Berthiaume, and Michael Mourez. "Proteolytic Processing Is Not Essential for Multiple Functions of the *Escherichia coli* Autotransporter Adhesin Involved in Diffuse Adherence (Aida-I)." *Journal of bacteriology* 188, no. 24 (2006): 8504-12.
65. Nakazawa, Masami, Mari Mukumoto, and Kazutaka Miyatake. "Production and Purification of Polyclonal Antibodies." In *High-Resolution Imaging of Cellular Proteins*, 49-59: Springer, 2016.
66. Mellies, Jay L, Fernando Navarro-Garcia, Iruka Okeke, Julie Frederickson, James P Nataro, and James B Kaper. "Espc Pathogenicity Island of Enteropathogenic *Escherichia coli* Encodes an Enterotoxin." *Infection and immunity* 69, no. 1 (2001): 315-24.
67. Provence, DL, and RIII Curtiss. "Role of Crl in Avian Pathogenic *Escherichia coli*: A Knockout Mutation of Crl Does Not Affect Hemagglutination Activity, Fibronectin Binding, or Curli Production." *Infection and immunity* 60, no. 11 (1992): 4460-67.

6.7 Supplement Figures of Article 2

Figure S1

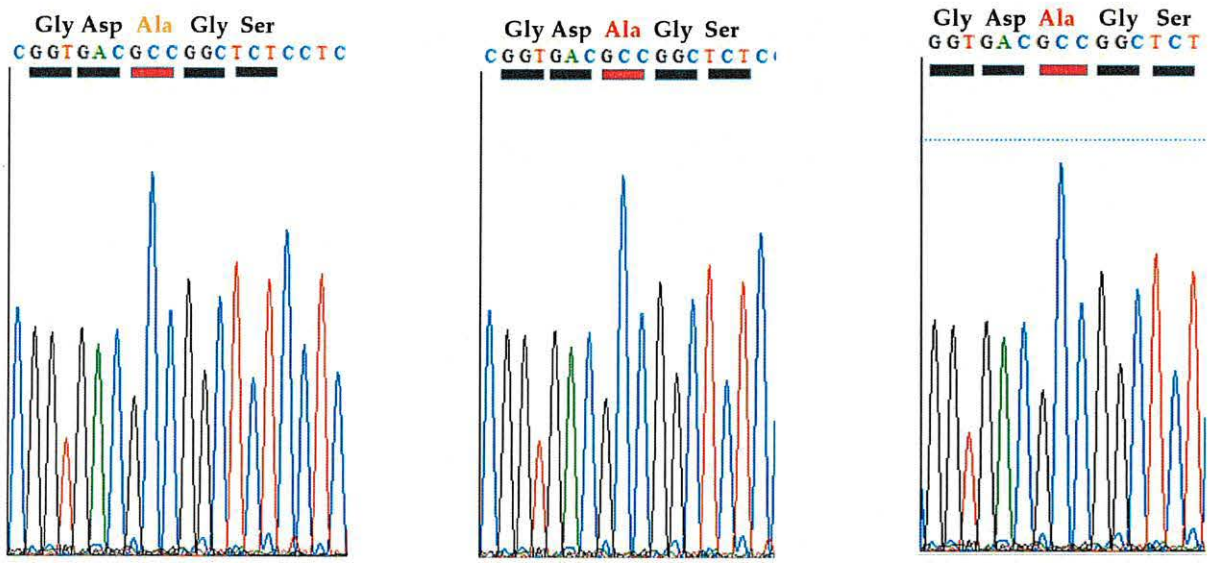

Figure S1. The sequencing chromatograms from the three mutated cloned fragments in the requisite serine protease motif (GDSGS) in the passenger domain of TagB, TagC and Sha where serine was replaced by alanine.

Figure S2

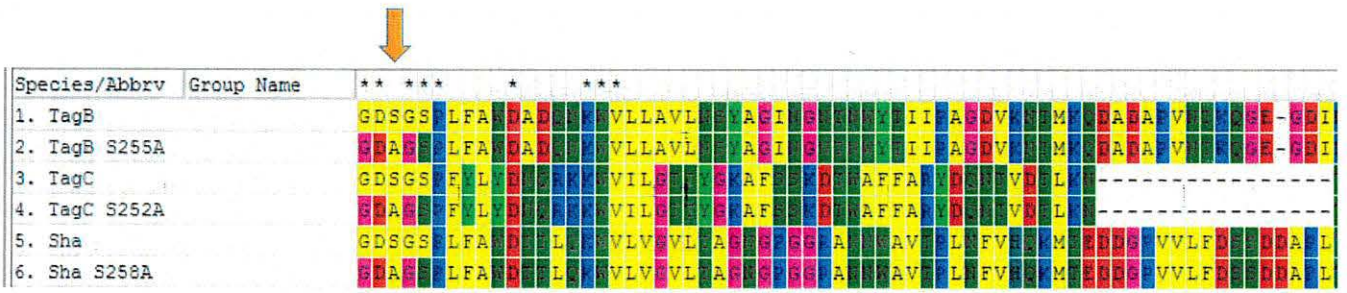

Figure S2. Pairwise sequence alignment of wild type and mutant TagB, TagC and Sha SPATEs by ClustalW. Red arrow shows the location of site directed mutation resulting from serine (S) of wild type protein into alanine (A).

Figure S3

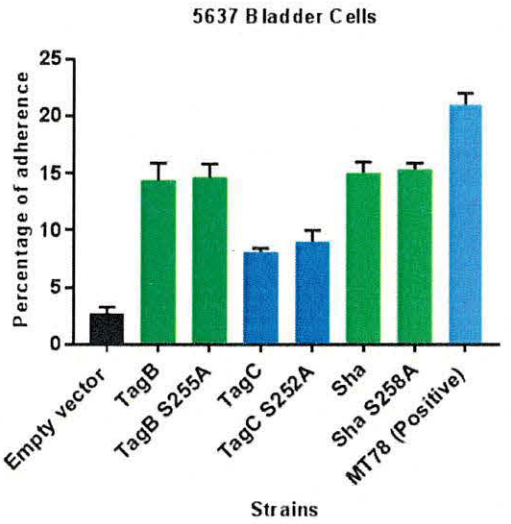

Figure S3. Comparative adherence of Wild-type and serine catalytic site SPATE mutants. Cell monolayers were infected with *E. coli fim*-negative ORN172 expressing SPATE proteins at a multiplicity of infection (MOI) of 10 and incubated at 37°C at 5% CO2 for 2 h. Adherent bacteria were enumerated by plating on LB agar. Empty vector (pBCsk+) was used as a negative-control and APEC MT78 [20] as a positive control for adherence. Data are the averages of three independent experiments. Error bars represent standard errors of the means.

Figure S4

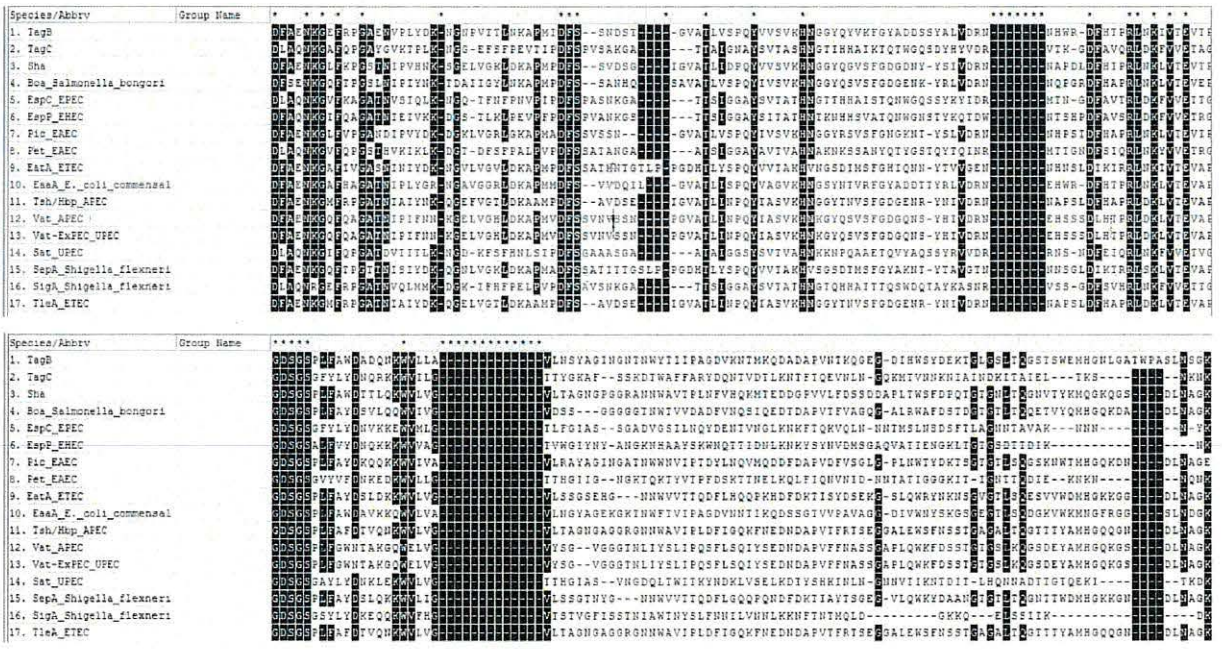

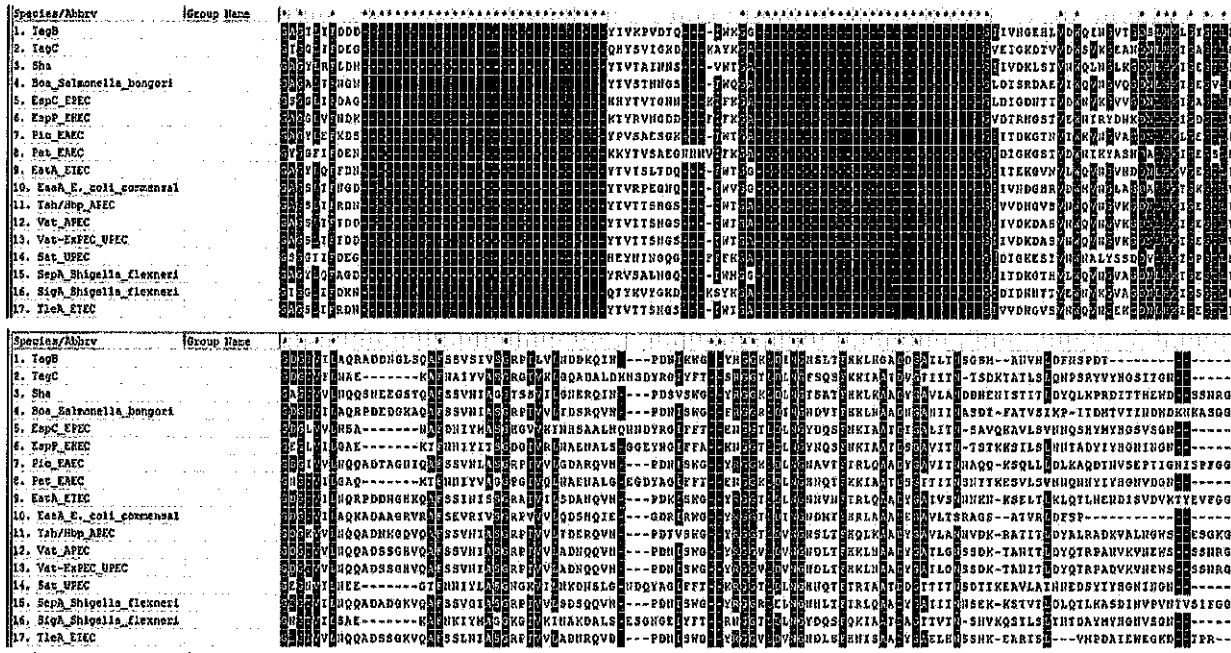

Figure S4. Multiple sequence alignment of SPATEs showing conserved residues (shaded in black and denoted with asterisk) in the passenger domain.

7 GENERAL DISCUSSION

Pathogenic microbes produce an array of toxins that alter or damage host cells and may contribute to virulence and colonization of host tissues. We determined that SPATEs including three previously uncharacterized ones, produced by *E. coli* QT598, contribute to its colonization and persistence inside the mammalian host. QT598 is an APEC O1: K1 strain belonging to phylogenetic group B2 has the capacity to encode 5 different SPATEs, the chromosomally encoded Vat, TagB, and TagC SPATEs as well as the plasmid-encoded Sha and Tsh SPATEs. The *tagB* and *tagC* genes are located in close proximity to each other on the chromosome of QT598 as well as in the genomes of some UPEC isolates in the sequence databases but are absent in the non-pathogenic *E. coli* strain MG1655, suggesting a potential role for these autotransporters in UPEC virulence. The co-localization of these two tandem SPATEs encoding genes when present in some UPEC strains suggests that the *tagBC* encoding island appears to be conserved among strains which have acquired it. In this regard, this thesis focused on the roles of TagB and TagC in pathogenesis of human and avian cells. TagB and TagC both harbor a predicted signal sequence, passenger domain, and β-domain which are conserved domains of SPATE proteins. Owing to the multiple functions of the different SPATEs, this thesis hypothesized that new TagB and TagC SPATEs could play a role in ExPEC pathogenesis by contributing to colonization of host tissues and potentially also promote bacterial persistence and systemic spread during infection.

7.1 Phenotypic properties of TagB and TagC – Adhesion, Autoaggregation, and Hemagglutination

Initially, we investigated the role of SPATEs in potential colonization of the host. This trait is important because bacterial colonization at the portal of entry is the initial stage of bacterial pathogenesis. We found that TagB and TagC adhered to both bladder and renal epithelial cells as well as to chicken fibroblasts *in vitro*. So, these proteins could help QT598 adhere to cells in the urinary tract and to avoid being expelled by the washing action of urine during voiding of the bladder. Since these proteins are located on the bacterial cell surface as seen in TEM micrographs, these proteins might mediate attachment of bacteria to host cell surfaces which are often decorated with extracellular matrix proteins such as collagen, laminin, elastin, glycoproteins such as fibrinogen or vitronectin; and integral host membrane proteins such as selectins, integrins and cadherins. Different bacterial adhesins can mediate adherence to present different proteins or host cell receptors on the target cell surface (tissue tropism). For example, YadA, a member of

trimeric autotransporter found in *Yersinia enterocolitica* binds to collagen, fibronectin and laminin (Nummelin *et al.*, 2004). The Autotransporter BabA from *Helicobacter pylori* binds to gastric mucosa by recognizing Lewis b blood group antigen present on red blood cells as well as in gastric mucosa to human integrins due to the presence of an RGD motif (Isberg & Van Nhieu, 1994). Likewise, AIDA-1 expressed by diffusely adhering *E. coli* strains binds to a glycoprotein of about 119 kDa (gp119) on HeLa cells (Laarmann & Schmidt, 2003). Currently, the receptors of the target tissues of TagB and TagC are not known, but attachment aided by these proteases could be the initial step required before degradation of target proteins such as extracellular matrix, mucosa, and cell junction complexes, which could lead to bacterial dissemination in the host. Interestingly, some of the new SPATEs of QT598 degraded biological substrates proteins such as mucin and gelatin. Sha demonstrated mucinase activity whereas TagC demonstrated gelatinase activity. This mucinase and gelatinase activity is not only important as a virulence factor but also can be used by bacteria as nutritive advantage to cleave biological substrates like mucosal polysaccharides for carbon and energy sources inside the hostile environment of the host (Maltby *et al.*, 2013). To verify the novel metabolic role for Sha mucinase we can test the growth kinetics of QT598 and its *sha* mutant in the minimal media where mucus is only the growth substrate. Furthur, to recapitulate the *in vivo* effect, we can perform competition experiments to compare the relative colonization fitness of the *sha* mutants for colonization of the mouse intestine in competition with their wild-type parent.

The molecular mechanisms of TagB and TagC mediated adherence in the human urinary tract are still unknown but our *in vitro* results suggest a competitive advantage for colonization in the bladder as well as in kidneys. Of note, we also observed the involvement of TagB and TagC in bacterial autoaggregation *in vitro* and the native expression of both tandem genes was detected in QT598 grown under *in vitro* as well as in the bladder during urinary tract infection in the murine model. Several studies have shown that aggregative bacteria resist host immune defenses such as complement attack and phagocytosis more efficiently than nonaggregated bacteria (Anderson *et al.*, 2003; Ochiai *et al.*, 1993). However, in contrast to *E. coli* K-12, the autoaggregation phenotype was absent in wild-type *E. coli* QT598. Furthermore, expression of either TagB or TagC on high-copy plasmids in QT598 still did not cause autoaggregation. The absence of aggregation was not likely to be due to transcriptional or translational changes in TagB and TagC gene or protein expression. It is most likely that other bacterial surface structures like capsule, LPS, flagella, and fimbriae in wild-type ExPEC strain QT598 hinder the interaction. Similarly, direct physical interference was reported in *E. coli* whereby the capsule shielded the function of self-recognizing protein Ag43 as well as AIDA-1 (Schembri *et al.*, 2004). In addition Ag43-Ag43

interaction was abolished by fimbriation even though the expression of fimbriae as well as Ag43 were completely independent processes (Hasman *et al.*, 1999). The capsule also interfered with but did not abolish the function of type 1 fimbriae in *Klebsiella pneumoniae* (Schembri *et al.*, 2005).

Autoaggregation can also contribute to interactions leading to more complex biofilms and the pathogenesis of ExPEC (Anderson *et al.*, 2003; Lehti *et al.*, 2010). Although, TagB and TagC did not contribute to biofilm formation, the Sha autotransporter led to increased biofilm production. The biofilm phenotype observed with Sha, however, was not seen when it was expressed in QT598, again possibly being masked by other surface structures made by this strain. It is still possible that under some conditions, the bacterial surface may be modified and lead to SPATE proteins mediating bacterial adherence or autoaggregation during infection.

The growth and survival of ExPEC outside the host in natural environment is equally important like its survival mechanism inside the host. Sewage could be the possible environmental site for dissemination or circulation of ExPEC due to presence of highly contaminated human fecal waste and possess many environmental stresses for *E. coli* – lack of nutrition, toxins, antibiotics, protozoan predators, solar radiation, temperature etc (Berthe *et al.*, 2013). So, the bacterial aggregates which are beneficial in human host pathology, also can have an important role for ExPEC survival in harsh environmental conditions. *Pseudomonas aeruginosa* induce cell aggregation to protect against detergents (Klebensberger *et al.*, 2007) and forms microcolonies to protect from grazing protozoans (Matz *et al.*, 2004).

Some autotransporters, as well as fimbriae, on the bacterial surface can mediate hemagglutination by agglutinating red blood cells (RBCs). Fimbrial hemagglutinins (type 1 fimbriae which are a mannose-specific adhesin and P fimbriae which recognize digalactoside units in the P-blood group antigen) are important adhesins present in *E. coli* (Harris *et al.*, 1990; Korhonen *et al.*, 1982). Hemagglutinin activities for SPATEs have been reported especially for members of the class 2 SPATEs (such as Tsh and Vat) which can bind to mucin-like leukocyte surface glycoproteins (Ruiz-Perez *et al.*, 2011). We tested erythrocytes obtained from a variety of species but TagC was negative for hemagglutination. The absence of hemagglutination activity for TagC is in good agreement with its classification as a class 1 SPATE. On the other hand, TagB showed some agglutination for sheep, bovine and pig erythrocytes. This could be because of domain 2 which are self-folding structures normally projected from the β-helix in some class 2 SPATEs, however, such domains are absent in TagB and TagC. In the case of IgAP (Immunoglobulin A1 proteases) produced by *Haemophilus influenzae* contains domain 2 which is believed to be a binding site for immunoglobulins which helps the correct positioning of the

antibody for cleavage by the active serine catalytic site present in the passenger domain (Johnson *et al.*, 2009).

Apart from the role of SPATEs in hemagglutination, we tested whether new SPATEs could contribute to serum resistance like Pic SPATE (Henderson *et al.*, 1999). In serum bactericidal assays in 10% human serum, all clones expressing SPATEs in K-12 background were as rapidly killed as *E. coli* K-12 containing the empty vector. Although wild-type ExPEC strain QT598 survived the action of 10% human serum efficiently, the deletion of the SPATE encoding genes had no appreciable effect on serum susceptibility (Appendix I). This suggests that SPATEs in QT598 have no role in serum resistance and that it is likely that other bacterial components like O-antigen, capsular polysaccharides, and outer membrane proteins may mediate resistance to complement-mediated killing (Cross *et al.*, 1986).

7.2 TagB and TagC are cytotoxins and are internalized by bladder epithelial cells

TagB and TagC are serine protease autotransporters harboring typical SPATE domains. Their proteolytic activity belongs to the trypsin clan of serine proteases and elicited cytopathic effects on bladder epithelial cells. Although the precise cytotoxic mechanisms of these SPATEs has not been determined, our results showed actin cytoskeleton disruption as a plausible mechanism. Actin stress fibers were conserved and the integrity of cells was normal when the bladder cells were treated with a serine catalytic site defective mutant protein or when wild-type protein was preincubated with a proteases inhibitor (PMSF), suggesting the role of a serine catalytic site to elicit the actin disruption or cytopathic phenotype. The actin cytoskeletal damage was not an indirect effect of cell epithelial proteins because these cytotoxins were internalized within 5 h and were found in the cytoplasm. By contrast, the catalytic site defective mutant was not internalized within epithelial cells. The internalization mechanism of these SPATE toxins is currently unknown. QT598 lacks any type 3 secretion mechanism, so the entry of these SPATEs into host cells is not dependent on a type 3 secretion system, as was shown for EspC in EPEC (Vidal & Navarro-García, 2006). Further, since the SPATEs isolated from culture supernatants were active and internalized, SPATE entry into host cells seems to be independent of any other bacterial transport systems. Another SPATE, Pet, which also induces cytotoxicity by cleaving fodrin and spectrin is internalized by host cells through an intracellular vesicular transport system (Navarro-García *et al.*, 2001). For our SPATEs, internalization by fluid-phase pinocytosis can be suspected but the inability of the serine catalytic site-defective mutant proteins to enter the cells suggests a serine protease dependent receptor-mediated endocytosis. Additional studies are needed to elucidate

the mechanism of entry of TagB and TagC proteins. For example, use of fluorescence microscopy-based techniques to specifically label components in the endocytic pathway such as early endosomes, late endosomes, or lysosomes; fractionation procedures; use of different drugs to inhibit protein transport pathways etc. Nonetheless, internalization of these proteins and subsequent cytotoxicity may play an important role in pathogenicity of ExPEC QT598 and other *E. coli* strains producing these SPATEs.

7.3 Assessment of roles of TagB and TagC in different animal models

QT598 was initially isolated from a young turkey poult and was found to be virulent in a subcutaneous infection model of 1-day-old chicks. We initially tested strain QT598 in a 21-day-old chicken air sac inoculation model. However, we failed to identify significant differences between the wild type and SPATE-negative mutant mainly since the wild-type strains were of low virulence and caused very limited disease in chickens. One explanation could be that the older chickens may have stronger immunity than the newly hatched ones. Therefore, we proceeded to infect 5-day-old chicks by the air sac route. Again, there was limited disease and no difference in bacterial counts observed between the wild-type and the SPATE mutant. However, the nature of the histopathological changes caused by QT598 was severe compared to SPATE mutant. Tissue lesions did vary in severity for airsacculitis and pericarditis with chicks infected with the QT598 when compared to SPATEs mutant (Appendix II). Changes in airsacs included mild diffuse thickening and neovascularization with mild fibrinous exudate while heart had vascularization, opacity, and cloudy fluid in the pericardial cavity (Appendix II). Taken together, our experiment suggested that QT598 was not virulent in the older chicken airsac inoculation model. Since QT598 was originally isolated from a 4-day-old turkey, it is quite possible that there may be a host-specific adaptation of this strain for systemic infection of turkeys, although it may be less able to infect chickens. A particularly interesting fact to support this potential host specificity is that among the 299 APEC strains that were screened for the *tagB* and *tagC* genes, the *tagB-tagC* positive isolates were only identified from infections from turkeys. We anticipate that systemic infection of young turkeys will reveal the role of virulence of these serine protease genes in this avian model. In host-pathogen interactions, there can be some instances where pathogens are highly specific to a single-host species instead of infecting a wide range of hosts. For example, enteropathogenic RDEC-1 strain of *E. coli* can elicit diarrhea in rabbits with heavy colonization in the ileal and cecal regions but not in guinea pigs or rats (Cheney *et al.*, 1980). Likewise, *Salmonella* Typhi and *Salmonella* Paratyphi A are normally asymptomatic in mice but cause gastroenteritis in healthy human adults (Vladoianu *et al.*, 1990). Among cross-species studies of ExPEC strains,

human ExPEC strain RS218 was more virulent in the mouse model compared to the duck model, while the APEC DE471 was more virulent in the duck model than in the mouse model (Zhang *et al.*, 2019).

Due to a poor level of infectivity of strain QT598 in the chicken systemic infection model and since the source of the strain was a turkey yolk sac infection, we tested strain QT598 as well as the SPATE mutant strain in a zebrafish yolk sac infection model. Zebrafish (*Danio rerio*) are extensively used in biomedical research to study the virulence mechanisms in host-pathogen interactions (Neely *et al.*, 2002; Van Der Sar *et al.*, 2003; Wiles *et al.*, 2009). Initial interest in studying zebrafish yolk sac for the pathogenesis stemmed from the fact that our working strain was isolated from 4-day-old turkey which might have died due to yolk sac infection. Zebrafish has a protruding yolk sac, which contains a supply of carbohydrates, lipids mainly triglycerides, and micronutrients to sustain metabolic function and growth. Turkey poults have higher risk of mortality within the first few days of life post-hatching (Carver *et al.*, 2000; Christensen *et al.*, 2003) and yolk sacculitis is a leading cause of death in poultry (Roehrig & Torrey, 2019). Yolk sacs of 48 hpf (hour post-fertilization) fish embryos were challenged with QT598 and its SPATE deletion mutant. Within 48 h, strain QT598 appeared to be lethal and had 30-40% death of the host while the SPATE deletion strain was avirulent and did not cause any embryo lethality. Thus, the SPATE mutant was significantly attenuated in the yolk sac (Appendix III). Of note, both strains grew at similar rates in BHI (Brain Heart Infusion) medium at 28.5°C, the optimum temperature of zebrafish growth. Thus, deletion of the SPATEs genes clearly attenuated the strain QT598 in the fish embryo yolk sac infection model. Normally, at 48 hpf the immune system of zebrafish is composed mainly of innate defenses, including antimicrobial peptides, complement, toll-like receptors, and phagocytes (Lieschke *et al.*, 2001). As such, it is likely that the SPATEs might play a role in either neutralizing some of these innate defenses or may promote systemic dissemination from the yolk sac to other organs and tissues. In the murine urinary tract infection model we also saw an attenuation of the SPATE mutant in the murine kidney, a highly vascularized organ. Further investigations are needed to clarify what role, these SPATEs may play in systemic infection and/or immune evasion.

To examine the link between adherence mediated by TagB and TagC to 5637 human bladder epithelial cells, we assessed their role for virulence in the murine UTI model. When mice were challenged transurethrally with QT598 when compared to its isogenic *tagBC* mutant, there were no significant differences in colonization in either the bladder or the kidneys. It is possible that since there are 5 SPATEs in QT598, the loss of *tagB* and *tagC* may be still be compensated by

the remaining three SPATEs. Deletion of all 5 SPATEs attenuated the strain in the kidneys, whereas deletion of only *sha* or deletion of both *tagB* and *tagC* did not. Further, it was also necessary to delete all 5 SPATEs from the strain to eliminate cytotoxicity of the bladder epithelial cell line. These observations strongly support the redundant roles of SPATEs for strain QT598. The SPATEs might work in combination or sequentially or have different functions in different host cells. It remains to be determined why a strain would need to have so many serine proteases, which ones may be more expressed or required in certain host niches or host species and whether there may be a hierarchy of expression or function of these SPATEs during infection.

We also cannot rule out that one limitation of our murine urinary tract model of pathogenesis is that this model does not fully recapitulate the original type of disease or the natural host model. However, similar SPATEs including TagB and TagC, Vat, and Tsh, are also sometimes present in UPEC, and some clades of pathogenic *E. coli* like QT598 are also associated with human systemic infections and UTIs. *In vitro* results demonstrated distinct phenotypes for the different SPATEs. For example, all the SPATEs from QT598 could induce cytopathic effects in 5637 bladder epithelial cells, but cellular phenotypes were different. TagB and TagC showed early activity by releasing LDH within 5 h, whereas the three other SPATEs were late cytotoxicity inducers and released LDH at 12 h, but not at 5 h. Thus, it is possible that the bacterium may cause either early or later cell damage depending on the level or type of specific toxin production in different host niches. The integrity of urothelial cells was shown to be compromised when mouse bladder *ex vivo* was exposed to Vat, which is also a SPATE produced by QT598 (Appendix IV). Vat did affect paracellular permeability of bladder epithelial cells and induced disassembly of tight junction proteins like Z0-1 and occludin (Appendix IV). We also found that all the SPATE genes were expressed *in vivo* but only the *sha* gene was strongly upregulated (by six-fold) in mouse bladder while TagB was upregulated in zebrafish by five-fold. It is therefore possible that gene regulation in addition to substrate specificity may also influence what SPATEs may be more important at certain stages of infection or in different host environments or species. We have seen redundancy in the iron acquisition systems of some bacteria. For instance, UPEC strain CFT073 was colonized well in the murine urinary tract with the disruption of aerobactin or enterobactin system but *iucB* and *entD* double mutant was attenuated (Torres *et al.*, 2001). Salmochelin receptor IroN mutants were defective for urothelial cell invasion (Feldmann *et al.*, 2007) and were outcompeted by the wild type during co-infection in the bladder, kidney and in urine (Russo *et al.*, 2002). In addition, heme acquisition mediated by ChuA is necessary for bladder and kidney colonization and was more important than Hma in kidney colonization (Hagan & Mobley, 2009). Further, the siderophore Yersiniabactin was shown to be more important than enterobactin for

Klebsiella pneumoniae during murine intranasal infection (Lawlor *et al.*, 2007). So, different iron acquisition systems may function more efficiently at specific infection sites. Likewise, there may be a similar distribution of roles for different SPATE proteins during different stages of infection or in specific cell types, tissues or host environments.

No discussion concerning the pathogenic *E. coli* strains would be complete without considering the potential zoonotic risk of APEC strains due to the array of common virulence factors shared between subsets of ExPEC (Johnson *et al.*, 2007). Our own strain of avian origin, irrespective of host source did colonize the urinary tract of mice and was virulent in zebrafish embryos demonstrating niche-adaptability and virulence. The concern regarding pathogenic *E.* coli from poultry is clearly a major issue for the poultry industry, but it is also an important matter for public health and food safety since there may also be a risk of dissemination of strains that may be multi-drug resistant and pathogenic from animal food products or fruits and vegetables contaminated by manure or feces of birds (Brower *et al.*, 2017; Johnson *et al.*, 2005b; Vincent *et al.*, 2010). It was reported that there was an increase in antimicrobial drug-resistant UTIs among women whose diet frequently included chicken and pork consumption (Manges *et al.*, 2007), suggesting that food derived from poultry and pork products may be an important source of UPEC strains. However, thus far, there are no clear studies linking a direct role of animal products as a reservoir of human ExPEC, mainly because it is difficult to rule out whether or not a potential acquisition of infection through the food can be due to human cross-contamination during food production, processing, handling, or especially preparation and consumption in the kitchen (Bélanger *et al.*, 2011). Nevertheless, there are certain subgroups of ExPEC that are common causes of both extraintestinal infections in poultry and infections in humans including urinary tract infections, meningitis, and sepsis.

8 CONCLUSION

In this thesis, TagB and TagC, two new members of the expanding family of serine protease autotransporters (SPATEs) were characterized, as well as the combined role of other SPATEs for virulence of an *E. coli* extraintestinal strain was determined.Today, extra-intestinal pathogenic *Escherichia coli* (ExPEC) represent an emerging pathogen associated with pandemic strains increasingly implicated in cases of urinary tract infections (UTIs), bacteremia, septicemia and meningitis in humans. Further, the avian pathotype of ExPEC, avian pathogenic *E. coli* (APEC), causes avian colibacillosis in domesticated and wild birds leading to severe economic losses to the poultry industry. These pathotypes exhibit considerable genome diversity characterized by the possession of different sets of virulence factors. A common trait to many of them is the presence of one or more SPATEs and they are considered as one of the important virulence factors and can be a potential therapeutic targets or vaccine antigens.

This dissertation has helped us in a greater understanding of ExPEC virulence and pathogenesis mediated by SPATEs. Novel SPATEs, TagB and TagC were characterized with a combination of bioinformatics, *in vitro* molecular analysis, and animal models. The investigation has demonstrated the presence of different SPATE genes among avian and human ExPEC isolates, but also demonstrated different biological activities of SPATEs including adhesion, autoaggregation, hemagglutination, cytotoxicity and proteolytic specificity against different host target proteins. Properties of TagB and TagC that promote adherence to bladder and kidney epithelial cells and ability to autoaggregate could allow the bacteria to persist in the urinary tract against the flushing action of urine and help in colonization. Besides, toxic activity of TagB and TagC characterized by dissolution of cytoplasm and nuclear vacuolation of bladder cell can be regarded as a key virulence factor during urinary tract infections. Further, gelatinase activity of TagC can help the bacteria to disseminate inside the host by penetrating the connective tissues. Based upon these variety of activities identified, it is justified to conclude that TagB and TagC are virulence determinants that may contribute to host-pathogen interactions and enhance the fitness of ExPEC during avian or human infections.

In addition, the research led to the finding that SPATE proteins are internalized in host bladder epithelial cells and lead to disruption of the actin cytoskeleton. Site-directed mutagenesis of the active-site serine residues (S255 and S252) in the putative serine protease motif of TagB and TagC did not abolish processing and secretion, adherence, or agglutination ability of the proteins. However, the substitution of serine with alanine rendered the enzyme inactive resulting in the loss

of protease activities and the ability to enter the host bladder cells. This demonstrated the importance of the serine catalytic site for the functionality of protease activity of TagB and TagC as well as the possible cell internalization mechanism.

The cumulative role of SPATEs of QT598 in ExPEC pathogenesis has been well demonstrated experimentally (*in vivo*) by our results of mouse and zebrafish yolksac model. An interesting finding in our animal model study - turkey strain QT598 was virulent in mice and zebrafish but not in the chickens. Also, no double mutation of *tagB* and *tagC* was proven to be important and lacked attenuation in murine UTI syndrome. Indeed, the study indicated a degree of possible functional redundancy in the spectrum of SPATEs. Interestingly, the *sha* gene was upregulated 6-fold in the murine bladder while TagB was upregulated 5-fold in the zebrafish. So, different animal infection models showed that different SPATEs may contribute specific roles in distinct animal infection models. SPATEs of QT598 include members of class 1 SPATEs (TagC) which are cytopathic in nature as well as members of class 2 (TagB, Vat, Tsh and Sha) which are immunomodulators. So, the success of QT598 colonization inside the host is likely due to the interplay of these proteins at different stages of infection.

Further, by observing the ability of avian strain QT598 to cause murine UTI, one can speculate that birds can be reservoirs for ExPEC strains that can potentially infect humans. However, to prove this hypothesis we will need more epidemiological studies. On contrary, the inability of turkey strain QT598 to cause infection in young chicks, provides evidence that host specificity is as, or more, important than similar virulence factors repertoire present among ExPEC strains. Further research is necessary to deeply analyze the factors involved in the host specificity and adaptation.

In conclusion, our data have significantly advanced understanding of SPATEs in the pathogenesis of extra-intestinal pathogenic *E. coli*. The proposed model of zebrafish yolksac can be instrumental to study other virulence factors involved in avian diseases.

9 PERSPECTIVES

In our study, we have shown a cumulative role for all 5 SPATEs during infection of mice during kidney colonization in a urinary tract infection model as well as for virulence in a zebrafish yolk sac infection model. All five SPATE genes were expressed *in vivo*, but the only *sha* was strongly upregulated in the mouse bladder. As such, it was not clear whether all the genes/proteins were equally important or whether there may be a functional or regulatory hierarchy of these systems during bacterial growth or during infection of the host. So, in future studies use of a transcriptional luciferase (*lux*) reporter consisting of *lux* under the control of the respective SPATE promoter could be useful to determine the level of expression during infection inside the host. This could be done initially in zebrafish and later extended to a murine infection model using biophotonic imaging. This will allow a more complete picture of SPATE regulation *in vivo*. With regards to regulation of SPATE gene expression, it has been shown that *vat* is regulated by the global regulator H-NS. Virtual footprint software (Münch *et al.*, 2005) has also suggested potential H-NS binding sites in the promoter regions of *tagB* and *tagC*. So, future experiments could be undertaken to confirm the role of H-NS in the regulation of *tagB* and *tagC* expression.

Another important future area to address is the mechanism of internalization of these proteins. We have identified actin disruption as a consequence of exposure to SPATEs, but the links between TagB and TagC internalization, cytopathic effects, and actin disorganization, and ExPEC pathogenesis need to be further elucidated. In addition, the effect of SPATEs on the host cellular fate (such as apoptosis, necropsy or autophagy), effects on the host immune response and inflammation should be further investigated. Further, identification of the cellular receptor target(s) of these proteins on host cells might lead to means of development of antimicrobial therapeutic targets. With respect to the biological targets, there is still much to be learned.

Finally, another interesting domain for future studies will be the effect of the biogenesis of SPATEs on fimbriae production and its role in virulence. Biogenesis of fimbriae and SPATEs are completely independent processes but both of them share BAM and TAM nanomachines to reach the outer membrane (Heinz *et al.*, 2015). As such, it may be of interest to determine if there is an order of affinity of either fimbriae or SPATE proteins for processing/export by the BAM and TAM systems, whether loss of TAM has any effect on secretion or biological activity of different SPATEs. Finally, it could also be of interest to pursue structure-function relationships of interaction between SPATE proteins and their host target substrates by crystallography and other biochemical or biophysical methods.

10 BIBLIOGRAPHY

Abraham JM, Freitag CS, Clements JR,Eisenstein BI (1985) An invertible element of DNA controls phase variation of type 1 fimbriae of *Escherichia coli*. *Proceedings of the National Academy of Sciences* 82(17):5724-5727.

Abreu AG, Fraga TR, Granados Martínez AP, Kondo MY, Juliano MA, Juliano L, Navarro-Garcia F, Isaac L, Barbosa AS,Elias WP (2015) The serine protease Pic from enteroaggregative *Escherichia coli* mediates immune evasion by the direct cleavage of complement proteins. *The Journal of infectious diseases* 212(1):106-115.

Anderson GG, Palermo JJ, Schilling JD, Roth R, Heuser J,Hultgren SJ (2003) Intracellular bacterial biofilm-like pods in urinary tract infections. *Science* 301(5629):105-107.

Antão E-M, Ewers C, Gürlebeck D, Preisinger R, Homeier T, Li G,Wieler LH (2009) Signature-tagged mutagenesis in a chicken infection model leads to the identification of a novel avian pathogenic *Escherichia coli* fimbrial adhesin. *PloS one* 4(11):e7796.

Ashkar AA, Mossman KL, Coombes BK, Gyles CL,Mackenzie R (2008) FimH adhesin of type 1 fimbriae is a potent inducer of innate antimicrobial responses which requires TLR4 and type 1 interferon signalling. *PLoS pathogens* 4(12):e1000233.

Bacher A, Eberhardt S, Fischer M, Kis K,Richter G (2000) Biosynthesis of vitamin B2 (riboflavin). *Annual review of nutrition* 20(1):153-167.

Backhed F, Alsen B, Roche N, Angstrom J, Euler Av, Breimer ME, Westerlund-Wikstrom B, Teneberg S,Richter-Dahlfors A (2002) GLYCOBIOLOGY AND EXTRACELLULAR MATRICES-Identification of target tissue glycosphingolipid receptors for uropathogenic, F1C-fimbriated *Escherichia coli* and its role in mucosal inflammation. *Journal of Biological Chemistry* 277(20):18198-18205.

Bäckhed F, Söderhäll M, Ekman P, Normark S,Richter-Dahlfors A (2001) Induction of innate immune responses by *Escherichia coli* and purified lipopolysaccharide correlate with organ-and cell-specific expression of Toll-like receptors within the human urinary tract. *Cellular microbiology* 3(3):153-158.

Baqui AH, Sack RB, Black RE, Haider K, Hossain A, Alim AA, Yunus M, Chowdhury H,Siddique A (1992) Enteropathogens associated with acute and persistent diarrhea in Bangladeshi children< 5 years of age. *Journal of infectious diseases* 166(4):792-796.

Bates Jr JM, Raffi HM, Prasadan K, Mascarenhas R, Laszik Z, Maeda N, Hultgren SJ,Kumar S (2004) Tamm-Horsfall protein knockout mice are more prone to urinary tract infection Rapid Communication. *Kidney international* 65(3):791-797.

Becknell B, Spencer JD, Carpenter AR, Chen X, Singh A, Ploeger S, Kline J, Ellsworth P, Li B,Proksch E (2013) Expression and antimicrobial function of beta-defensin 1 in the lower urinary tract. *PloS one* 8(10):e77714.

Bélanger L, Garenaux A, Harel J, Boulianne M, Nadeau E,Dozois CM (2011) *Escherichia coli* from animal reservoirs as a potential source of human extraintestinal pathogenic *E. coli*. *FEMS Immunology & Medical Microbiology* 62(1):1-10.

Bentley R & Meganathan R (1982) Biosynthesis of vitamin K (menaquinone) in bacteria. *Microbiological reviews* 46(3):241.

Benz I & Schmidt MA (1992) AIDA-I, the adhesin involved in diffuse adherence of the diarrhoeagenic *Escherichia coli* strain 2787 (O126: H27), is synthesized via a precursor molecule. *Molecular microbiology* 6(11):1539-1546.

Berthe, T., Ratajczak, M., Clermont, O., Denamur, E. and Petit, F. (2013) Evidence for coexistence of distinct *Escherichia coli* populations in various aquatic environments and their survival in estuary water. Appl Environ Microbiol 79, 4684–4693

Bertrand N, Houle S, LeBihan G, Poirier É, Dozois CM,Harel J (2010) Increased Pho regulon activation correlates with decreased virulence of an avian pathogenic *Escherichia coli* O78 strain. *Infection and immunity* 78(12):5324-5331.

Bilge S, Clausen C, Lau W,Moseley S (1989) Molecular characterization of a fimbrial adhesin, F1845, mediating diffuse adherence of diarrhea-associated *Escherichia coli* to HEp-2 cells. *Journal of bacteriology* 171(8):4281-4289.

Bjarke Olsen P & Klemm P (1994) Localization of promoters in the fim gene cluster and the effect of H-NS on the transcription of *fimB* and *fimE*. *FEMS microbiology letters* 116(1):95-100.

Bonacorsi S, Clermont O, Houdouin V, Cordevant C, Brahimi N, Marecat A, Tinsley C, Nassif X, Lange M,Bingen E (2003) Molecular analysis and experimental virulence of French and North American *Escherichia coli* neonatal meningitis isolates: identification of a new virulent clone. *The Journal of infectious diseases* 187(12):1895-1906.

Boyd EF & Hartl DL (1998) Chromosomal regions specific to pathogenic isolates of *Escherichia coli* have a phylogenetically clustered distribution. *Journal of bacteriology* 180(5):1159-1165.

Brauner A, Jacobson S,Kühn I (1992) Urinary *Escherichia coli* causing recurrent infections--a prospective follow-up of biochemical phenotypes. *Clinical nephrology* 38(6):318-323.

Brower CH, Mandal S, Hayer S, Sran M, Zehra A, Patel SJ, Kaur R, Chatterjee L, Mishra S,Das B (2017) The prevalence of extended-spectrum beta-lactamase-producing multidrug-resistant *Escherichia coli* in poultry chickens and variation according to farming practices in Punjab, India. *Environmental health perspectives* 125(7):077015.

Brown P, Ki M,Foxman B (2005) Acute pyelonephritis among adults. *Pharmacoeconomics* 23(11):1123-1142.

Brunder W, Schmidt H,Karch H (1997) EspP, a novel extracellular serine protease of enterohaemorrhagic *Escherichia coli* O157: H7 cleaves human coagulation factor V. *Molecular microbiology* 24(4):767-778.

Brzuszkiewicz E, Brüggemann H, Liesegang H, Emmerth M, Ölschläger T, Nagy G, Albermann K, Wagner C, Buchrieser C,Emődy L (2006) How to become a uropathogen: comparative genomic analysis of extraintestinal pathogenic *Escherichia coli* strains. *Proceedings of the National Academy of Sciences* 103(34):12879-12884.

Carver DK, Fetrow J, Gerig T, Correa MT, Krueger KK,Barnes HJ (2000) Use of statistical modeling to assess risk for early poult mortality in commercial turkey flocks. *Journal of Applied Poultry Research* 9(3):303-318.

Caza M, Lépine F, Milot S,Dozois CM (2008) Specific roles of the iroBCDEN genes in virulence of an avian pathogenic *Escherichia coli* O78 strain and in production of salmochelins. *Infection and immunity* 76(8):3539-3549.

Chaffer M, Heller E,Schwartsburd B (1999) Relationship between resistance to complement, virulence and outer membrane protein patterns in pathogenic *Escherichia coli* O2 isolates. *Veterinary microbiology* 64(4):323-332.

Chaturvedi KS, Hung CS, Crowley JR, Stapleton AE,Henderson JP (2012) The siderophore yersiniabactin binds copper to protect pathogens during infection. *Nature chemical biology* 8(8):731.

Cheney CP, Schad PA, Formal SB,Boedeker EC (1980) Species specificity of in vitro *Escherichia coli* adherence to host intestinal cell membranes and its correlation with in vitro colonization and infectivity. *Infection and immunity* 28(3):1019-1027.

Choudhury D, Thompson A, Stojanoff V, Langermann S, Pinkner J, Hultgren SJ,Knight SD (1999) X-ray structure of the FimC-FimH chaperone-adhesin complex from uropathogenic *Escherichia coli*. *Science* 285(5430):1061-1066.

Chouikha I, Germon P, Brée A, Gilot P, Moulin-Schouleur M,Schouler C (2006) A selC-associated genomic island of the extraintestinal avian pathogenic *Escherichia coli* strain BEN2908 is involved in carbohydrate uptake and virulence. *Journal of bacteriology* 188(3):977-987.

Christensen VL, Ort DT,Grimes JL (2003) Physiological factors associated with weak neonatal poults (Meleagris gallopavo). *Int. J. Poult. Sci* 2:7-14.

Chromek M, Slamová Z, Bergman P, Kovács L, Podracká Lu, Ehrén I, Hökfelt T, Gudmundsson GH, Gallo RL,Agerberth B (2006) The antimicrobial peptide cathelicidin protects the urinary tract against invasive bacterial infection. *Nature medicine* 12(6):636.

Clermont O, Christenson JK, Denamur E,Gordon DM (2013) The C lermont E scherichia *coli* phylo-typing method revisited: improvement of specificity and detection of new phylo-groups. *Environmental microbiology reports* 5(1):58-65.

Connell I, Agace W, Klemm P, Schembri M, Märild S,Svanborg C (1996) Type 1 fimbrial expression enhances *Escherichia coli* virulence for the urinary tract. *Proceedings of the National Academy of Sciences* 93(18):9827-9832.

Cookson ST & Nataro JP (1996) Characterization of HEp-2 cell projection formation induced by diffusely adherent *Escherichia coli*. *Microbial pathogenesis* 21(6):421-434.

Cortes MA, Gibon J, Chanteloup NK, Moulin-Schouleur M, Gilot P,Germon P (2008) Inactivation of ibeA and ibeT results in decreased expression of type 1 fimbriae in extraintestinal pathogenic *Escherichia coli* strain BEN2908. *Infection and immunity* 76(9):4129-4136.

Cross AS, Kim KS, Wright DC, Sadoff JC,Gemski P (1986) Role of lipopolysaccharide and capsule in the serum resistance of bacteremic strains of *Escherichia coli*. *Journal of infectious diseases* 154(3):497-503.

Czeczulin JR, Balepur S, Hicks S, Phillips A, Hall R, Kothary MH, Navarro-Garcia F,Nataro JP (1997) Aggregative adherence fimbria II, a second fimbrial antigen mediating aggregative adherence in enteroaggregative *Escherichia coli*. *Infection and immunity* 65(10):4135-4145.

Danzeisen JL, Wannemuehler Y, Nolan LK,Johnson TJ (2013) Comparison of multilocus sequence analysis and virulence genotyping of *Escherichia coli* from live birds, retail poultry meat, and human extraintestinal infection. *Avian diseases* 57(1):104-108.

de Paiva JB, Leite JL, da Silva LPM, Rojas TCG, de Pace F, Conceição RA, Sperandio V,da Silveira WD (2015) Influence of the major nitrite transporter NirC on the virulence of a Swollen Head Syndrome avian pathogenic E. coli (APEC) strain. *Veterinary microbiology* 175(1):123-131.

Dhakal BK & Mulvey MA (2012) The UPEC pore-forming toxin α-hemolysin triggers proteolysis of host proteins to disrupt cell adhesion, inflammatory, and survival pathways. *Cell host & microbe* 11(1):58-69.

Dho-Moulin M & Fairbrother JM (1999) Avian pathogenic *Escherichia coli* (APEC). *Veterinary research* 30(2-3):299-316.

Dietzman DE, Fischer GW,Schoenknecht FD (1974) Neonatal *Escherichia coli* septicemia—bacterial counts in blood. *The Journal of pediatrics* 85(1):128-130.

Dobrindt U, Blum-Oehler G, Hartsch T, Gottschalk G, Ron EZ, Fünfstück R,Hacker J (2001) S-Fimbria-Encoding Determinant sfa I Is Located on Pathogenicity Island III536 of Uropathogenic*Escherichia coli* Strain 536. *Infection and immunity* 69(7):4248-4256.

Dozois CM, Dho-Moulin M, Brée A, Fairbrother JM, Desautels C,Curtiss R (2000) Relationship between the Tsh autotransporter and pathogenicity of avian *Escherichia coli* and localization and analysis of the Tsh genetic region. *Infection and immunity* 68(7):4145-4154.

Dozois CM, Fairbrother JM, Harel J,Bossé M (1992) pap-and pil-related DNA sequences and other virulence determinants associated with *Escherichia coli* isolated from septicemic chickens and turkeys. *Infection and immunity* 60(7):2648-2656.

Dutta PR, Cappello R, Navarro-García F,Nataro JP (2002) Functional comparison of serine protease autotransporters of Enterobacteriaceae. *Infection and immunity* 70(12):7105-7113.

Ejrnæs K (2011) Bacterial characteristics of importance for recurrent urinary tract infections caused by *Escherichia coli*. *Dan Med Bull* 58(4):B4187.

Ejrnaes K, Sandvang D, Lundgren B, Ferry S, Holm S, Monsen T, Lundholm R,Frimodt-Moller N (2006) Pulsed-field gel electrophoresis typing of *Escherichia coli* strains from samples collected before and after pivmecillinam or placebo treatment of uncomplicated community-acquired urinary tract infection in women. *Journal of Clinical Microbiology* 44(5):1776-1781.

Emery D, Nagaraja KV, Shaw D, Newman J,White D (1992) Virulence factors of *Escherichia coli* associated with colisepticemia in chickens and turkeys. *Avian diseases* :504-511.

Endo Y, Tsurugi K, Yutsudo T, Takeda Y, Ogasawara T,Igarashi K (1988) Site of action of a Vero toxin (VT2) from *Escherichia coli* O157: H7 and of Shiga toxin on eukaryotic ribosomes: RNA N-glycosidase activity of the toxins. *European Journal of Biochemistry* 171(1-2):45-50.

Eslava C, Navarro-García F, Czeczulin JR, Henderson IR, Cravioto A,Nataro JP (1998) Pet, an autotransporter enterotoxin from enteroaggregative *Escherichia coli*. *Infection and immunity* 66(7):3155-3163.

Ewers C, Janßen T, Kießling S, Philipp H-C,Wieler LH (2004) Molecular epidemiology of avian pathogenic *Escherichia coli* (APEC) isolated from colisepticemia in poultry. *Veterinary microbiology* 104(1-2):91-101.

Fasano A, Noriega F, Liao F, Wang W,Levine M (1997) Effect of shigella enterotoxin 1 (ShET1) on rabbit intestine in vitro and in vivo. *Gut* 40(4):505-511.

Feldmann F, Sorsa LJ, Hildinger K,Schubert S (2007) The salmochelin siderophore receptor IroN contributes to invasion of urothelial cells by extraintestinal pathogenic *Escherichia coli* in vitro. *Infection and immunity* 75(6):3183-3187.

Fléchard M, Cortes MA, Répérant M,Germon P (2012) New role for the ibeA gene in H2O2 stress resistance of *Escherichia coli*. *Journal of bacteriology* 194(17):4550-4560.

Foley SL, Horne SM, Giddings CW, Robinson M,Nolan LK (2000) Iss from a virulent avian *Escherichia coli*. *Avian diseases* :185-191.

Foxman B (1990) Recurring urinary tract infection: incidence and risk factors. *American journal of public health* 80(3):331-333.

Foxman B (2010) The epidemiology of urinary tract infection. *Nature Reviews Urology* 7(12):653.

Foxman B (2014) Urinary tract infection syndromes: occurrence, recurrence, bacteriology, risk factors, and disease burden. *Infectious disease clinics of North America* 28(1):1-13.

Foxman B, Marsh J, Gillespie B, Rubin N, Koopman JS,Spear S (1997) Condom use and first-time urinary tract infection. *Epidemiology* :637-641.

Fraser ME, Fujinaga M, Cherney MM, Melton-Celsa AR, Twiddy EM, O'Brien AD,James MN (2004) Structure of Shiga toxin type 2 (Stx2) from *Escherichia coli* O157: H7. *Journal of Biological Chemistry* 279(26):27511-27517.

Frendéus B, Wachtler C, Hedlund M, Fischer H, Samuelsson P, Svensson M,Svanborg C (2001) *Escherichia coli* P fimbriae utilize the Toll-like receptor 4 pathway for cell activation. *Molecular microbiology* 40(1):37-51.

Gao Q, Jia X, Wang X, Xiong L, Gao S,Liu X (2015a) The avian pathogenic *Escherichia coli* O2 strain E058 carrying the defined aerobactin-defective iucD or iucDiutA mutation is less virulent in the chicken. *Infection, Genetics and Evolution* 30:267-277.

Gao Q, Wang X, Xu H, Xu Y, Ling J, Zhang D, Gao S,Liu X (2012) Roles of iron acquisition systems in virulence of extraintestinal pathogenic *Escherichia coli*: salmochelin and aerobactin contribute more to virulence than heme in a chicken infection model. *BMC microbiology* 12(1):143.

Gao Q, Ye Z, Wang X, Mu X, Gao S,Liu X (2015b) RstA is required for the virulence of an avian pathogenic *Escherichia coli* O2 strain E058. *Infection, Genetics and Evolution* 29:180-188.

Garénaux A, Caza M,Dozois CM (2011) The Ins and Outs of siderophore mediated iron uptake by extra-intestinal pathogenic *Escherichia coli*. *Veterinary microbiology* 153(1-2):89-98.

Germon P, Chen Y-H, He L, Blanco JE, Bree A, Schouler C, Huang S-H,Moulin-Schouleur M (2005) ibeA, a virulence factor of avian pathogenic *Escherichia coli*. *Microbiology* 151(4):1179-1186.

Girón JA, Levine MM,Kaper JB (1994) Longus: a long pilus ultrastructure produced by human enterotoxigenic *Escherichia coli*. *Molecular microbiology* 12(1):71-82.

Goluszko P, Popov V, Selvarangan R, Nowicki S, Pham T,Nowicki BJ (1997) Dr fimbriae operon of uropathogenic *Escherichia coli* mediate microtubule-dependent invasion to the HeLa epithelial cell line. *Journal of infectious diseases* 176(1):158-167.

Grabe M, Bjerklund-Johansen T, Botto H, Çek M, Naber K, Tenke P,Wagenlehner F (2015) Guidelines on urological infections. *European association of urology* 182.

Guignot J, Chaplais C, Coconnier-Polter MH,Servin AL (2007) The secreted autotransporter toxin, Sat, functions as a virulence factor in Afa/Dr diffusely adhering *Escherichia coli* by promoting lesions in tight junction of polarized epithelial cells. *Cellular microbiology* 9(1):204-221.

Guignot J, Segura A,Van Nhieu GT (2015) The serine protease EspC from enteropathogenic *Escherichia coli* regulates pore formation and cytotoxicity mediated by the type III secretion system. *PLoS pathogens* 11(7):e1005013.

Guyer DM, Henderson IR, Nataro JP,Mobley HL (2000) Identification of sat, an autotransporter toxin produced by uropathogenic *Escherichia coli*. *Molecular microbiology* 38(1):53-66.

Guyer DM, Radulovic S, Jones F-E,Mobley HL (2002) Sat, the secreted autotransporter toxin of uropathogenic *Escherichia coli*, is a vacuolating cytotoxin for bladder and kidney epithelial cells. *Infection and immunity* 70(8):4539-4546.

Hagan EC & Mobley HL (2009) Haem acquisition is facilitated by a novel receptor Hma and required by uropathogenic *Escherichia coli* for kidney infection. *Molecular microbiology* 71(1):79-91.

Hantke K, Nicholson G, Rabsch W,Winkelmann G (2003) Salmochelins, siderophores of Salmonella enterica and uropathogenic *Escherichia coli* strains, are recognized by the outer membrane receptor IroN. *Proceedings of the National Academy of Sciences* 100(7):3677-3682.

Harrington SM, Sheikh J, Henderson IR, Ruiz-Perez F, Cohen PS,Nataro JP (2009) The Pic protease of enteroaggregative *Escherichia coli* promotes intestinal colonization and growth in the presence of mucin. *Infection and immunity* 77(6):2465-2473.

Harris SL, Elliott DA, Blake M, Must L, Messenger M,Orndorff P (1990) Isolation and characterization of mutants with lesions affecting pellicle formation and erythrocyte agglutination by type 1 piliated *Escherichia coli*. *Journal of bacteriology* 172(11):6411-6418.

Hasman H, Chakraborty T,Klemm P (1999) Antigen-43-Mediated Autoaggregation of *Escherichia coli* Is Blocked by Fimbriation. *Journal of bacteriology* 181(16):4834-4841.

Hedlund M, Frendéus B, Wachtler C, Hang L, Fischer H,Svanborg C (2001) Type 1 fimbriae deliver an LPS-and TLR4-dependent activation signal to CD14-negative cells. *Molecular microbiology* 39(3):542-552.

Hedlund M, Wachtler C, Johansson E, Hang L, Somerville J, Darveau R,Svanborg C (1999) P fimbriae-dependent, lipopolysaccharide-independent activation of epithelial cytokine responses. *Molecular microbiology* 33(4):693-703.

Heimer SR, Rasko DA, Lockatell CV, Johnson DE,Mobley HL (2004) Autotransporter genes pic and tsh are associated with *Escherichia coli* strains that cause acute pyelonephritis and are expressed during urinary tract infection. *Infection and immunity* 72(1):593-597.

Heinz E, Selkrig J, Belousoff MJ,Lithgow T (2015) Evolution of the translocation and assembly module (TAM). *Genome biology and evolution* 7(6):1628-1643.

Henderson, I. R., Czeczulin, J., Eslava, C., Noriega, F., & Nataro, J. P. (1999). Characterization of pic, a secreted protease of Shigella flexneri and enteroaggregative Escherichia coli. Infection and immunity, 67(11), 5587–5596.

Henderson JP, Crowley JR, Pinkner JS, Walker JN, Tsukayama P, Stamm WE, Hooton TM,Hultgren SJ (2009) Quantitative metabolomics reveals an epigenetic blueprint for iron acquisition in uropathogenic *Escherichia coli*. *PLoS pathogens* 5(2):e1000305.

Herren CD, Mitra A, Palaniyandi SK, Coleman A, Elankumaran S,Mukhopadhyay S (2006) The BarA-UvrY two-component system regulates virulence in avian pathogenic *Escherichia coli* O78: K80: H9. *Infection and immunity* 74(8):4900-4909.

Hill M & Drasar B (1975) The normal colonic bacterial flora. *Gut* 16(4):318.

Hooton TM (2001) Recurrent urinary tract infection in women. *International journal of antimicrobial agents* 17(4):259-268.

Hooton TM, Bradley SF, Cardenas DD, Colgan R, Geerlings SE, Rice JC, Saint S, Schaeffer AJ, Tambayh PA,Tenke P (2010) Diagnosis, prevention, and treatment of catheter-associated urinary tract infection in adults: 2009 International Clinical Practice Guidelines from the Infectious Diseases Society of America. *Clinical infectious diseases* 50(5):625-663.

Hopkins WJ, Helsey DM, Lorentzeh DF,Uehling DT (1998) A comparative study of major histocompatibility complex and red blood cell antigen phenotypes as risk factors for recurrent urinary tract infections in women. *The Journal of infectious diseases* 177(5):1296-1301.

Huang S-H, Wan Z-S, Chen Y-H, Jong AY,Kim KS (2001) Further characterization of *Escherichia coli* brain microvascular endothelial cell invasion gene ibeA by deletion, complementation, and protein expression. *The Journal of infectious diseases* 183(7):1071-1078.

Hudault S, Guignot J,Servin AL (2001) *Escherichia coli* strains colonising the gastrointestinal tract protect germfree mice againstSalmonella typhimuriuminfection. *Gut* 49(1):47-55.

Isberg RR & Van Nhieu GT (1994) Binding and internalization of microorganisms by integrin receptors. *Trends in microbiology* 2(1):10-14.

Jakobsen L, Hammerum AM,Frimodt-Møller N (2010) Detection of clonal group A *Escherichia coli* isolates from broiler chickens, broiler chicken meat, community-dwelling humans, and urinary tract infection (UTI) patients and their virulence in a mouse UTI model. *Appl. Environ. Microbiol.* 76(24):8281-8284.

Johnson JR, Delavari P, Kuskowski M,Stell AL (2001) Phylogenetic distribution of extraintestinal virulence-associated traits in *Escherichia coli*. *The Journal of infectious diseases* 183(1):78-88.

Johnson JR, Jelacic S, Schoening LM, Clabots C, Shaikh N, Mobley HL,Tarr PI (2005a) The IrgA homologue adhesin Iha is an *Escherichia coli* virulence factor in murine urinary tract infection. *Infection and immunity* 73(2):965-971.

Johnson JR, Kuskowski MA, Smith K, O'Bryan TT,Tatini S (2005b) Antimicrobial-resistant and extraintestinal pathogenic *Escherichia coli* in retail foods. *The Journal of infectious diseases* 191(7):1040-1049.

Johnson JR & Stell AL (2000) Extended virulence genotypes of *Escherichia coli* strains from patients with urosepsis in relation to phylogeny and host compromise. *The Journal of infectious diseases* 181(1):261-272.

Johnson TA, Qiu J, Plaut AG,Holyoak T (2009) Active-site gating regulates substrate selectivity in a chymotrypsin-like serine protease: the structure of Haemophilus influenzae immunoglobulin A1 protease. *Journal of molecular biology* 389(3):559-574.

Johnson TJ, Kariyawasam S, Wannemuehler Y, Mangiamele P, Johnson SJ, Doetkott C, Skyberg JA, Lynne AM, Johnson JR,Nolan LK (2007) The genome sequence of avian pathogenic *Escherichia coli* strain O1: K1: H7 shares strong similarities with human extraintestinal pathogenic E. coli genomes. *Journal of bacteriology* 189(8):3228-3236.

Johnson TJ, Siek KE, Johnson SJ,Nolan LK (2006) DNA sequence of a ColV plasmid and prevalence of selected plasmid-encoded virulence genes among avian *Escherichia coli* strains. *Journal of bacteriology* 188(2):745-758.

Jones NL, Islur A, Haq R, Mascarenhas M, Karmali MA, Perdue MH, Zanke BW,Sherman PM (2000) *Escherichia coli* Shiga toxins induce apoptosis in epithelial cells that is regulated by the Bcl-2 family. *American Journal of Physiology-Gastrointestinal and Liver Physiology* 278(5):G811-G819.

Jones RL, Peterson CM, Grady RW,Cerami A (1980) Low molecular weight iron-binding factor from mammalian tissue that potentiates bacterial growth. *Journal of Experimental Medicine* 151(2):418-428.

Justice SS, Hung C, Theriot JA, Fletcher DA, Anderson GG, Footer MJ,Hultgren SJ (2004) Differentiation and developmental pathways of uropathogenic *Escherichia coli* in urinary tract pathogenesis. *Proceedings of the National Academy of Sciences* 101(5):1333-1338.

Kaper JB, Nataro JP,Mobley HL (2004) Pathogenic *escherichia coli*. *Nature reviews microbiology* 2(2):123.

Kariyawasam S & Nolan LK (2009) Pap mutant of avian pathogenic *Escherichia coli* O1, an O1: K1: H7 strain, is attenuated in vivo. *Avian diseases* 53(2):255-260.

Kenny B (2001) Mechanism of action of EPEC type III effector molecules. *International journal of medical microbiology* 291(6-7):469-477.

Kerrn M, Struve C, Blom J, Frimodt-Møller N,Krogfelt K (2005) Intracellular persistence of *Escherichia coli* in urinary bladders from mecillinam-treated mice. *Journal of Antimicrobial Chemotherapy* 55(3):383-386.

Khac HV, Holoda E, Pilipcinec E, Blanco M, Blanco JE, Mora A, Dahbi G, López C, González EA,Blanco J (2006) Serotypes, virulence genes, and PFGE profiles of *Escherichia coli* isolated from pigs with postweaning diarrhoea in Slovakia. *BMC Veterinary Research* 2(1):10.

Khan NA, Shin S, Chung JW, Kim KJ, Elliott S, Wang Y,Kim KS (2003) Outer membrane protein A and cytotoxic necrotizing factor-1 use diverse signaling mechanisms for *Escherichia coli* K1 invasion of human brain microvascular endothelial cells. *Microbial pathogenesis* 35(1):35-42.

Khan NA, Wang Y, Kim KJ, Chung JW, Wass CA,Kim KS (2002) Cytotoxic necrotizing factor-1 contributes to *Escherichia coli* K1 invasion of the central nervous system. *Journal of Biological Chemistry* 277(18):15607-15612.

Kim KJ, Elliott SJ, Di Cello F, Stins MF,Kim KS (2003) The K1 capsule modulates trafficking of *E. coli*-containing vacuoles and enhances intracellular bacterial survival in human brain microvascular endothelial cells. *Cellular microbiology* 5(4):245-252.

Kim KS, Itabashi H, Gemski P, Sadoff J, Warren RL,Cross AS (1992) The K1 capsule is the critical determinant in the development of *Escherichia coli* meningitis in the rat. *The Journal of clinical investigation* 90(3):897-905.

Klebensberger J, Lautenschlager K, Bressler D, Wingender J, Philipp B. Detergent-induced cell aggregation in subpopulations of Pseudomonas aeruginosa as a preadaptive survival strategy. Environ Microbiol. 2007;9(9):2247-2259. doi:10.1111/j.1462-2920.2007.01339.x

Klumpp DJ, Weiser AC, Sengupta S, Forrestal SG, Batler RA,Schaeffer AJ (2001) Uropathogenic *Escherichia coli* potentiates type 1 pilus-induced apoptosis by suppressing NF-κB. *Infection and immunity* 69(11):6689-6695.

Korhonen T, Väisänen-Rhen V, Rhen M, Pere A, Parkkinen J,Finne J (1984) *Escherichia coli* fimbriae recognizing sialyl galactosides. *Journal of bacteriology* 159(2):762-766.

Korhonen T, Väisänen V, Saxén H, Hultberg H,Svenson SB (1982) P-antigen-recognizing fimbriae from human uropathogenic *Escherichia coli* strains. *Infection and immunity* 37(1):286-291.

Korhonen TK, Parkkinen J, Hacker J, Finne J, Pere A, Rhen M,Holthöfer H (1986) Binding of *Escherichia coli* S fimbriae to human kidney epithelium. *Infection and immunity* 54(2):322-327.

Koschinski A, Repp H, Unver B, Dreyer F, Brockmeier D, Valeva A, Bhakdi S, Walev I, Koschinski A,Repp H (2006) Why *Escherichia coli* α-hemolysin induces calcium oscillations in mammalian cells--the pore is on its own. *The FASEB journal* 20(7):973-975.

Kostakioti M & Stathopoulos C (2004) Functional analysis of the Tsh autotransporter from an avian pathogenic *Escherichia coli* strain. *Infection and immunity* 72(10):5548-5554.

Kumar P, Luo Q, Vickers TJ, Sheikh A, Lewis WG,Fleckenstein JM (2014) EatA, an immunogenic protective antigen of enterotoxigenic *Escherichia coli,* degrades intestinal mucin. *Infection and immunity* 82(2):500-508.

La Ragione R, Cooley W,Woodward MJ (2000) The role of fimbriae and flagella in the adherence of avian strains of *Escherichia coli* O78: K80 to tissue culture cells and tracheal and gut explants. *Journal of Medical Microbiology* 49(4):327-338.

Laarmann S & Schmidt MA (2003) The *Escherichia coli* AIDA autotransporter adhesin recognizes an integral membrane glycoprotein as receptor. *Microbiology* 149(7):1871-1882.

Labigne-Roussel AF, Lark D, Schoolnik G,Falkow S (1984) Cloning and expression of an afimbrial adhesin (AFA-I) responsible for P blood group-independent, mannose-resistant hemagglutination from a pyelonephritic *Escherichia coli* strain. *Infection and immunity* 46(1):251-259.

Lamarche MG, Dozois CM, Daigle F, Caza M, Curtiss R, Dubreuil JD,Harel J (2005) Inactivation of the pst system reduces the virulence of an avian pathogenic *Escherichia coli* O78 strain. *Infection and immunity* 73(7):4138-4145.

Lane M & Mobley H (2007) Role of P-fimbrial-mediated adherence in pyelonephritis and persistence of uropathogenic *Escherichia coli* (UPEC) in the mammalian kidney. *Kidney international* 72(1):19-25.

Lawlor MS, O'Connor C,Miller VL (2007) Yersiniabactin is a virulence factor for Klebsiella pneumoniae during pulmonary infection. *Infection and immunity* 75(3):1463-1472.

Lehti TA, Bauchart P, Heikkinen J, Hacker J, Korhonen TK, Dobrindt U,Westerlund-Wikström B (2010) Mat fimbriae promote biofilm formation by meningitis-associated *Escherichia coli. Microbiology* 156(8):2408-2417.

Li G, Feng Y, Kariyawasam S, Tivendale KA, Wannemuehler Y, Zhou F, Logue CM, Miller CL,Nolan LK (2010) AatA is a novel autotransporter and virulence factor of avian pathogenic *Escherichia coli. Infection and immunity* 78(3):898-906.

Li G, Tivendale KA, Liu P, Feng Y, Wannemuehler Y, Cai W, Mangiamele P, Johnson TJ, Constantinidou C,Penn CW (2011) Transcriptome analysis of avian pathogenic *Escherichia coli* O1 in chicken serum reveals adaptive responses to systemic infection. *Infection and immunity* 79(5):1951-1960.

Lieschke GJ, Oates AC, Crowhurst MO, Ward AC,Layton JE (2001) Morphologic and functional characterization of granulocytes and macrophages in embryonic and adult zebrafish. *Blood, The Journal of the American Society of Hematology* 98(10):3087-3096.

Liévin-Le Moal V, Comenge Y, Ruby V, Amsellem R, Nicolas V,Servin AL (2011) Secreted autotransporter toxin (Sat) triggers autophagy in epithelial cells that relies on cell detachment. *Cellular microbiology* 13(7):992-1013.

Lund B, Lindberg F, Marklund B-I,Normark S (1987) The PapG protein is the alpha-D-galactopyranosyl-(1---4)-beta-D-galactopyranose-binding adhesin of uropathogenic *Escherichia coli. Proceedings of the National Academy of Sciences* 84(16):5898-5902.

Lymberopoulos MH, Houle S, Daigle F, Léveillé S, Brée A, Moulin-Schouleur M, Johnson JR,Dozois CM (2006) Characterization of Stg fimbriae from an avian pathogenic *Escherichia coli* O78: K80 strain

and assessment of their contribution to colonization of the chicken respiratory tract. *Journal of bacteriology* 188(18):6449-6459.

Maldonado-Contreras A, Birtley JR, Boll E, Zhao Y, Mumy KL, Toscano J, Ayehunie S, Reinecker H-C, Stern LJ,McCormick BA (2017) Shigella depends on SepA to destabilize the intestinal epithelial integrity via cofilin activation. *Gut microbes* 8(6):544-560.

Maltby R, Leatham-Jensen MP, Gibson T, Cohen PS, Conway T. Nutritional basis for colonization resistance by human commensal Escherichia coli strains HS and Nissle 1917 against E. coli O157:H7 in the mouse intestine. PLoS One. 2013;8(1):e53957. doi:10.1371/journal.pone.0053957

Matz, C., Bergfeld, T., Rice, S. A., & Kjelleberg, S. (2004). Microcolonies, quorum sensing and cytotoxicity determine the survival of Pseudomonas aeruginosa biofilms exposed to protozoan grazing. Environmental microbiology, 6(3), 218-226.

Manges AR, Smith SP, Lau BJ, Nuval CJ, Eisenberg JN, Dietrich PS,Riley LW (2007) Retail meat consumption and the acquisition of antimicrobial resistant *Escherichia coli* causing urinary tract infections: a case–control study. *Foodborne pathogens and disease* 4(4):419-431.

Martinez JJ, Mulvey MA, Schilling JD, Pinkner JS,Hultgren SJ (2000) Type 1 pilus-mediated bacterial invasion of bladder epithelial cells. *The EMBO journal* 19(12):2803-2812.

McDaniel TK, Jarvis KG, Donnenberg MS,Kaper JB (1995) A genetic locus of enterocyte effacement conserved among diverse enterobacterial pathogens. *Proceedings of the National Academy of Sciences* 92(5):1664-1668.

McPeake S, Smyth J,Ball H (2005) Characterisation of avian pathogenic *Escherichia coli* (APEC) associated with colisepticaemia compared to faecal isolates from healthy birds. *Veterinary microbiology* 110(3-4):245-253.

Mellata M, Ameiss K, Mo H,Curtiss R (2010) Characterization of the contribution to virulence of three large plasmids of avian pathogenic *Escherichia coli* χ7122 (O78: K80: H9). *Infection and immunity* 78(4):1528-1541.

Mellata M, Dho-Moulin M, Dozois CM, Curtiss III R, Brown PK, Arné P, Brée A, Desautels C,Fairbrother JM (2003) Role of virulence factors in resistance of avian pathogenic *Escherichia coli* to serum and in pathogenicity. *Infection and immunity* 71(1):536-540.

Mellies JL, Navarro-Garcia F, Okeke I, Frederickson J, Nataro JP,Kaper JB (2001) espC pathogenicity island of enteropathogenic *Escherichia coli* encodes an enterotoxin. *Infection and immunity* 69(1):315-324.

Menard R, Sansonetti PJ,Parsot C (1993) Nonpolar mutagenesis of the ipa genes defines IpaB, IpaC, and IpaD as effectors of Shigella flexneri entry into epithelial cells. *Journal of bacteriology* 175(18):5899-5906.

Mills M, Meysick KC,O'Brien AD (2000) Cytotoxic necrotizing factor type 1 of uropathogenic *Escherichia coli* kills cultured human uroepithelial 5637 cells by an apoptotic mechanism. *Infection and immunity* 68(10):5869-5880.

Miraglia AG, Travaglione S, Meschini S, Falzano L, Matarrese P, Quaranta MG, Viora M, Fiorentini C,Fabbri A (2007) Cytotoxic necrotizing factor 1 prevents apoptosis via the Akt/IκB kinase pathway: role of nuclear factor-κB and Bcl-2. *Molecular biology of the cell* 18(7):2735-2744.

Miyazaki Y & Ichikawa I (2003) Ontogeny of congenital anomalies of the kidney and urinary tract, CAKUT. *Pediatrics international* 45(5):598-604.

Moll A, Manning P,Timmis K (1980) Plasmid-determined resistance to serum bactericidal activity: a major outer membrane protein, the traT gene product, is responsible for plasmid-specified serum resistance in *Escherichia coli*. *Infection and immunity* 28(2):359-367.

Moon H, Whipp S, Argenzio R, Levine M,Giannella R (1983) Attaching and effacing activities of rabbit and human enteropathogenic *Escherichia coli* in pig and rabbit intestines. *Infection and immunity* 41(3):1340-1351.

Mossman KL, Mian MF, Lauzon NM, Gyles CL, Lichty B, Mackenzie R, Gill N,Ashkar AA (2008) Cutting edge: FimH adhesin of type 1 fimbriae is a novel TLR4 ligand. *The Journal of Immunology* 181(10):6702-6706.

Moulin-Schouleur M, Répérant M, Laurent S, Brée A, Mignon-Grasteau S, Germon P, Rasschaert D,Schouler C (2007) Extraintestinal pathogenic *Escherichia coli* strains of avian and human origin:

link between phylogenetic relationships and common virulence patterns. *Journal of Clinical Microbiology* 45(10):3366-3376.

Mulvey MA, Schilling JD,Hultgren SJ (2001) Establishment of a persistent *Escherichia coli* reservoir during the acute phase of a bladder infection. *Infection and immunity* 69(7):4572-4579.

Münch R, Hiller K, Grote A, Scheer M, Klein J, Schobert M,Jahn D (2005) Virtual Footprint and PRODORIC: an integrative framework for regulon prediction in prokaryotes. *Bioinformatics* 21(22):4187-4189.

Mysorekar IU & Hultgren SJ (2006) Mechanisms of uropathogenic *Escherichia coli* persistence and eradication from the urinary tract. *Proceedings of the National Academy of Sciences* 103(38):14170-14175.

Nataro JP & Kaper JB (1998) Diarrheagenic *escherichia coli. Clinical microbiology reviews* 11(1):142-201.

Nataro JP, Kaper JB, Robins-Browne R, Prado V, Vial P,Levine MM (1987) Patterns of adherence of diarrheagenic *Escherichia coli* to HEp-2 cells. *The Pediatric infectious disease journal* 6(9):829-831.

Nataro JP, Seriwatana J, Fasano A, Maneval DR, Guers LD, Noriega F, Dubovsky F, Levine MM,Morris J (1995) Identification and cloning of a novel plasmid-encoded enterotoxin of enteroinvasive *Escherichia coli* and Shigella strains. *Infection and immunity* 63(12):4721-4728.

Navarro-García F, Canizalez-Roman A, Luna J, Sears C,Nataro JP (2001) Plasmid-Encoded Toxin of Enteroaggregative*Escherichia coli* is Internalized by Epithelial Cells. *Infection and immunity* 69(2):1053-1060.

Navarro-Garcia F, Gutierrez-Jimenez J, Garcia-Tovar C, Castro LA, Salazar-Gonzalez H,Cordova V (2010) Pic, an autotransporter protein secreted by different pathogens in the Enterobacteriaceae family, is a potent mucus secretagogue. *Infection and immunity* 78(10):4101-4109.

Neely MN, Pfeifer JD,Caparon M (2002) Streptococcus-zebrafish model of bacterial pathogenesis. *Infection and immunity* 70(7):3904-3914.

Nhu NTK, Phan M-D, Peters KM, Lo AW, Forde BM, Chong TM, Yin W-F, Chan K-G, Chromek M,Brauner A (2018) Discovery of New Genes Involved in Curli Production by a Uropathogenic *Escherichia coli* Strain from the Highly Virulent O45: K1: H7 Lineage. *MBio* 9(4):e01462-01418.

Nicolle LE (2003) Asymptomatic bacteriuria: when to screen and when to treat. *Infectious Disease Clinics* 17(2):367-394.

Nolan LK, Horne S, Giddings C, Foley S, Johnson T, Lynne A,Skyberg J (2003) Resistance to serum complement, iss, and virulence of avian *Escherichia coli. Veterinary research communications* 27(2):101-110.

Norton R, Macklin K,McMurtrey B (2000) The association of various isolates of *Escherichia coli* from the United States with induced cellulitis and colibacillosis in young broiler chickens. *Avian Pathology* 29(6):571-574.

Nummelin H, Merckel MC, Leo JC, Lankinen H, Skurnik M,Goldman A (2004) The Yersinia adhesin YadA collagen-binding domain structure is a novel left-handed parallel β-roll. *The EMBO journal* 23(4):701-711.

Ochiai K, Kurita-Ochiai T, Kamino Y,Ikeda T (1993) Effect of co-aggregation on the pathogenicity of oral bacteria. *Journal of Medical Microbiology* 39(3):183-190.

Ochoa TJ, Barletta F, Contreras C,Mercado E (2008) New insights into the epidemiology of enteropathogenic *Escherichia coli* infection. *Transactions of the Royal Society of Tropical Medicine and Hygiene* 102(9):852-856.

Olsen RH, Chadfield MS, Christensen JP, Scheutz F, Christensen H,Bisgaard M (2011) Clonality and virulence traits of *Escherichia coli* associated with haemorrhagic septicaemia in turkeys. *Avian Pathology* 40(6):587-595.

Pak J, Pu Y, Zhang Z-T, Hasty DL,Wu X-R (2001) Tamm-Horsfall protein binds to type 1 fimbriated *Escherichia coli* and prevents E. coli from binding to uroplakin Ia and Ib receptors. *Journal of Biological Chemistry* 276(13):9924-9930.

Parham NJ, Srinivasan U, Desvaux M, Foxman B, Marrs CF,Henderson IR (2004) PicU, a second serine protease autotransporter of uropathogenic *Escherichia coli. FEMS microbiology letters* 230(1):73-83.

Parreira V & Gyles C (2003) A novel pathogenicity island integrated adjacent to the thrW tRNA gene of avian pathogenic *Escherichia coli* encodes a vacuolating autotransporter toxin. *Infection and immunity* 71(9):5087-5096.

Patel SK, Dotson J, Allen KP,Fleckenstein JM (2004) Identification and molecular characterization of EatA, an autotransporter protein of enterotoxigenic *Escherichia coli. Infection and immunity* 72(3):1786-1794.

Pham TQ, Goluszko P, Popov V, Nowicki S,Nowicki BJ (1997) Molecular cloning and characterization of Dr-II, a nonfimbrial adhesin-I-like adhesin isolated from gestational pyelonephritis-associated *Escherichia coli* that binds to decay-accelerating factor. *Infection and immunity* 65(10):4309-4318.

Picard B, Garcia JS, Gouriou S, Duriez P, Brahimi N, Bingen E, Elion J,Denamur E (1999) The link between phylogeny and virulence in*Escherichia coli* extraintestinal infection. *Infection and immunity* 67(2):546-553.

Prasadarao NV, Wass CA, Hacker J, Jann K,Kim KS (1993) Adhesion of S-fimbriated *Escherichia coli* to brain glycolipids mediated by sfaA gene-encoded protein of S-fimbriae. *Journal of Biological Chemistry* 268(14):10356-10363.

Raffatellu M, George MD, Akiyama Y, Hornsby MJ, Nuccio S-P, Paixao TA, Butler BP, Chu H, Santos RL,Berger T (2009) Lipocalin-2 resistance of Salmonella enterica serotype Typhimurium confers an advantage during life in the inflamed intestine. *Cell host & microbe* 5(5):476.

Rasko DA, Phillips JA, Li X,Mobley HL (2001) Identification of DNA sequences from a second pathogenicity island of uropathogenic *Escherichia coli* CFT073: probes specific for uropathogenic populations. *The Journal of infectious diseases* 184(8):1041-1049.

Restieri C, Garriss G, Locas M-C,Dozois CM (2007) Autotransporter-encoding sequences are phylogenetically distributed among *Escherichia coli* clinical isolates and reference strains. *Appl. Environ. Microbiol.* 73(5):1553-1562.

Riley LW, Remis RS, Helgerson SD, McGee HB, Wells JG, Davis BR, Hebert RJ, Olcott ES, Johnson LM,Hargrett NT (1983) Hemorrhagic colitis associated with a rare *Escherichia coli* serotype. *New England Journal of Medicine* 308(12):681-685.

Rippere-Lampe KE, O'Brien AD, Conran R,Lockman HA (2001) Mutation of the gene encoding cytotoxic necrotizing factor type 1 (cnf 1) attenuates the virulence of uropathogenic *Escherichia coli*. *Infection and immunity* 69(6):3954-3964.

Robbins JB, McCracken Jr GH, Gotschlich EC, Ørskov F, Ørskov I,Hanson LA (1974) *Escherichia coli* K1 capsular polysaccharide associated with neonatal meningitis. *New England Journal of Medicine* 290(22):1216-1220.

Rodriguez-Siek KE, Giddings CW, Doetkott C, Johnson TJ, Fakhr MK,Nolan LK (2005) Comparison of *Escherichia coli* isolates implicated in human urinary tract infection and avian colibacillosis. *Microbiology* 151(6):2097-2110.

Roehrig C & Torrey S (2019) Mortality and early feeding behavior of female turkey poults during the first week of life. *Frontiers in veterinary science* 6:129.

Ruiz-Perez F, Wahid R, Faherty CS, Kolappaswamy K, Rodriguez L, Santiago A, Murphy E, Cross A, Sztein MB,Nataro JP (2011) Serine protease autotransporters from Shigella flexneri and pathogenic *Escherichia coli* target a broad range of leukocyte glycoproteins. *Proceedings of the National Academy of Sciences* 108(31):12881-12886.

Russo TA, Davidson BA, Genagon SA, Warholic NM, MacDonald U, Pawlicki PD, Beanan JM, Olson R, Holm BA,Knight III PR (2005) E. coli virulence factor hemolysin induces neutrophil apoptosis and necrosis/lysis in vitro and necrosis/lysis and lung injury in a rat pneumonia model. *American Journal of Physiology-Lung Cellular and Molecular Physiology* 289(2):L207-L216.

Russo TA, McFadden CD, Carlino-MacDonald UB, Beanan JM, Barnard TJ,Johnson JR (2002) IroN functions as a siderophore receptor and is a urovirulence factor in an extraintestinal pathogenic isolate of *Escherichia coli. Infection and immunity* 70(12):7156-7160.

Sabri M, Caza M, Proulx J, Lymberopoulos MH, Brée A, Moulin-Schouleur M, Curtiss R,Dozois CM (2008) Contribution of the SitABCD, MntH, and FeoB metal transporters to the virulence of avian pathogenic *Escherichia coli* O78 strain χ7122. *Infection and immunity* 76(2):601-611.

Sabri M, Houle S,Dozois CM (2009) Roles of the extraintestinal pathogenic *Escherichia coli* ZnuACB and ZupT zinc transporters during urinary tract infection. *Infection and immunity* 77(3):1155-1164.

Saif Y, Barnes HJ, Glisson J, Fadly A, McDougald L,Swayne D (2003) Diseases of poultry. *Diseases of poultry.* (Ed. 11).

Sarff L, McCracken Jr G, Schiffer M, Glode M,Robbins J (I. Orskov, and F. Orskov. 1975. Epidemiology of *Escherichia coli* KI in healthy and diseased newborns. *Lancet i* :1099-1104.

Savarino SJ, McVeigh A, Watson J, Cravioto A, Molina J, Echeverria P, Bhan MK, Levine MM,Fasano A (1996) Enteroaggregative *Escherichia coli* heat-stable enterotoxin is not restricted to enteroaggregative E. coli. *Journal of infectious diseases* 173(4):1019-1022.

Schembri MA, Blom J, Krogfelt KA,Klemm P (2005) Capsule and fimbria interaction in Klebsiella pneumoniae. *Infection and immunity* 73(8):4626-4633.

Schembri MA, Dalsgaard D,Klemm P (2004) Capsule shields the function of short bacterial adhesins. *Journal of bacteriology* 186(5):1249-1257.

Schmiemann G, Kniehl E, Gebhardt K, Matejczyk MM,Hummers-Pradier E (2010) The diagnosis of urinary tract infection: a systematic review. *Deutsches Ärzteblatt International* 107(21):361.

Schneeberger C, Kazemier BM,Geerlings SE (2014) Asymptomatic bacteriuria and urinary tract infections in special patient groups: women with diabetes mellitus and pregnant women. *Current opinion in infectious diseases* 27(1):108-114.

Scholes D, Hooton TM, Roberts PL, Stapleton AE, Gupta K,Stamm WE (2000) Risk factors for recurrent urinary tract infection in young women. *The Journal of infectious diseases* 182(4):1177-1182.

Schönwald S, Begovac J,Skerk V (1999) Urinary tract infections in HIV disease. *International journal of antimicrobial agents* 11(3-4):309-311.

Serapio-Palacios A & Navarro-Garcia F (2016) EspC, an autotransporter protein secreted by enteropathogenic *Escherichia coli,* causes apoptosis and necrosis through caspase and calpain activation, including direct procaspase-3 cleavage. *MBio* 7(3):e00479-00416.

Smelov V, Naber K,Johansen TEB (2016) Improved classification of urinary tract infection: future considerations. *European Urology Supplements* 15(4):71-80.

Smith YC, Rasmussen SB, Grande KK, Conran RM,O'Brien AD (2008) Hemolysin of uropathogenic *Escherichia coli* evokes extensive shedding of the uroepithelium and hemorrhage in bladder tissue within the first 24 hours after intraurethral inoculation of mice. *Infection and immunity* 76(7):2978-2990.

Song J, Bishop BL, Li G, Grady R, Stapleton A,Abraham SN (2009) TLR4-mediated expulsion of bacteria from infected bladder epithelial cells. *Proceedings of the National Academy of Sciences* 106(35):14966-14971.

Spangler BD (1992) Structure and function of cholera toxin and the related *Escherichia coli* heat-labile enterotoxin. *Microbiology and Molecular Biology Reviews* 56(4):622-647.

Spencer JD, Schwaderer AL, Becknell B, Watson J,Hains DS (2014) The innate immune response during urinary tract infection and pyelonephritis. *Pediatric Nephrology* 29(7):1139-1149.

Stein M, Kenny B, Stein MA,Finlay BB (1996) Characterization of EspC, a 110-kilodalton protein secreted by enteropathogenic *Escherichia coli* which is homologous to members of the immunoglobulin A protease-like family of secreted proteins. *Journal of bacteriology* 178(22):6546-6554.

Stojiljkovic I & Perkins-Balding D (2002) Processing of heme and heme-containing proteins by bacteria. *DNA and cell biology* 21(4):281-295.

Taddei CR, Fasano A, Ferreira AJ, Trabulsi LR,Martinez MB (2005) Secreted autotransporter toxin produced by a diffusely adhering *Escherichia coli* strain causes intestinal damage in animal model assays. *FEMS microbiology letters* 250(2):263-269.

Teng C-H, Cai M, Shin S, Xie Y, Kim K-J, Khan NA, Di Cello F,Kim KS (2005) *Escherichia coli* K1 RS218 interacts with human brain microvascular endothelial cells via type 1 fimbria bacteria in the fimbriated state. *Infection and immunity* 73(5):2923-2931.

Teng C-H, Tseng Y-T, Maruvada R, Pearce D, Xie Y, Paul-Satyaseela M,Kim KS (2010) NlpI contributes to *Escherichia coli* K1 strain RS218 interaction with human brain microvascular endothelial cells. *Infection and immunity* 78(7):3090-3096.

Thumbikat P, Waltenbaugh C, Schaeffer AJ,Klumpp DJ (2006) Antigen-specific responses accelerate bacterial clearance in the bladder. *The Journal of Immunology* 176(5):3080-3086.

Tivendale KA, Logue CM, Kariyawasam S, Jordan D, Hussein A, Li G, Wannemuehler Y,Nolan LK (2010) Avian-pathogenic *Escherichia coli* strains are similar to neonatal meningitis E. coli strains and are

able to cause meningitis in the rat model of human disease. *Infection and immunity* 78(8):3412-3419.

Torres AG, Redford P, Welch RA,Payne SM (2001) TonB-dependent systems of uropathogenic *Escherichia coli*: aerobactin and heme transport and TonB are required for virulence in the mouse. *Infection and immunity* 69(10):6179-6185.

Tóth I, Hérault F, Beutin L,Oswald E (2003) Production of cytolethal distending toxins by pathogenic *Escherichia coli* strains isolated from human and animal sources: establishment of the existence of a new cdt variant (type IV). *Journal of Clinical Microbiology* 41(9):4285-4291.

Tuttle J, Gomez T, Doyle M, Wells J, Zhao T, Tauxe R,Griffin P (1999) Lessons from a large outbreak of *Escherichia coli* O157 [ratio] H7 infections: insights into the infectious dose and method of widespread contamination of hamburger patties. *Epidemiology & Infection* 122(2):185-192.

Valdebenito M, Crumbliss AL, Winkelmann G,Hantke K (2006) Environmental factors influence the production of enterobactin, salmochelin, aerobactin, and yersiniabactin in *Escherichia coli* strain Nissle 1917. *International journal of medical microbiology* 296(8):513-520.

Valle J, Mabbett AN, Ulett GC, Toledo-Arana A, Wecker K, Totsika M, Schembri MA, Ghigo J-M,Beloin C (2008) UpaG, a new member of the trimeric autotransporter family of adhesins in uropathogenic *Escherichia coli*. *Journal of bacteriology* 190(12):4147-4161.

Van Der Sar AM, Musters RJ, Van Eeden FJ, Appelmelk BJ, Vandenbroucke-Grauls CM,Bitter W (2003) Zebrafish embryos as a model host for the real time analysis of Salmonella typhimurium infections. *Cellular microbiology* 5(9):601-611.

Vidal JE & Navarro-García F (2006) Efficient translocation of EspC into epithelial cells depends on enteropathogenic *Escherichia coli* and host cell contact. *Infection and immunity* 74(4):2293-2303.

Villaseca JM, Navarro-García F, Mendoza-Hernández G, Nataro JP, Cravioto A,Eslava C (2000) Pet toxin from enteroaggregative *Escherichia coli* produces cellular damage associated with fodrin disruption. *Infection and immunity* 68(10):5920-5927.

Vincent C, Boerlin P, Daignault D, Dozois CM, Dutil L, Galanakis C, Reid-Smith RJ, Tellier P-P, Tellis PA,Ziebell K (2010) Food reservoir for *Escherichia coli* causing urinary tract infections. *Emerging infectious diseases* 16(1):88.

Visvikis O, Boyer L, Torrino S, Doye A, Lemonnier M, Lorès P, Rolando M, Flatau G, Mettouchi A,Bouvard D (2011) *Escherichia coli* producing CNF1 toxin hijacks Tollip to trigger Rac1-dependent cell invasion. *Traffic* 12(5):579-590.

Vladoianu I-R, Chang HR,Pechère J-C (1990) Expression of host resistance to Salmonella typhi and Salmonella typhimurium: bacterial survival within macrophages of murine and human origin. *Microbial pathogenesis* 8(2):83-90.

Wang Y, Tang C, Yu X, Xia M,Yue H (2010) Distribution of serotypes and virulence-associated genes in pathogenic *Escherichia coli* isolated from ducks. *Avian Pathology* 39(4):297-302.

Wei B, Cha S-Y, Kang M, Park I-J, Moon O-K, Park C-K,Jang H-K (2013) Development and application of a multiplex PCR assay for rapid detection of 4 major bacterial pathogens in ducks. *Poultry science* 92(5):1164-1170.

Weiss A, Joerss H,Brockmeyer J (2014) Structural and functional characterization of cleavage and inactivation of human serine protease inhibitors by the bacterial SPATE protease EspPα from enterohemorrhagic E. coli. *PloS one* 9(10):e111363.

Welch RA, Burland V, Plunkett G, Redford P, Roesch P, Rasko D, Buckles E, Liou S-R, Boutin A,Hackett J (2002) Extensive mosaic structure revealed by the complete genome sequence of uropathogenic *Escherichia coli*. *Proceedings of the National Academy of Sciences* 99(26):17020-17024.

Wiles TJ, Bower JM, Redd MJ,Mulvey MA (2009) Use of zebrafish to probe the divergent virulence potentials and toxin requirements of extraintestinal pathogenic *Escherichia coli*. *PLoS pathogens* 5(12).

Wu X-R, Sun T-T,Medina JJ (1996) In vitro binding of type 1-fimbriated *Escherichia coli* to uroplakins Ia and Ib: relation to urinary tract infections. *Proceedings of the National Academy of Sciences* 93(18):9630-9635.

Wullt B, Bergsten G, Connell H, Röllano P, Gebretsadik N, Hull R,Svanborg C (2000) P fimbriae enhance the early establishment of *Escherichia coli* in the human urinary tract. *Molecular microbiology* 38(3):456-464.

Xicohtencatl-Cortes J, Saldaña Z, Deng W, Castañeda E, Freer E, Tarr PI, Finlay BB, Puente JL,Girón JA (2010) Bacterial macroscopic rope-like fibers with cytopathic and adhesive properties. *Journal of Biological Chemistry* 285(42):32336-32342.

Xie Y, Kolisnychenko V, Paul-Satyaseela M, Elliott S, Parthasarathy G, Yao Y, Plunkett III G, Blattner FR,Kim KS (2006) Identification and Characterization of *Escherichia coli* RS218–Derived Islands in the Pathogenesis of E. coli Meningitis. *The Journal of infectious diseases* 194(3):358-364.

Yang C-C & Konisky J (1984) Colicin V-treated *Escherichia coli* does not generate membrane potential. *Journal of bacteriology* 158(2):757-759.

Zalewska-Pia B, Pia R, Olszewski M,Kur J (2015) Identification of antigen Ag43 in uropathogenic Escherichia coli Dr+ strains and defining its role in the pathogenesis of urinary tract infections. *Microbiology* 161(5):1034-1049.

Zhang H, Chen X, Nolan LK, Zhang W,Li G (2019) Identification of Host Adaptation Genes in Extraintestinal Pathogenic *Escherichia coli* during Infection in Different Hosts. *Infection and immunity* 87(12).

Zhou G, Mo W-J, Sebbel P, Min G, Neubert TA, Glockshuber R, Wu X-R, Sun T-T,Kong X-P (2001) Uroplakin Ia is the urothelial receptor for uropathogenic *Escherichia coli*: evidence from in vitro FimH binding. *Journal of cell science* 114(22):4095-4103.

APPENDIX I SERUM BACTERICIDAL ASSAY

Serum resistance assay

Cultures of QT598 and its SPATEs mutant were grown to an OD_{600} of 0.6 and equal volumes (50 µL) of standardized cultures and pooled human sera were mixed and incubated for 4h at 37°C in triplicate. Viable counts were performed to estimate the number of bacterial cells before and at hourly intervals after serum treatment.

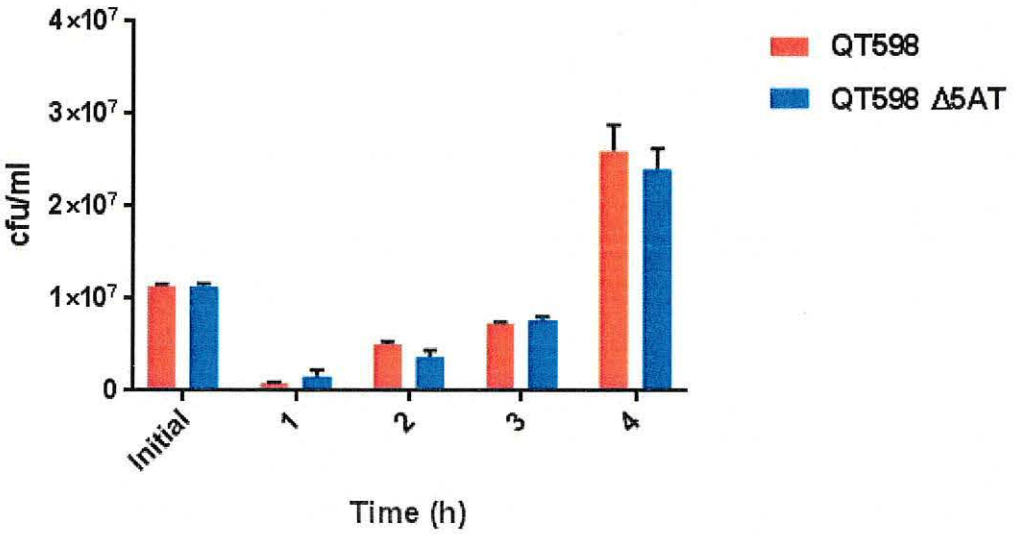

Supplement Figure I Human serum bactericidal assay

Effect of 10% human serum on survival of APEC strain QT598 and its Δ5 SPATEs mutant was determined. The serum-bacterium suspensions were incubated at 37°C for 4 h in a humidified 5% CO_2 atmosphere with an initial bacterial inoculum of approximately 10^7 CFU/ml. The counts of viable bacteria were estimated on hourly basis on MacConkey agar. Results are from a representative experiment from three independent assays. (Unpublished)

APPENDIX II CHICKEN SYSTEMIC AIR-SAC INFECTION MODEL

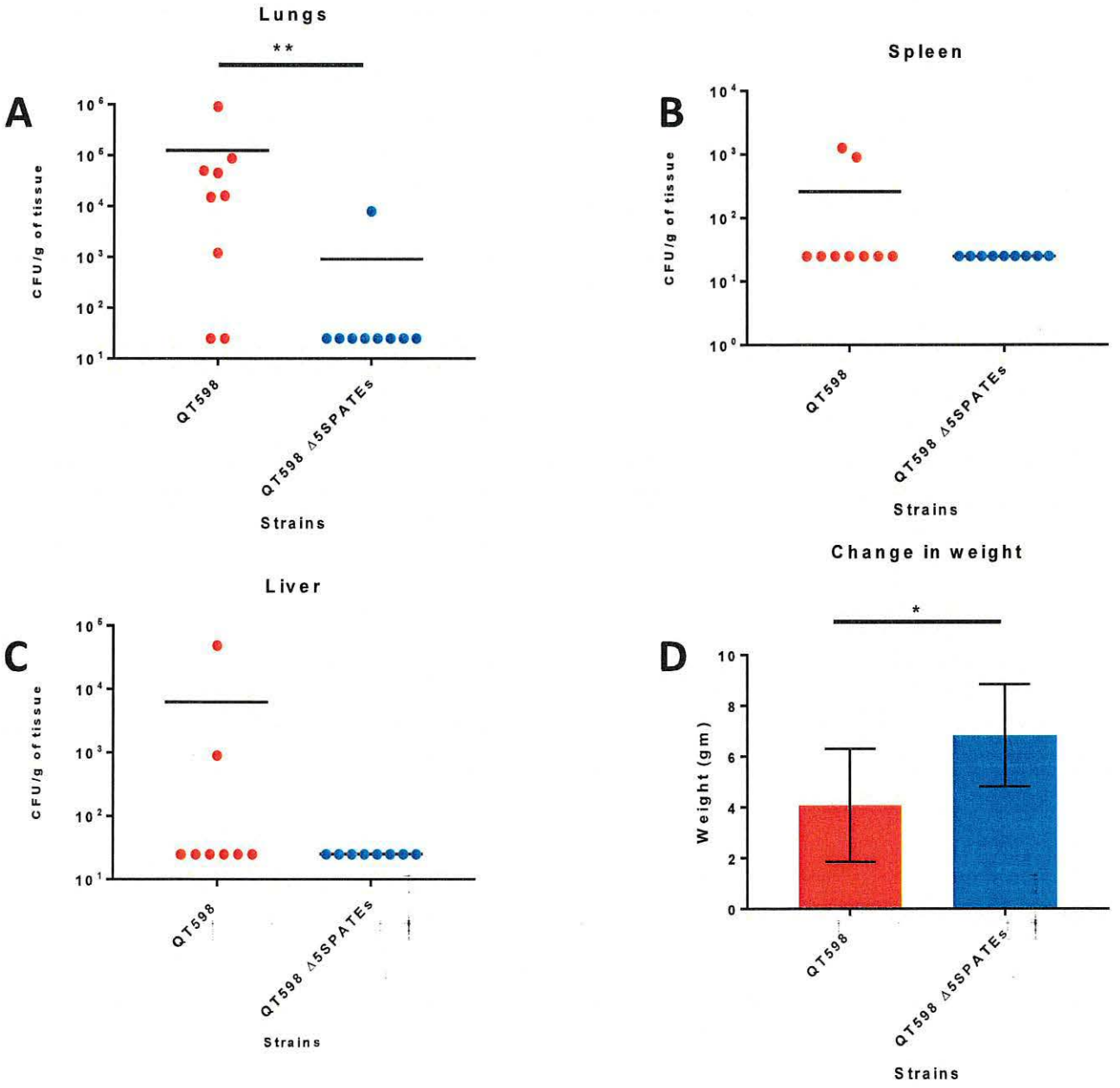

Supplement Figure II Role of the SPATEs for QT598 in the chicken sac infection model

Bacterial numbers present in the lungs (A), spleen (B), and liver (C) of the infected chickens. The bacterial counts are reported as CFU per gram of tissue. Data points represent bacterial counts from tissues isolated from different chickens (n=10) 48h post-infection. D. Weight differences between chickens before and after the infections. Represented values are means and standard deviation. (* $p < 0.05$, ** $p < 0.01$, Mann-Whitney Test). (Unpublished)

Supplement Table I Production of inflammatory lesions in air sacs and extra-respiratory organs of chickens inoculated with QT598 and its SPATEs mutant (Unpublished)

Strains	Mean Lesion Score ± SD		
	Air Sac[a]	Pericardium[b]	Liver[c]
QT598	2.5 ± 0.91	0.83 ± 0.57	0
QT598 Δ5SPATEs	1.65 ± 0.35	0	0

[a] Lesion scoring values for severity of aerosacculitis ± standard deviation: 0, normal; 1, slight edema; 2, mild diffuse thickening and neovascularization of air sacs with mild fibrinous exudate; 3, moderate fibrinous exudate; 4, severe extensive fibrinous exudate.

[b] Combined lesion scoring values for severity of pericarditis and perihepatitis ± standard deviation. Heart and pericardium: 0, normal; 1, vascularization, opacity, cloudy fluid in the pericardial cavity; 2, acute pericarditis.

[c] Combined lesion scoring values for severity of pericarditis and perihepatitis ± standard deviation. Liver: 0, normal; 1, slight amounts of fibrinous exudate; 2, marked perihepatitis.

Lesion scoring notations were used from (Mellata *et al.*, 2003).

APPENDIX III YOLKSAC INFECTION MODEL OF ZEBRAFISH

To measure the virulence potential of QT598 and its SPATEs mutant, a zebrafish yolksac local infection model was used as in (Wiles *et al.*, 2009). Briefly, 48 hpf (hours post fertilization) zebrafish embryos were infected. During the experiment each embryo was kept separately. Prior to injection, 48 hpf embryos were briefly anesthetized with 0.77 mM ethyl 3-aminobenzoate methanesulfonate salt (tricaine) (Sigma-Aldrich), and embedded in 0.8% low melt agarose (Thermo Fisher Scientific, St. Laurent, QC, Canada) without tricaine. Flaming/Brown Micropipette Puller Model P97 (Sutter Instrument, USA) was used to pull capillary tips for injections. Approximately 1 nl of bacteria (around 3000 CFU) were injected directly into the yolk sac using Narishige IM-200 microinjector stand and Eppendorf femtojet 4i microinjection pump setup.

For each experiment, average CFU introduced per injection was determined by adding 10 drops of each inoculum into 1 ml PBS, which was then serially diluted and plated on MacConkey agar plates. So, each group was inoculated with approximately 3000 CFU of each strain into the yolk sac. Embryos that were injected in the yolk sac were carefully extracted from the agar and placed individually into wells of a 96-well microtiter plate containing sterile fish water lacking both tricaine and methylene blue. Fish were scored death with the complete absence of heart rhythm and blood flow. Survival graphs include data from three or more independent experiments in which groups of 15 to 20 embryos were injected in yolksac. To quantify bacterial burden during the course of infection, embryos from each infection group were collected at 48 hpi and individually homogenized in 0.5 mL PBS. Homogenates were serially diluted and plated on Mac Conkey agar, incubated overnight at 37 °C and CFUs were counted. Both the survival trial and the quantification trial were run in biological triplicates.

Reference

Wiles TJ, Bower JM, Redd MJ,Mulvey MA (2009) Use of zebrafish to probe the divergent virulence potentials and toxin requirements of extraintestinal pathogenic *Escherichia coli. PLoS pathogens* 5(12).

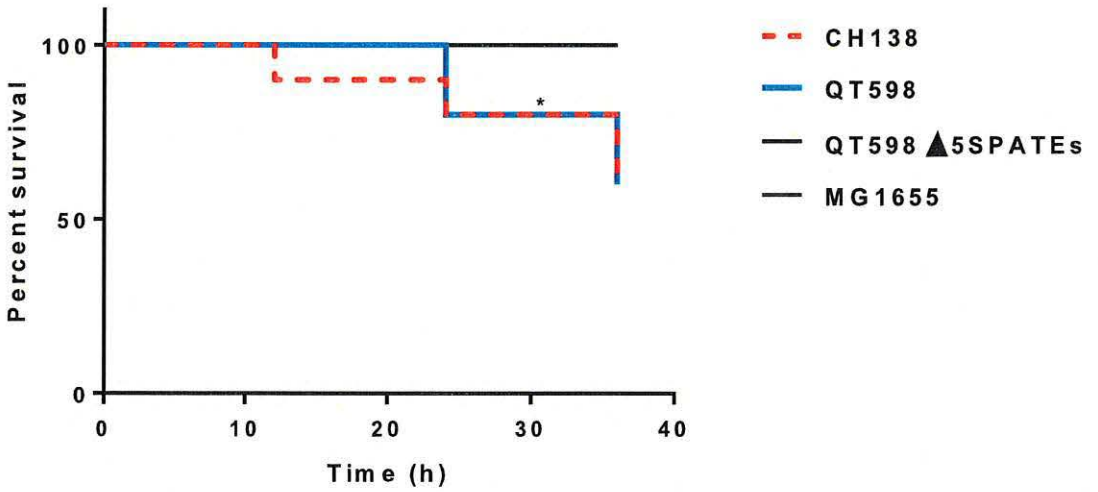

Supplement Figure III Survival curve of infected zebrafish embryos

The yolksac of 48 hpf embryos were inoculated with PBS containing CH138, QT598, QT598 ΔSPATEs and MG1655 at 3000 CFU doses. Data are presented as log-rank test for trend for survival curves, * p<0.05, n = 30 to 40 embryos pooled from 3 experiments. (Unpublished)

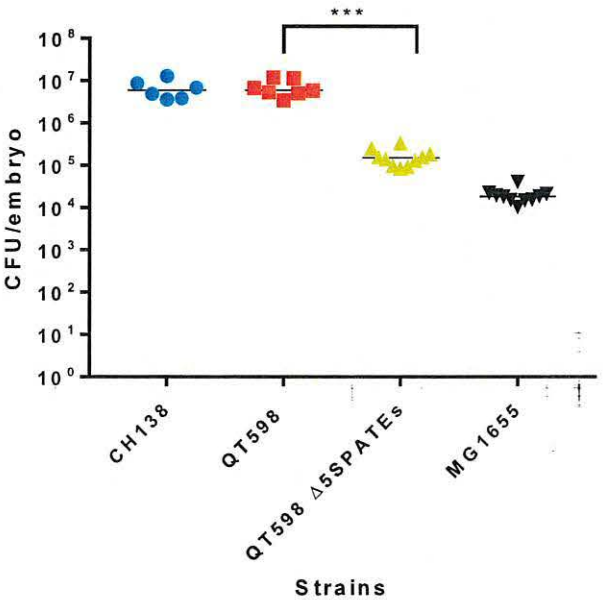

Supplement Figure IV Bacterial burdens in infected embryos

Bacteria were enumerated from embryos at 48 hpi. Bar denotes median values of the groups, n = 10 embryos per time point. Pooled from 3 independent experiments (*p < 0.001, Mann–Whitney Test) (Unpublished)**

APPENDIX IV BLADDER EPITHELIAL DAMAGE BY VAT SPATE

The vacuolating autotransporter toxin (Vat) of *Escherichia coli* causes cell cytoskeleton changes and produces non-lysosomal vacuole formation in bladder epithelial cells

Juan Manuel Díaz [1], Charles M. Dozois [2], Francisco Javier Avelar-González [3], Eduardo Hernández-Cuellar[1], Pravil Pokharel [2], Alfredo Salazar-de Santiago [1], Alma Lilián Guerrero-Barrera[1*].

[1] Laboratorio de Biología Celular y Tisular, Departamento de Morfología, Universidad Autónoma de Aguascalientes (UAA), Aguascalientes, Mexico.

[2] Institut national de recherche scientifique (INRS)-Centre Armand-Fappier Santé Biotechnologie, Laval, Quebec, Canadá.

[3] Laboratorio de Ciencias Ambientales, Departamento de Fisiología y Farmacología, Universidad Autónoma de Aguascalientes (UAA), Aguascalientes, Mexico.

*Correspondence:
Dra. Alma Lilian Guerrero Barrera. aliliammx@yahoo.com

frontiers in Cellular and Infection Microbiology

ORIGINAL RESEARCH
published: 26 June 2020
doi: 10.3389/fcimb.2020.00299

The Vacuolating Autotransporter Toxin (Vat) of *Escherichia coli* Causes Cell Cytoskeleton Changes and Produces Non-lysosomal Vacuole Formation in Bladder Epithelial Cells

Juan Manuel Díaz[1], *Charles M. Dozois*[2], *Francisco Javier Avelar-González*[3], *Eduardo Hernández-Cuellar*[1], *Pravil Pokharel*[2], *Alfredo Salazar de Santiago*[1] *and Alma Lilian Guerrero-Barrera*[1]*

[1] *Departamento de Morfología, Universidad Autónoma de Aguascalientes (UAA), Aguascalientes, Mexico,* [2] *Institut National de Recherche Scientifique (INRS)-Centre Armand-Fappier Santé Biotechnologie, Laval, QC, Canada,* [3] *Departamento de Fisiología y Farmacología, Universidad Autónoma de Aguascalientes (UAA), Aguascalientes, Mexico*

OPEN ACCESS

Edited by:
Ulrich Dobrindt,
University of Münster, Germany

Reviewed by:
Lee-Ann H. Allen,
The University of Iowa, United States
Alain L. Servin,
Institut National de la Santé et de la Recherche Médicale (INSERM), France

***Correspondence:**
Alma Lilian Guerrero-Barrera
alguerre@correo.uaa.mx

Specialty section:
This article was submitted to Bacteria and Host, a section of the journal Frontiers in Cellular and Infection Microbiology

Received: *09 November 2019*
Accepted: *19 May 2020*
Published: *26 June 2020*

Citation:
Díaz JM, Dozois CM, Avelar-González FJ, Hernández-Cuellar E, Pokharel P, de Santiago AS and Guerrero-Barrera AL (2020) The Vacuolating Autotransporter Toxin (Vat) of Escherichia coli Causes Cell Cytoskeleton Changes and Produces Non-lysosomal Vacuole Formation in Bladder Epithelial Cells. Front. Cell. Infect. Microbiol. 10:299. doi: 10.3389/fcimb.2020.00299

Urinary tract infections (UTIs) affect more than 150 million people, with a cost of over 3.5 billion dollars, each year. *Escherichia coli* is associated with 70–80% of UTIs. Uropathogenic *E. coli* (UPEC) has virulence factors including adhesins, siderophores, and toxins that damage host cells. Vacuolating autotransporter toxin (Vat) is a member of serine protease autotransporter proteins of *Enterobacteriaceae* (SPATEs) present in some uropathogenic *E. coli* (UPEC) strains. Vat has been identified in 20–36% of UPEC and is present in almost 68% of urosepsis isolates. However, the mechanism of action of Vat on host cells is not well-known. Thus, in this study the effect of Vat in a urothelium model of bladder cells was investigated. Several toxin concentrations were tested for different time periods, resulting in 15–47% of cellular damage as measured by the LDH assay. Vat induced vacuole formation on the urothelium model in a time-dependent manner. Vat treatment showed loss of the intercellular contacts on the bladder cell monolayer, observed by Scanning Electron Microscopy. This was also shown using antibodies against ZO-1 and occludin by immunofluorescence. Additionally, changes in permeability of the epithelial monolayer was demonstrated with a fluorescence-based permeability assay. Cellular damage was also evaluated by the identification of cytoskeletal changes produced by Vat. Thus, after Vat treatment, cells presented F-actin distribution changes and loss of stress fibers in comparison with control cells. Vat also modified tubulin, but it was not found to affect Arp3 distribution. In order to find the nature of the vacuoles generated by Vat, the Lysotracker deep red fluorescent dye for the detection of acidic organelles was used. Cells treated with Vat showed generation of some vacuoles without acidic content. An *ex vivo* experiment with mouse bladder exposed to Vat demonstrated

loss of integrity of the urothelium. In conclusion, Vat induced cellular damage, vacuole formation, and urothelial barrier dysregulation of bladder epithelial cells. Further studies are needed to elucidate the role of these vacuoles induced by Vat and their relationship with the pathogenesis of urinary tract infection.

Keywords: urinary tract infection, *Escherichia coli*, virulence factors, vat, cell damage, vacuoles, cytoskeleton, cell junctions

INTRODUCTION

Urinary tract infections (UTIs) are a public health problem that affects more than 150 million people, with an estimated cost of over 3.5 billion dollars each year (Flores-Mireles et al., 2015). For the development of the disease, several risk factors exist such as diabetes, vaginal infections, sexual activity, presence of a urinary catheter, neurological disease, immunosuppression, and kidney transplantation (Foxman, 2003; Nielubowicz and Mobley, 2010).

UTIs are caused mainly by bacteria, but sometimes can be provoked by yeast or other fungi. The most frequent cause of UTIs is uropathogenic *Escherichia coli* (UPEC), with a prevalence of 70 to 80% worldwide (Flores-Mireles et al., 2015; Ramírez-Castillo et al., 2018). *Escherichia coli* is typically found in the gastrointestinal tract as part of the microbiota, and certain commensal *E. coli* strains residing in the gut have the potential to cause UTIs. The difference between purely commensal *E. coli* strains and UPEC is the presence of certain virulence factors in the pathogenic strains (Terlizzi et al., 2017). UPEC has the capacity to attach, colonize and invade the urinary tract through production of several virulence factors including adhesins, siderophores, capsular polysaccharides and the production of toxins (Kaper et al., 2004; Crépin et al., 2012; López-Banda et al., 2014).

One of the virulence factors identified in some UPEC is the Vacuolating autotransporter toxin (Vat), which is a member of the serine protease autotransporter proteins of *Enterobacteriaceae* (SPATEs). The Vat toxin is a ~110 kDa secreted protein exported by the Type Va secretion system and belongs to the class II cytotoxic SPATEs (Henderson and Nataro, 2001; Dutta et al., 2002; Nichols et al., 2016). The *vat* gene has been identified in both avian pathogenic *E. coli* (APEC) and UPEC strains. It has been shown to generate the formation of vacuoles in chicken embryo fibroblasts and contribute to the development of cellulitis in chickens (Parreira and Gyles, 2003). Although the mechanism of action of Vat and its implication in the development of UTIs is not entirely known, the gene sequences encoding the toxin were detected in 36% of UPEC strains (Ramírez-Castillo et al., 2018). In a different study, the *vat* gene was found in patients with cystitis (57.9%), pyelonephritis (59.3%), prostatitis (72.4%) and septicemia (64.7%) (Parham et al., 2005; Spurbeck et al., 2012; Nichols et al., 2016). Also, our group recently published the prevalence of *vat* genes in UPEC from Guadeloupe (Habouria et al., 2019) where *vat* sequences were found in 333 isolates (48.7%) of the UTI strains. Despite the fact that Vat is one of the most prevalent SPATEs in UPEC, the mechanism of action and specific activity of this protein during urinary infection has not been determined (Welch, 2016).

The bladder epithelial cell is an *in vitro* cell culture model extensively studied because of the interaction of these cells during the pathogenesis of infection (McLellan and Hunstad, 2016). The urothelium plays a significant role as a barrier against biotic and abiotic agents, and disruption of this barrier may lead to urinary tract disease (Parsons, 2007). The characteristics of the urothelial wall are mainly imparted by the integrity of the bladder cells. Interestingly, enteroaggregative and enteropathogenic *Escherichia coli* induce epithelial cell damage that involves virulence factors such as SPATEs (Gates and Peifer, 2005; Khurana, 2006; Windoffer et al., 2011; Sanchez-Villamil et al., 2019). Thus, the objective of this study was to determine the effects of the vacuolating autotransporter toxin, Vat, from *Escherichia coli* on human epithelial bladder cells, in order to elucidate the mechanism of action of this toxin, and to serve as a basis for a more detailed study of this virulence factor, serving as a precedent of its function *in vivo*.

MATERIALS AND METHODS

Bacterial Strains and Cell Culture

The *vat* autotransporter encoding gene was amplified by PCR using specific primers (Forward: TATTGGATCCTCCGCTCTGAACCGCCACGC; Reverse: CAAGCTTCGTAATCAGATAATCGCAGC) from pathogenic *E. coli* strain QT598 (Genbank accession QDB64244.1) (Habouria et al., 2019), which with the exception of a single Arg_{534} to His_{534} substitution is identical to Vat (c0393) from UPEC strain CFT073. PCR products contained 15 bp extensions homologous to the pUCmT multi-cloning site. Linearized pUCmT digested with *Xho*I and *BamHI* was used to clone inserts by fusion reaction with the Quick-fusion cloning kit (Biotool, #B2261). The plasmid clones were transformed into *E. coli* DH5α then into *E. coli* BL21 for protein production (Habouria et al., 2019). The model to test the cytotoxicity of Vat was performed with human urinary bladder epithelial cell line ATCC 5637 (American Type Culture Collection HTB-9). The cells were maintained in RPMI 1640 (Sigma-Aldrich, #R7509) supplemented with 10% heat-inactivated fetal calf serum (Invitrogen, #16000044) without antibiotics.

Vat Production and Concentration

Escherichia coli BL21 (pUCmT::*vat*) was grown in 200 ml of Lennox Broth (LB) medium with ampicillin (100 μg/ml) overnight (37°C/100 rpm). The culture was centrifuged (2,370 × g for 10 min at 4°C) and the supernatant filtered through a 0.22 μm membrane filter (Corning Inc, # R7509) (Salvadori et al., 2001). The protein from the sterile supernatant was

concentrated through a 50 kDa centrifugal filter unit (Millipore, #UFC905024) by centrifugation (2,370 × g for 10 min at 4°C). Quantification of the protein was determined by Bradford assay, and the absorbance was measured at 595 nm, using a microplate reader (Bio-Rad, #028007). To determine the concentration of the protein the measurements were overlapped with a standard linear curve. The protein was visualized using Coomassie blue staining (**Figure 1**) after separation by sodium dodecyl sulfate-polyacrylamide gel electrophoresis (SDS-PAGE) (Dutta et al., 2002).

Cytotoxic Effect of Vat Toxin Measured by Lactate Dehydrogenase Release Assay

Confluent cultures of the 5637 cell line were grown in 96-well plates and were treated with different Vat concentrations from the concentrated supernatant sample (5, 25, 50, 75, 100 μg/ml) in a final volume of 100 μl of RPMI per well, and incubated at different times (3, 6, 12, and 24 h) (Dutta et al., 2002). Parreira and Gyles, 2003). The culture supernatant from *E. coli* BL21 containing the empty vector (pUCmT) was added volume/volume as a negative control to compare to bladder cells exposed to Vat supernatant. Cell damage was determined by lactate dehydrogenase (LDH) release using the LDH-Cytotoxicity Assay Kit II (Biovision, #K313) according to the manufacturer's instructions; the absorbance was measured at an optical density of 495 nm using a microplate reader (Fanizza et al., 2009). The background control (RPMI 1640-medium only) and the lysis control (treatment with Triton X-100) (Sigma, #T8787) were used (Peidaee et al., 2013). All the samples were tested by triplicate ($n = 3$). The results were obtained and analyzed statistically using Dunnett's multiple comparisons tests.

Evaluation of Vacuole Formation in Bladder Cells Following Exposure to Vat

The concentrated supernatant of the toxin was tested to determine the effect on bladder cells *in vitro* as reported previously for the effect of Vat on chicken fibroblast cell culture (Parreira and Gyles, 2003). The 5637-bladder cell line was grown in 8-well Lab-Tek chambers (Nunc, #Z734853) until ~60% confluence. The monolayers were exposed to 50 μg/ml of the Vat toxin per well with a total volume of 300 μl RPMI 1640 and incubated for 0.5, 1, 3, 6, and 12 h at 37°C with 5% CO_2 (Greune et al., 2009; Habouria et al., 2019). After incubation, the cells were washed three times with PBS and stained with Giemsa dye (Hu et al., 2015). Vacuole formation was observed by optical microscope (Zeiss, Primo star). A random semiquantitative analysis of the images of the vacuolated cells per well was done, and the results were statistically analyzed using a one-way ANOVA multiple comparisons test.

Evaluation of Changes on Epithelial Bladder Cell Junctions Induced by Vat

Cultures of bladder cells were grown in 8-well Lab-Tek II chamber slides until reaching 100% confluence. The cultures were exposed to 50 μg/ml of Vat for 6 h, 12 h and 24 h; supernatant from a clone containing the empty vector was used as a negative control. The integrity of the urothelial monolayer was observed by Scanning Electron Microscopy. After exposure to Vat for different time points, samples were fixed with 2.5% Glutaraldehyde for 24 h, after that, the samples were dehydrated using increasing concentrations of ethanol (60, 70, 80, 90, 96, and 100%), incubating for 10 min in each step. At the end, the samples were dried at 37°C/5% CO_2 for 12 h (Nordestgaard and Rostgaard, 1985). The slide was covered with 100 Å of gold, using Denton Vacuum Desk II. Images were obtained and analyzed under JEOL JSM 5900LV, Scanning Electron Microscope.

The cell-cell distribution of ZO-1 and Occludin, tight junction molecules, were analyzed by immunofluorescence, using the same toxin exposition protocol as described above. Epithelial cells were fixed with 3.7% formaldehyde. After washing with PBS, the cells were permeabilized with 0.1% Triton X-100 for 5 min and then incubated with blocking solution, PBS / 5% BSA for 30 min. To label ZO-1 and Occludin, it was used a primary antibody Anti-ZO-1 (Abcam, #ab221547) and Anti-Occludin (Abcam, #ab216327) respectively, incubating for 2 h at 37°C. Secondary antibody anti-rabbit conjugated with Alexa fluor 488 for ZO-1 (Sigma-Aldrich, #SAB4600387) and Alexa fluor 594 (ThermoFisher, #A-11012) for Occludin. The samples were incubated for 2 h at 37°C. Then, samples were mounted with ProLong Gold (Invitrogen, # P36930) antifade reagent (Bercier et al., 2018). Images were obtained using a confocal microscope (Zeiss, LSM700) with Zen Black software (2012).

Fluorescence-Based Permeability Assay

Permeability changes following exposure of the bladder cell monolayer with Vat, were evaluated by a paracellular permeability assay using FITC-Dextran 4 (FD4) (Sigma-Aldrich, #60842-46-8) according to the method of Bercier et al. (2018). Briefly, 5637 Bladder cells were seeded and incubated until 100% confluence on Transwell polyester membrane cell culture inserts (Sigma-Aldrich, #CLS3472). The Basolateral space was filled with 300 μl PBS at the start the experiment. The apical chamber was filled with 300 μl of RPMI containing 50 μl/ml of Vat and 1 mg/ml of FD-4. The control was established using the empty vector supernatant in the same amount of cell media and FD4. The permeability measurement was made at 6, 12, and 24 h using a FP-8000 Series Fluorometer. The numeric results were interpreted as Relative Fluorescent Units (Bercier et al., 2018). All the experiments were performed by triplicate and the data analyzed statistically using two-way ANOVA comparisons tests.

Evaluation of Cell Damage and Cytoskeletal Changes Caused by Exposure to Vat

The F-actin, α-tubulin and Arp3 protein distribution changes produced following Vat treatment were evaluated using bladder cell cultures. Cell monolayers were cultured in 8-well Lab-Tek chambers until 60% confluency was reached and cells were then incubated with 50 μg of the Vat protein for 6 h; as a control to rule out a possible LPS effect on samples, cells were incubated with the toxin simultaneously with 50 μg/ml of polymyxin B

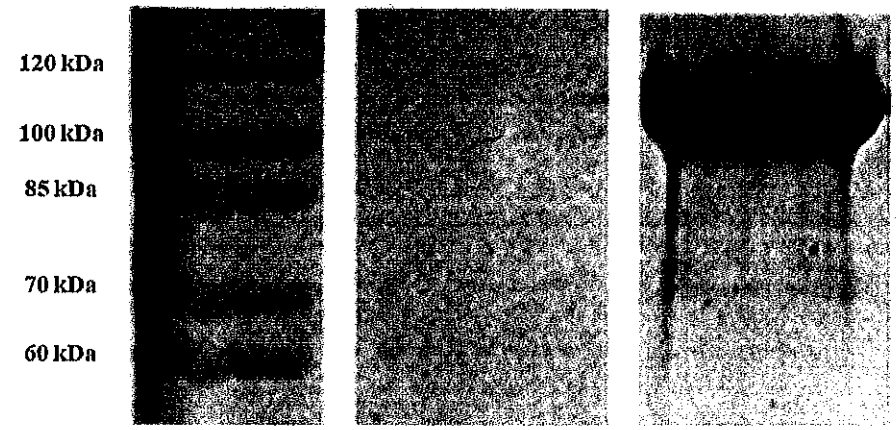

FIGURE 1 | Overexpression of Vat protein detected by SDS-PAGE. The filtered supernatants from overnight cultures of *E. coli* BL21 (pUCmT::vat) and *E. coli* BL21 empty vector were concentrated by Amicon filter units and the protein from the supernatant was migrated next to a protein marker (10–200 kDa). The gel was stained with Coomassie Blue.

(InvivoGen, #1405-20-5) (Tsuzuki et al., 2001; Lu et al., 2017). Cells incubated with 50 μg/ml of heat-inactivated Vat at 95°C for 20 min provided another control (Salvadori et al., 2001; Simon et al., 2018). After incubation, the cells were washed three times with PBS and were fixed.

F-Actin labeling was done by permeabilizing the samples and incubating with Alexa Fluor 488 phalloidin (Invitrogen, #A12379) at 37°C, during 60 min (Guerrero-Barrera et al., 1996). To observe the effect on α-tubulin after Vat incubation, samples were permeabilized and blocked as described above. To label tubulin in cells, anti-α-Tubulin (Sigma, #T5168) at 10 μg/ml was used as the primary antibody and incubated for 2 h at 37°C. This was followed by incubation with a secondary antibody conjugated with Alexa fluor 488 for 2 h at 37°C. The samples were mounted (Invitrogen, # P36930) and images were obtained by confocal microscope.

Labeling of Acidic Organelles in Bladder Cells After Exposure to Vat

Samples were processed for fluorescence detection of acidic organelles with Lysotracker Deep Red staining (Thermo Fisher, # L12492) (Chen et al., 2015; Magryś et al., 2018). Bladder cells plated on 8-well glass slides were treated with 50 μg/ml of Vat for 6 h. After incubation, cells were washed three time with PBS and were exposed to 300 μl of RPMI added with Lysotracker Deep Red reagent at 10 nM. After 1 h of incubation at 37°C, samples were washed and mounted with Prolong Gold prior to analysis by confocal microscopy (Nagahama et al., 2011).

Ex vivo Culture of Murine Urinary Bladder Exposed to Vat

The animal protocol for this study was approved by the animal ethics committee of the Autonomous University of Aguascalientes, México in accordance with the NIH ethical program. Eight BALB/c female mice were sedated and euthanized to obtain by midline laparotomy urinary bladders. The procedure was developed under sterile conditions (Durnin et al., 2018; Gabella, 2019). In 12-well plates (Corning, #3513) the bladders were placed in RPMI 1640 supplemented with 100 μg/mL streptomycin, 100 U/mL penicillin, 50 mg/L gentamicin. The tissues were exposed to 25, 50, and 100 μg of Vat toxin and incubated for 24 or 48 h at 37°C in 5% CO_2. The control tissue was incubated for 48 h with supernatant from a clone containing the empty vector. Another control used was simply RPMI 1640 medium for 48 h in order to observe possible changes in the tissue during the cell culture time period (Kannan and Baseman, 2006). Formalin-fixed bladders were dehydrated and cleared automatically with a Histokinette (Leica, #TP1020). Next, the tissues were embedded in paraffin and 5 μm thick sections were obtained (Kim et al., 2010; Najafzadeh et al., 2011). Tissues were stained with hematoxylin and eosin (Prophet et al., 1995) and observed under an optical microscope with a 40X objective (Zeiss, Primo star).

Statistical Methods

GraphPad Prism 8.0 was the software used to evaluate the quantitative data in this study. Dunnett's multiple comparisons tests were used to analyze the presence of statistically significant differences ($P \leq 0.05$) between the cells exposed to empty vector supernatant or following exposure to different concentrations of Vat for the LDH release assay. One-way ANOVA, and the multiple comparisons test was used to evaluate the quantity of vacuolated cells per field generated depending on the exposure time to Vat. Two-way ANOVA was used for statistical comparisons of samples from the fluorescence-based cell permeability assay.

RESULTS

Cytotoxic Effect of Vat Toxin Measured by Lactate Dehydrogenase Release Assay

LDH release from cells to the extracellular media is considered an indicator of cell membrane integrity damage (Fanizza et al., 2009; Radin et al., 2011). Vat treatment of bladder cells with different toxin concentrations (5, 25, 50, 75, 100 μg/ml) at different times (3, 6, 12, and 24 h) showed statistically significant differences in comparison with the *E. coli* empty vector supernatant treatment ($P \leq 0.05$) (**Figure 2**). LDH released to the media was dependent on the time of exposure and concentration of Vat.

Vacuole Formation in Bladder Cells Exposed to Vat

The bladder cells exposed to Vat during 6 h showed vacuole formation that increased in numbers with the time of exposition (**Figure 3A**). There were no vacuoles observed following exposure to toxin for 0.5 or 1 h. Statistically significant vacuole production (**Supplementary Image 1**) was found after 3 h of exposure to the toxin (**Figure 3B**).

Evaluation of Changes to Epithelial Cell Junctions Following Exposure to Vat

Scanning Electronic Microscopy analysis of the bladder cell monolayer, showed increased spacing between cells when it was exposed to Vat, as well as changes in cell morphology (**Figure 4**). After 6 h of treatment, these spaces appeared in the monolayer when compared to the control cells. This damage increased with time of exposure and resembled alterations between cell-cell junctions. In order to characterize cellular alterations due to Vat, the localization of two important tight junction molecules, ZO-1 and Occludin, were evaluated. Vat induced discontinuities in the pattern of distribution of both ZO-1 and Occludin in bladder epithelial cells following 12 and 24 h of treatment (**Figure 4**).

Fluorescence-Based Permeability Assay for Epithelial Bladder Monolayer Cell Culture Treated With Vat Toxin

Changes in monolayer integrity were confirmed by the permeability assay. The quantification of FD4 fluorescence in the supernatants of basolateral transwell chambers showed a significative difference in permeability at 12 and 24 h of toxin exposure with respect to the control (**Figure 5**). The fluorescence increased by ~2-fold from 12 to 24 h of exposure.

Evaluation of Cell Damage Induced by Vat Through Cytoskeletal Changes

Bladder cell cultures exposed to Vat were analyzed for alterations of the cytoskeleton components actin and tubulin by confocal microscopy. After 6 h of exposure to Vat toxin, cells labeled with phalloidin, revealed changes in F-actin distribution with a diffuse pattern (**Figure 6B**) resulting in round cell shape, loss of integrity of stress fibers, and disruption of cell-cell interactions. In the control cells treated with the empty vector supernatant, the F-actin cytoskeleton was intact with well-defined stress fibers distributed along with the cytoplasm (**Figure 6A**). In control cells, tubulin showed mainly a peripheral distribution and a normal cell shape (**Figure 6C**). When cells were treated with Vat toxin, this pattern changed, and tubulin was more diffuse at the cell surface, and correlated with the altered morphology of the cells (**Figure 6D**). Toxin activity was validated using control samples, testing the cells with heat-inactivated toxin and by the addition of polymyxin B to inhibit any potential cellular changes that might be caused by traces of LPS present in the culture supernatants (**Supplementary Image 2**).

Labeling of Acidic Organelles After Exposure to Vat

Acidic organelles were found using Lysotracker Deep Red. **Figure 7** shows cells after 12 h of Vat treatment (**Figure 7B**),

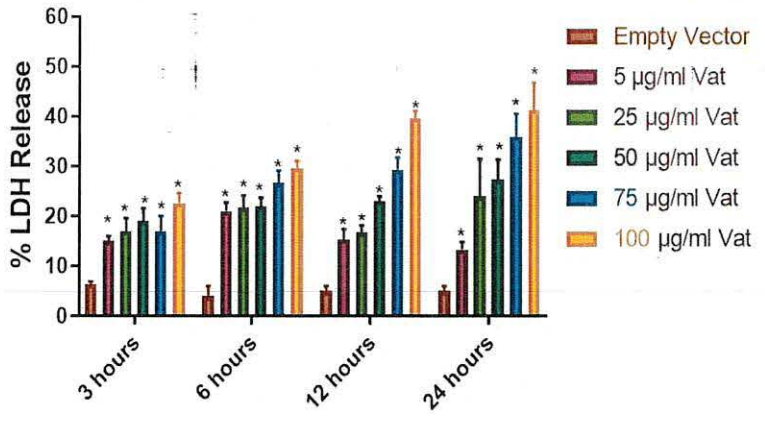

FIGURE 2 | Cellular damage provoked by Vat toxin measured by LDH release. Cells from human urinary bladder cell line 5,637 were exposed during 3, 6, 12, and 24 h to 5, 25, 50, 75, and 100 μg/ml of Vat toxin. As a control supernatant from the empty vector was used. After incubation, LDH in the cell culture supernatant was measured. All toxin concentrations showed statistically significant differences compared to the control in a dose- and time-dependent manner. The percentage of cell damage after toxin exposure resulted in 15 to 47% LDH release (*$p \leq 0.05$, two-way ANOVA, Dunnett's test).

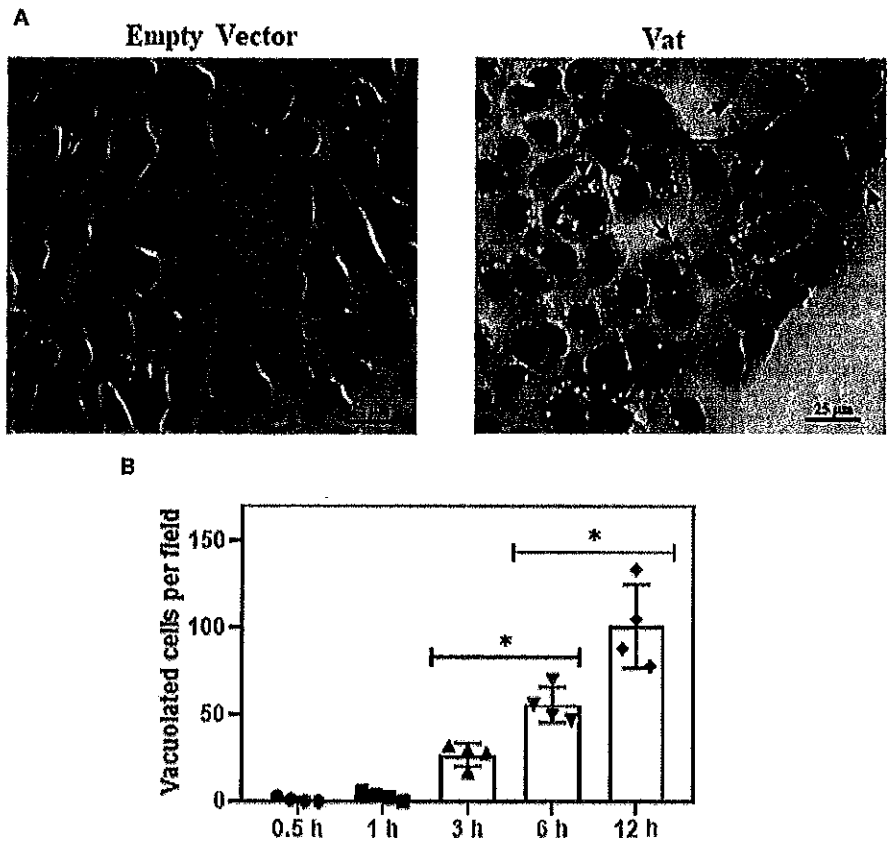

FIGURE 3 | Effect of Vat in human urinary bladder cells 5637 at different time of exposition **(A)** Control cells exposed to empty vector for 6 h, showing normal cell shape and distribution on the monolayer. The cells incubated for 6 h with 50 µg/ml of Vat toxin, exhibit cytoplasmic vacuole formation (black arrows). **(B)** Plotted results of the vacuole formation showed a significative difference between 3 to 6 h and 6 to 12 h. (*$p \leq 0.05$, ANOVA, Dunnett's).

with the distribution of acidic organelles. A merged image combining bright field and fluorescence (**Figure 7C**) identifies cells containing multiple vacuoles that are not fluorescent (white arrows), whereas acidic organelles are shown with black arrows. **Supplementary Image 3** shows that acidic organelles are also produced by control cells. By contrast the vacuoles produced by Vat are not labeled with Lysotracker.

Ex vivo Culture of Murine Urinary Bladder Tissue Exposed to Vat

Bladder tissues exposed to different concentrations of Vat for 24 and 48 h showed partial cell desquamation of the urothelial cells (Black arrow) in comparison with the controls. This effect was dependent on toxin concentration (**Figure 8**). With 25 µg/ml of toxin at 24 h (**Figure 7C**), the most superficial urothelial cells showed exfoliation from the underlying tissue. Treatment with 50 µg/ml of Vat for 24 h (**Figure 8D**) caused extended changes in epithelial cell integrity, affecting deeper stratum. Higher concentrations of Vat resulted in a thinner urothelium in comparison with other samples, this suggests that Vat caused a loss of normal integrity of the epithelial cell barrier. Also, Vat treatment showed an alteration of the urinary bladder lamina propria. After 48 h of incubation with 25 µg/ml of Vat, the transitional epithelium was absent and the lamina propria was loose and disorganized (**Figure 8F**). Treatment with 50 µg/ml of toxin increased damage to the lamina propria, resulting in loss of the normal bladder structure (**Figure 8G**). Similar results were observed with 100 µg/ml of Vat at 48 h (**Figure 8H**). Tissue changes were compared with bladder exposed to supernatant from bacteria containing only the empty vector or only with RPMI 1640 cell culture medium for 48 h in order to validate the *ex vivo* experiments and the action of Vat toxin on tissues (**Figures 8A,B**).

Discussion

Exposure of bladder cells to the Vacuolating autotransporter toxin caused vacuole formation, and these changes resembled cytological changes observed previously in avian cell models (Parreira and Gyles, 2003; Nichols et al., 2016). Also, cell rounding of the bladder cells and the alteration in cell-cell contact could result in the loss of integrity of the urothelial barrier. This epithelial disruption has also been observed with another vacuolating toxin, VacA, from *Helicobacter pylori* (Tombola et al., 1999; de Bernard et al., 2004; Bercier et al., 2018).

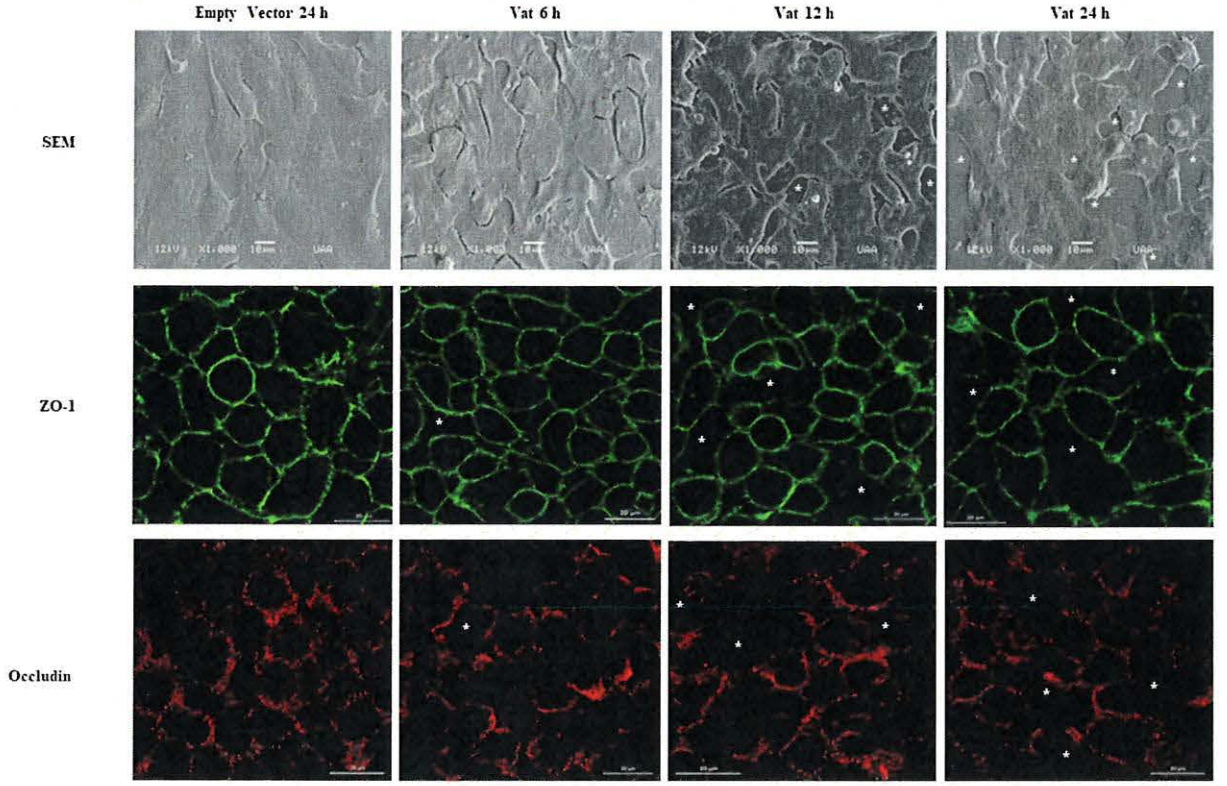

FIGURE 4 | Modification of cell junctions of the bladder urothelial monolayer after incubation with Vat. Analysis by scanning electron microscopy revealed loss of integrity of the cell monolayer (White asterisks) starting at 6 h. The changes in the monolayer are more visible at 12 and 24 h after exposure to the toxin in comparison to the control. The immunofluorescence labeling of ZO-1 and Occludin proteins show cell junction disruption in the cell monolayer.

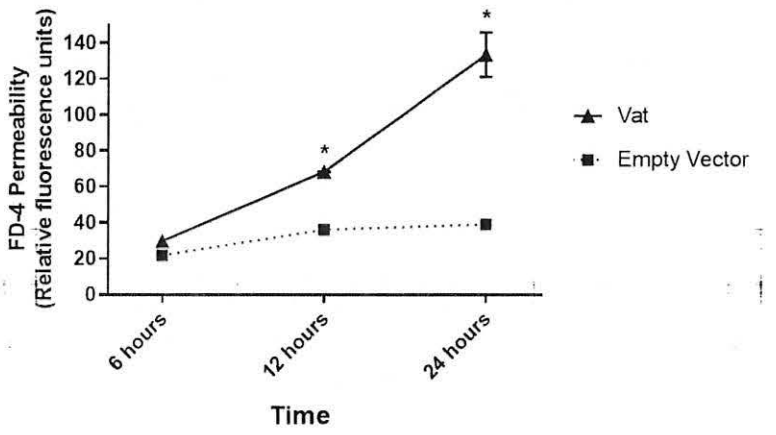

FIGURE 5 | Fluorescence-based permeability assay of a bladder epithelial cell monolayer treated with Vat toxin. The quantitative method showed changes in the permeability of the monolayer exposed to the toxin. Comparison between the Vat toxin and the empty vector control supernatant had statistically significant differences at 6 and 12 h of incubation (*$p \leq 0.05$, two-way ANOVA).

Lactate Dehydrogenase (LDH) is a cytoplasmic enzyme that is released into the extracellular medium when cell membrane integrity is compromised. Time of exposure and dose effect on cytotoxic activity of Vat was assessed by LDH release and suggests that a high concentration and exposure time of at least 6 h was required to achieve a high level (>50%) of cytotoxicity for bladder cells *in vitro*. These results in comparison to other bacterial toxins from *Escherichia coli*, *Helicobacter pylori* and *Clostridioides difficile* toxin (Grossmann et al., 2000; Roberts et al., 2001; Radin et al., 2011), suggest that Vat likely plays a subtle role in the pathogenesis of UTIs (Roberts et al., 2001; Peterson et al., 2009).

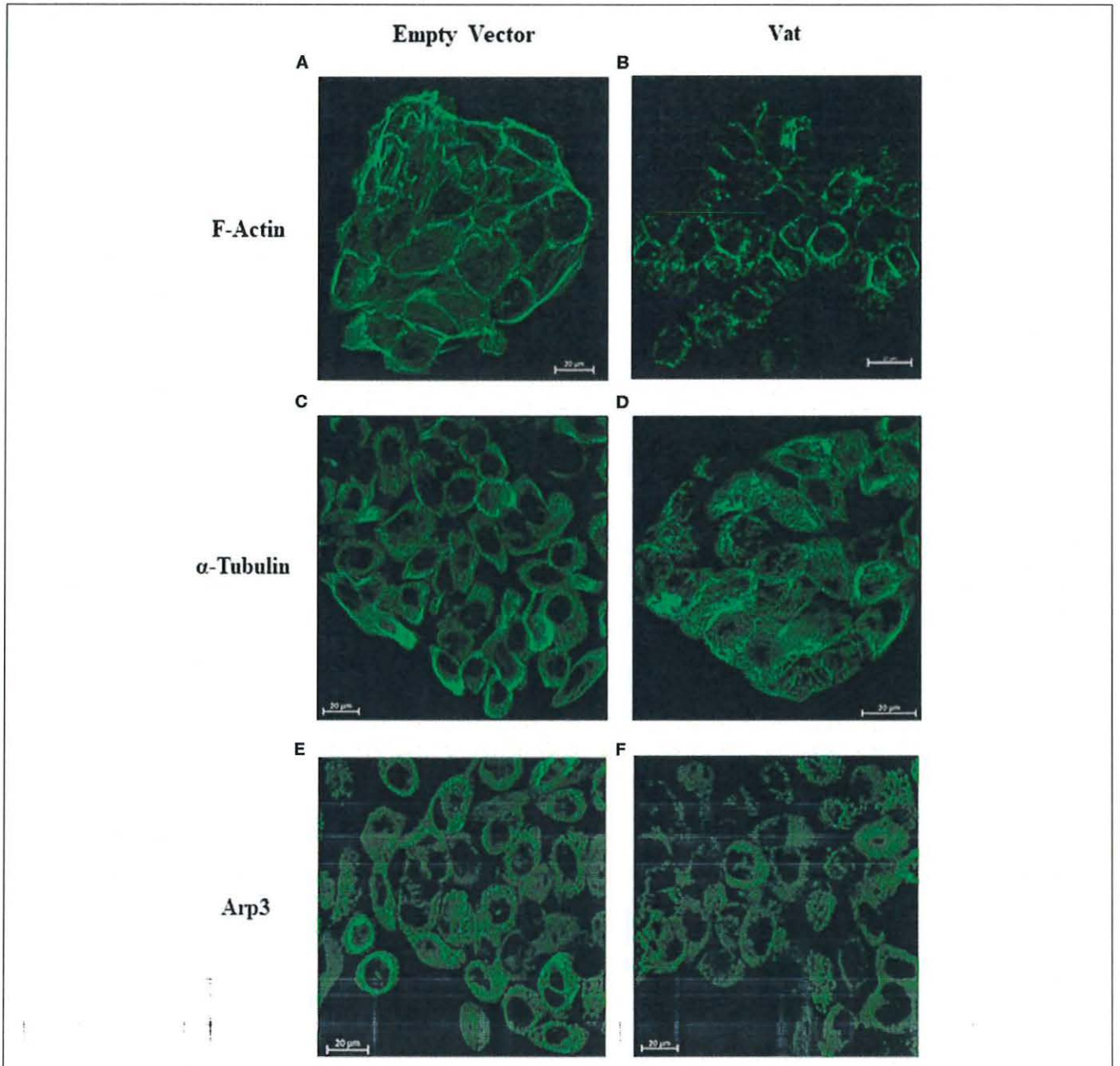

FIGURE 6 | Changes in the distribution of F-actin, α-Tubulin, and Arp3 cytoskeletal proteins detected after Vat treatment of bladder cells observed by confocal microscopy. The negative control cells **(A)** showed a normal distribution of actin stress fibers with a normal cell shape and appearance. After exposure to Vat **(B)** the cells acquired a rounded shape with loss of the cytoplasmic actin stress fibers. Normal tubulin distribution was observed in the control cells **(C)** with its presence throughout the cell. Once cells were exposed to Vat **(D)** the distribution of tubulin was altered. Arp3 demonstrated a cytoplasmic dotted distribution **(E)** on the untreated cells, and there was no evident change in Arp3 distribution when cells were treated with Vat **(F)**.

Cell damage can also be evaluated through cytoskeletal changes such as distribution of F-actin and tubulin that have an effect on cell morphology and cell-cell association. Alfaro-Aco and Petry (2015) have proposed that actin and tubulin cytoskeleton components play a critical role in cytoprotection, intercellular junction maintenance, shape definition and intracellular vesicular transport (Tang et al., 2014; Gefen and Weihs, 2015; Tran and Ten Hagen, 2017). Damage to these cytoskeletal components, as observed after the exposure to Vat, affects the normal cell distribution and morphology *in vitro*. The alteration and redistribution of F-actin and α-tubulin in the cytoskeleton correlated with the morphological changes in cells, a decrease in monolayer integrity and the desquamation of cells from the substrate, a phenomenon similar to what occurs

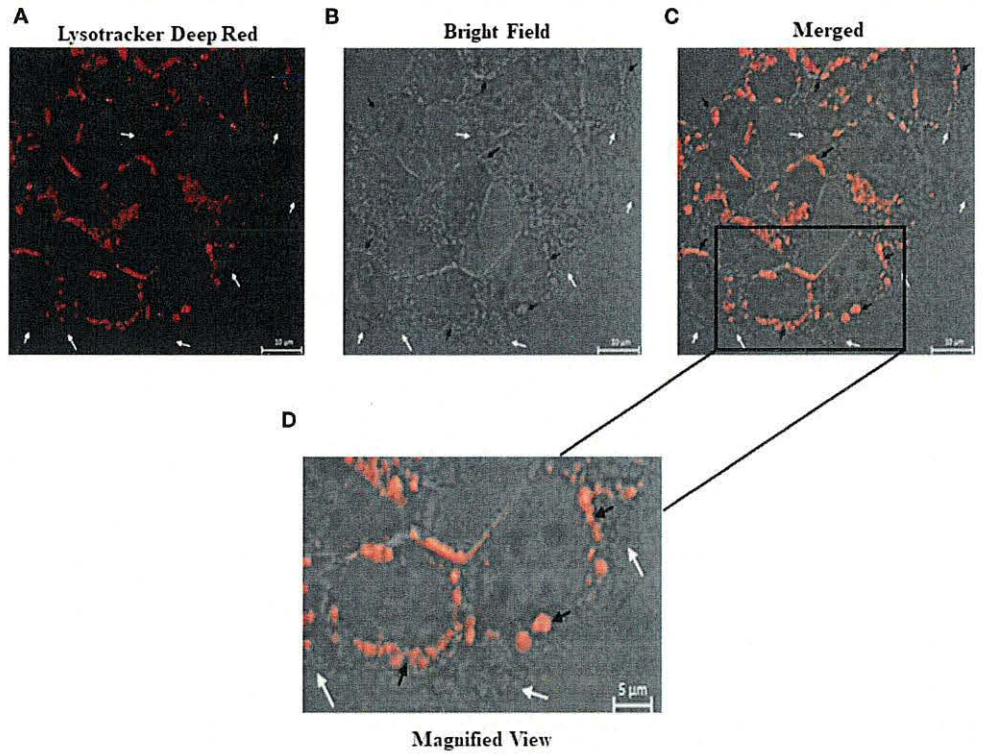

FIGURE 7 | Characterization of the vacuoles produced in bladder epithelial cells after treatment with Vat. After 12 h of Vat exposure, samples were labeled with Lysotracker deep red to identify acidic organelles **(A–C)**. The vacuoles that incorporated Lysotracker reagent (Black arrows) show a red color. Some other vacuoles were identified in the samples which did not have an acidic content (White arrows) **(C,D)**.

following exposure of cells to other SPATEs (Dautin, 2010; Liévin-Le Moal et al., 2011; Glotfelty et al., 2014; Gasic and Mitchison, 2019).

Vacuole formation within mammalian cells affects cell homeostasis. A variety of secreted bacterial toxins can induce vacuole production in cells with different functions in its pathogenesis in the host (Lee et al., 2015; Shubin et al., 2016; Magryś et al., 2018). In order to determine the nature of the vacuoles generated by the Vat toxin, the presence of acidic organelles was determined in bladder cells. The results obtained in this study by the overlaying of fluorescence confocal microscopy and bright field image, reveals acidic content in some vacuoles generated by Vat as well as others vacuoles with non-acidic characteristics inside of them (Nagahama et al., 2011; Chen et al., 2015). The non-lysosomal nature of some vacuoles in bladder cells treated with Vat is of interest and merits further investigation (Appelqvist et al., 2013; Ram and Ramakrishna, 2014; Shubin et al., 2016).

Finally, our *ex vivo* experiment suggests that Vat can induce detachment of epithelial cells comprising the urothelium of the bladder, possibly as a direct effect of the toxin on the adhesion molecules of the cell surface or due to an indirect effect caused by changes in the morphology of the cells as a consequence of alterations to the cytoskeleton. Further, the lamina propia underlying the urothelium of the bladder was affected by Vat at the highest concentration. This suggests that some connective tissue molecules may be targeted by the toxin. Proteolytic activity of Vat has been shown to exhibit an elastase-like activity (Habouria et al., 2019). This result is in agreement with our *in vitro* experiments in which we observed the loss of intercellular contacts of cells from the monolayer and in its integrity showed with the permeability assay.

In conclusion, the effect of the vacuolating autotransporter toxin from *Escherichia coli* was investigated by using a bladder epithelial cell model. Cytotoxicity of Vat was dose-dependent and suggested that Vat most likely acts as a cytopathic toxin that alters bladder cell function with a limited degree of cell death. Vat caused vacuole formation on bladder cells similar to the cytopathic effects that were previously reported following exposure of avian cells to *E. coli* culture supernatants containing Vat. Also, the Vat toxin caused alterations on cell junctions, affecting monolayer integrity, causing redistribution of tight junction proteins and increasing urothelial cell permeability. Furthermore, redistribution of actin and tubulin in bladder epithelial cells occurred simultaneously with morphological changes on cells. In addition, our results suggest that some vacuoles on epithelial cells induced by Vat have not acidic content. Finally, our *ex vivo* experiments on murine bladder demonstrated that Vat caused alterations of the urothelium and lamina propria of the bladder. It will be of future interest to

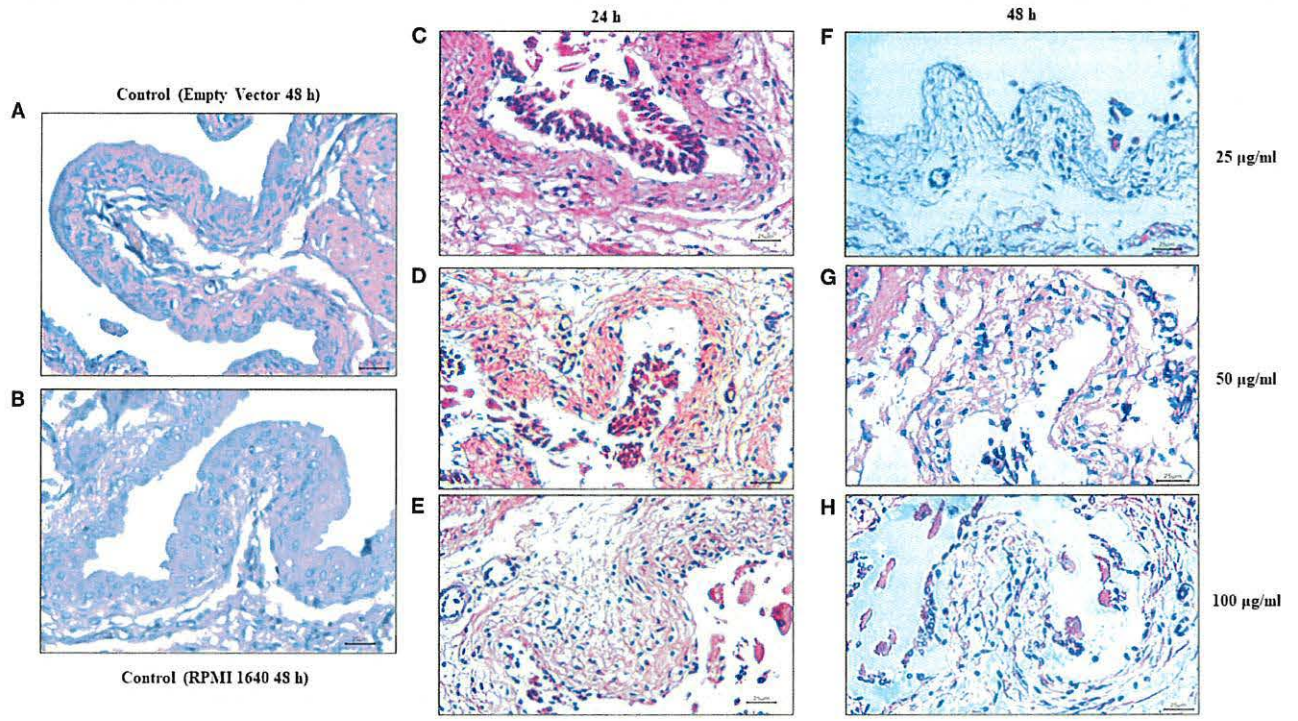

FIGURE 8 | Effect of Vat on urinary bladder tissues. Mouse urinary bladders were incubated *ex vivo* with 25, 50, and 100 µg/ml of Vat toxin supernatant for 24 h or for 48 h. After 24 h of Vat treatment **(C–E)**, detachment of the urothelium from the underlying connective tissue was observed (Black arrows). This effect was dependent on the toxin concentration. After 48 h of incubation, alterations in the lamina propria (Black asterisk) were visible on bladder samples with a loose and disorganized connective tissue **(F–H)**. Those changes were compared with bladders exposed to the empty vector supernatant and the control containing only RPMI 1640 medium **(A,B)**.

investigate whether Vat targets an adhesion molecule on the epithelial cell surface or a specific component of the lamina propria. As well, characterization of the composition of the vacuoles induced by Vat may provide further evidence of how this toxin contributes to the pathogenesis of UTIs caused by UPEC.

DATA AVAILABILITY STATEMENT

All datasets generated for this study are included in the article/**Supplementary Material**.

ETHICS STATEMENT

This study was reviewed and approved by the ethics committee for the use of animals in the teaching and research of The Autonomous University of Aguascalientes.

AUTHOR CONTRIBUTIONS

JD was the primary author of the manuscript. CD and PP contributed to optimization of protein production and revision of the manuscript. FA-G provided expertise in statistical analysis. EH-C advised for the planning and design of some experiments. AS contributed to the development of experimental work. AG-B proposed the line of research and was responsible for major funding of the project.

FUNDING

This work was funded through the support of CONACyT scholarship (572462). Universidad Autonoma de Aguascalientes, Mexico Award number: PIBT16-3 to ALGB. The project was supported by Special Resource UAA for Research 2017 and 2018, as well as Fonds de recherche du Québec–Nature et technologies (FRQ-NT) and the Centre de recherche en infectiologie porcine et avicole (CRIPA) that provided an international internship, #264179, to JMDV. CD was funded by NSERC Discovery grant 2019-06642.

ACKNOWLEDGMENTS

We thank Dr. Josée Harel and Dr. Cécile Crost for their support and guidance on the cooperative funding through the CRIPA FRQ-NT funded internship program. We thank Adriana Cecilia Moreno Flores for technical assistance with confocal microscopy, also to Sébastien Houle and Fabiola Galindo Guerrero for their technical assistance.

SUPPLEMENTARY MATERIAL

The Supplementary Material for this article can be found online at: https://www.frontiersin.org/articles/10.3389/fcimb.2020.00299/full#supplementary-material

Supplementary Image 1 | Kinetics of vacuole formation induced by Vat toxin on human urinary bladder cell line 5,637. Kinetics of vacuole formation (Black arrows) showed cytoplasmic vacuoles after 3 h of toxin exposure, with vacuole formation increasing over time.

Supplementary Image 2 | Distribution of F-actin, α-Tubulin, and Arp3 cytoskeletal proteins detected after treatment of bladder epithelial cells with Vat observed by confocal microscopy. The negative control cells **(A)** show a normal distribution of actin stress fibers with a homogeneous pattern. A similar pattern was observed in samples exposed to 50 μg of heat-inactivated Vat toxin **(B)**. After exposure to Vat **(C)**, the cells acquired a rounded shape with a loss of the cytoplasmic actin stress fibers. This effect was also observed in cells treated with Vat together with polymyxin B **(D)**. Tubulin was distributed throughout the cell in control cells **(E)** with its presence throughout the cell. Cells incubated with the toxin after heat inactivation have a similar tubulin pattern as those treated with the empty vector supernatant **(F)**. Once cells were exposed to Vat **(G)**, the tubulin pattern showed cytoplasmic rearrangement resembling the morphological changes in cell shape **(H)**. The presence of Polymyxin B in the cell culture did not alter the effect of the toxin on cells. Arp3 had a cytoplasmic dotted distribution **(I)** in untreated control cells. This was also the case with cells exposed to the inactivated toxin **(J)**. Cells after treatment with Vat **(K)** with or without polymyxin B **(L)**, showed a homogeneous cytoplasmic distribution of Arp3 in contrast to the control cells.

Supplementary Image 3 | Characterization of the vacuoles in bladder epithelial cells treated with Vat. After exposure to Vat toxin, cells were stained with Lysotracker deep red and visualized. Vacuoles with acidic content (Black arrows) with a perinuclear distribution were observed and other vacuoles without lysotracker staining were also observed (White arrows). The samples exposed to supernatant from bacteria contain the empty vector did not produce vacuoles (Bright-field microscopy), and the slight lysotracker staining may indicate a basal level of lysosomes in these cells.

REFERENCES

Alfaro-Aco, R., and Petry, S. (2015). Building the microtubule cytoskeleton piece by piece. *J. Biol. Chem.* 290, 17154–17162. doi: 10.1074/jbc.R115.638452

Appelqvist, H., Wäster, P., Kågedal, K., and Öllinger, K. (2013). The lysosome: from waste bag to potential therapeutic target. *J. Mol. Cell Biol.* 5, 214–226. doi: 10.1093/jmcb/mjt022

Bercier, P., Gottschalk, M., and Grenier, D. (2018). Effects of actinobacillus pleuropneumoniae on barrier function and inflammatory response of pig tracheal epithelial cells. *Pathog. Dis.* 77:fty079. doi: 10.1093/femspd/fty079

Chen, X., Bi, Y., Wang, T., Li, P., Yan, X., Hou, S., et al. (2015). Lysosomal targeting with stable and sensitive fluorescent probes (superior lysoprobes): applications for lysosome labeling and tracking during apoptosis. *Sci. Rep.* 5:9004. doi: 10.1038/srep09004

Crépin, S., Houle, S., Charbonneau, M., Mourez, M., Harel, J., and Dozois, C. (2012). Decreased expression of type 1 fimbriae by apstmutant of uropathogenic *Escherichia coli* reduces urinary tract infection. *Infect. Immun.* 80, 2802–2815. doi: 10.1128/IAI.00162-12

Dautin, N. (2010). Serine protease autotransporters of enterobacteriaceae (SPATEs): biogenesis and function. *Toxins* 2, 1179–1206. doi: 10.3390/toxins2061179

de Bernard, M., Cappon, A., Del Giudice, G., Rappuoli, R., and Montecucco, C. (2004). The multiple cellular activities of the VacA cytotoxin of Helicobacter pylori. *Int. J. Med. Microbiol.* 293, 589–597. doi: 10.1078/1438-4221-00299

Durnin, L., Kwok, B., Kukadia, P., McAvera, R., Corrigan, R., Ward, S., et al. (2018). An *ex vivo* bladder model with detrusor smooth muscle removed to analyse biologically active mediators released from the suburothelium. *J. Physiol.* 597, 1467–1485. doi: 10.1113/JP276924

Dutta, P. R., Cappello, R., Navarro-García, F., and Nataro, J. P. (2002). Functional comparison of serine protease autotransporters of Enterobacteriaceae. *Infect. Immun.* 70, 7105–7113. doi: 10.1128/iai.70.12.7105-7113.2002

Fanizza, C., Fresegna, A., Maiello, R., Paba, B., and Cavallo, D. (2009). Evaluation of cytotoxic concentration-time response in A549 cells exposed to respirable-quartz. *J. Appl. Toxicol.* 29, 537–544. doi: 10.1002/jat.1440

Flores-Mireles, A., Walker, J., Caparon, M., and Hultgren, S. (2015). Urinary tract infections: epidemiology, mechanisms of infection and treatment options. *Nat. Rev. Microbiol.* 13, 269–284. doi: 10.1038/nrmicro3432

Foxman, B. (2003). Epidemiology of urinary tract infections: incidence, morbidity, and economic costs. *Dis. Month* 49, 53–70. doi: 10.1067/mda.2003.7

Gabella, G. (2019). Lamina propria: the connective tissue of rat urinary bladder mucosa. *Neurourol. Urodyn.* 38, 2093–2103. doi: 10.1002/nau.24085

Gasic, I., and Mitchison, T. (2019). Autoregulation and repair in microtubule homeostasis. *Curr. Opin. Cell Biol.* 56, 80–87. doi: 10.1016/j.ceb.2018.10.003

Gates, J., and Peifer, M. (2005). Can 1000 reviews be wrong? Actin, α-catenin, and adherens junctions. *Cell* 123, 769–772. doi: 10.1016/j.cell.2005.11.009

Gefen, A., and Weihs, D. (2015). Mechanical cytoprotection: a review of cytoskeleton-protection approaches for cells. *J. Biomech.* 49, 1321–1329. doi: 10.1016/j.jbiomech.2015.10.030

Glotfelty, L., Zahs, A., Iancu, C., Shen, L., and Hecht, G. (2014). Microtubules are required for efficient epithelial tight junction homeostasis and restoration. *Am. J. Physiol. Cell Physiol.* 307, C245–C254. doi: 10.1152/ajpcell.00336.2013

Greune, L., Kemper, B., Dobrindt, U., Geelen, J., Kim, K., Schmidt, M., et al. (2009). Vacuolisation of human microvascular endothelial cells by enterohaemorrhagic *Escherichia coli*. *Thromb. Haemost.* 102, 1080–1092. doi: 10.1160/TH09-07-0499

Grossmann, E., Longo, W., Kaminski, D., Smith, G., Murphy, C., Durham, R., et al. (2000). Clostridium difficile toxin: cytoskeletal changes and lactate dehydrogenase release in hepatocytes. *J. Surg. Res.* 88, 165–172. doi: 10.1006/jsre.1999.5736

Guerrero-Barrera, A., Garcia-Cuellar, C., Villalba, J., Segura-Nieto, M., Gomez-Lojero, C., Reyes, M., et al. (1996). Actin-related proteins in anabaena spp. and *Escherichia coli*. *Microbiology* 142, 1133–1140. doi: 10.1099/13500872-142-5-1133

Habouria, H., Pokharel, P., Maris, S., Garénaux, A., Bessaiah, H., Houle, S., et al. (2019). Three new serine-protease autotransporters of Enterobacteriaceae (SPATEs) from extra-intestinal pathogenic *Escherichia coli* and combined role of SPATEs for cytotoxicity and colonization of the mouse kidney. *Virulence* 10, 568–587. doi: 10.1080/21505594.2019.1624102

Henderson, I., and Nataro, J. (2001). Virulence functions of autotransporter proteins. *Infect. Immun.* 69, 1231–1243. doi: 10.1128/IAI.69.3.1231-1243.2001

Hu, X., Laguerre, V., Packert, D., Nakasone, A., and Moscinski, L. (2015). A simple and efficient method for preparing cell slides and staining without using cytocentrifuge and cytoclips. *Int. J. Cell Biol.* 2015, 1–4. doi: 10.1155/2015/813216

Kannan, T. R., and Baseman, J. B. (2006). ADP-ribosylating and vacuolating cytotoxin of *Mycoplasma pneumoniae* represents unique virulence determinant among bacterial pathogens. *Proc. Natl. Acad. Sci. U. S. A.* 103, 6724–6729. doi: 10.1073/pnas.0510644103

Kaper, J., Nataro, J., and Mobley, H. (2004). Pathogenic *Escherichia coli*. *Nat. Rev. Microbiol.* 2, 123–140. doi: 10.1038/nrmicro818

Khurana, S. (2006). *Aspects of the Cytoskeleton, Vol 37*. Burlington: Elsevier.

Kim, S., Song, S., Ahn, K., Kwon, D., Park, K., and Ryu, S. (2010). Changes in aquaporin 1 expression in rat urinary bladder after partial bladder outlet obstruction: preliminary report. *Korean J. Urol.* 51:281. doi: 10.4111/kju.2010.51.4.281

Lee, J.-H., McBrayer, M. K., Wolfe, D. M., Haslett, L. J., Kumar, A., Sato, Y., et al. (2015). Presenilin 1 maintains lysosomal Ca2+ homeostasis via TRPML1 by Regulating vATPase-Mediated lysosome acidification. *Cell Rep.* 12, 1430–1444.

Lièvin-Le Moal, V., Comenge, Y., Ruby, V., Amsellem, R., Nicolas, V., and Servin, A. (2011). Secreted autotransporter toxin (Sat) triggers autophagy in

epithelial cells that relies on cell detachment. *Cell. Microbiol.* 13, 992–1013. doi: 10.1111/j.1462-5822.2011.01595.x

López-Banda, D., Carrillo-Casas, E., Leyva-Leyva, M., Orozco-Hoyuela, G., Manjarrez-Hernández, Á., Arroyo-Escalante, S., et al. (2014). Identification of virulence factors genes inescherichia coliisolates from women with urinary tract infection in Mexico. *BioMed. Res. Int.* 2014, 1–10. doi: 10.1155/2014/959206

Lu, X. X., Jiang, Y. F., Li, H., Ou, Y. Y., Zhang, Z. D., DI, H. Y., et al. (2017). Polymyxin B as an inhibitor of lipopolysaccharides contamination of herb crude polysaccharides in mononuclear cells. *Chin. J. Nat. Med.* 15, 487–494. doi: 10.1016/S1875-5364(17)30074-2

Magryś, A., Deryło, K., Bogut, A., Olender, A., and Tchórzewski, M. (2018). Intraphagolysosomal conditions predispose to *Staphylococcus epidermidis* small colony variants persistence in macrophages. *PLoS ONE* 13:e0207312. doi: 10.1371/journal.pone.0207312

McLellan, L., and Hunstad, D. (2016). Urinary tract infection: pathogenesis and outlook. *Trends Mol. Med.* 22, 946–957. doi: 10.1016/j.molmed.2016.09.003

Nagahama, M., Itohayashi, Y., Hara, H., Higashihara, M., Fukatani, Y., Takagishi, T., et al. (2011). Cellular vacuolation induced by clostridium perfringens epsilon-toxin. *FEBS J.* 278, 3395–3407. doi: 10.1111/j.1742-4658.2011.08263.x

Najafzadeh, H., Masoodi, A., Rezaie, A., and Mehrzadi, S. (2011). Comparison of the effect of vanadium and deferoxamine on acetaminophen toxicity in rats. *Indian J. Pharmacol.* 43, 429–432. doi: 10.4103/0253-7613.83115

Nichols, K., Totsika, M., Moriel, D., Lo, A., Yang, J., Wurpel, D., et al. (2016). Molecular characterization of the vacuolating autotransporter toxin in uropathogenic *Escherichia coli*. *J. Bacteriol.* 198, 1487–1498. doi: 10.1128/JB.00791-15

Nielubowicz, G., and Mobley, H. (2010). Host–pathogen interactions in urinary tract infection. *Nat. Rev. Urol.* 7, 430–441. doi: 10.1038/nrurol.2010.101

Nordestgaard, B., and Rostgaard, J. (1985). Critical-point drying versus freeze drying for scanning electron microscopy: a quantitative and qualitative study on isolated hepatocytes. *J. Microsc.* 137, 189–207. doi: 10.1111/j.1365-2818.1985.tb02577.x

Parham, N., Pollard, S., Desvaux, M., Scott-Tucker, A., Liu, C., Fivian, A., et al. (2005). Distribution of the serine protease autotransporters of the enterobacteriaceae among extraintestinal clinical isolates of *Escherichia coli*. *J. Clin. Microbiol.* 43, 4076–4082. doi: 10.1128/JCM.43.8.4076-4082.2005

Parreira, V., and Gyles, C. (2003). A novel pathogenicity island integrated adjacent to the thrW tRNA gene of avian pathogenic *Escherichia coli* encodes a vacuolating autotransporter toxin. *Infect. Immun.* 71, 5087–5096. doi: 10.1128/IAI.71.9.5087-5096.2003

Parsons, C. (2007). The role of the urinary epithelium in the pathogenesis of interstitial cystitis/prostatitis/urethritis. *Urology* 69, S9–S16. doi: 10.1016/j.urology.2006.03.084

Peidaee, P., Almansour, N., Shukla, R., and Pirogova, E. (2013). The cytotoxic effects of low intensity visible and infrared light on human breast cancer (MCF7) cells. *Comput. Struct. Biotechnol. J.* 6:e201303015. doi: 10.5936/csbj.201303015

Peterson, D., Collier, J., Katterman, M., Turner, R., and Riley, M. (2009). Cytotoxicity of bacterial-derived toxins to immortal lung epithelial and macrophage cells. *Appl. Biochem. Biotechnol.* 160, 751–763. doi: 10.1007/s12010-009-8526-y

Prophet, E., Mills, B., Arrington, J., and Sobin, L. (1995). *Laboratory Methods in Histotechnology*. Washington: American Registry of Pathology.

Radin, J., González-Rivera, C., Ivie, S., McClain, M., and Cover, T. (2011). Helicobacter pylori VacA induces programmed necrosis in gastric epithelial cells. *Infect. Immun.* 79, 2535–2543. doi: 10.1128/IAI.01370-10

Ram, B. M., and Ramakrishna, G. (2014). Endoplasmic reticulum vacuolation and unfolded protein response leading to paraptosis like cell death in cyclosporine A treated cancer cervix cells is mediated by cyclophilin B inhibition. *Biochim. Biophys. Acta* 1843, 2497–2512. doi: 10.1016/j.bbamcr.2014.06.020

Ramírez-Castillo, F., Moreno-Flores, A., Avelar-González, F., Márquez-Díaz, F., Harel, J., and Guerrero-Barrera, A. (2018). An evaluation of multidrug-resistant *Escherichia coli* isolates in urinary tract infections from aguascalientes, Mexico: cross-sectional study. *Ann. Clin. Microbiol. Antimicrob.* 17:34. doi: 10.1186/s12941-018-0286-5

Roberts, P., Davis, K., Garstka, W., and Bhunia, A. (2001). Lactate dehydrogenase release assay from Vero cells to distinguish verotoxin producing *Escherichia coli* from non-verotoxin producing strains. *J. Microbiol. Methods* 43, 171–181. doi: 10.1016/S0167-7012(00)00222-0

Salvadori, M., Yano, T., Carvalho, H., Parreira, V., and Gyles, C. (2001). Vacuolating cytotoxin produced by avian pathogenic *Escherichia coli*. *Avian Dis.* 45, 43–51. doi: 10.2307/1593010

Sanchez-Villamil, J., Navarro-Garcia, F., Castillo-Romero, A., Gutierrez-Gutierrez, F., Tapia, D., and Tapia-Pastrana, G. (2019). Curcumin blocks cytotoxicity of enteroaggregative and enteropathogenic *Escherichia coli* by blocking pet and EspC proteolytic release from bacterial outer membrane. *Front. Cell. Infect. Microbiol.* 9:334. doi: 10.3389/fcimb.2019.00334

Shubin, A. V., Demidyuk, I. V., Komissarov, A. A., Rafieva, L. M., and Kostrov, S. V. (2016). Cytoplasmic vacuolization in cell death and survival. *Oncotarget* 7, 55863–55889. doi: 10.18632/oncotarget.10150

Simon, J., Müller, J., Ghazaryan, A., Morsbach, S., Mailänder, V., and Landfester, K. (2018). Protein denaturation caused by heat inactivation detrimentally affects biomolecular corona formation and cellular uptake. *Nanoscale* 10, 21096–21105. doi: 10.1039/C8NR07424K

Spurbeck, R., Dinh, P., Walk, S., Stapleton, A., Hooton, T., Nolan, L., et al. (2012). *Escherichia coli* isolates that carryvat, fyuA, chuA, andyfcV efficiently colonize the urinary tract. *Infect. Immun.* 80, 4115–4122. doi: 10.1128/IAI.00752-12

Tang, E., Mok, K., Lee, W., and Cheng, C. (2014). EB1 regulates tubulin and actin cytoskeletal networks at the sertoli cell blood-testis barrier in male rats: an *in vitro* study. *Endocrinology* 156, 680–693. doi: 10.1210/en.2014-1720

Terlizzi, M., Gribaudo, G., and Maffei, M. (2017). UroPathogenic *Escherichia coli* (UPEC) infections: virulence factors, bladder responses, antibiotic, and non-antibiotic antimicrobial strategies. *Front. Microbiol.* 8:1566. doi: 10.3389/fmicb.2017.01566

Tombola, F., Carlesso, C., Szabò, I., de Bernard, M., Reyrat, J., Telford, J., et al. (1999). Helicobacter pylori vacuolating toxin forms anion-selective channels in planar lipid bilayers: possible implications for the mechanism of cellular vacuolation. *Biophys. J.* 76, 1401–1409. doi: 10.1016/S0006-3495(99)77301-7

Tran, D., and Ten Hagen, K. (2017). Real-time insights into regulated exocytosis. *J. Cell Sci.* 130, 1355–1363. doi: 10.1242/jcs.193425

Tsuzuki, H., Tani, T., Ueyama, H., and Kodama, M. (2001). Lipopolysaccharide: neutralization by polymyxin B shuts down the signaling pathway of nuclear factor κB in peripheral blood mononuclear cells, even during activation. *J. Surg. Res.* 100, 127–134. doi: 10.1006/jsre.2001.6227

Welch, R. (2016). Uropathogenic *Escherichia coli*-associated exotoxins. *Microbiol. Spectr.* 4. doi: 10.1128/microbiolspec.UTI-0011-2012

Windoffer, R., Beil, M., Magin, T., and Leube, R. (2011). Cytoskeleton in motion: the dynamics of keratin intermediate filaments in epithelia. *J. Cell Biol.* 194, 669–678. doi: 10.1083/jcb.201008095

Conflict of Interest: The authors declare that the research was conducted in the absence of any commercial or financial relationships that could be construed as a potential conflict of interest.